frontiers | Research Topics

Specific macroscopic brain changes in psychotic disorders

Edited by
Felix Brandl, Franziska Knolle, Stefan Borgwardt and Chun Meng

Published in
Frontiers in Human Neuroscience

ISSN 1664-8714
ISBN 978-2-8325-2352-0
DOI 10.3389/978-2-8325-2352-0

About Frontiers

Frontiers is more than just an open access publisher of scholarly articles: it is a pioneering approach to the world of academia, radically improving the way scholarly research is managed. The grand vision of Frontiers is a world where all people have an equal opportunity to seek, share and generate knowledge. Frontiers provides immediate and permanent online open access to all its publications, but this alone is not enough to realize our grand goals.

Frontiers journal series

The Frontiers journal series is a multi-tier and interdisciplinary set of open-access, online journals, promising a paradigm shift from the current review, selection and dissemination processes in academic publishing. All Frontiers journals are driven by researchers for researchers; therefore, they constitute a service to the scholarly community. At the same time, the *Frontiers journal series* operates on a revolutionary invention, the tiered publishing system, initially addressing specific communities of scholars, and gradually climbing up to broader public understanding, thus serving the interests of the lay society, too.

Dedication to quality

Each Frontiers article is a landmark of the highest quality, thanks to genuinely collaborative interactions between authors and review editors, who include some of the world's best academicians. Research must be certified by peers before entering a stream of knowledge that may eventually reach the public - and shape society; therefore, Frontiers only applies the most rigorous and unbiased reviews. Frontiers revolutionizes research publishing by freely delivering the most outstanding research, evaluated with no bias from both the academic and social point of view. By applying the most advanced information technologies, Frontiers is catapulting scholarly publishing into a new generation.

What are Frontiers Research Topics?

Frontiers Research Topics are very popular trademarks of the *Frontiers journals series*: they are collections of at least ten articles, all centered on a particular subject. With their unique mix of varied contributions from Original Research to Review Articles, Frontiers Research Topics unify the most influential researchers, the latest key findings and historical advances in a hot research area.

Find out more on how to host your own Frontiers Research Topic or contribute to one as an author by contacting the Frontiers editorial office: frontiersin.org/about/contact

Specific macroscopic brain changes in psychotic disorders

Topic editors

Felix Brandl — Technical University of Munich, Germany
Franziska Knolle — Technical University of Munich, Germany
Stefan Borgwardt — University of Lübeck, Germany
Chun Meng — University of Electronic Science and Technology of China, China

Citation

Brandl, F., Knolle, F., Borgwardt, S., Meng, C., eds. (2023). *Specific macroscopic brain changes in psychotic disorders*. Lausanne: Frontiers Media SA.
doi: 10.3389/978-2-8325-2352-0

Table of contents

frontiers | Frontiers in Human Neuroscience

TYPE Editorial
PUBLISHED 06 February 2023
DOI 10.3389/fnhum.2023.1141866

OPEN ACCESS

EDITED AND REVIEWED BY
Mingzhou Ding,
University of Florida, United States

*CORRESPONDENCE
Felix Brandl
✉ felix.brandl@tum.de

SPECIALTY SECTION
This article was submitted to Brain Imaging and Stimulation, a section of the journal Frontiers in Human Neuroscience

RECEIVED 10 January 2023
ACCEPTED 11 January 2023
PUBLISHED 06 February 2023

CITATION
Brandl F, Knolle F, Meng C and Borgwardt S (2023) Editorial: Specific macroscopic brain changes in psychotic disorders. *Front. Hum. Neurosci.* 17:1141866. doi: 10.3389/fnhum.2023.1141866

Editorial: Specific macroscopic brain changes in psychotic disorders

Felix Brandl[1,2]*, Franziska Knolle[2,3], Chun Meng[4] and Stefan Borgwardt[5]

[1]Department of Psychiatry and Psychotherapy, School of Medicine, Technical University of Munich, Munich, Germany, [2]TUM-NIC Neuroimaging Center, School of Medicine, Technical University of Munich, Munich, Germany, [3]Department of Neuroradiology, School of Medicine, Technical University of Munich, Munich, Germany, [4]School of Life Science and Technology, University of Electronic Science and Technology of China, Chengdu, China, [5]Department of Psychiatry, University of Lübeck, Lübeck, Germany

KEYWORDS

psychotic disorders, schizophrenia, brain changes, specific, macroscopic

Editorial on the Research Topic
Specific macroscopic brain changes in psychotic disorders

Psychotic disorders, covering mainly the schizophrenia spectrum and substance-induced psychosis, affect more than 1% of the population, are often chronic, and comprise debilitating symptoms like hallucinations, delusions, and cognitive impairments (American Psychiatric Association, 2013; McCutcheon et al., 2020). In recent years, many studies and meta-analyses have shown an association between psychotic disorders and macroscopic brain changes, particularly changes of brain structure, function, perfusion, and metabolism measured by magnetic resonance imaging (MRI) and positron emission tomography (PET) (McCutcheon et al., 2018; van Erp et al., 2018; Brandl et al., 2019; Gong et al., 2020; Sukumar et al., 2020). However, psychotic disorders overlap with other psychiatric disorders on the level of both symptoms and macroscopic brain changes (Goodkind et al., 2015; Kebets et al., 2019; Sha et al., 2019).

Therefore, we are yet to fully understand the macroscopic brain changes that are specific to psychotic disorders. Investigating changes specific to psychotic disorders may not only improve our pathophysiological and mechanistic understanding, but also—in the mid to long term—enable imaging-based differential diagnosis at early disease stages, and, thereby, informing the development of prognostic markers and specific treatment strategies. To achieve this, transdiagnostic approaches are necessary, for example comparisons of macroscopic brain changes in psychotic disorders, such as schizophrenia, with those in affective disorders, such as bipolar disorder or major depression (Brandl et al., 2019).

This Research Topic provides original studies and reviews examining macroscopic brain changes that are specific to psychotic disorders. The term "psychotic disorders" is understood as in DSM-5, covering mostly the schizophrenia spectrum and substance-induced psychosis (American Psychiatric Association, 2013). "Macroscopic brain changes" is understood as alterations of brain regions or systems in the millimeter/centimeter scale, which are detectable by *in-vivo* brain imaging. Finally, "specific" means that changes are more pronounced in psychotic disorders than in other psychiatric disorders, e.g., bipolar disorder.

Rootes-Murdy et al. compared gray matter alterations and symptom profiles of patients with schizophrenia and patients with bipolar I disorder, using a large structural MRI dataset. They showed that in general, patients with schizophrenia tend to have more severe symptom profiles and gray matter alterations, particularly in the temporal poles, than patients with bipolar I disorder. However, diagnostic boundaries were not clearly

related to structural differences or distinct symptom profiles. They concluded that both disorders may track along an extensive spectrum of symptoms and brain correlates.

Schaub et al. started from observations that seasonal birth in winter and spring increases the risk of psychiatric disorders, for example schizophrenia and depression, possibly through pathological processes during neurodevelopment. They tested the effects of season of birth on gray matter volume (based on structural MRI) in a transdiagnostic sample of patients with schizophrenia and depression. They observed an effect of season of birth only in depression, but not in schizophrenia. Interestingly, and contrary to their expectations, hippocampal volume was lower in summer-born depressed individuals compared to winter-born individuals.

Takahashi et al. studied whether Heschl's gyrus duplication, a gyrification variant with increased prevalence in schizophrenia, is also present in bipolar disorder and major depression. Using structural MRI data, they showed a significantly higher prevalence of Heschl's gyrus duplication in patients with bipolar disorder, but not in patients with major depression, compared to healthy subjects. They concluded that the neurodevelopmental pathology of Heschl's gyrus duplication partly overlaps between schizophrenia and bipolar disorder, while its contribution in major depression appears distinct.

Cao et al. investigated the dyssynchrony of local brain activation in schizophrenia *via* a surface-based two-dimensional regional homogeneity approach, using resting-state fMRI data. They identified multiple aberrances both at the global and the local level, as well as links with illness duration and negative symptom severity. Some of their findings overlapped with abnormalities in bipolar disorder and depression, as reported in the literature. They concluded that the surface-based two-dimensional regional homogeneity approach could help with further exploring pathophysiological mechanisms of schizophrenia.

Rasmussen et al. examined associations between white matter microstructure and sleep-wake disturbances in individuals at ultra-high risk for psychosis. They used data from diffusion MRI, sleep questionnaire, and actigraphy. They observed an association between white matter microstructure of the corpus callosum and sleep disturbances in individuals at ultra-high risk for psychosis. They concluded that their findings suggest sleep disturbances as a potential treatment target.

Liang et al. investigated the link between structural MRI-based cortical thickness, MRS-based glutamate levels in the dorsal anterior cingulate cortex, and language dysfunction in patients with first-episode psychosis. Using a clustering approach, they identified a patient subgroup with widespread cortical thinning, higher glutamate levels in the dorsal anterior cingulate cortex, and reduced syntactic complexity and lexical cohesion. They concluded that their findings support the presence of detectable neurobiological subtypes of schizophrenia.

Salvador et al. applied a regularization approach (ridge regression), i.e., an innovative method to assess resting-state functional connectivity abnormalities, to resting-state fMRI data from patients with schizophrenia and healthy controls. They also compared their results to other measures of brain connectivity and dimensionality reduction. They observed widespread connectivity reductions in schizophrenia; the regularization approach outperformed the other methods. They concluded that regularization is a simple and sensitive alternative for quantifying functional brain connectivity.

In their Methods paper, Blair et al. propose a novel method for estimating complexity of brain activity, whose alteration in psychiatric disorders has already been shown by several studies. This method relies on dynamic functional connectivity to capture the distributed nature of brain activity and entropy measures to estimate global signal complexity. They applied their method to a sample of patients with obsessive-compulsive disorder, showing the robustness and consistency of this method compared with the existing literature.

In their Hypothesis and Theory paper, Liddle and Liddle review electrophysiological and fMRI-based evidence indicating imprecise predictive coding (i.e., the process of generating models of the world that are successively updated by sensory information) as a core pathological process in schizophrenia. They discuss macroscopic and molecular brain changes and their link with imprecise predictive coding and symptoms of schizophrenia, particularly disorganized and impoverished mental activity.

In conclusion, this Research Topic combines original studies and reviews concerning macroscopic brain changes in psychotic disorders, particularly compared to other psychiatric disorders such as bipolar disorder or major depression, and outlines promising areas for future research.

Author contributions

All authors listed have made a substantial, direct, and intellectual contribution to the work and approved it for publication.

Acknowledgments

The Topic Editors express their gratitude to all the contributors for submitting their work to this Research Topic, to the Review Editors and external reviewers who participated in the review process, and to the Editorial and Production teams of Frontiers for their valuable assistance through the various stages of the publication process.

Conflict of interest

The authors declare that the research was conducted in the absence of any commercial or financial relationships that could be construed as a potential conflict of interest.

Publisher's note

References

American Psychiatric Association (2013). *Diagnostic and Statistical Manual of Mental Disorders, Fifth Edition (DSM-5)*. Arlington, VA, American Psychiatric Publishing. doi: 10.1176/appi.books.9780890425596

Brandl, F., Avram, M., Weise, B., Shang, J., Simões, B., Bertram, T., et al. (2019). Specific substantial dysconnectivity in schizophrenia: a transdiagnostic multimodal meta-analysis of resting-state functional and structural magnetic resonance imaging studies. *Biol. Psychiatry* 85, 573–583. doi: 10.1016/j.biopsych.2018.12.003

Gong, J., Wang, J., Luo, X., Chen, G., Huang, H., Huang, R., et al. (2020). Abnormalities of intrinsic regional brain activity in first-episode and chronic schizophrenia: a meta-analysis of resting-state functional MRI. *J. Psychiatry Neurosci.* 45, 55–68. doi: 10.1503/jpn.180245

Goodkind, M., Eickhoff, S. B., Oathes, D. J., Jiang, Y., Chang, A., Jones-Hagata, L. B., et al. (2015). Identification of a common neurobiological substrate for mental illness. *JAMA Psychiatry* 72, 305–315. doi: 10.1001/jamapsychiatry.2014.2206

Kebets, V., Holmes, A. J., Orban, C., Tang, S., Li, J., Sun, N., et al. (2019). Somatosensory-motor dysconnectivity spans multiple transdiagnostic dimensions of psychopathology. *Biol. Psychiatry* 86, 779–791. doi: 10.1016/j.biopsych.2019.06.013

McCutcheon, R., Beck, K., Jauhar, S., and Howes, O. D. (2018). Defining the locus of dopaminergic dysfunction in schizophrenia: a meta-analysis and test of the mesolimbic hypothesis. *Schizophr. Bull.* 44, 1301–1311. doi: 10.1093/schbul/sbx180

McCutcheon, R. A., Reis Marques, T., and Howes, O. D. (2020). Schizophrenia-an overview. *JAMA Psychiatry* 77, 201–210. doi: 10.1001/jamapsychiatry.2019.3360

Sha, Z., Wager, T. D., Mechelli, A., and He, Y. (2019). Common dysfunction of large-scale neurocognitive networks across psychiatric disorders. *Biol. Psychiatry* 85, 379–388. doi: 10.1016/j.biopsych.2018.11.011

Sukumar, N., Sabesan, P., Anazodo, U., and Palaniyappan, L. (2020). Neurovascular uncoupling in schizophrenia: a bimodal meta-analysis of brain perfusion and glucose metabolism. *Front. Psychiatry* 11, 754. doi: 10.3389/fpsyt.2020.00754

van Erp, T. G. M., Walton, E., Hibar, D. P., Schmaal, L., Jiang, W., Glahn, D. C., et al. (2018). Cortical brain abnormalities in 4474 individuals with schizophrenia and 5098 control subjects via the enhancing neuro imaging genetics through meta analysis (ENIGMA) consortium. *Biol. Psychiatry* 84, 644–654. doi: 10.1016/j.biopsych.2018.04.023

frontiers in Human Neuroscience

ORIGINAL RESEARCH
published: 06 December 2021
doi: 10.3389/fnhum.2021.750879

Surface-Based Spontaneous Oscillation in Schizophrenia: A Resting-State Functional Magnetic Resonance Imaging Study

Xianyu Cao[1,2], Huan Huang[1,2], Bei Zhang[1,2], Yuchao Jiang[1,2], Hui He[1,2], Mingjun Duan[1,2,3], Sisi Jiang[1,2,3], Ying Tan[4], Dezhong Yao[1,2,3]*, Chao Li[1,2]* and Cheng Luo[1,2,3]*

[1] MOE Key Lab for Neuroinformation, High-Field Magnetic Resonance Brain Imaging Key Laboratory of Sichuan Province, The Clinical Hospital of Chengdu Brain Science Institute, University of Electronic Science and Technology of China, Chengdu, China, [2] High-Field Magnetic Resonance Brain Imaging Key Laboratory of Sichuan Province, Center for Information in Medicine, University of Electronic Science and Technology of China, Chengdu, China, [3] Research Unit of NeuroInformation (2019RU035), Chinese Academy of Medical Sciences, Chengdu, China, [4] The Key Laboratory for Computer Systems of State Ethnic Affairs Commission, Southwest Minzu University, Chengdu, China

OPEN ACCESS

Edited by:
Felix Brandl,
Technical University of Munich, Germany

Reviewed by:
Fengmei Lu,
Chengdu No.4 People's Hospital, China
Bochao Cheng,
Sichuan University, China

***Correspondence:**
Ying Tan
ty7499@swun.edu.cn
Dezhong Yao
dyao@uestc.edu.cn
Chao Li
lichao0906@hotmail.com

Specialty section:
This article was submitted to Brain Imaging and Stimulation, a section of the journal Frontiers in Human Neuroscience

Received: 31 July 2021
Accepted: 05 November 2021
Published: 06 December 2021

Citation:
Cao X, Huang H, Zhang B, Jiang Y, He H, Duan M, Jiang S, Tan Y, Yao D, Li C and Luo C (2021) Surface-Based Spontaneous Oscillation in Schizophrenia: A Resting-State Functional Magnetic Resonance Imaging Study. Front. Hum. Neurosci. 15:750879. doi: 10.3389/fnhum.2021.750879

Schizophrenia (SZ) is considered as a self-disorder with disordered local synchronous activation. Previous studies have reported widespread dyssynchrony of local activation in patients with SZ, which may be one of the crucial physiological mechanisms of SZ. To further verify this assumption, this work used a surface-based two-dimensional regional homogeneity (2dReHo) approach to compare the local neural synchronous spontaneous oscillation between patients with SZ and healthy controls (HC), instead of the volume-based regional homogeneity approach described in previous study. Ninety-seven SZ patients and 126 HC were recruited to this study, and we found the SZ showed abnormal 2dReHo across the cortical surface. Specifically, at the global level, the SZ patients showed significantly reduced global 2dReHo; at the vertex level, the foci with increased 2dReHo in SZ were located in the default mode network (DMN), frontoparietal network (FPN), and limbic network (LN); however, foci with decreased 2dReHo were located in the somatomotor network (SMN), auditory network (AN), and visual network (VN). Additionally, this work found positive correlations between the 2dReHo of bilateral rectus and illness duration, as well as a significant positive correlation between the 2dReHo of right orbital inferior frontal gyrus (OIFG) with the negative scores of the positive and negative syndrome scale in the SZ patients. Therefore, the 2dReHo could provide some effective features contributed to explore the pathophysiology mechanism of SZ.

Keywords: schizophrenia, fMRI, spontaneous neuronal activity, surface-base, resting state

INTRODUCTION

Schizophrenia (SZ) is commonly considered as a heterogeneous psychiatric disorder with a wide range of clinical and biological manifestations, which also is included among the world's top 10 causes of long-term disability (Dong et al., 2017; Luo et al., 2020). These manifestations include positive symptoms (hallucination, delusions, and disturbed emotions), negative symptoms

(affective flattening, avolition-apathy, alogia, social withdrawal, and attention impairment), and cognitive dysfunction (processing speed, attention/vigilance, working memory) (Schultz and Andreasen, 1999; Tomasik et al., 2016; Jiang et al., 2019). However, the clear neuronal mechanisms underlying these symptoms remain unclear.

As a number of researchers continue to study SZ, various theories have been proposed to explain these different symptoms. In the study of SZ sensory and perceptual disorders, the bottom-up and top-down brain system integration theory proposes that the bottom-up functional impairment will lead to the abnormality of sensory mechanism (Javitt and Freedman, 2015), whereas the abnormality of top-down cognitive mechanism is the cause of cognitive failure (Allen et al., 2012). Specifically, auditory hallucinations are thought to result from the failure of top-down inhibitory control over bottom-up perceptual processes (Hugdahl, 2009). Furthermore, the pathophysiology underlying SZ has been attributed to functional abnormalities of the brain, which can be partially explained by spontaneous brain activity (Xu et al., 2015; Zhang et al., 2021). Previous studies have demonstrated that the SZ has exhibited functional changes in both task-evoked activation and spontaneous brain activity (Light et al., 2006; Jiang et al., 2020). SZ is regarded as a neurodevelopmental disorder, and its symptoms occur spontaneously. Therefore, investigating spontaneous brain activities in SZ can help us understand the pathophysiology underlying SZ.

The development and application of functional magnetic resonance imaging (fMRI) provide a new way to explore the neural activity of SZ (Biswal et al., 1995; Luo et al., 2020). Several works have revealed abnormal functional connectivity (FC) in patients with SZ, including the default mode network (DMN) (Bluhm et al., 2007; Canuet et al., 2011), the frontoparietal network (FPN) (Chen et al., 2017), thalamus (Wang et al., 2020), hippocampus (Ho et al., 2016), and temporoparietal area (Jiang et al., 2018; Huang et al., 2020); these findings suggested that abnormal neural activity in these region may be the alterations characteristic of SZ. In addition, a review has demonstrated that abnormal spontaneous brain activity in SZ were mainly located in the somatosensory cortex, occipital cortex (OC), medial temporal cortex (MTC), and medial prefrontal cortex (MPFC) (Xu et al., 2015); abnormal activation patterns within these regions may reflect different aspect symptoms in the SZ.

Regional homogeneity (ReHo), which measures the similarity or synchronism of the time series of a given voxel with its neighboring voxel within a single region, is the most widely used to reflect the local neural synchronous spontaneous oscillation in the brain (Zang et al., 2004). Since the blood oxygenation level dependent signal of fMRI reflects neural activity, abnormal ReHo is probably related to the temporal variation of regional spontaneous neural activity (Logothetis and Wandell, 2004). According to previous studies on subjects with a first-episode drug-naïve patients with SZ comorbid with depression (Fang et al., 2021), unipolar depression, and bipolar disorder (Liu et al., 2020) and SZ (Kuhn and Gallinat, 2013), abnormal ReHo may provide new insights into the potential pathophysiological mechanisms of psychiatric disorders. In addition, abnormal neural activities are associated with clinical symptoms and cognitive dysfunction, and ReHo may be used to evaluate the severity of clinical symptoms and cognitive dysfunction (Gao et al., 2020).

In recent years, ReHo has been widely used to investigate SZ pathophysiology (Zalesky et al., 2012; Cui et al., 2016; Zhao et al., 2018). Increased ReHo may represent neural hyperactivity in the brain regional area and vice versa (Zang et al., 2004). However, to our knowledge, all previous studies examined ReHo in patients with SZ to explore the abnormalities of regional functional synchronization at the voxel level (Xu et al., 2015; Chen et al., 2020). This volume-based ReHo (3dReHo) approach ignores the intersubject variability of cortical folding patterns, and voxels near the boundary between the gray and white matter show a significant partial volume effect (Li et al., 2014). A previous work has demonstrated that volume-based smoothing causes contamination of the primary motor cortex by somatosensory cortical responses, leading to false positive motor activation (Brodoehl et al., 2020). Therefore, in our work, we used a surface-based two-dimensional ReHo (2dReHo) method (Bo et al., 2019), which focuses on neural activation in the cerebral cortex, decreases signal contamination considerably between neighboring functional brain regions, and improves the validity of the activity results (Jiang and Zuo, 2016; Brodoehl et al., 2020).

In our work, with this relatively new 2dReHo approach, 97 patients with SZ were recruited to explore the abnormal local functional homogeneity of spontaneous neuronal activity and its correlations with symptomatic severity. We hypothesized that patients with SZ may have extensive abnormal local synchronization of spontaneous neuronal activity across the cortical mantle, and the 2dReHo could provide more accurate and persuasive evidences to expound the pathophysiological hypothesis of SZ.

MATERIALS AND METHODS

Participants

Ninety-seven patients with SZ (29 women, 41.0 $\pm$ 11.5 years old) were recruited from the inpatient in the Clinical Hospital of Chengdu Brain Science Institute in University of Electronic Science and Technology of China. The diagnosis of SZ was according to the structured clinical interview for Diagnostic and Statistical Manual of mental disorder (DSM-IV) criteria. All patients were treated with antipsychotics. Clinical symptomatic severity was evaluated by the positive and negative syndrome scale (PANSS) (Kay et al., 1987). In this work, 126 healthy controls (HC) (42 women, 38.0 $\pm$ 14.9 years old) who matched in age and gender with SZ were also enrolled from the local community through advertisements. The exclusion criteria for both groups included history of major medical or neurological illness, traumatic brain injury, first- and second-degree relatives with a history of mental illness, current drug or alcohol abuse, and MRI contraindications. Additionally, four SZ patients and one HC were excluded because they failed to accomplish all of T1 and resting-state fMRI data acquisitions, or their head-motion was beyond 2 mm or 2°. These patients were part of

our previous studies and more details can be found in prior published works (Jiang et al., 2020). Written informed consents were signed by all participants before the MRI scanning, and the Ethics Committee of the Clinical Hospital of Chengdu Brain Science Institute approved the work (No. CDFH2014030501).

Data Acquisition

High-resolution T1-weighted images and Resting-state fMRI were collected on a 3.0 Tesla scanner (GE Discovery MR 750) with an 8-channel standard whole head coil at the MRI Center of University of Electronic Science and Technology of China. During the scanning, sponges were used to reduce the noise of head movements, and participants were requested to keep their minds wandering during the resting-state scan with eyes closed without falling asleep. Three-dimensional T1-weighted data were obtained by using a fast-spoiled gradient echo sequence [repetition time (TR) = 6.008 ms; echo time (TE) = 1.984 ms; flip angle (FA) = 9°; field of view (FOV) = 25.6 × 25.6 cm^2; matrix size = 256 × 256; slice thickness = 1 mm, no gap, and slice number = 156]. Resting-state functional data were obtained with the use of a gradient-echo echo-planar imaging (EPI) sequence (TR = 2,000 ms; TE = 30 ms; FA = 90°; FOV = 24 × 24 cm^2; matrix size = 64 × 64; slice thickness = 4 mm, no gap and slice number = 35). Scanning time lasting 510 s (255 volumes).

Data Preprocessing

Both the structural and functional image preprocessing were performed using a surface-based resting-state fMRI data analysis toolbox (DPABISurf[1], Yan et al., 2016). The structural image processing steps consisted of: (1) spatial adaptive non-local mean filter was used to remove MRI spatial noise (Xing et al., 2011), (2) intensity correction, (3) skull-stripped, (4) brain tissue segmentation, cerebrospinal fluid (CSF), white matter (WM), and gray matter (GM), (5) brain surface reconstruction *via* the recon-all command in FREESURFER (version 6.0.1) (Dale et al., 1999), and (6) spatial normalization from individual native space to fsaverage space (Fischl, 2012). The functional image processing steps consisted of: (1) remove the first 10 volumes, (2) skull-stripped, (3) slice timing correction, (4) head motion correction, (5) nuisance correction by regressing out the WM and CSF mean time series according the WM and CSF masks segmented by FREESURFER as well as the Friston-24 motion time series (Friston et al., 1996), except for the global signal, as it may be the basis for alterations in neural information flow in SZ patients (Yang et al., 2014), (6) band-pass temporal filtering (0.01–0.1 Hz), (7) boundary-based registration (BBR) algorithm was used to register individual structural and functional images (Greve and Fischl, 2009), and (8) projection of the individual preprocessed volume-based function image onto a standard cortical surface (fsaverage5). Specifically, we calculated the midpoints of each pair of vertices on the pia meningeal and white matter surfaces generated by FREESURFER. Through BBR algorithm, we could get the registration matrix between the native fMRI volume and structural volume of each subject. Then, we choose fsaverage5 surface space as the target surface for projection and interpolation. For each subject's vertex in the fsaverage5 space, its corresponding coordinates in the native structural space were calculated first, and then its corresponding coordinates in the fMRI space were calculated. Finally, according to these given coordinates, the fMRI values are interpolated using the trilinear interpolation method.

[1]http://rfmri.org/DPABISurf

Cortical Surface-Based 2dReHo

In our study, 2dReHo was used to explore the abnormal local functional homogeneity of spontaneous neuronal activity. For each subject, the 2dReHo is obtained by calculating Kendall's concordance coefficient (KCC) of the given vertex and the nearest neighbors' time series (Zuo et al., 2013). This calculation was repeated for all vertices on both hemispheres, resulting in a 2dReHo map of both hemispheres. Specifically, for each vertex, we determined its 18 nearest vertices, based on which we calculated the KCC of fMRI time series of all 19 vertices. Of note, if we try to keep the same length of neighbors for certain vertices or voxel, the number of neighbors is different; for 2dReHo, the length-one and length-two calculation recruits 6 and 18 neighbors, respectively, whereas the 3dReHo recruits 26 neighbors. Moreover, previous studies have shown that the spatial pattern of length-two neighbors 2dReHo is highly similar to length-one neighbors 2dReHo's pattern (Zuo et al., 2013). Based on the above reasons, we chose 18 vertices as our calculation criteria. Finally, Gaussian spatial smoothing was performed for the 2dReHo maps using a 10-mm full-width half maximum Gaussian kernel (Zuo et al., 2013).

Statistical Analysis

The demographic and psychometric data were analyzed using SPSS 28.0. Two-sample *t*-tests were used to compare age and

TABLE 1 | Demographic data for SZ vs. HC participants.

Characteristic	Patients		Health controls		*P*-value
	Mean	SD	Mean	SD	
Number	97		126		
Gender (male/female)	68/29		84/42		0.67[a]
Age (years)	41.0	11.5	38.0	14.9	0.10[b]
Education (years)[c]	11.8	3.1	10.9	3.4	0.08[b]
Duration of illness (years)	16.3	10.9			
Chlorpromazine equivalents (mg/day)	324.5	157.1			
PANSS score					
PANSS-positive[d]	13.32	5.89			
PANSS-negative[d]	20.70	6.06			
PANSS-general[d]	28.19	5.86			
PANSS-total[d]	62.21	13.26			

PANSS, positive and negative syndrome scale; SZ, schizophrenia; HC, healthy controls.
[a] χ^2 *test.*
[b] *Two-sample t-test.*
[c] *Data of 76 patients and 111 controls available.*
[d] *Data of 64 patients available.*

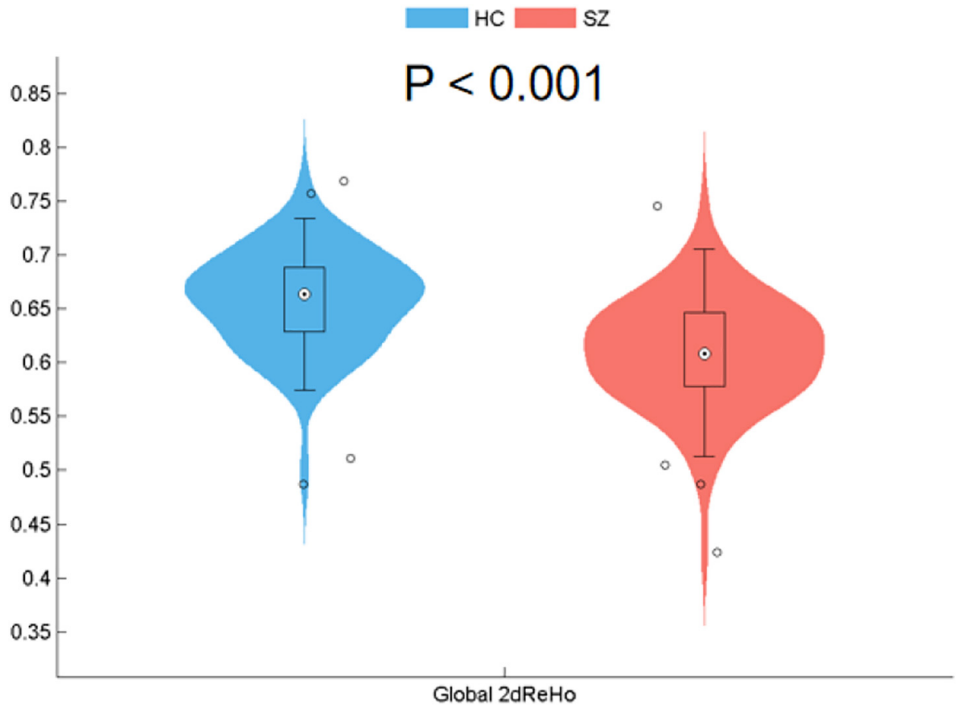

FIGURE 1 | Reduced surface-based 2dReHo in SZ patients compared with HC at the global level ($p < 0.001$) across the cortical surface. Global 2dReHo, global mean two-dimensional regional homogeneity. SZ, schizophrenia; HC, healthy control.

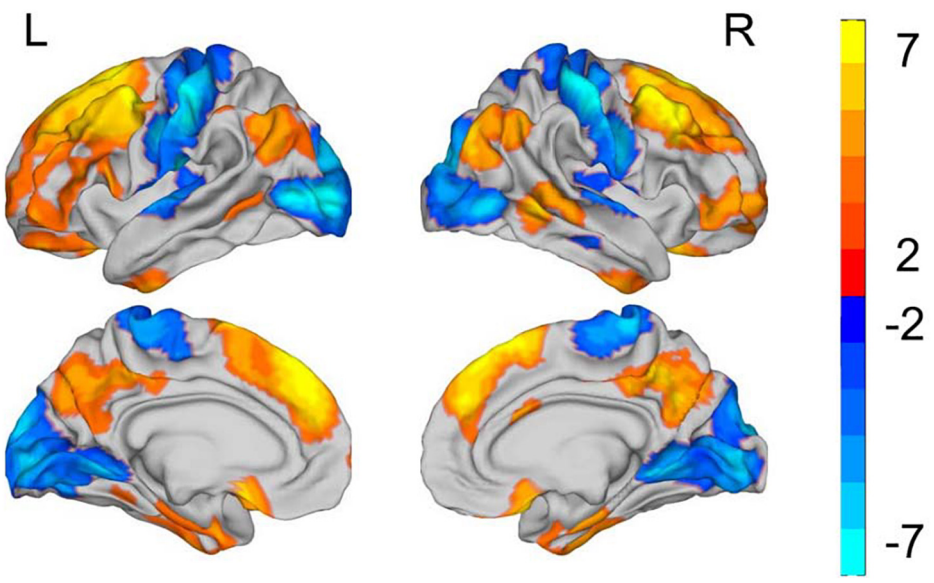

FIGURE 2 | Group differences in the surface-based 2dReHo. L refers to **left side** of brain. R refers to **right side** of brain. All results are shown after FDR corrected ($p < 0.05$). The color bar represents T values of the two-sample *t*-test; the yellow regions represent higher and blue regions represent lower 2dReHo in the patient group compared with the control group.

years of education. The chi-square test was performed to compare the difference in the gender between SZ and HC groups.

To compare the 2dReHo differences between the SZ and HC groups, the two-sample *t*-test was performed between the surface maps of SZ and HC groups by DPABISurf. Multiple comparisons correction was performed using the false discovery rate (FDR) corrected. The 2dReHo in the regions with significant differences between the two groups were extracted. Subsequently,

the Spearman rank correlation analysis was used to evaluate the relationship between the 2dReHo in these regions and clinical variables (illness duration, PANSS subscales, and total scores) after regressing out age and gender.

RESULTS

Demographic and Clinical Characteristics

The remaining 93 patients with SZ (28 women, 40.0 ± 11.5 years old) and 125 controls (41 women, 37.6 ± 14.9 years old) were matched in age ($p = 0.09$), gender ($p = 0.67$), and education years ($p = 0.08$). More demographic and clinical information of the patients are summarized, as shown in **Table 1**.

Surface-Based 2dReHo Differences Between Schizophrenia and Healthy Controls

At the global level, the patients with SZ showed a significant reduction in the global 2dReHo of the cortical surface ($t = -7.336$, $p < 0.001$) compared with HC (**Figure 1**).

At the vertex level, patients with SZ showed significantly increased 2dReHo in regions widely distributed across DMN (bilateral middle temporal gyrus and precuneus), FPN (bilateral frontal and parietal cortex), and limbic network (LN) (inferior temporal gyrus and rectus) (**Figure 2** and **Table 2**). Moreover, reduced 2dReHo was observed in the somatomotor network (SMN) (bilateral postcentral gyrus), auditory network (AN) (heschl and superior temporal gyrus), and visual network (VN) (bilateral occipital cortex) in SZ group (**Figure 2** and **Table 2**).

Relationships Between Surface-Based 2dReHo and Clinical Variables

After multiple comparisons correction by the FDR ($p < 0.05$, FDR corrected), the 2dReHo of left rectus ($r = 0.536$, $p < 0.001$) and right rectus ($r = 0.427$, $p < 0.001$) showed significantly positive correlations with illness duration in the SZ group. Moreover, the 2dReHo in the right orbital inferior frontal gyrus (OIFG) ($r = 0.251$, $p = 0.039$, without corrected) exhibited significant positive correlation with the PANSS negative scores (**Figure 3**).

TABLE 2 | Group differences in the surface-based 2dReHo.

Brain regions (peak index) (AAL)	Peak index[a]	Peak T value	Cluster size (mm^2)[b]
Left hemisphere			
Default mode network			
Frontal_Mid_L	8,062	6.95	8154.28
Precuneus_L	9,718	4.49	1607.18
Angular_L	5,108	4.23	1116.1
Temporal_Mid_L	4,344	3.18	138.16
Frontoparietal network			
Parietal_Inf_L	2,044	4.16	106.04
Limbic network			
Rectus_L	430	5.11	925.2
Temporal_Inf_L	5,539	3.76	846.3
Somatomotor network			
Postcentral_L	8,726	−7.02	5664.69
Visual network			
Occipital_Mid_L	5,283	−7.59	5904.62
Auditory network			
Temporal_Sup_L	1,172	−5.66	730.33
Right hemisphere			
Default mode network			
Frontal_Mid_R	3,607	6.35	4417.62
Precuneus_R	9,354	5.15	1561.81
Angular _R	784	4.39	1298.13
Temporal_Mid_R	5,640	4.45	736.1
Frontoparietal network			
Frontal_Inf_Orb_R	7,613	4.02	1130.25
Limbic network			
Rectus_R	514	4.96	813.26
Temporal_Inf_R	5,486	3.97	657.19
Somatomotor network			
Postcentral_R	1,071	−7.54	5387.76
Visual network			
Occipital_Sup_R	6,872	−6.37	6116.6
Auditory network			
Heschl_R	1,309	−3.28	260.62

L, left side of brain; R, right side of brain; AAL, automated anatomical labeling atlas.
[a]The index of the vertex with the peak T value.
[b]The cluster size represents the number of vertices within the cluster.

DISCUSSION

To the best of our knowledge, this is the first work to investigate the abnormal local functional homogeneity of spontaneous neural oscillation in patients with SZ. At the global level, our work indicated that compared with HC, the SZ patients showed significantly reduced global 2dReHo. As for the vertex level, we demonstrated significantly enhanced 2dReHo in the DMN, FPN, and LN, and also significantly reduced 2dReHo in the primary perception networks (SMN, AN, and VN) in SZ. These results suggested that the SZ is associated with abnormal synchronization of spontaneous neural oscillation in the regional brain. Moreover, the relationships between the 2dReHo abnormalities and clinical variables, including illness duration, PANSS subscales, and total scores were evaluated in patients with SZ. The results indicated that the 2dReHo of bilateral rectus were significantly positive related with illness duration, and also the 2dReHo in the right OIFG exhibited significant positive correlation with the PANSS positive scores.

Recently, several studies have investigated the ReHo abnormalities in SZ, but with inconsistent results. The reasons for these inconsistencies are complex and it is necessary to reconcile the heterogeneity of different findings. Of note, our results are highly consistent with those of a previous metaanalysis on 3dReHo in the SZ (Xu et al., 2015), which demonstrated

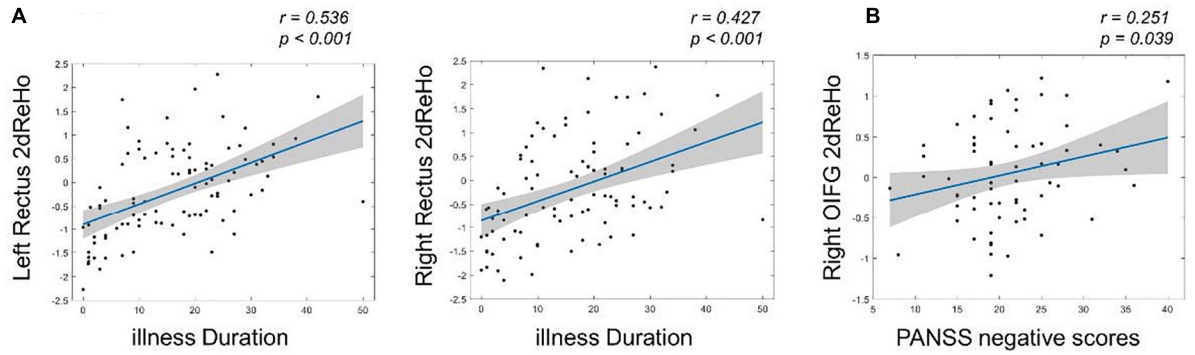

FIGURE 3 | The relationships between surface-based 2dReHo and clinical variables in patients with SZ by using Spearman rank correlation analysis. **(A)** The left and right rectus 2dReHo were significantly positive correlated with the illness duration (FDR corrected, $p < 0.05$); **(B)** the right OIFG 2dReHo exhibited significant positive correlation with the PANSS negative scores. OIFG, orbital inferior frontal gyrus.

an increased spontaneous brain activity in the striatum, MTC, and MPFC, and a decreased activity in the sensorimotor and visual cortex. The results indicated that our 2dReHo results may provide more accurate and persuasive evidences to expound the abnormal synchronization of spontaneous neural activity of SZ. Moreover, at the vertex level, the patients with SZ exhibited decreased 2dReHo in the SMN, the precentral gyrus, and the postcentral gyrus, which was consistent with previous studies (Liu et al., 2006). This finding was understandable as patients with SZ commonly illustrate a variety of symptoms, including psychomotor and fine motor, and also abnormalities in touch, temperature, pain, tension, and vibration (Chen et al., 2015). In addition, the posterior central gyrus may be associated with the processing of multimotion-related cognitive functions, which was abnormal in SZ (Elvevag and Goldberg, 2000). In general, patients with SZ exhibited reduced global 2dReHo across the cortical surface, which revealed that SZ showed deactivation in synchronization of spontaneous neural oscillation across the global cortices.

Patients with SZ exhibited reduced 2dReHo in the occipital lobe, which may serve as the underlying functional basis of visual preliminary processing defects, such as perceptual closure, object recognition, and face processing (Pastrnak et al., 2017). The same reduction exists in drug-naive patients with bipolar disorder (Fang et al., 2021). Notably, OC is the main region of extrastriate body area (EBA), and the functional abnormalities of OC may lead to error, which selectively responds to the viewing of body parts and mental imagery of embodied self-location. Previous analysis showed that the brain injury of EBA was mainly related to the autoscopic phenomena (Heydrich and Blanke, 2013). Therefore, the relative reduction of 2dReHo in the OC may impair the perception of body ownership in patients with SZ.

Interestingly, a significant increase of 2dReHo was found in widespread brain regions, including the bilateral frontal and parietal, temporal cortex, and precuneus. Actually, increased ReHo in the medial frontal cortex (MFC) in SZ seems to contradict some previous fMRI findings (Hill et al., 2004; Whalley et al., 2008; Pomarol-Clotet et al., 2010); however, consistent with a metaanalysis of depressive patients, increased ReHo in the superior and inferior frontal gyrus were associated with depressive symptoms (Iwabuchi et al., 2015; Fang et al., 2021). This might be explained by the hypotheses that 2dReHo can obtain more neglected information about local activation of the brain compared with ReHo (Li et al., 2014; Jiang and Zuo, 2016). In addition, the reliability of hemodynamic-induced prefrontal dysfunction in SZ seems controversial. A recent study also showed differences in ReHo among different types of SZ (Gao et al., 2018). Furthermore, several current studies have reported increased activation in the prefrontal cortex in SZ responding to performing working memory tasks (Tan et al., 2006, 2007). In fact, the MFC in patients with SZ shows task-related inactivation failure (Whitfield-Gabrieli et al., 2009). Our finding of increased 2dReHo in MFC may explain the hyperfrontality responding to abnormality of task-performance in the patients of SZ. Moreover, a previous study of electroconvulsive therapy (ECT) in depressive patients also showed a decrease in ReHo values in bilateral SFG after ECT.

Our study demonstrated widespread abnormalities in the consistent activation of local brain regions in patients with SZ, including two higher-order intrinsic brain networks (DMN, FPN), and some low-level networks (SMN, VN). The DMN and FPN are two higher-order intrinsic brain networks with functional heterogeneities, which appear to be crucial for both daily general functioning and physiopathology (Khadka et al., 2013). DMN, the most prominent network at rest, can be considered as the baseline of brain processing (Calhoun et al., 2009; Whitfield-Gabrieli and Ford, 2012). The DMN often shows deactivation during tasks requiring external attention, while it increases activity during unconstrained thought (Mason et al., 2007), introspection (Svoboda et al., 2006), and self-related processing (Lin et al., 2011). Failure of this function may result in individuals mistakenly attributing internally generated thoughts as exogenous (Frith, 1995). For FPN, it is often evoked by various cognitive tasks (Dosenbach et al., 2007; Cole et al., 2013), and multiple executive functions subserved by the FPN including working memory and sustained attention (Das et al., 2020). The dysfunction of FPN may be one of the abnormal neural mechanisms of SZ (Dong et al., 2018, 2019). In addition,

this work found that the 2dReHo of right OIFG in FPN was also significantly positively correlated with the PANSS negative scores, and bilateral rectus was associated with illness duration, which provided evidence that the local brain activity might predict the severity of SZ. Furthermore, a previous work showed the disconnection between DMN and FPN in SZ. Specifically, the connectivity between the FPN and the DMN decreased with greater working memory load in healthy participants, but increased in patients with SZ (Godwin et al., 2017). This was consistent with our results that both FPN and DMN were hyperactivated in SZ. Moreover, the decrease of 2dReHo in the low-level primary perceptual networks including SMN, AN, and VN indicates that the consistency of spontaneous activation is reduced, which were well-documented for the deficits of perceptual processing and multisensory integration in SZ.

It would be noted that the resting state fMRI features such as ReHo, which reflect the regional neural spontaneous oscillation in temporal and/or spatial domain, the most widely used to investigate the potential pathophysiological mechanisms of various psychiatric disorders (Zang et al., 2004). However, many of the studies in these illnesses reported similar alteration of neural spontaneous oscillation in DMN and FPN (Zuo et al., 2013; Jiang and Zuo, 2016), which would reflect that the domain-general function was interrupted due to common and/or similar symptoms across psychiatric disorders. Thus, domain-specific network or its relationship with domain-general function might be important to the specific psychiatric disorder. In general, the disrupted interaction between primary perception system and high-order cognitive function was found in SZ rather than depression or bipolar disorder (Dong et al., 2018). Consistent with the hypotheses of uncoupling between high- and low-order brain functional networks in SZ, the opposite alteration between high-order networks (increased in DMN and FPN) and low-order networks (decreased in VN, AN, and SMN) was observed in this work, which might provide a specific insight to understand the potential pathophysiological mechanisms of SZ.

There are several limitations in this study. First, all patients were medicated and the negative symptoms were dominant, which may lead to a certain bias in our results. Second, our present 2dReHo approach can only analyze functional abnormalities in the cortex rather subcortical regions, but the subcortical regions have been proven to be key regions in the emotional regulation circuit. Third, the instructions associated with the resting state approach may have potential impact, leading to confounding results. Fourth, the physiological origin and functional significance of ReHo remain unclear, which limits the exploration of the physiological basis of 2dReHo.

CONCLUSION

Using the 2dReHo method, SZ patients showed enhanced surface-based spontaneous neural oscillation in two higher-order functional networks including DMN and FPN, as well as reduced 2dReHo in the low-order perceptual networks: SMN, AN, and VN. Dysfunction of these functional networks was closely related to the symptoms of SZ. Therefore, these findings indicated that the 2dReHo might provide the effective approach to explore the pathophysiology mechanism of SZ.

DATA AVAILABILITY STATEMENT

The raw data supporting the conclusions of this article will be made available by the authors, without undue reservation.

ETHICS STATEMENT

The studies involving human participants were reviewed and approved by the Ethics Committee of the Clinical Hospital of Chengdu Brain Science Institute. The patients/participants provided their written informed consent to participate in this study. Written informed consent was obtained from the individual(s) for the publication of any potentially identifiable images or data included in this article.

AUTHOR CONTRIBUTIONS

YT, DY, and CLu designed the study and supervised the project. CLi, XC, and MD managed the experiments and data collection. YJ, HHe, BZ, HHu, and XC undertook the data analysis. XC, HHu, YT, YJ, and CLu wrote and revised the manuscript. All the authors reviewed the manuscript and approved the final manuscript.

FUNDING

This work was partly supported by the grants from the National Natural Science Foundation of China (Grant Nos. U2033217, 61933003, 81960249, 62003076, U1833130, and 62003058), the CAMS Innovation Fund for Medical Sciences (CIFMS) (No. 2019-I2M-5-039), and the Project funded by China Postdoctoral Science Foundation (No. 2021TQ0061).

REFERENCES

Allen, P., Modinos, G., Hubl, D., Shields, G., Cachia, A., Jardri, R., et al. (2012). Neuroimaging auditory hallucinations in schizophrenia: from neuroanatomy to neurochemistry and beyond. *Schizophr. Bull.* 38, 695–703. doi: 10.1093/schbul/sbs066

Biswal, B., Yetkin, F. Z., Haughton, V. M., and Hyde, J. S. (1995). Functional connectivity in the motor cortex of resting human brain using echo-planar mri. *Magn. Reson. Med.* 34, 537–541. doi: 10.1002/mrm.1910340409

Bluhm, R. L., Jodi, M., Lanius, R. A., Osuch, E. A., Kristine, B., Rwj, N., et al. (2007). Spontaneous low-frequency fluctuations in the BOLD signal in schizophrenic patients: anomalies in the default network. *Schizophr. Bull.* 33, 1004–1012.

Bo, Z., Fei, W., Dong, H. M., Jiang, X. W., Wei, S. N., Miao, C., et al. (2019). Surface-based regional homogeneity in bipolar disorder: a resting-state fMRI study. *Psychiatry Res.* 278, 199–204. doi: 10.1016/j.psychres.2019.05.045

Brodoehl, S., Gaser, C., Dahnke, R., Witte, O. W., and Klingner, C. M. (2020). Surface-based analysis increases the specificity of cortical activation patterns and connectivity results. *Sci. Rep.* 10:5737.

Calhoun, V. D., Eichele, T., and Pearlson, G. (2009). Functional brain networks in schizophrenia: a review. *Front. Hum. Neurosci.* 3:17. doi: 10.3389/neuro.09.017.2009

Canuet, L., Ishii, R., Pascual-Marqui, R. D., Iwase, M., Kurimoto, R., Aoki, Y., et al. (2011). Resting-State EEG source localization and functional connectivity in schizophrenia-like psychosis of epilepsy. *PLoS One* 6:e27863. doi: 10.1371/journal.pone.0027863

Chen, K., Azeez, A., Chen, D. Y., and Biswal, B. B. (2020). Resting-state functional connectivity: signal origins and analytic methods. *Neuroimage Clin. N Am.* 30:15. doi: 10.1016/j.nic.2019.09.012

Chen, X., Duan, M. J., Xie, Q. K., Lai, Y. X., Dong, L., Cao, W. F., et al. (2015). Functional disconnection between the visual cortex and the sensorimotor cortex suggests a potential mechanism for self-disorder in schizophrenia. *Schizophr. Res.* 166, 151–157. doi: 10.1016/j.schres.2015.06.014

Chen, X., Liu, C., He, H., Chang, X., Jiang, Y., Li, Y., et al. (2017). Transdiagnostic differences in the resting-state functional connectivity of the prefrontal cortex in depression and schizophrenia. *J. Affect. Disord.* 217, 118–124. doi: 10.1016/j.jad.2017.04.001

Cole, M. W., Reynolds, J. R., Power, J. D., Repovs, G., Anticevic, A., and Braver, T. S. (2013). Multi-task connectivity reveals flexible hubs for adaptive task control. *Nat. Neurosci.* 16, 1348–U247. doi: 10.1038/nn.3470

Cui, L. B., Liu, K., Li, C., Wang, L. X., Guo, F., Tian, P., et al. (2016). Putamen-related regional and network functional deficits in first-episode schizophrenia with auditory verbal hallucinations. *Schizophr. Res.* 173, 13–22. doi: 10.1016/j.schres.2016.02.039

Dale, A. M., Fischl, B., and Sereno, M. I. (1999). Cortical surface-based analysis - I. Segmentation and surface reconstruction. *Neuroimage* 9, 179–194.

Das, T. K., Kumar, J., Francis, S., Liddle, P. F., and Palaniyappan, L. (2020). Parietal lobe and disorganisation syndrome in schizophrenia and psychotic bipolar disorder: a bimodal connectivity study. *Psychiatry Res. Neuroimaging* 303:111139. doi: 10.1016/j.pscychresns.2020.111139

Dong, D., Duan, M., Wang, Y., Zhang, X., Jia, X., Li, Y., et al. (2019). Reconfiguration of dynamic functional connectivity in sensory and perceptual system in schizophrenia. *Cereb. Cortex* 29, 3577–3589.

Dong, D., Wang, Y., Chang, X., Jiang, Y., Klugah-Brown, B., Luo, C., et al. (2017). Shared abnormality of white matter integrity in schizophrenia and bipolar disorder: a comparative voxel-based meta-analysis. *Schizophr. Res.* 185, 41–50. doi: 10.1016/j.schres.2017.01.005

Dong, D., Wang, Y., Chang, X., Luo, C., and Yao, D. (2018). Dysfunction of large-scale brain networks in schizophrenia: a meta-analysis of resting-state functional connectivity. *Schizophr. Bull.* 44, 168–181. doi: 10.1093/schbul/sbx034

Dosenbach, N. U. F., Fair, D. A., Miezin, F. M., Cohen, A. L., Wenger, K. K., Dosenbach, R. A. T., et al. (2007). Distinct brain networks for adaptive and stable task control in humans. *Proc. Natl. Acad. Sci. U.S.A.* 104:11073. doi: 10.1073/pnas.0704320104

Elvevag, B., and Goldberg, T. E. (2000). Cognitive impairment in schizophrenia is the core of the disorder. *Crit. Rev. Neurobiol.* 14, 1–21.

Fang, X. Y., Zhang, R. R., Bao, C. X., Zhou, M., Yan, W., Lu, S. P., et al. (2021). Abnormal regional homogeneity (ReHo) and fractional amplitude of low frequency fluctuations (fALFF) in first-episode drug-naive schizophrenia patients comorbid with depression. *Brain Imaging Behav.* 15, 2627–2636. doi: 10.1007/s11682-021-00465-0

Fischl, B. (2012). FreeSurfer. *Neuroimage* 62, 774–781. doi: 10.1016/j.neuroimage.2012.01.021

Friston, K. J., Williams, S., Howard, R., Frackowiak, R. S. J., and Turner, R. (1996). Movement-related effects in fMRI time-series. *Magn. Reson. Med.* 35, 346–355. doi: 10.1002/mrm.1910350312

Frith, C. (1995). Functional imaging and cognitive abnormalities. *Lancet* 346, 615–620. doi: 10.1016/s0140-6736(95)91441-2

Gao, S. Z., Lu, S. P., Shi, X. M., Ming, Y. D., Xiao, C. Y., Sun, J., et al. (2018). Distinguishing between treatment-resistant and non-treatment-resistant schizophrenia using regional homogeneity. *Front.Psychiatry* 9:282. doi: 10.3389/fpsyt.2018.00282

Gao, S. Z., Ming, Y. D., Wang, J. Y., Gu, Y., Ni, S. L., Lu, S. P., et al. (2020). Enhanced prefrontal regional homogeneity and its correlations with cognitive dysfunction/psychopathology in patients with first-diagnosed and drug-naive schizophrenia. *Front. Psychiatry* 11:580570. doi: 10.3389/fpsyt.2020.580570

Godwin, D., Ji, A., Kandala, S., and Mamah, D. (2017). Functional connectivity of cognitive brain networks in schizophrenia during a working memory task. *Front. Psychiatry* 8:294. doi: 10.3389/fpsyt.2017.00294

Greve, D. N., and Fischl, B. (2009). Accurate and robust brain image alignment using boundary-based registration. *Neuroimage* 48, 63–72. doi: 10.1016/j.neuroimage.2009.06.060

Heydrich, L., and Blanke, O. (2013). Distinct illusory own-body perceptions caused by damage to posterior insula and extrastriate cortex. *Brain* 136, 790–803. doi: 10.1093/brain/aws364

Hill, K., Mann, L., Laws, K. R., Stephenson, C. M. E., Nimmo-Smith, I., and McKenna, P. J. (2004). Hypofrontality in schizophrenia: a meta-analysis of functional imaging studies. *Acta Psychiatr. Scand.* 110, 243–256. doi: 10.1111/j.1600-0447.2004.00376.x

Ho, N. F., Iglesias, J. E., Sum, M. Y., Kuswanto, C. N., Sitoh, Y. Y., De Souza, J., et al. (2016). Progression from selective to general involvement of hippocampal subfields in schizophrenia. *Mol. Psychiatry* 22, 142–152. doi: 10.1038/mp.2016.4

Huang, H., Botao, Z., Jiang, Y., Tang, Y., Zhang, T., Tang, X., et al. (2020). Aberrant resting-state functional connectivity of salience network in first-episode schizophrenia. *Brain Imaging Behav.* 14, 1350–1360. doi: 10.1007/s11682-019-00040-8

Hugdahl, K. (2009). "Hearing voices": auditory hallucinations as failure of top-down control of bottom-up perceptual processes. *Scand. J. Psychol.* 50, 553–560. doi: 10.1111/j.1467-9450.2009.00775.x

Iwabuchi, S. J., Krishnadas, R., Li, C., Auer, D. P., Radua, J., and Palaniyappan, L. (2015). Localized connectivity in depression: a meta-analysis of resting state functional imaging studies. *Neurosci. Biobehav. Rev.* 51, 77–86. doi: 10.1016/j.neubiorev.2015.01.006

Javitt, D. C., and Freedman, R. (2015). Sensory processing dysfunction in the personal experience and neuronal machinery of schizophrenia. *Am. J. Psychiatry* 172, 17–31. doi: 10.1176/appi.ajp.2014.13121691

Jiang, L., and Zuo, X. N. (2016). regional homogeneity: a multimodal, multiscale neuroimaging marker of the human connectome. *Neuroscientist* 22, 486–505. doi: 10.1177/1073858415595004

Jiang, Y., Luo, C., Li, X., Duan, M., He, H., Chen, X., et al. (2018). Progressive reduction in gray matter in patients with schizophrenia assessed with mr imaging by using causal network analysis. *Radiology* 287, 633–642. doi: 10.1148/radiol.2017171832

Jiang, Y., Xu, L., Li, X., Tang, Y., Wang, P., Li, C., et al. (2019). Common increased hippocampal volume but specific changes in functional connectivity in schizophrenia patients in remission and non-remission following electroconvulsive therapy: a preliminary study. *Neuroimage Clin.* 24:102081. doi: 10.1016/j.nicl.2019.102081

Jiang, Y., Yao, D., Zhou, J., Tan, Y., Huang, H., Wang, M., et al. (2020). Characteristics of disrupted topological organization in white matter functional connectome in schizophrenia. *Psychol. Med.* doi: 10.1017/S0033291720003141 [Epub ahead of print].

Kay, S. R., Fiszbein, A., and Opler, L. A. (1987). The positive and negative syndrome scale (PANSS) for schizophrenia. *Schizophr. Bull.* 13, 261–276. doi: 10.1093/schbul/13.2.261

Khadka, S., Meda, S. A., Stevens, M. C., Glahn, D. C., Calhoun, V. D., Sweeney, J. A., et al. (2013). Is aberrant functional connectivity a psychosis endophenotype? A resting state functional magnetic resonance imaging study. *Biol. Psychiatry* 74, 458–466. doi: 10.1016/j.biopsych.2013.04.024

Kuhn, S., and Gallinat, J. (2013). Resting-State brain activity in schizophrenia and major depression: a quantitative meta-analysis. *Schizophr. Bull.* 39, 358–365. doi: 10.1093/schbul/sbr151

Li, H. J., Cao, X. H., Zhu, X. T., Zhang, A. X., Hou, X. H., Xu, Y., et al. (2014). Surface-based regional homogeneity in first-episode, drug-nave major depression: a resting-state fMRI study. *Biomed. Res. Int.* 2014, 1–8. doi: 10.1155/2014/374828

Light, G. A., Hsu, J. L., Hsieh, M. H., Meyer-Gomes, K., Sprock, J., Swerdlow, N., et al. (2006). Gamma band EEG oscillations reveal neural network cortical coherence dysfunction in schizophrenia patients. *Biol. Psychiatry* 60, 1231–1240. doi: 10.1016/j.biopsych.2006.03.055

Lin, P., Hasson, U., Jovicich, J., and Robinson, S. (2011). A neuronal basis for task-negative responses in the human brain. *Cereb. Cortex* 21, 821–830. doi: 10.1093/cercor/bhq151

Liu, H. H., Liu, Z. N., Liang, M., Hao, Y. H., Tan, L. H., Kuang, F., et al. (2006). Decreased regional homogeneity in schizophrenia: a resting state functional magnetic resonance imaging study. *Neuroreport* 17, 19–22.

Liu, P. H., Li, Q., Zhang, A. X., Liu, Z. F., Sun, N., Yang, C. X., et al. (2020). Similar and different regional homogeneity changes between bipolar disorder and unipolar depression: a resting-state fMRI study. *Neuropsychiatr. Dis. Treat.* 16, 1087–1093. doi: 10.2147/NDT.S249489

Logothetis, N. K., and Wandell, B. A. (2004). Interpreting the BOLD signal. *Annu. Rev. Physiol.* 66, 735–769. doi: 10.1146/annurev.physiol.66.082602.092845

Luo, Y., He, H., Duan, M., Huang, H., and Luo, C. (2020). Dynamic functional connectivity strength within different frequency-band in schizophrenia. *Front. Psychiatry* 10:995. doi: 10.3389/fpsyt.2019.00995

Mason, M. F., Norton, M. I., Van Horn, J. D., Wegner, D. M., Grafton, S. T., and Macrae, C. N. (2007). Wandering minds: the default network and stimulus-independent thought. *Science* 315, 393–395. doi: 10.1126/science.1131295

Pastrnak, M., Dorazilova, A., and Rodriguez, M. (2017). Visual perception and its impairments in schizophrenia - summary article. *Cesk Psychol.* 61, 593–604.

Pomarol-Clotet, E., Canales-Rodriguez, E. J., Salvador, R., Sarro, S., Gomar, J. J., Vila, F., et al. (2010). Medial prefrontal cortex pathology in schizophrenia as revealed by convergent findings from multimodal imaging. *Mol. Psychiatr.* 15, 823–830. doi: 10.1038/mp.2009.146

Schultz, S. K., and Andreasen, N. C. (1999). Schizophrenia. *Lancet* 353, 1425–1430.

Svoboda, E., McKinnon, M. C., and Levine, B. (2006). The functional neuroanatomy of autobiographical memory: a meta-analysis. . *Neuropsychologia* 44, 2189–2208.

Tan, H. Y., Callicott, J. H., and Weinberger, D. R. (2007). Dysfunctional and compensatory prefrontal cortical systems, genes and the pathogenesis of schizophrenia. *Cereb. Cortex* 17, I171–I181. doi: 10.1093/cercor/bhm069

Tan, H. Y., Sust, S., Buckholtz, J. W., Mattay, V. S., Meyer-Lindenberg, A., Egan, M. F., et al. (2006). Dysfunctional prefrontal regional specialization and compensation in schizophrenia. *Am. J. Psychiatry* 163, 1969–1977. doi: 10.1176/ajp.2006.163.11.1969

Tomasik, J., Rahmoune, H., Guest, P. C., and Bahn, S. (2016). Neuroimmune biomarkers in schizophrenia. *Schizophr. Res.* 176, 3–13. doi: 10.1016/j.schres.2014.07.025

Wang, J., Jiang, Y., Tang, Y., Xia, M., Curtin, A., Li, J., et al. (2020). Altered functional connectivity of the thalamus induced by modified electroconvulsive therapy for schizophrenia. *Schizophr. Res.* 218, 209–218. doi: 10.1016/j.schres.2019.12.044

Whalley, H. C., Mowatt, L., Stanfield, A. C., Hall, J., Johnstone, E. C., Lawrie, S. M., et al. (2008). Hypofrontality in subjects at high genetic risk of schizophrenia with depressive symptoms. *J. Affect. Disord.* 109, 99–106. doi: 10.1016/j.jad.2007.11.009

Whitfield-Gabrieli, S., and Ford, J. M. (2012). Default mode network activity and connectivity in psychopathology. *Annu. Rev. Clin. Psychol.* 8:49. doi: 10.1146/annurev-clinpsy-032511-143049

Whitfield-Gabrieli, S., Thermenos, H. W., Milanovic, S., Tsuang, M. T., Faraone, S. V., McCarley, R. W., et al. (2009). Hyperactivity and hyperconnectivity of the default network in schizophrenia and in first-degree relatives persons with schizophrenia (vol 106, pg 1279, 2009). *Proc. Natl. Acad. Sci. U.S.A.* 106, 4572–4572. doi: 10.1073/pnas.0809141106

Xing, X. X., Zhou, Y. L., Adelstein, J. S., and Zuo, X. N. (2011). PDE-based spatial smoothing: a practical demonstration of impacts on MRI brain extraction, tissue segmentation and registration. *Magn. Reson. Imaging* 29, 731–738. doi: 10.1016/j.mri.2011.02.007

Xu, Y. J., Zhuo, C. J., Qin, W., Zhu, J. J., and Yu, C. S. (2015). Altered spontaneous brain activity in schizophrenia: a meta-analysis and a large-sample study. *Biomed. Re.s Int.* 2015:204628. doi: 10.1155/2015/204628

Yan, C. G., Wang, X. D., Zuo, X. N., and Zang, Y. F. (2016). DPABI: data processing & analysis for (resting-state) brain imaging. *Neuroinformatics* 14, 339–351.

Yang, G. J., Murray, J. D., Repovs, G., Cole, M. W., Savic, A., Glasser, M. F., et al. (2014). Altered global brain signal in schizophrenia. *Proc. Natl. Acad. Sci. U.S.A.* 111, 7438–7443.

Zalesky, A., Fornito, A., Egan, G. F., Pantelis, C., and Bullmore, E. T. (2012). The relationship between regional and inter-regional functional connectivity deficits in schizophrenia. *Hum. Brain Mapp.* 33, 2535–2549. doi: 10.1002/hbm.21379

Zang, Y. F., Jiang, T. Z., Lu, Y. L., He, Y., and Tian, L. X. (2004). Regional homogeneity approach to fMRI data analysis. *Neuroimage* 22, 394–400. doi: 10.1016/j.neuroimage.2003.12.030

Zhang, N., Niu, Y., Sun, J., An, W. C., Li, D. D., Wei, J., et al. (2021). Altered complexity of spontaneous brain activity in schizophrenia and bipolar disorder patients. *J. Magn. Reson. Imaging* 54, 586–595.

Zhao, C., Zhu, J. J., Liu, X. Y., Pu, C. C., Lai, Y. Y., Chen, L., et al. (2018). Structural and functional brain abnormalities in schizophrenia: a cross-sectional study at different stages of the disease. *Prog. Neuropsychopharmacol. Biol. Psychiatry* 83, 27–32. doi: 10.1016/j.pnpbp.2017.12.017

Zuo, X. N., Xu, T., Jiang, L., Yang, Z., Cao, X. Y., He, Y., et al. (2013). Toward reliable characterization of functional homogeneity in the human brain: preprocessing, scan duration, imaging resolution and computational space. *Neuroimage* 65, 374–386. doi: 10.1016/j.neuroimage.2012.10.017

Conflict of Interest: The authors declare that the research was conducted in the absence of any commercial or financial relationships that could be construed as a potential conflict of interest.

Publisher's Note: All claims expressed in this article are solely those of the authors and do not necessarily represent those of their affiliated organizations, or those of the publisher, the editors and the reviewers. Any product that may be evaluated in this article, or claim that may be made by its manufacturer, is not guaranteed or endorsed by the publisher.

frontiers in Human Neuroscience

HYPOTHESIS AND THEORY
published: 03 March 2022
doi: 10.3389/fnhum.2022.818711

Imprecise Predictive Coding Is at the Core of Classical Schizophrenia

Peter F. Liddle and Elizabeth B. Liddle*

Centre for Translational Neuroimaging for Mental Health, School of Medicine, Institute of Mental Health, University of Nottingham, Nottingham, United Kingdom

Current diagnostic criteria for schizophrenia place emphasis on delusions and hallucinations, whereas the classical descriptions of schizophrenia by Kraepelin and Bleuler emphasized disorganization and impoverishment of mental activity. Despite the availability of antipsychotic medication for treating delusions and hallucinations, many patients continue to experience persisting disability. Improving treatment requires a better understanding of the processes leading to persisting disability. We recently introduced the term classical schizophrenia to describe cases with disorganized and impoverished mental activity, cognitive impairment and predisposition to persisting disability. Recent evidence reveals that a polygenic score indicating risk for schizophrenia predicts severity of the features of classical schizophrenia: disorganization, and to a lesser extent, impoverishment of mental activity and cognitive impairment. Current understanding of brain function attributes a cardinal role to predictive coding: the process of generating models of the world that are successively updated in light of confirmation or contradiction by subsequent sensory information. It has been proposed that abnormalities of these predictive processes account for delusions and hallucinations. Here we examine the evidence provided by electrophysiology and fMRI indicating that imprecise predictive coding is the core pathological process in classical schizophrenia, accounting for disorganization, psychomotor poverty and cognitive impairment. Functional imaging reveals aberrant brain activity at network hubs engaged during encoding of predictions. We discuss the possibility that frequent prediction errors might promote excess release of the neurotransmitter, dopamine, thereby accounting for the occurrence of episodes of florid psychotic symptoms including delusions and hallucinations in classical schizophrenia. While the predictive coding hypotheses partially accounts for the time-course of classical schizophrenia, the overall body of evidence indicates that environmental factors also contribute. We discuss the evidence that chronic inflammation is a mechanism that might link diverse genetic and environmental etiological factors, and contribute to the proposed imprecision of predictive coding.

Keywords: classical schizophrenia, disorganization, psychomotor poverty, negative symptoms, predictive coding, prediction error, polygenic risk score, inflammation

OPEN ACCESS

Edited by:
Chun Meng,
University of Electronic Science and Technology of China, China

Reviewed by:
Zhiqiang Sha,
Max Planck Institute for Psycholinguistics, Netherlands
Mary V. Seeman,
University of Toronto, Canada
Martin Dietz,
Aarhus University, Denmark

****Correspondence:***
Peter F. Liddle
peter.liddle@nottingham.ac.uk

Specialty section:
This article was submitted to Brain Imaging and Stimulation, a section of the journal Frontiers in Human Neuroscience

Received: *19 November 2021*
Accepted: *14 February 2022*
Published: *03 March 2022*

Citation:
Liddle PF and Liddle EB (2022) Imprecise Predictive Coding Is at the Core of Classical Schizophrenia. Front. Hum. Neurosci. 16:818711. doi: 10.3389/fnhum.2022.818711

INTRODUCTION

Schizophrenia remains an enigma. We know a large amount about causal factors. We also know a large amount about diverse pathological mechanisms, in both psychological and neuronal terms. We have had effective antipsychotic medications for more than 60 years. Despite all this, a substantial proportion of patients with schizophrenia still experience long term disability and shortened life expectancy.

A major issue is the heterogeneity of schizophrenia. Modern diagnostic criteria identify a spectrum of non-affective psychoses all characterized by a distorted perception of reality (American Psychiatric Association, 2013; World Health Organisation, 2018). Schizophrenia itself lies at the severe end, while at the mild end lies schizotypal personality disorder, in which the distortion of reality might not achieve psychotic intensity.

However, the heterogeneity is not simply degree of psychotic intensity. The presentation that we call schizophrenia is typically characterized by other features, some of which are associated with long term disability. This raises the question: is there a cluster of related psychological and/or neuronal processes that are associated with a tendency toward persisting disability, and which lie at the core of what we might call classical schizophrenia? Identifying such a core might open the door to therapies that lead to better long-term outcomes.

Liddle (2019) introduced the term classical schizophrenia to denote a disorder exhibiting not only the central features in the classical descriptions by Bleuler (1911) and Kraepelin (1919), but also characterized by pathophysiological processes that predispose to persisting disability. Liddle proposed disorganized mental activity, impoverished mental activity, and cognitive impairments as the three characteristic features of classical schizophrenia. The features of classical schizophrenia are summarized in **Table 1**.

Rathnaiah et al. (2020) demonstrated that the severity of classical schizophrenia can be estimated using symptom scores assessed using the Positive and Negative Symptom Scale (PANSS) (Kay et al., 1987); the Comprehensive Assessment of Symptoms and History (CASH) (Andreasen et al., 1992); or Symptoms and Signs of Psychotic Illness (SSPI) (Liddle et al., 2002).

TABLE 1 | Clinical Features of classical schizophrenia (based on Liddle, 2019).

Core features	Persistent disorganization	Disorganized thought Disorganized affect Disorganized behavior
	Persistent impoverished mental activity	Poverty of speech Flat affect Diminished spontaneous movement
	Cognitive impairment	Slow speed of processing Impaired executive function Impaired working memory
Secondary features	Persistent impairment of role function	Impaired occupational function Impaired social function
	Reality distortion (typically episodic)	Delusions Hallucinations

Several lines of evidence support Liddle's proposal. In a large non-clinical sample of young people, Dominguez et al. (2010) found that disorganization and negative symptoms predicted both subsequent overt psychosis and severity of functional impairment. Consistent with this, Ziermans et al. (2014) found greater disorganization in cases at high risk of schizophrenia, and that disorganization predicted poorer long term functional outcome. Perhaps most tellingly, Legge et al. (2021) found that genetic risk for schizophrenia was significantly correlated with disorganization (manifest as formal thought disorder and/or inappropriate affect), expressive negative symptoms (affective flattening and alogia), and impaired cognition, but not significantly with reality distortion. The finding of an association between polygenic risk score and disorganization is consistent with previous studies that have identified disorganization symptoms as the symptom cluster in schizophrenia with greatest heritability. However, the association between polygenic risk score for schizophrenia with not only disorganization but also with expressive negative symptoms and cognitive impairment suggests a heritable component for Liddle's proposal for a cluster of traits constituting the core of a classical presentation of schizophrenia that is associated with long term disability.

To test the validity of this concept of a core of correlated features (disorganization, negative symptoms, cognitive impairments) associated with impaired role function, Rathnaiah et al. (2020) recruited a sample of patients in stable phase of illness, and used confirmatory factor analysis to verify a latent variable reflecting shared variance between these features. The verification of such a variable supports the proposition that these clinical features should be regarded as core features of classical schizophrenia. However it should be noted that the shared genetic origins do not necessarily account fully for the mutual relationships between these clinical features. As we shall discuss subsequently (in the section entitled Gene-Environment Interactions), it is likely that both genes and environment contribute to the clinical profile in an individual case.

In this paper we propose a plausible pathological mechanism at the core of classical schizophrenia in terms of an abnormality of predictive coding. Predictive coding refers to a range of mechanisms by which the brain generates internal models of the world that are successively updated in light of confirmation or contradiction by subsequent sensory information. **Table 2** summarizes the predictive coding terminology employed in this manuscript.

Multiple lines of evidence indicate that predictive coding plays a cardinal role at multiple stages in the processing of information by the human brain, accounting for its efficiency. Instead of having to generate a fresh model with each volley of sensory of input, it needs only to match its predicted state against the state arising from relevant sensory input, and adjust for discrepancies. A discrepancy between the predictions and the sensory input represents a prediction error. If the prediction error exceeds the level expected from

TABLE 2 | Terminology relevant to predictive coding.

Predictive coding	The mechanisms by which the brain makes predictions about the world, and successively updates them in light of further sensory information.
Forward model	The predictive model of the sensory consequences of an action. As the action is executed, the predicted sensory consequences are compared with actual sensory input. In the case of a mismatch, the motor command is updated, and a revised prediction generated.
Prediction error	The mismatch between predicted and actual brain-state. For instance, when the sensory consequences of an action are accurately predicted, the sensory input is down-weighted. Unpredicted sensory consequences constitute a "prediction error" and are likely to be more salient.
Salience of prediction errors	A prediction error means that the actual sensory input was unpredicted and therefore salient, in the sense of being more noticeable or "surprising." The sensory input is also behaviorally salient as it indicates the need to adjust the internally generated prediction. A "salience network," including insula and anterior cingulate cortex, plays a role in detecting and responding to salient information in general.
Teaching signal	The neural signal that indicates a prediction error and the need to adjust strategy and generate an updated prediction. The teaching signal is associated with release of dopamine from midbrain dopaminergic neurons, particularly when the error is in the value of a reward. It is likely that the teaching signal also produces enduring changes in expectations that guide prediction in similar circumstances in future.

statistical noise, the predictive model of the world is updated. In Bayesian terms, the predictive prior is updated in light of the probability of the actual sensory input, given the prior likelihood, to provide an improved predictive model (posterior). In an influential account, Friston (2009) describes this process of minimizing surprise as the minimization of Free Energy (i.e., minimizing the amount correction likely to be required).

In the domain of perception, the predictive coding hypothesis provides an efficient mechanism by which an internally generated "feedforward" model requires only minor correction from "feedback" sensory confirmation (Rao and Ballard, 1999). What we perceive reflects our internally generated prediction after adjustment to minimize discrepancy with the sensory input, and explains why the world appears to stay still when we move our eyes, even though the image on the retina changes position.

More generally in the domain of motor control, we develop a forward model of the state of our brain and body as we execute an intended action (Wolpert and Ghahramani, 2000). Throughout execution, we compare our forward model with the incoming proprioceptive and external signals. We continuously adjust our action to minimize the discrepancy between prediction and sensory input. Thus, in this framework, the control of action is achieved via minimization of the discrepancy between endogenous prediction and sensory input. As the sensory consequences of our own actions are better predicted than the sensory consequences of an externally generated perturbation, this mechanism allows us to distinguish "self-caused" from "other-caused" sensory signals, and to discount the salience of the former—a mechanism postulated to explain "why you can't tickle yourself" (Blakemore et al., 2000).

Predictive coding deficits have been invoked to account for delusions and hallucinations in psychotic disorders (Corlett et al., 2009). In the case of a motor act, if the proprioceptive and tactile feedback does not match the prediction generated by the motor command, the action might be perceived as alien. In more general terms, Adams et al. (2013) discuss the way in which imbalances between the precision of internally generated predictions and the weight allocated to precision of sensory evidence might account for both what they regard as "trait" phenomena of schizophrenia (which might include both disorganization and impoverishment of mental activity) and "state" phenomena (acute psychotic symptoms such as hallucinations). In particular they propose that trait abnormalities might arise from a decrease in the precision of internally generated predictions (or failure to down-weight sensory evidence), while acute psychotic symptoms might arise from a compensatory increase in the precision of internally generated predictions (or decrease in weight allocated to sensory information). They suggest that abnormality of glutamatergic or GABAergic transmission might play a cardinal role in trait abnormalities, while over activity of dopaminergic transmission might play a cardinal role in the acute psychotic state.

Brown and Kuperberg (2015) have reviewed the evidence that predictive coding deficits play a role in formal thought disorder, a key feature of disorganization. Sterzer et al. (2019) argue that schizophrenia involves a pervasive alteration in predictive coding at multiple hierarchical levels, including sensory and motor systems and also cognitive and value-based decision-making processes. They propose that impairments in various brain areas implicated in predictive coding account for the variety of psychotic experiences.

In this paper we examine the evidence that imprecision of internally generated predictions lies at the core of classical schizophrenia. Imprecise predictive models result in failure to down-weight what would otherwise be expected sensory stimuli, increasing their salience and the rate of error signals. Our hypothesis is similar to the proposal of Adams et al. (2013) that trait abnormalities might arise from a decrease in the precision of internally generated predictions (or failure to down-weight sensory evidence), but we propose that this "trait" reflects the "core" process in the pathway to classical schizophrenia: persistently imprecise predictions generate percepts that are both salient and tangential, reflected in disorganization symptoms, while a steady stream of minor error signals elevate net background dopamine levels and increase the risk of acute psychosis. Conversely, over-time, chronic errors may reduce the efficiency of decision-making, slowing cognition and action and giving rise to the psychomotor poverty and cognitive impairments of classical schizophrenia.

In accord with the observation that the genetic variants expressed in glutamatergic and GABAergic neurons contribute to the polygenic risk score for schizophrenia associated with the clinical features of classical schizophrenia (Legge et al., 2021), taken together with the proposal by Adams et al. (2013) that

reduced synaptic gain arising from abnormality of glutamatergic or GABAergic transmission might play a cardinal role in trait abnormalities, we propose that classical schizophrenia arises from imprecise priors resulting from reduced synaptic gain in pyramidal neurons.

In this account we place emphasis on the role of imprecise predictions in disorganization of mental activity, and to a lesser extent, in impoverished mental activity. Nonetheless, we discuss the possible mechanism by which such a core process might account for the diverse aspects of schizophrenia, including the occurrence of at least transient episodes of reality distortion. We explore the way in which interaction between genetic prediction and environmental factors might account for the characteristic time-course of the illness.

EVIDENCE FOR EXCESSIVELY IMPRECISE PREDICTIONS

To support our proposal, we will examine evidence derived from studies of five types of brain processes: Mismatch Negativity (MMN); oddball target detection; self-initiated action; perceptual organization, and Post-movement Beta Rebound (PMBR).

Mismatch Negativity

MMN is an electrophysiological feature elicited by deviant acoustic stimuli delivered within a train of repetitive standard stimuli: The deviant stimuli elicit a greater negativity in the scalp potential compared to the standard stimuli, at approximately 200 ms after the presentation of the deviant stimulus. The MMN occurs even when there is no requirement to make a response (unlike the requirement in an "oddball" target detection task). In fact, the stimuli of interest are usually presented while the participant engages in some other activity such as watching a silent movie. Typically, the deviant stimuli differ from the standard stimuli in features such as such as pitch, duration, or intensity. MMN appears to reflect an automatic "change detection" process when an acoustic event violates expectation, even when it has no direct behavioral relevance.

Reduction of MMN amplitude is well established in schizophrenia. Interestingly, a meta-analysis by Erickson et al. (2016) of data acquired in over a hundred cases at various phases of illness indicated that MMN impairment appears to reflect vulnerability to disease progression in individuals at high risk of schizophrenia on the grounds of clinical features rather than a genetically determined risk for the condition. The association with vulnerability to disease progression suggests that the clinical features that predict severe illness may share a substrate with processes underlying reduced MMN, namely impaired detection of statistical irregularities in the environment.

Predictive Coding and Mismatch Negativity

Kirihara et al. (2020) reviewed the evidence indicating that reduced MMN amplitude might reflect altered predictive coding in schizophrenia. Studies using variants of the paradigm such as variation in the probability of the deviant stimuli and paradigms in which deviants entailed omission of expected stimuli, indicated that predictive coding is impaired in schizophrenia. For example, Baldeweg et al. (2004) measured MMN using a modified version of the "roving oddball" paradigm in which the last tone of each of a series of separate trains of auditory stimuli differs in duration from other stimuli. They found that healthy controls showed larger MMN amplitudes for oddballs following longer trains of repeated standards than for short trains, while MMN was not affected by the length of the train of repeated stimuli in patients with schizophrenia. These observations suggest less effective predictive coding in the patients. In light of inconsistent evidence regarding the role of familial factors underlying the MMN deficits in schizophrenia, we will return to the question of whether or not the MMN deficit is relevant to disease progression when we consider the role of gene-environment interactions in the cause of classical schizophrenia in the section entitled Gene-Environment Interactions.

Modeling Mismatch Negativity Deficits in Schizophrenia

The proposal that the MMN abnormality in schizophrenia reflects an abnormality of predictive coding is also supported by various mathematical models of the abnormality of MMN in schizophrenia. For example, Adams et al. (2021) developed a model of MMN employing Dynamic Causal Modeling. Their model comprised a distributed hierarchical network of brain regions implicated in generation of MMN: the inferior frontal gyrus, superior temporal gyrus and auditory cortex. They modeled the local circuits in the network nodes with inhibitory interneurons and spiny stellate cells interacting with superficial and deep pyramidal cells. The hierarchical model parameters were estimated according to Bayesian principles. The model successfully predicted a reduction in MMN in schizophrenia on the basis of local circuit parameters representing decreased synaptic gain in pyramidal cells in the patients. Synaptic gain of a neuron is the ratio of output signal to input. It can be adjusted by changes in synaptic strength mediated by glutamatergic and GABAergic transmission. The modeled decrease in synaptic gain represented increased self-inhibition of the pyramidal cells.

Using similar local circuit parameters, Adams et al. (2021) also applied Dynamic Causal Modeling to resting state EEG data, responses to steady state 40 Hz auditory stimulation, and resting state fMRI data in the same sample of patients. In all paradigms, the model was best fitted by local circuit parameters representing reduced synaptic gain in pyramidal neurons. In an analysis of relationships with symptoms, disinhibition in auditory areas predicted severity of positive symptoms.

Perhaps contrary to the evidence from meta-analysis (Erickson et al., 2016) indicating that MMN deficits in schizophrenia show no substantial familial influence, Adams et al. (2021) observed a decrease in MMN in first degree relatives of patients with schizophrenia.

Oddball Target Detection

Oddball target detection tasks differ from MMN-eliciting tasks by requiring a motor response to the oddball stimulus. In typical oddball target detection paradigms, auditory tones at a particular frequency are presented randomly within a series of identical

non-target stimuli, such has tones with a frequency different from the target. The participant is required to make a response, usually a button press, to target tones while refraining from responding to non-target tones. The oddball target stimuli elicit a characteristic series of event related potentials (ERPs), including a large positive-going deflection of the scalp potential, the P300, in a time window extending from 300 to 450 ms after the stimulus. The magnitude of the P300 is modulated by variation in target characteristics. Magnitude increases with decreasing target probability, suggesting, that like the MMN, P300 indexes the degree to which an internally generated expectation is violated.

A reduction in the magnitude of the P300 in schizophrenia is one of the best documented physiological abnormalities in schizophrenia. Many of the important clinical correlates of the P300 were described over two decades ago in Ford's Presidential Address to the Society for Psychophysiological Research (Ford, 1999). Reduced P300 is both a state and a trait marker. In severe illness, the abnormality of the P300 is correlated with positive symptom score; it is also correlated with severity of persisting negative symptoms. Detectable abnormality persists even after symptom resolution. More recent studies confirm that deficits in P300 amplitude in both auditory and visual modalities emerge early in the course of illness, and precede onset of overt psychosis (Hamilton et al., 2019). P300 amplitude is also reduced in siblings of cases, suggesting a genetic contribution (Winterer et al., 2004; Groom et al., 2008).

The oddball target detection task entails perception, decision making and generation of motor responses, and thus might be expected to be a sensitive, though not specific, marker of abnormality in predictive coding. Oddball target detection tasks have only occasionally been addressed from the predictive coding perspective (e.g., Kolossa et al., 2012), at least in part because of difficulty distinguishing P300 modulations arising from mismatch in predictions regarding sensory stimuli, from mismatch related to the selection of response. Nonetheless, the theories of the role of predictive coding proposed by Friston (2009); Sterzer et al. (2019) and others imply that predictive coding plays a central role in the processes that contribute to perception and evaluation of the stimuli and/or planning the response in the oddball target detection task. As we shall discuss in the section entitled Brain Regions Engaged in Predictive Coding the brain regions engaged during predictive coding in healthy controls exhibit a marked overlap with the regions engaged during oddball target detection. In this section we will examine differences between patients and healthy controls in the effects of manipulations that modify endogenous ("top–down") influence on the processing of information. Within a predictive coding framework, these manipulations would be expected to modify internally generated predictions. However, in the case of the fMRI data, we cannot distinguish effects arising from abnormality of the generation of predictions from differences attributable to abnormality of the response to prediction errors.

Reduced Signal to Noise Ratio

Precise predictive coding requires precise representation of both the content and timing of the neural representation of the coded information. An important parameter in modeling brain activity according to a predictive coding framework is the degree of confidence in the prediction (Adams et al., 2013). The ratio of signal-to noise in the neural representation of prediction would be expected to influence the confidence in the prediction. There is a substantial body of evidence regarding diminished cortical signal-to-noise ratio in patients with schizophrenia during the processing of information. Winterer et al. (2004) assessed background noise in frontal brain regions in discrete frequency bands across a range of frequencies extending from 0.5 to 45 Hz during auditory oddball processing. They quantified noise as the activity that did not exhibit a consistent temporal relationship to the presentation of the stimuli. They reported pronounced broadband cortical background noise over frontal cortex in patients with schizophrenia. A similar but less marked excess of noise was observed in clinically unaffected siblings. The frontal background noise predicted poor performance on frontal lobe cognitive tasks. There was a high intraclass correlation between sib-pairs suggesting high heritability of cortical background noise.

Inter-Trial Coherence and Phase Resetting

In a predictive coding framework, the brain needs not only to predict the causes of sensory input and the upstream neural consequences of that input but also when these events are likely to occur. Arnal and Giraud (2012) argue that slow endogenous cortical activity reflected in cortical delta (1–4 Hz) and theta band (4–8 Hz) oscillations play a role in predictive timing. In particular, delta band oscillations might play a role in the temporal organization of speech. In the context of selecting and responding to a target stimulus, transient bursts of low frequency oscillations might play a role in timing of neural events. The major features of the time-course of event-locked electrical potentials can be described as a superposition of transient delta and theta oscillations that are time-locked to the presentation of stimuli. The degree of phase locking is reflected in the consistency of the oscillatory phase across trial and can be quantified as inter-trail coherence (ITC) in the frequency band of interest. Consistency of phase of oscillations evoked by an event is achieved in part by consistent re-setting of the phase of ongoing cortical oscillations and partly by the addition of new oscillations with a phase that is locked to the event of interest (Martínez-Montes et al., 2008).

In a study of auditory oddball processing in schizophrenia, Doege et al. (2010) demonstrated that patients with schizophrenia exhibit significantly less ITC in the delta band and also significant less re-setting of the phase of ongoing delta oscillations, in comparison with healthy control participants. The resulting inconsistency of the phase of delta oscillations across trials contributed to the decrease in the observed magnitude of the P300. Furthermore the severity of the abnormality of phase resetting in the delta band was correlated with the severity of disorganization.

Processing of Speech Sounds During Oddball Target Detection

Healthy individuals exhibit increased neural activity in the left superior temporal gyrus in response to speech sounds compared to complex non-speech sounds. Ngan et al. (2003) employed fMRI to identify the pattern of brain activation associated with

processing speech sounds in comparison with non-speech sounds in patients with schizophrenia, during an auditory oddball target-detection task in which the target stimuli were either speech sounds (such as "lif") or non-speech sounds matched for acoustic complexity.

In comparison with healthy controls, patients with schizophrenia exhibited greater and more extensive activation for speech sounds in left superior frontal cortex, left temporo-parietal junction and right temporal cortex. The magnitude of the difference in activity in the left temporo-parietal junction was significantly correlated with severity of disorganization of speech. The finding of more extensive activation is consistent with the hypothesis that neural representation of speech sounds is less precise in patients. The more extensive activation of right temporal cortex suggests less clearly defined hemispheric lateralization of the processing of speech sounds, while the more extensive activation in the left temporo-parietal region suggests more widespread activation in brain regions normally engaged in processing speech sounds. The correlation of the aberrant activity in left temporo-parietal junction with severity of disorganization of speech suggests that disorganization of speech in schizophrenia is associated with failure to suppress inappropriate sounds related to speech.

Activity During Processing of Non-target Stimuli

Studies employing fMRI reveal widespread activation of the brain during the processing of target stimuli during the auditory oddball task (Kiehl et al., 2005). Furthermore, at least in well-established cases of schizophrenia, the activation during processing of target stimuli is diminished (Kiehl and Liddle, 2001). Performance of patients is usually impaired insofar as reaction times to targets are significantly longer in patients and there is a tendency toward more errors of omission in response to targets and errors of commission by failing to suppress response to non-targets (Kiehl and Liddle, 2001).

To minimize possible confounds in assessing brain activation arising from individual differences in task difficulty, Liddle et al. (2013) employed fMRI to assess brain activation during the processing of target stimuli and also the processing of non-target stimuli in an easy variant of the task in which the probability of targets was equal to that of non-targets, in early phase cases and also non-affected siblings of cases. Patients with schizophrenia and siblings showed significant hyper-activation to non-targets in brain areas activated by targets in all groups. The regions exhibiting hyperactivity included left superior frontal gyrus, fronto-insular cortex and bilateral temporo-parietal junction. In addition the patients and the siblings exhibited less deactivation to non-targets in Default Mode Network areas, including the precuneus, in which activity was suppressed during processing of targets in all groups.

These findings suggest that inefficient cerebral recruitment is a vulnerability marker for schizophrenia, made manifest by less suppression of activity in brain areas normally deactivated in response to task stimuli, and increased activation of areas normally activated in response to task stimuli. These findings are consistent with the hypothesis that vulnerability for schizophrenia is associated with inappropriate internally generated allocation of behavioral salience to non-target stimuli. With a predictive coding framework, this might be described as lack of precision in specification of prior expectation.

In a further test of the hypothesis that schizophrenia is associated with inappropriate internally generated allocation of behavioral salience to non-target stimuli, Liddle et al. (2016) employed Magnetoencephalography (MEG) to measure beta oscillations in the insula (a cardinal node of the salience network) during a relevance modulation task designed to compare activity during the processing of task-relevant stimuli with that during processing of task-irrelevant stimuli. The stimuli were images of either butterflies or ladybirds. The task-relevant stimulus type alternated between blocks. Beta oscillations were selected as the relevant measure on account of the evidence that beta oscillation mediate endogenously generated long range integrative signals (Fries, 2015). As predicted, healthy participants exhibited greater beta synchronization in the insula following processing of behaviorally relevant, as compared to irrelevant, stimuli. Patients with schizophrenia showed the reverse pattern: a greater beta synchronization during processing of irrelevant than relevant stimuli. Within a predictive coding framework, this might be described as inaccurate endogenous specification of expectation.

Self-Generated Action

Using EEG, Ford et al. (2008) examined phase synchronization of brain oscillations in various frequency bands across trials (quantified as Phase Locking Factor, PLF) during self-paced button-pressing. Participants were required to press a button at will at time intervals of approximately 1–2 s. They argued that if PLF in sensorimotor cortex immediately preceding the motor action represents the "efference copy" of the action plan, it should be maximal in the hemisphere contralateral to the finger making the movement. Furthermore, if the role of the efference copy is to dampen the subsequent tactile sensory experience associated with the button press, the magnitude of the efference copy should related to the subsequent neural activity in sensori-motor cortex immediately after the button press.

They observed that in healthy controls, gamma band neural synchrony preceding the button press was maximal over the contra-lateral sensorimotor cortex, and was correlated with the amplitude of the somatosensory ERP evoked by the press. These effects were reduced in patients with schizophrenia. Furthermore, beta band neural synchrony preceding the button press was also reduced in patients. This reduction in beta synchrony was most marked in patients with avolition/apathy assessed using the Scale for the Assessment of Negative Symptoms (SANS).

It is noteworthy that volition/apathy scale employed in SANS contains items related to role function that reflect both disorganization and impoverishment of mental activity. In particular, in chronic illness, scores for poor grooming and hygiene, and for impersistence at school or work, are correlated more strongly with disorganization, whereas physical anergia is correlated more strongly with impoverished mental activity (Liddle, 1987).

Perceptual Organization

Perceptual organization is the process of organizing sensory information into coherent patterns that represent objects, groups of objects and whole scenes, and our bodily relationship to them. Perceptual organization entails interpreting sensory input in light of internally generated predictions about relationships between percepts. Imprecise predictions would be expected to lead to impaired perceptual organization. There is extensive evidence for abnormalities of visual perceptual organization in schizophrenia. In a meta-analysis, Silverstein and Keane (2011) found that abnormalities of the organization of complex visual information are consistently found in schizophrenia, but are rare in other psychotic disorders such as bipolar mood disorder. Furthermore, in schizophrenia, these abnormalities are associated with severity of disorganization symptoms, and with poor premorbid functioning and poor prognosis. Thus, they are associated with features of classical schizophrenia. However, in light of evidence that disorders of perceptual organization are not prominent in the early phase of illness, Silverstein and Keane (2011) concluded that impairment of perceptual organization reflects illness progression.

In an fMRI study Silverstein et al. (2009) found that during a contour integration task, patients with schizophrenia exhibited diminished activation of visual association cortex during a perceptual organization task in comparison with healthy controls. Furthermore, patients with schizophrenia exhibited less activation compared with healthy controls in frontal, parietal and temporal regions during conditions in which integrated forms were perceived compared to random stimuli. In contrast the patients exhibited greater activation than controls in those brain areas during perception of random stimuli compared with integrated forms. These observations suggest a deficit in attentional enhancement of the perception of coherent forms relative to background information.

In a study of individuals with schizophrenia, first degree relatives of people with schizophrenia, individuals with bipolar disorder and healthy controls, Chen et al. (2005) found impairment of visual motion integration in the patients with schizophrenia, but not in the first-degree relatives, nor in patients with bipolar disorder, suggesting specificity to schizophrenia but indicating that it is not a familial trait.

In a structural and functional imaging study of schizophrenia and bipolar disorder, Palaniyappan and Liddle (2014) found that in comparison with bipolar disorder, schizophrenia was associated with increased functional connectivity between visual cortex and other regions of the brain during a working memory task, consistent with inadequate down-weighting of sensory evidence. Furthermore, Palaniyappan and Liddle (2014) found that the aberrant functional connectivity of the visual processing system predicted burden of persistent symptoms, consistent with the hypothesis that this abnormality in visual processing is specifically associated with classical schizophrenia.

Post-movement Beta Rebound

Further evidence of imprecise prediction in schizophrenia is provided by abnormalities of the phenomenon of Post-movement Beta Rebound (PMBR). Beta synchrony decreases during the execution of a movement but then rebounds to a level higher than the baseline level over a period of several seconds following the movement. The magnitude of this rebound is influenced by the confidence in the motor plan. For example, Tan et al. (2014) assessed brain oscillations during a task in which healthy participants were required to move a joystick with the aim of moving a cursor toward a visual target presented on a computer screen. Unbeknownst to the participant, the relationship between the direction of movement the joystick and the motion of the cursor was manipulated during the task, creating uncertainty about the motor plan and inducing inaccurate responses. Tan et al. (2014) found that in the healthy participants, the magnitude of PMBR was lower when the error in direction of movement of the cursor was larger. In a subsequent study of healthy participants, Tan et al. (2016) employed Bayesian modeling to estimate the anticipated uncertainly in the environmental feedback and the uncertainty in the feedforward estimation. They concluded that magnitude of PMBR reflects the confidence in the internal feedforward estimation during sensorimotor integration based on updating of plans according to Bayesian principles. A high amplitude PMBR might be regarded as an index of confidence in the current motor plan, whereas a low amplitude PMBR might indicate the need for adaptive changes driven by the sensory feedback.

Several studies reveal that the magnitude of PMBR is decreased in schizophrenia. Robson et al. (2016) found that the decrease in magnitude of PMBR is correlated with the severity of persisting symptoms during a stable phase of illness. In a partially overlapping sample of cases, Rathnaiah et al. (2020) demonstrated that the reduction in PMBR was correlated with severity of classical schizophrenia quantified by a latent variable representing the shared variance between severity of disorganization, psychomotor poverty, cognitive impairment and impairment of role function, as discussed in the Introduction.

In a study using MEG to measure oscillatory activity following a simple finger abduction movement, in separate samples of early phase cases of schizophrenia (within 6 weeks of commencement of antipsychotic medication) and cases with well-established illness (of duration at least 10 years), Gascoyne et al. (2021) confirmed that PMBR was significantly reduced in both samples of cases relative to matched healthy controls. The reduction was greater in the well-established cases. In the well-established cases the magnitude of the reduction was correlated with severity of disorganization symptoms.

In a MEG study of oscillations following a finger abduction movement in a non-clinical sample, Hunt et al. (2018) found that magnitude of PMBR was inversely correlated with severity of schizotypal features. The greatest contribution to the relative diminution of PMBR came from schizotypal features reflecting disorganization of mental activity. Schizotypal features reflecting impoverishment of mental activity also made a lesser but nonetheless significant contribution to the PMBR deficit.

Although PMBR is usually quantified by averaging the beta power across a time window following movement, observation of data acquired in single trials reveals that the smooth peak of beta activity observed in trial averaged data actually represents

the superposition of transient bursts of beta activity with duration of order 150 ms occurring with increased probability in the PMBR time window. In a study employing concurrent EEG and fMRI to assess brain activity during the n-back working memory task, Briley et al. (2021) confirmed that beta-burst rate following button press responses was diminished in schizophrenia, and also in psychotic bipolar disorder, compared with healthy controls. The reduction was less marked in the bipolar cases. Furthermore, the magnitude of the deficit was correlated with severity of disorganization. Multivariate analysis confirmed that shared variance between the features of classical schizophrenia: disorganization, psychomotor poverty and cognitive impairment, was significantly correlated with the reduction beta-burst rate. The findings in bipolar disorder suggest that at least some cases satisfying DSM IV criteria for bipolar disorder exhibit features characteristic of classical schizophrenia.

Furthermore, the analysis by Briley et al. (2021) of the BOLD signal assessed using fMRI revealed that beta-bursts are associated with the reactivation of a pattern of brain activity representing task-relevant content of working memory. In the context of the n-back task, in which the target stimuli were letters of the alphabet, the spatial distribution of BOLD signal associated with the occurrence of beta-bursts included areas implicated in the articulation of speech, processing of speech sounds and also sensorimotor areas engaged in the required motor response. In patients with schizophrenia or psychotic bipolar disorder, the BOLD activation was more extensive than in healthy controls, consistent with less precise representation of the content of working memory. Furthermore, the occurrence of beta-bursts was also associated with suppression of activity in brain regions expected to be engaged in the ongoing executive processing during the working memory blocks, implying that beta-bursts are associated not only with reactivation of the response-relevant brain activity but suppression of competing brain activity.

On the basis of study of beta-bursts in humans, primates and rodents, Sherman et al. (2016) proposed a neuronal model of beta-burst generation in which the characteristic time-course of a beta-burst is generated by coincident arrival of relatively broad peak of neural activity in middle layers of the cerebral cortex (via thalamo-cortical fibers) with the arrival of strong spike of activity in superficial layers of cortex. Such a model is potentially consistent with the hypothesis that beta-bursts play a role in the comparison of an intended action with the sensorimotor feedback from the action. A large amplitude beta-burst might confirm the timing and content of the planned response, while diminution of the amplitude of the beta-bursts, as seen in patients with schizophrenia, might indicate less precise prediction.

MACROSCOPIC BRAIN CHANGES

Gray Matter Abnormalities in Schizophrenia

Many studies report widespread gray matter deficits in psychotic disorder. A mega-analysis of structural MRI studies employing Voxel Based Morphometry revealed deficits in schizophrenia that are most marked in insula and anterior cingulate cortex and also occur in association cortex sites implicated in executive function and attention, including lateral frontal cortex and parietal cortex (Gupta et al., 2015).

The gray matter reductions reported in mental disorders can reflect diminution of cortical thickness, surface area or gyrification. Diminished gyrification, especially in the insula, might be more specific to schizophrenia (Sheffield et al., 2021). Patterns of gyrification are largely determined during prenatal development, consistent with a developmental origin for classical schizophrenia. However, it should be noted that some evidence from longitudinal studies indicates that frontal gyrification can diminish during the early years of a schizophrenic illness (Palaniyappan et al., 2013). Evidence suggests that in schizophrenia, local gyrification in a region is related to density of long range connections with that region (White and Hilgetag, 2011).

Although reduction of local gyrification index in schizophrenia compared with healthy control participants has been reported in diverse brain regions, the most marked reductions occur in left insula and frontal operculum, left superior and middle frontal gyrus, temporo-parietal junction bilaterally and precuneus (Palaniyappan and Liddle, 2012). These regions contain major hubs in brain networks engaged in the regulation of attention (Seeley et al., 2007).

In the combined structural and functional imaging study comparing schizophrenia with bipolar disorder discussed in the section entitled Perceptual Organization, Palaniyappan and Liddle (2014) confirmed that in the contrast of patients with schizophrenia with healthy controls, the patients exhibited diminished gyrification in left insula, left superior frontal gyrus, regions in the vicinity of the tempo-parietal junction bilaterally, and left precuneus and posterior cingulate. They also conducted a conjunction analysis to identify brain regions exhibiting both diminished gyrification and increased functional connectivity in patients with schizophrenia relative to patients with bipolar disorder. They observed a conjunction of these effects (assessed at a lenient threshold) in left anterior insula, left middle temporal gyrus, left precuneus and posterior cingulate, and in visual processing areas in the lingual gyrus and calcarine fissure bilaterally.

Brain Regions Engaged in Predictive Coding

Although it might be expected that brain regions engaged in perception of diverse sensory stimuli and in the planning of diverse actions might be engaged during predictive coding, fMRI studies suggest that predictive processing commonly engages certain brain regions. Ficco et al. (2021) performed a meta-analysis of 45 studies of paradigms involving prediction violation, and 39 studies of task entailing encoding of predictions. They employed Activation Likelihood Estimation (ALE) to identify sites of activity common to the different studies, and also a meta-analytic connectivity method (Seed-Voxel Correlations Consensus, SVC). The ALE analysis identified sites in left anterior insula and left inferior frontal gyrus that were active during prediction violation. The tasks that involved prediction

encoding engaged a distinguishable set of sites including right insula, bilateral inferior parietal lobule, the cuneus and the right middle frontal gyrus. Nonetheless, the connectivity analysis demonstrated that the sites engaged in prediction violation were connected to the sites engaged in prediction encoding. The SVC analysis identified a large, bilateral predictive network, which containing many network nodes involved in task driven attention and execution, including insula and dorsal ACC; lateral frontal cortex and parietal cortex and also sites in the cerebellum.

Given that violations of prediction will have high salience, the involvement of the insula in detecting prediction violation is consistent with its role in the processing of salient stimuli (Seeley et al., 2007; Sridharan et al., 2008). It is noteworthy that left insula is the site of greatest gray matter reduction in schizophrenia revealed by mega-analysis of Voxel Based Morphometry data (Gupta et al., 2015), as well as the site of the most marked abnormalities of gyrification in schizophrenia (Palaniyappan and Liddle, 2012). Furthermore, in the stable phase of schizophrenia, disorganization is associated with diminished resting state cerebral blood flow in the left fronto-insular cortex, and also in temporo-parietal junction bilaterally (Liddle et al., 1992).

Figure 1 illustrates the similarity between the regions with most marked reduction of local gyrification in schizophrenia (Palaniyappan and Liddle, 2012) and the regions exhibiting an aberrant increase in activity in patients with schizophrenia relative to controls during processing of non-target stimuli in a target detection task (Liddle et al., 2013) and during processing of word sounds relative to non-word sounds (Ngan et al., 2003).

It should be noted that the aberrant activity in the precuneus during processing of non-target stimuli is in a region of the Default Mode Network in which patients fail to exhibit the normal level of suppression of activity during processing of target stimuli. All of the regions depicted in **Figure 1** in which patients exhibit aberrant activation lie within the network of sites engaged during predictive coding identified in the SVC analysis by Ficco et al. (2021), apart from the site in the precuneus, which Ficco et al. (2021) found to be anti-correlated with the predictive coding network.

MOLECULAR BRAIN ABNORMALITIES

Modeling of EEG signals associated with Mismatch Negativity suggests that reduced synaptic gain arising from abnormality of glutamatergic or GABAergic transmission might play a cardinal role in aberrant predictive coding in schizophrenia (Adams et al., 2013, 2021).

Post mortem studies reveal consistent evidence of abnormalities of the morphology of dendrites of pyramidal (glutamatergic) neurons in the cerebral cortex, and of reduced levels of the protein synaptophysin, a sensitive marker for synaptic terminals, in frontal cortex and hippocampus, in schizophrenia (Hu et al., 2015; Osimo et al., 2019). *In vivo* measurements using Magnetic Resonance Spectroscopy (MRS) have been less consistent. Meta-analysis of MRS findings reveals decreased glutamate levels in frontal regions, especially anterior

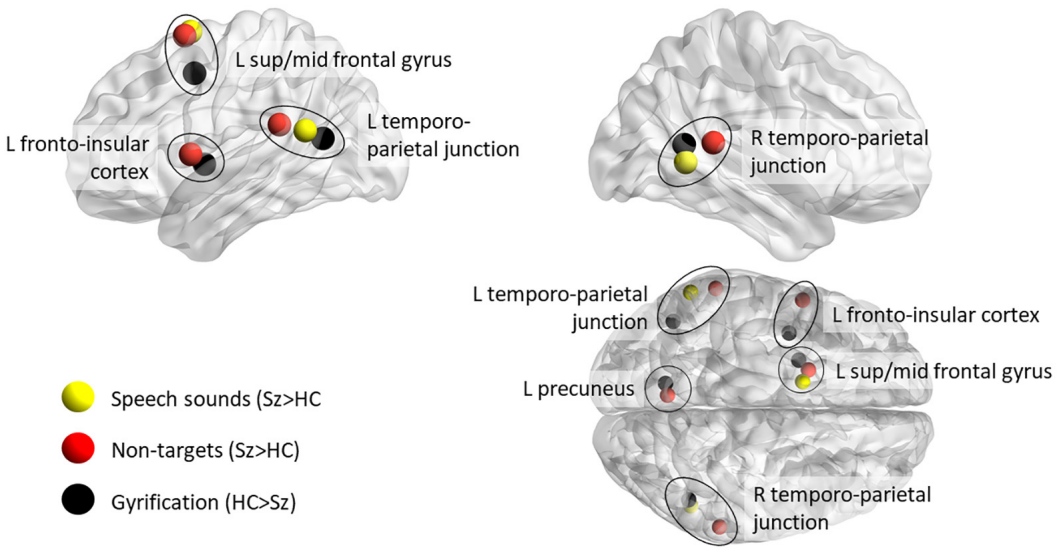

FIGURE 1 | Comparison of regions of aberrant increase of brain activity in patients with schizophrenia during tasks likely to involve endogenous coding of predictions, with the regions in which local gyrification index is diminished in patients relative to healthy controls. Red spheres depict the loci of local maxima in clusters of voxels exhibiting greater activity in patients with schizophrenia relative to healthy controls during processing of non-target stimuli in a target detection task (Liddle et al., 2013); yellow spheres depict local maxima of aberrant activity in patients during processing of word sounds relative to non-word sounds (Ngan et al., 2003). The black spheres depict the local maxima in clusters of reduced local gyrification in schizophrenia compared with healthy controls (Palaniyappan and Liddle, 2012). Note that the clusters were irregular is shape and many extended beyond the sphere depicting the local maximum. In particular, the region of diminished gyrification with peak difference between patients and controls in the left middle frontal gyrus extended into superior frontal gyrus. The brain loci were visualized using Brain Net Viewer (Xia et al., 2013).

cingulate cortex, in both first episode psychosis and established schizophrenia (Sydnor and Roalf, 2020). However, a recent mega-analysis suggests that the reduction in glutamate might be attributable, at least in part, to antipsychotic medication (Merritt et al., 2021).

Post mortem studies also provide evidence for reduced transcription of genes implicated in GABA transmission in frontal cortex in schizophrenia (Hashimoto et al., 2008). *In vivo* measurements using MRS have been inconsistent but a recent meta-analysis indicates a significant reduction of GABA levels in anterior cingulate cortex, and a trend toward reduction in other frontal regions (Kumar et al., 2021).

THE RELATIONSHIP BETWEEN DISORGANIZATION AND PSYCHOMOTOR POVERTY

As discussed in the Introduction, Legge et al. (2021) found that the polygenic risk for schizophrenia is associated with both disorganization and with expressive negative symptoms. They also found a significant correlation between severity of disorganization and expressive negative symptoms in their cases. The expressive negative symptoms identified by Legge et al. (2021) (flat affect and alogia) are similar to the core negative symptoms reflecting impoverishment of mental activity, which Liddle (1987) labeled psychomotor poverty.

The findings of Legge et al. (2021) are consistent with the identification by McGorry et al. (1998) in a large sample of cases of First Episode Psychosis of a Bleulerian factor with contributions from symptoms reflecting disorganization and also symptoms reflecting psychomotor poverty. A similar factor with loadings on disorganization and psychomotor poverty symptoms was identified in another large study of first episode cases by Tonna et al. (2019). Furthermore these finding are consistent with the finding by Rathnaiah et al. (2020) of a latent variable with loadings on both disorganization and psychomotor poverty in stable cases of established schizophrenia (as referred to in the Introduction).

On the other hand, numerous other studies of the relationships between symptoms of schizophrenia report that disorganization and psychomotor poverty are distinguishable dimensions of psychopathology (Bilder et al., 1985; Liddle, 1987; Arndt et al., 1991). Thus, within an account of the pathological mechanism of classical schizophrenia it is necessary to propose a mechanism that accounts for the observation that disorganization and psychomotor poverty are related but nonetheless distinguishable clusters of symptoms.

Our proposal that imprecise predictive coding is a core feature of classical schizophrenia could account for the observed relationship between disorganization and psychomotor poverty, as both are potential consequences of imprecise prediction. Firstly, imprecise predictions will give rise to imprecise prediction errors and thus to erratic updating of predictions, leading, in turn, to poorly organized perception and action, manifest as disorganization symptoms. Secondly, if predictions are so imprecise that the prediction error is too diffuse to facilitate a coherently refined action plan, the process of generating action might be slowed or even fail to reach execution threshold at all, and manifest as impoverishment of motor activity. Furthermore, inconsistent updating of predictions over an extended period might result in a failure of consistent reinforcement of the pattern of neural activity coding the predictions, resulting in weakening of predictions and to diminished initiation of mental activity and behavior.

This possibility is supported by evidence regarding verbal fluency in schizophrenia. Allen et al. (1993) administered a verbal fluency test in which the person was required to generate as many words as possible within a given category in a 2 min period, on multiple occasions several days apart. They found that patients with schizophrenia do not suffer from diminished store of words. The variation between samples of words generated on different days suggested that cases with marked disorganization exhibit an inefficient search strategy, while cases with marked impoverishment of mental activity appear to terminate the search prematurely. This is consistent with the possibility that over an extended period of frequently occurring mismatches between predictions and experience, synapses in the networks engaged in generating specific predictions become weaker resulting in reduced ability to initiate a search for words.

CONTRIBUTIONS TO COGNITIVE IMPAIRMENT IN SCHIZOPHRENIA

In the study of polygenic risk scores and schizophrenia referred to in the Introduction, Legge et al. (2021) also examined the degree to which the polygenic risk for cognitive impairment contributes to clinical features of schizophrenia. Not surprisingly, they reported that the polygenic score for cognitive impairment occurring in diverse conditions contributes to cognitive impairment in schizophrenia. Thus the genetic contribution to cognitive impairment in schizophrenia arises from two distinguishable groups of genetic variants: the variants contributing to the polygenic risk for schizophrenia and from the variants contributing to polygenic risk for cognitive impairment in general. On further analysis Legge et al. (2021) found evidence that the polygenic risk score for schizophrenia contributes to cognitive decline rather than premorbid cognitive performance.

The evidence suggesting that the polygenic risk for schizophrenia predisposes to cognitive decline indicates that the expression of risk genes unfolds over time. It is plausible that disorganization is an early manifestation of the genetic risk for schizophrenia and that both psychomotor poverty and cognitive impairment develop over time as consequence of persisting lack of precision of predictions. This interpretation accounts for the evidence that the association of disorganization and psychomotor poverty with cognitive impairment is stronger in the chronic phase of schizophrenia than in the early phase. For example, Liddle and Morris (1991) found that in the stable phase of chronic schizophrenia disorganization is associated with impaired selection of mental activity (e.g., increased Stroop effect; unusual word choice during a verbal fluency test); whilst psychomotor poverty associated with impaired

initiation of mental activity (e.g., decreased verbal fluency). Furthermore, this evidence for progression over time provides a pointer toward strategies for ameliorating at least some of the cognitive impairment of schizophrenia, and in turn, ameliorating impairment of role function that might arise from those impairments. Identification of the nature of the relevant neuronal processes offers the prospect of approaches to treatments that might prevent or reverse long term disabilities.

REALITY DISTORTION IN CLASSICAL SCHIZOPHRENIA

Reality distortion occurs in all psychotic illnesses, and is therefore not unique to schizophrenia. Nonetheless, reality distortion plays a major part in diagnostic criteria for schizophrenia employed in current clinical practice (American Psychiatric Association, 2013; World Health Organisation, 2018). The frequent occurrence of reality distortion in schizophrenia is unlikely to merely be an artifact of current diagnostic criteria. Simple schizophrenia, characterized by classical features without overt reality distortion and first identified by Diem in 1905, is relatively rare (Lally et al., 2019). Thus, an adequate description of classical schizophrenia must account for frequent occurrence of reality distortion in classical schizophrenia. In this regard it is noteworthy, as mentioned in the introduction, that in their longitudinal study of the emergence of psychotic illness in a large non-clinical sample of young people Dominguez et al. (2010) reported that prior disorganization and negative symptoms predicted onset of subsequent overt psychosis.

The hypothesis that the core aspect of classical schizophrenia is imprecise coding of predictions provides a possible clue to the mechanism by which the classical features of disorganization together with psychomotor poverty might precede the development of reality distortion and florid psychosis. Prediction errors are associated with the release of dopamine, which modulates the "teaching signal" responsible for updating of predictions (Schultz, 1998). Persisting imprecision of prediction would lead to frequent but unreliable prediction errors, leading to an increase in net dopamine (Jenkinson and Brown, 2011), increased dopaminergic transmission and amplification of unreliable teaching signals. In some circumstances, the strengthening of erroneous predictions might, lead either to delusional misinterpretation of exogenous signals or to misinterpretation of endogenously generated signals as exogenous signals (i.e., hallucinations). At times of stress, when levels of stress tend to magnify dopaminergic signals, classical schizophrenia might develop into florid psychosis.

TIME-COURSE OF CLASSICAL SCHIZOPHRENIA

The evidence regarding relationships between disorganization, psychomotor poverty and cognitive impairment, and also the relationships between these classical clinical features and reality distortion, indicates that the manifestations of classical schizophrenia evolve over time. It is therefore appropriate to summarize the time-course characteristic of classical schizophrenia.

Prior to Illness Onset

Features of classical schizophrenia are discernible before illness onset in cases that subsequently develop schizophrenia. As mentioned in earlier, Dominguez et al. (2010) performed a 10 year follow-up study of a representative sample of over three thousand young people, recruited at age 14–24 years. Symptoms were assessed at three time points: at time 1, negative/disorganized score was based in scores for "indifference" and "thought incoherence"; at times 2 and 3; additional items measuring negative symptoms were also included. Negative/disorganized symptoms predicted positive symptoms over time. The co-occurrence of positive and negative/disorganized symptoms predicted functional impairment.

Classical Features Occurring During the Prodrome

In many cases of schizophrenia, symptoms emerge gradually during a prodromal period. In one of the most comprehensive studies of the prodrome, Hafner et al. (1995) interviewed 232 cases in their first episode of overt schizophrenia, using an interview schedule designed to delineate the time-course and nature of the prodromal features. In that sample, the mean duration of the prodrome was 5 years. Non-specific symptoms such as restlessness, depression and anxiety were the most common symptoms. Nonetheless the ten most common features included features characteristic of classical schizophrenia: difficulty with thinking and concentration; lack of energy and slowness; poor work performance; and reduced interpersonal communication.

Several studies using computerized analysis of speech samples have demonstrated that subtle disorganization of speech in cases at risk predicts onset of overt psychosis and subsequent severity of negative symptoms (Bedi et al., 2015; Mota et al., 2017). As mentioned in the Introduction, Ziermans et al. (2014) performed a comprehensive assessment of symptoms and cognition in a sample of individuals identified as being at high risk of psychosis on the basis of clinical features. They found that severity of disorganization predicted poor functional outcome at 6 years ($r = 0.55$, $p < 0.001$).

In contrast, meta-analysis of the predictive power of duration of untreated psychosis (DUP) reveals that DUP has only very weak power to predict functional outcome. In a comprehensive meta-analysis, Penttilä et al. (2014) found a weak though statistically significant correlation between DUP and social function, but no significant correlation between DUP and occupational function.

Long Term Evolution of Symptoms in Classical Cases

Pfohl and Winokur (1982) delineated the evolution of symptoms over a period of 35 years in a sample of hebephrenic/catatonic

schizophrenia identified in a cohort of 500 cases admitted to mental hospital in a period 1935–1945, prior to the introduction of antipsychotic medication. At initial assessment, the hebephrenic/catatonic cases were characterized by disorganization of mental activity. The investigators examined case records reporting the presence or absence of 28 different symptoms assessed systematically on a yearly basis during the follow-up period. They found that symptoms reflecting reality distortion, such as hallucinations and delusions, had onset in the early phase of overt illness and in many cases, resolved within the first 5 years. In contrast, features characteristic of classical schizophrenia, such as loosening of associations, weakened volition, diminished social interaction and lack of engagement in productive activity were very prevalent in the early phases and usually persisted beyond 5 years. Furthermore, symptoms such incoherence of speech and flatness of affect became more prevalent in the longer term.

GENE-ENVIRONMENT INTERACTIONS

As discussed in sections "The Relationship Between Disorganization and Psychomotor Poverty" and "Reality Distortion in Classical Schizophrenia," life-long imprecision in predictive coding might in itself lead to an evolving course of illness. Imprecise predictive coding might initially produce disorganization and lead to psychomotor poverty, while predisposing to episodic reality distortion. However, such processes do not fully account for the characteristic time-course of classical schizophrenia. There is evidence that a diverse number of environmental factors might contribute to schizophrenia: maternal infection, obstetric complications, childhood abuse, brain injury, substance abuse (Gilmore, 2010).

Furthermore, the concept of Classical Schizophrenia embraces a specific clinical profile within the diverse clinical conditions that would be diagnosed as schizophrenia (or as a condition within the schizophrenia spectrum) according to either DSM-5 (American Psychiatric Association, 2013) or ICD-11 (World Health Organisation, 2018). It is likely that diverse environmental factors, and perhaps other genetic variants, contribute to the cause of psychotic conditions that do not exhibit the profile of classical schizophrenia.

Inflammation is a plausible process that might link diverse environmental factors to genetic factors contributing to schizophrenia. Watanabe et al. (2010) have reviewed the evidence suggesting that inflammatory processes mediated by cytokines such as epidermal growth factor (EGF) and interleukins provide a common pathway linking genetic and environmental factors. Genome wide association studies have revealed evidence of multiple genetic variants implicated in immune mechanisms, most notably variants of immunity-related genes located on chromosome 6 in the vicinity of the Major Histocompatibility Locus, are associated with schizophrenia (Shi et al., 2009).

Many of the environmental factors that predispose to schizophrenia involve stress on body tissues, including infection or metabolic processes that are associated with inflammation. Inflammatory cytokines, are elevated at onset of illness (Lesh et al., 2018) and through the course of the illness (Rodrigues-Amorim et al., 2018). It is noteworthy that in contrast to cytokine elevation observed in bipolar mood disorder, there is evidence that cytokine elevation observed at the onset of schizophrenia is associated with deficits in cerebral gray matter (Lesh et al., 2018). In light of the evidence for gray matter deficits in classical schizophrenia discussed in the section entitled Macroscopic Brain Changes, it is pertinent to ask whether or not inflammation might contribute to the clinical profile of classical schizophrenia.

Our hypothesis that the imprecision of predictive coding is a core process in classical schizophrenia raises the question: might inflammation impair predictive coding and in particular, be associated with electrophysiological abnormalities such as reduced MMN and PMBR? Emerging evidence supports this hypothesis. Jodo et al. (2019) demonstrated that neonatal exposure to the inflammatory cytokine, EGF, results in deficits of MMN in rats. In elderly men, persisting prostatitis and urinary tract infection is associated with cognitive deficits and with abnormality of MMN (Urios et al., 2019). Successful treatment with the phosphodiesterase-5 inhibitor, tadalafil, resulted in reduction of levels of the inflammatory cytokine, IL-6, recovery of the MMN to the level observed in healthy controls, and significant improvement in cognitive function (Urios et al., 2019). Investigation of the relationships between markers of inflammation and electrophysiological markers indicative of imprecise predictive coding, such as MMN and PMBR in schizophrenia is warranted.

DISCUSSION

In accord with our overarching goal of understanding of the processes that lead to poor functional outcome in schizophrenia, we have identified a specific clinical profile that we have designated "classical schizophrenia." Classical schizophrenia is characterized by disorganized and impoverished mental activity that predispose to reality distortion, and is associated with risk of persisting impairment of role function. We have assembled evidence supporting the hypothesis that the core pathological process in classical schizophrenia is imprecise predictive coding.

This concept of classical schizophrenia is consistent with subtle but widespread abnormalities of brain structure, predominantly in association cortex. Some evidence indicates that abnormal gyrification, particularly in insula, lateral frontal cortex and superior temporal gyrus, is characteristic of classical schizophrenia. Evidence indicates that these regions play an important role in generating predictions and/or responding to prediction error.

While there is evidence that the genetic variants that contribute to the polygenic risk score for schizophrenia are especially predictive of the clinical profile of classical schizophrenia, it is likely that interaction between genes and environmental factors influence the time-course of classical schizophrenia. In particular, it is plausible that inflammation plays a cardinal role in mediating these interactions. Emerging evidence suggests that inflammation might contribute to the

predictive coding deficits that we propose are at the core of classical schizophrenia. However, further evidence that inflammation might contribute to imprecise predictive coding is required. In particular, investigation of the relationship between inflammation and electrophysiological markers, such as MMN and PMBR, and also the relationships between inflammation and the proposed characteristic regional brain abnormalities revealed by structural and functional fMRI, is warranted.

In light of the association between polygenic risk score and the classical profile, it is noteworthy that Landi et al. (2021) demonstrated that polygenic risk score predicts poor outcome (quantified by measures such as course of disorder, classified as Continuous chronic illness/Continuous chronic illness with deterioration). However Landi et al. (2021) reported that the polygenic risk score does not add to the accuracy of prediction based on detailed analysis of electronic case records.

There is need for more sensitive measures of disorganization, both for the purpose of investigating mechanism and also for clinical prediction in early phase of illness. There is promising evidence that automated analysis of speech samples might help meet this need (see section entitled Classical Features Occurring During the Prodrome). In light of the observation that disorganization is also manifest as inappropriate affect, automated processing of facial expressions of emotion might also be helpful.

Furthermore, it would be of potential value to develop procedures for quantifying imprecise predictive coding from relevant measurements of brain function that might feasibly be employed in routine clinical practice. The evidence suggesting that PMBR is associated with predictive coding, together with the evidence that reduced PMBR is associated with clinical features of classical schizophrenia, raises the possibility that an assessment of beta oscillations using the clinically accessible technique of EEG, recorded during an appropriate attentional task, might have prognostic value.

One outstanding issue is whether or not classical schizophrenia is best regarded as a discrete category of psychotic illness, or alternatively, that the clinical profile of classical schizophrenia reflects a continuously distributed dimension of variation within the spectrum of psychotic illnesses. In light of the likelihood that a multiplicity of genes and environmental factors contribute to the cause of classical schizophrenia, there is likely to be a degree of heterogeneity within classical schizophrenia. A sharp categorical boundary is unlikely to exist. Nonetheless for the practical purposes of making a diagnosis and planning treatment, it would be useful to determine the degree to which classical schizophrenia can be identified as an illness that is categorically distinct from cases of psychotic illness that do not exhibit the classical profile.

In this paper we have discussed the evidence from studies of groups of cases, that the classical features reflecting disorganized or impoverished mental activity and cognitive impairment (listed in **Table 1**) predict long term disability. So far there is limited evidence that assessment of the relevant symptoms and cognitive measures are sufficiently sensitive and reliable to provide clinically useful estimates of prognosis in an individual case. However, the evidence that classical features are correlated with electrophysiological features such as inter-trial coherence during target detection tasks (Doege et al., 2010) and beta-bursts related to movement (Rathnaiah et al., 2020; Briley et al., 2021; Gascoyne et al., 2021) indicates a practical approach to enhancing prediction. It is practical to measure these electrophysiological features in routine clinical practice. It is plausible that a combination of measures of symptoms and cognition, together with such electrophysiological measurements would provide an estimate of risk of persisting disability that would facilitate planning treatment for an individual. The next step toward developing an effective predictive procedure would be identification of the optimal combination of these clinical and electrophysiological measurements at baseline for predicting role function in a longitudinal study of early phase cases over a period of a year or preferably longer.

We have also presented evidence from electrophysiological and brain imaging studies suggesting that the relevant pathological process entails imprecise predictive coding. Further investigation of the proposed pathophysiological mechanism might lead to development of improved treatment strategies. For example the modeling of the role of abnormal neural signaling in local circuits and also in long range connections in the electrophysiological features associated with classical schizophrenia, similar to the modeling performed by Adams et al. (2021), has the potential to lead to proposals for neuromodulation therapies effective in treating the features of classical schizophrenia.

DATA AVAILABILITY STATEMENT

The original contributions presented in the study are included in the article/supplementary material, further inquiries can be directed to the corresponding author/s.

AUTHOR CONTRIBUTIONS

PL proposed the concept of classical schizophrenia and drafted the manuscript. EL revised the manuscript. Both authors developed the hypotheses regarding the role of impaired predictive coding and approved the final draft.

FUNDING

This work was supported by the Medical Research Council (Grant No. G0601442) to PL and the National Institute for Health Research (NIHR) Nottingham Biomedical Research Centre.

ACKNOWLEDGMENTS

We are grateful to Drs. Mohan Rathnaiah, Lena Palaniyappan and Paul Briley for helpful discussions regarding the concept of Classical Schizophrenia.

REFERENCES

Adams, R. A., Pinotsis, D., Tsirlis, K., Unruh, L., Mahajan, A., Horas, A. M., et al. (2021). Computational modeling of electroencephalography and functional magnetic resonance imaging paradigms indicates a consistent loss of pyramidal cell synaptic gain in schizophrenia. *Biol. Psychiatry* 91, 202–215. doi: 10.1016/j.biopsych.2021.07.024

Adams, R. A., Stephan, K. E., Brown, H. R., Frith, C. D., and Friston, K. J. (2013). The computational anatomy of psychosis. *Front. Psychiatry* 4:47. doi: 10.3389/fpsyt.2013.00047

Allen, H. A., Liddle, P. F., and Frith, C. D. (1993). Negative features, retrieval processes and verbal fluency in schizophrenia. *Br. J. Psychiatry* 163, 769–775. doi: 10.1192/bjp.163.6.769

American Psychiatric Association (2013). *DSM 5*. Virginia, VA: American Psychiatric Association.

Andreasen, N. C., Flaum, M., and Arndt, S. (1992). The comprehensive assessment of symptoms and history (CASH). An instrument for assessing diagnosis and psychopathology. *Arch. Gen. Psychiatry* 49, 615–623. doi: 10.1001/archpsyc.1992.01820080023004

Arnal, L. H., and Giraud, A.-L. (2012). Cortical oscillations and sensory predictions. *Trends Cogn. Sci.* 16, 390–398. doi: 10.1016/j.tics.2012.05.003

Arndt, S., Alliger, R. J., and Andreasen, N. C. (1991). The distinction of positive and negative symptoms. The failure of a two-dimensional model. *Br. J. Psychiatry* 158, 317–322. doi: 10.1192/bjp.158.3.317

Baldeweg, T., Klugman, A., Gruzelier, J., and Hirsch, S. R. (2004). Mismatch negativity potentials and cognitive impairment in schizophrenia. *Schizophr. Res.* 69, 203–217. doi: 10.1016/j.schres.2003.09.009

Bedi, G., Carrillo, F., Cecchi, G. A., Slezak, D. F., Sigman, M., Mota, N. B., et al. (2015). Automated analysis of free speech predicts psychosis onset in high-risk youths. *NPJ Schizophr.* 1:15030. doi: 10.1038/npjschz.2015.30

Bilder, R. M., Mukherjee, S., Rieder, R. O., and Pandurangi, A. K. (1985). Symptomatic and neuropsychological components of defect states. *Schizophr. Bull.* 11, 409–419. doi: 10.1093/schbul/11.3.409

Blakemore, S. J., Wolpert, D., and Frith, C. (2000). Why can't you tickle yourself? *Neuroreport* 11, R11–R16.

Bleuler, E. (1911). *Dementia Praecox or the Group of Schizophrenias (trans J Zinkin 1951)*. London: Allen & Unwin.

Briley, P. M., Liddle, E. B., Simmonite, M., Jansen, M., White, T. P., Balain, V., et al. (2021). Regional brain correlates of beta bursts in health and psychosis: a concurrent electroencephalography and functional magnetic resonance imaging study. *Biol. Psychiatry Cogn. Neurosci. Neuroimaging* 6, 1145–1156. doi: 10.1016/j.bpsc.2020.10.018

Brown, M., and Kuperberg, G. R. A. (2015). Hierarchical generative framework of language processing: linking language perception. interpretation, and production abnormalities in schizophrenia. *Front. Hum. Neurosci.* 9:643. doi: 10.3389/fnhum.2015.00643

Chen, Y., Bidwell, L. C., and Holzman, P. S. (2005). Visual motion integration in schizophrenia patients, their first-degree relatives, and patients with bipolar disorder. *Schizophr. Res.* 74, 271–281. doi: 10.1016/j.schres.2004.04.002

Corlett, P. R., Frith, C. D., and Fletcher, P. C. (2009). From drugs to deprivation: a Bayesian framework for understanding models of psychosis. *Psychopharmacology* 206, 515–530. doi: 10.1007/s00213-009-1561-0

Doege, K., Jansen, M., Mallikarjun, P., Liddle, E. B., and Liddle, P. F. (2010). How much does phase resetting contribute to event-related EEG abnormalities in schizophrenia? *Neurosci. Lett.* 481, 1–5. doi: 10.1016/j.neulet.2010.06.008

Dominguez, M.-G., Saka, M. C., Lieb, R., Wittchen, H.-U., and van Os, J. (2010). Early expression of negative/disorganized symptoms predicting psychotic experiences and subsequent clinical psychosis: a 10-year study. *Am. J. Psychiatry* 167, 1075–1082. doi: 10.1176/appi.ajp.2010.09060883

Erickson, M. A., Ruffle, A., and Gold, J. M. A. (2016). Meta-Analysis of mismatch negativity in schizophrenia: from clinical risk to disease specificity and progression. *Biol. Psychiatry* 79, 980–987. doi: 10.1016/j.biopsych.2015.08.025

Ficco, L., Mancuso, L., Manuello, J., Teneggi, A., Liloia, D., Duca, S., et al. (2021). Disentangling predictive processing in the brain: a meta-analytic study in favour of a predictive network. *Sci. Rep.* 11:16258. doi: 10.1038/s41598-021-95603-5

Ford, J. M. (1999). Schizophrenia: the broken P300 and beyond. *Psychophysiology* 36, 667–682.

Ford, J. M., Roach, B. J., Faustman, W. O., and Mathalon, D. H. (2008). Out-of-synch and out-of-sorts: dysfunction of motor-sensory communication in schizophrenia. *Biol. Psychiatry* 63, 736–743. doi: 10.1016/j.biopsych.2007.09.013

Fries, P. (2015). Rhythms for cognition: communication through coherence. *Neuron* 88, 220–235. doi: 10.1016/j.neuron.2015.09.034

Friston, K. (2009). The free-energy principle: a rough guide to the brain? *Trends Cogn. Sci.* 13, 293–301. doi: 10.1016/j.tics.2009.04.005

Gascoyne, L. E., Brookes, M. J., Rathnaiah, M., Katshu, M. Z. U. H., Koelewijn, L., Williams, G., et al. (2021). Motor-related oscillatory activity in schizophrenia according to phase of illness and clinical symptom severity. *Neuroimage Clin.* 29:102524. doi: 10.1016/j.nicl.2020.102524

Gilmore, J. H. (2010). Understanding what causes schizophrenia: a developmental perspective. *Am. J. Psychiatry* 167, 8–10. doi: 10.1176/appi.ajp.2009.09111588

Groom, M. J., Bates, A. T., Jackson, G. M., Calton, T. G., Liddle, P. F., and Hollis, C. (2008). Event-related potentials in adolescents with schizophrenia and their siblings: a comparison with attention-deficit/hyperactivity disorder. *Biol. Psychiatry* 63, 784–792. doi: 10.1016/j.biopsych.2007.09.018

Gupta, C. N., Calhoun, V. D., Rachakonda, S., Chen, J., Patel, V., Liu, J., et al. (2015). Patterns of gray matter abnormalities in schizophrenia based on an international mega-analysis. *Schizophr. Bull.* 41, 1133–1142. doi: 10.1093/schbul/sbu177

Hafner, H., Maurer, K., Loffler, W., Bustamante, S., an der Heiden, W., Riechler-Rossler, A., et al. (1995). "Onset and early course of schizophrenia," in *Search for the Causes of Schizophrenia,* eds. H. Hafner and W. F. Gattaz (Berlin: Springer-Verlag), 43–66.

Hamilton, H. K., Woods, S. W., Roach, B. J., Llerena, K., McGlashan, T. H., Srihari, V. H., et al. (2019). Auditory and visual oddball stimulus processing deficits in schizophrenia and the psychosis risk syndrome: forecasting psychosis risk with P300. *Schizophr. Bull.* 45, 1068–1080. doi: 10.1093/schbul/sby167

Hashimoto, T., Arion, D., Unger, T., Maldonado-Avilés, J. G., Morris, H. M., Volk, D. W., et al. (2008). Alterations in GABA-related transcriptome in the dorsolateral prefrontal cortex of subjects with schizophrenia. *Mol. Psychiatry* 13, 147–161. doi: 10.1038/sj.mp.4002011

Hu, W., MacDonald, M. L., Elswick, D. E., and Sweet, R. A. (2015). The glutamate hypothesis of schizophrenia: evidence from human brain tissue studies. *Ann. N. Y. Acad. Sci.* 1338, 38–57. doi: 10.1111/nyas.12547

Hunt, B. A. E., Liddle, E. B., Gascoyne, L. E., Magazzini, L., Routley, B. C., Singh, K. D., et al. (2018). Attenuated Post-movement beta rebound associated with schizotypal features in healthy people. *Schizophr. Bull.* 45, 883–891. doi: 10.1093/schbul/sby117

Jenkinson, N., and Brown, P. (2011). New insights into the relationship between dopamine, beta oscillations and motor function. *Trends Neurosci.* 34, 611–618. doi: 10.1016/j.tins.2011.09.003

Jodo, E., Inaba, H., Narihara, I., Sotoyama, H., Kitayama, E., Yabe, H., et al. (2019). Neonatal exposure to an inflammatory cytokine, epidermal growth factor, results in the deficits of mismatch negativity in rats. *Sci. Rep.* 9:7503. doi: 10.1038/s41598-019-43923-y

Kay, S. R., Fiszbein, A., and Opler, L. A. (1987). The positive and negative syndrome scale (PANSS) for schizophrenia. *Schizophr. Bull.* 13, 261–276.

Kiehl, K. A., and Liddle, P. F. (2001). An event-related functional magnetic resonance imaging study of an auditory oddball task in schizophrenia. *Schizophr. Res.* 48, 159–171. doi: 10.1016/s0920-9964(00)00117-1

Kiehl, K. A., Stevens, M. C., Laurens, K. R., Pearlson, G., Calhoun, V. D., and Liddle, P. F. (2005). An adaptive reflexive processing model of neurocognitive function: supporting evidence from a large scale (n = 100) fMRI study of an auditory oddball task. *Neuroimage* 25, 899–915. doi: 10.1016/j.neuroimage.2004.12.035

Kirihara, K., Tada, M., Koshiyama, D., Fujioka, M., Usui, K., Araki, T., et al. (2020). A predictive coding perspective on mismatch negativity impairment in schizophrenia. *Front. Psychiatry* 11:660. doi: 10.3389/fpsyt.2020.00660

Kolossa, A., Fingscheidt, T., Wessel, K., and Kopp, B. (2012). A model-based approach to trial-by-trial p300 amplitude fluctuations. *Front. Hum. Neurosci.* 6:359. doi: 10.3389/fnhum.2012.00359

Kraepelin, E. (1919). *Dementia Praecox and Paraphrenia (trans M Barclay)*. Edinburgh: Livingstone.

Kumar, V., Vajawat, B., and Rao, N. P. (2021). Frontal GABA in schizophrenia: a meta-analysis of 1H-MRS studies. *World J. Biol. Psychiatry* 22, 1–13. doi: 10.1080/15622975.2020.1731925

Lally, J., Maloudi, S., Krivoy, A., and Murphy, K. C. (2019). Simple schizophrenia: a forgotten diagnosis in psychiatry. *J. Nerv. Ment. Dis.* 207, 721–725. doi: 10.1097/NMD.0000000000000936

Landi, I., Kaji, D. A., Cotter, L., Van Vleck, T., Belbin, G., Preuss, M., et al. (2021). Prognostic value of polygenic risk scores for adults with psychosis. *Nat. Med.* 27, 1576–1581. doi: 10.1038/s41591-021-01475-7

Legge, S. E., Cardno, A. G., Allardyce, J., Dennison, C., Hubbard, L., Pardiñas, A. F., et al. (2021). Associations between schizophrenia polygenic liability, symptom dimensions, and cognitive ability in schizophrenia. *JAMA Psychiatry* 78, 1143–1151. doi: 10.1001/jamapsychiatry.2021.1961

Lesh, T. A., Careaga, M., Rose, D. R., McAllister, A. K., Van de Water, J., Carter, C. S., et al. (2018). Cytokine alterations in first-episode schizophrenia and bipolar disorder: relationships to brain structure and symptoms. *J. Neuroinflammation* 15:165. doi: 10.1186/s12974-018-1197-2

Liddle, E. B., Bates, A. T., Das, D., White, T. P., Groom, M. J., Jansen, M., et al. (2013). Inefficient cerebral recruitment as a vulnerability marker for schizophrenia. *Psychol. Med.* 43, 169–182. doi: 10.1017/S0033291712000992

Liddle, E. B., Price, D., Palaniyappan, L., Brookes, M. J., Robson, S. E., Hall, E. L., et al. (2016). Abnormal salience signaling in schizophrenia: the role of integrative beta oscillations. *Hum. Brain Mapp.* 37, 1361–1374. doi: 10.1002/hbm.23107

Liddle, P. F. (1987). The symptoms of chronic schizophrenia. A re-examination of the positive-negative dichotomy. *Br. J. Psychiatry* 151, 145–151. doi: 10.1192/bjp.151.2.145

Liddle, P. F. (2019). The core deficit of classical schizophrenia: implications for predicting the functional outcome of psychotic illness and developing effective treatments. *Can. J. Psychiatry.* 64, 680–685. doi: 10.1177/0706743719870515

Liddle, P. F., and Morris, D. L. (1991). Schizophrenic syndromes and frontal lobe performance. *Br. J. Psychiatry* 158, 340–345. doi: 10.1192/bjp.158.3.340

Liddle, P. F., Friston, K. J., Frith, C. D., Hirsch, S. R., Jones, T., and Frackowiak, R. S. (1992). Patterns of cerebral blood flow in schizophrenia. *Br. J. Psychiatry* 160, 179–186.

Liddle, P. F., Ngan, E. T. C., Duffield, G., Kho, K., and Warren, A. J. (2002). Signs and symptoms of psychotic illness (SSPI): a rating scale. *Br. J. Psychiatry* 180, 45–50. doi: 10.1192/bjp.180.1.45

Martínez-Montes, E., Cuspineda-Bravo, E. R., El-Deredy, W., Sánchez-Bornot, J. M., Lage-Castellanos, A., and Valdés-Sosa, P. A. (2008). Exploring event-related brain dynamics with tests on complex valued time-frequency representations. *Stat. Med.* 27, 2922–2947. doi: 10.1002/sim.3132

McGorry, P. D., Bell, R. C., Dudgeon, P. L., and Jackson, H. J. (1998). The dimensional structure of first episode psychosis: an exploratory factor analysis. *Psychol. Med.* 28, 935–947. doi: 10.1017/s0033291798006771

Merritt, K., McGuire, P. K., and Egerton, A., (2021). Association of age, antipsychotic medication, and symptom severity in schizophrenia with proton magnetic resonance spectroscopy brain glutamate level: a mega-analysis of individual participant-level data. *JAMA Psychiatry* 78, 667–681. doi: 10.1001/jamapsychiatry.2021.0380

Mota, N. B., Copelli, M., and Ribeiro, S. (2017). Thought disorder measured as random speech structure classifies negative symptoms and schizophrenia diagnosis 6 months in advance. *NPJ Schizophr.* 3:18. doi: 10.1038/s41537-017-0019-3

Ngan, E. T. C., Vouloumanos, A., Cairo, T. A., Laurens, K. R., Bates, A. T., Anderson, C. M., et al. (2003). Abnormal processing of speech during oddball target detection in schizophrenia. *Neuroimage* 20, 889–897. doi: 10.1016/S1053-8119(03)00385-9

Osimo, E. F., Beck, K., Reis Marques, T., and Howes, O. D. (2019). Synaptic loss in schizophrenia: a meta-analysis and systematic review of synaptic protein and mRNA measures. *Mol. Psychiatry* 24, 549–561. doi: 10.1038/s41380-018-0041-5

Palaniyappan, L., and Liddle, P. F. (2012). Aberrant cortical gyrification in schizophrenia: a surface-based morphometry study. *J. Psychiatry Neurosci.* 37, 399–406. doi: 10.1503/jpn.110119

Palaniyappan, L., and Liddle, P. F. (2014). Diagnostic discontinuity in psychosis: a combined study of cortical gyrification and functional connectivity. *Schizophr. Bull.* 40, 675–684. doi: 10.1093/schbul/sbt050

Palaniyappan, L., Crow, T. J., Hough, M., Voets, N. L., Liddle, P. F., James, S., et al. (2013). Gyrification of Broca's region is anomalously lateralized at onset of schizophrenia in adolescence and regresses at 2 year follow-up. *Schizophr. Res.* 147, 39–45. doi: 10.1016/j.schres.2013.03.028

Penttilä, M., Jääskeläinen, E., Hirvonen, N., Isohanni, M., and Miettunen, J. (2014). Duration of untreated psychosis as predictor of long-term outcome in schizophrenia: systematic review and meta-analysis. *Br. J. Psychiatry* 205, 88–94. doi: 10.1192/bjp.bp.113.127753

Pfohl, B., and Winokur, G. (1982). The evolution of symptoms in institutionalized hebephrenic/catatonic schizophrenics. *Br. J. Psychiatry* 141, 567–572. doi: 10.1192/bjp.141.6.567

Rao, R. P., and Ballard, D. H. (1999). Predictive coding in the visual cortex: a functional interpretation of some extra-classical receptive-field effects. *Nat. Neurosci.* 2, 79–87. doi: 10.1038/4580

Rathnaiah, M., Liddle, E. B., Gascoyne, L., Kumar, J., Z, Ul Haq, Katshu, M., et al. (2020). Quantifying the core deficit in classical schizophrenia. *Schizophr. Bull. Open* 1:sgaa031. doi: 10.1093/schizbullopen/sgaa031

Robson, S. E., Brookes, M. J., Hall, E. L., Palaniyappan, L., Kumar, J., Skelton, M., et al. (2016). Abnormal visuomotor processing in schizophrenia. *Neuroimage* 12, 869–878. doi: 10.1016/j.nicl.2015.08.005

Rodrigues-Amorim, D., Rivera-Baltanás, T., Spuch, C., Caruncho, H. J., González-Fernandez, Á, Olivares, J. M., et al. (2018). Cytokines dysregulation in schizophrenia: a systematic review of psychoneuroimmune relationship. *Schizophr. Res.* 197, 19–33. doi: 10.1016/j.schres.2017.11.023

Schultz, W. (1998). Predictive reward signal of dopamine neurons. *J. Neurophysiol.* 80, 1–27. doi: 10.1152/jn.1998.80.1.1

Seeley, W. W., Menon, V., Schatzberg, A. F., Keller, J., Glover, G. H., Kenna, H., et al. (2007). Dissociable intrinsic connectivity networks for salience processing and executive control. *J. Neurosci.* 27, 2349–2356. doi: 10.1523/JNEUROSCI.5587-06.2007

Sheffield, J. M., Huang, A. S., Rogers, B. P., Blackford, J. U., Heckers, S., and Woodward, N. D. (2021). Insula sub-regions across the psychosis spectrum: morphology and clinical correlates. *Transl. Psychiatry* 11:346. doi: 10.1038/s41398-021-01461-0

Sherman, M. A., Lee, S., Law, R., Haegens, S., Thorn, C. A., Hämäläinen, M. S., et al. (2016). Neural mechanisms of transient neocortical beta rhythms: converging evidence from humans, computational modeling, monkeys, and mice. *Proc. Natl. Acad. Sci. U.S.A.* 113, E4885–E4894. doi: 10.1073/pnas.1604135113

Shi, J., Levinson, D. F., Duan, J., Sanders, A. R., Zheng, Y., Pe'er, I., et al. (2009). Common variants on chromosome 6p22.1 are associated with schizophrenia. *Nature* 460, 753–757. doi: 10.1038/nature08192

Silverstein, S. M., and Keane, B. P. (2011). Perceptual organization impairment in schizophrenia and associated brain mechanisms: review of research from 2005 to 2010. *Schizophr. Bull.* 37, 690–699. doi: 10.1093/schbul/sbr052

Silverstein, S. M., Berten, S., Essex, B., Kovács, I., Susmaras, T., and Little, D. M. (2009). An fMRI examination of visual integration in schizophrenia. *J. Integr. Neurosci.* 8, 175–202. doi: 10.1142/s0219635209002113

Sridharan, D., Levitin, D. J., and Menon, V. (2008). A critical role for the right fronto-insular cortex in switching between central-executive and default-mode networks. *PNAS* 105, 12569–12574. doi: 10.1073/pnas.0800005105

Sterzer, P., Voss, M., Schlagenhauf, F., and Heinz, A. (2019). Decision-making in schizophrenia: a predictive-coding perspective. *Neuroimage* 190, 133–143. doi: 10.1016/j.neuroimage.2018.05.074

Sydnor, V. J., and Roalf, D. R. (2020). A meta-analysis of ultra-high field glutamate, glutamine, GABA and glutathione 1HMRS in psychosis: implications for studies of psychosis risk. *Schizophr. Res.* 226, 61–69. doi: 10.1016/j.schres.2020.06.028

Tan, H., Jenkinson, N., and Brown, P. (2014). Dynamic neural correlates of motor error monitoring and adaptation during trial-to-trial learning. *J. Neurosci.* 34, 5678–5688. doi: 10.1523/JNEUROSCI.4739-13.2014

Tan, H., Wade, C., and Brown, P. (2016). Post-Movement beta activity in sensorimotor cortex indexes confidence in the estimations from internal models. *J. Neurosci.* 36, 1516–1528. doi: 10.1523/JNEUROSCI.3204-15.2016

Tonna, M., Ossola, P., Marchesi, C., Bettini, E., Lasalvia, A., Bonetto, C., et al. (2019). Dimensional structure of first episode psychosis. *Early Interv. Psychiatry* 13, 1431–1438.

Urios, A., Ordoño, F., García-García, R., Mangas-Losada, A., Leone, P., José Gallego, J., et al. (2019). Tadalafil treatment improves inflammation, cognitive function, and mismatch negativity of patients with low urinary tract symptoms and erectile dysfunction. *Sci. Rep.* 9:17119. doi: 10.1038/s41598-019-53136-y

Watanabe, Y., Someya, T., and Nawa, H. (2010). Cytokine hypothesis of schizophrenia pathogenesis: evidence from human studies and animal models. *Psychiatry Clin. Neurosci.* 64, 217–230. doi: 10.1111/j.1440-1819.2010.02094.x

White, T., and Hilgetag, C. C. (2011). Gyrification and neural connectivity in schizophrenia. *Dev. Psychopathol.* 23, 339–352. doi: 10.1017/S0954579410000842

Winterer, G., Coppola, R., Goldberg, T. E., Egan, M. F., Jones, D. W., Sanchez, C. E., et al. (2004). Prefrontal broadband noise, working memory, and genetic risk for schizophrenia. *Am. J. Psychiatry* 161, 490–500. doi: 10.1176/appi.ajp.161.3.490

Wolpert, D. M., and Ghahramani, Z. (2000). Computational principles of movement neuroscience. *Nat. Neurosci.* 3, 1212–1217. doi: 10.1038/81497

World Health Organisation (2018). *ICD-11 [Internet]*. Available online at: https://icd.who.int/en (accessed May 29, 2021).

Xia, M., Wang, J., and He, Y. (2013). BrainNet viewer: a network visualization tool for human brain connectomics. *PLoS One* 8:e68910. doi: 10.1371/journal.pone.0068910

Ziermans, T., de Wit, S., Schothorst, P., Sprong, M., van Engeland, H., Kahn, R., et al. (2014). Neurocognitive and clinical predictors of long-term outcome in adolescents at ultra-high risk for psychosis: a 6-year follow-up. *PLoS One* 9:e93994. doi: 10.1371/journal.pone.0093994

Conflict of Interest: The authors declare that the research was conducted in the absence of any commercial or financial relationships that could be construed as a potential conflict of interest.

frontiers | Frontiers in Human Neuroscience

ORIGINAL RESEARCH
published: 11 May 2022
doi: 10.3389/fnhum.2022.878028

Regularized Functional Connectivity in Schizophrenia

Raymond Salvador[1,2], Paola Fuentes-Claramonte[1,2], María Ángeles García-León[1,2], Núria Ramiro[3], Joan Soler-Vidal[1,2,4], María Llanos Torres[5], Pilar Salgado-Pineda[1,2], Josep Munuera[6], Aristotle Voineskos[7,8] and Edith Pomarol-Clotet[1,2]*

[1] FIDMAG Germanes Hospitalàries Research Foundation, Barcelona, Spain, [2] Centro de Investigación Biomédica en Red de Salud Mental, Barcelona, Spain, [3] Department of Psychiatry, Hospital Sant Rafael, Barcelona, Spain, [4] Benito Menni Centre Assistencial en Salut Mental, Sant Boi de Llobregat, Barcelona, Spain, [5] Hospital Mare de Déu de la Mercé, Unitat Polivalent, Barcelona, Spain, [6] Department of Diagnostic Imaging, Hospital Sant Joan de Déu, Barcelona, Spain, [7] Campbell Family Mental Health Research Institute, Toronto, ON, Canada, [8] Department of Psychiatry, University of Toronto, Toronto, ON, Canada

OPEN ACCESS

Edited by:
Franziska Knolle, Technical University of Munich, Germany

Reviewed by:
Zonglei Zhen, Beijing Normal University, China
Mete Ozay, Samsung Research and Development Institute, United Kingdom
Jing Wang, Xinyang Normal University, China
Lena Kaethe Linda Oestreich, The University of Queensland, Australia

***Correspondence:**
Raymond Salvador
rsalvador@fidmag.com

Specialty section:
This article was submitted to Brain Imaging and Stimulation, a section of the journal Frontiers in Human Neuroscience

Received: *17 February 2022*
Accepted: *04 April 2022*
Published: *11 May 2022*

Citation:
Salvador R, Fuentes-Claramonte P, García-León MÁ, Ramiro N, Soler-Vidal J, Torres ML, Salgado-Pineda P, Munuera J, Voineskos A and Pomarol-Clotet E (2022) Regularized Functional Connectivity in Schizophrenia. Front. Hum. Neurosci. 16:878028. doi: 10.3389/fnhum.2022.878028

Regularization may be used as an alternative to dimensionality reduction when the number of variables in a model is much larger than the number of available observations. In a recent study from our group regularized regression was employed to quantify brain functional connectivity in a sample of healthy controls using a brain parcellation and resting state fMRI images. Here regularization is applied to evaluate resting state connectivity abnormalities at the voxel level in a sample of patients with schizophrenia. Specifically, ridge regression is implemented with different degrees of regularization. Results are compared to those delivered by the weighted global brain connectivity method (GBC), which is based on averaged bivariate correlations and from the non-redundant connectivity method (NRC), a dimensionality reduction approach that applies supervised principal component regressions. Ridge regression is able to detect a larger set of abnormally connected regions than both GBC and NRC methods, including schizophrenia related connectivity reductions in fronto-medial, somatosensory and occipital structures. Due to its multivariate nature, the proposed method is much more sensitive to group abnormalities than the GBC, but it also outperforms the NRC, which is multivariate too. Voxel based regularized regression is a simple and sensitive alternative for quantifying brain functional connectivity.

Keywords: resting state fMRI, schizophrenia, functional connectivity, ridge regression, global brain connectivity

INTRODUCTION

Usage of regularization methods is obiquitous in estimating problems involving high dimensionality data (Bühlmann and Van De Geer, 2011). In MRI, where voxels are the primary unit of information representation, there may be from tens to hundreds of thousands of values characterizing an imaged brain. However, comprehensive analyses on such large data entities have been usually preceded by dimensionality reduction steps such as principal component analysis, independent component analysis, and partial least squares (Calhoun et al., 2009; McIntosh and Misic, 2013; Salvador et al., 2017) which drastically reduce the number of variables to be considered in the following analyses.

Specifically, in the field of functional connectivity one may use this newly generated subset of low dimensionality variables to fit linear models quantifying the connectivity between a single voxel and the remaining gray matter voxels of the brain (Salvador et al., 2017). These models may be

considered as truly multivariate models, in contrast to other voxel level connectivity measures that are simple averages of bivariate correlations between the target voxel and the rest of voxels in the brain, as proposed by the weighted Global Brain Connectivity (GBC) method (Cole et al., 2010).

As an alternative to dimensionality reduction methods, regularization techniques allow fitting models directly to the original data by applying constraints on the parameter estimates of the fitted models (Hastie et al., 2009). This approach was recently proposed by our group and applied to analyze age and gender related connectivity patterns in a sample of healthy controls scanned at rest (Salvador et al., 2020). In this first study, mean time series from 246 regions of interest (ROIs) from the Brainnetome atlas (Fan et al., 2016) were used as input data for the regularized regressions (ridge and random forest regressions) and results obtained were compared to those delivered by the GBC, finding distinct connectivity patterns between both approximations, which were especially relevant in the age-related analyses (Salvador et al., 2020).

Such methods may also be useful in improving understanding of psychiatric disorders, such as schizophrenia. One of the most accepted ethiological hypotheses for schizophrenia is the dysconnection hypothesis (Weinberger, 1993; Friston and Frith, 1995) which states that symptoms in patients with schizophrenia arise from abnormalities in brain connectivity at several levels (Friston et al., 2016). While there are many MRI connectivity studies with significant results summarized in recent meta-analyses (e.g., Zhou et al., 2015; Giraldo-Chica and Woodward, 2017). the application and evaluation of newly developed connectivity methods remains of high interest in schizophrenia.

Here we apply one of the regularization methods used in our previous study (ridge regression) to evaluate differences in resting state connectivity between a sample of N = 74 patients with schizophrenia and N = 74 healthy controls matched for gender, age, and premorbid IQ. The association with clinical severity is also evaluated in a larger sample of N = 148 patients. Results are compared to those provided by the GBC method and by the non-redundant connectivity method (NRC) (Salvador et al., 2017), a dimensionality reduction approach that applies supervised principal component regressions (Bair et al., 2006; Hastie et al., 2009). We also extend the previous implementation of ridge regression by directly considering voxels instead of ROIs as inputs for the analyses.

MATERIALS AND METHODS

Regularized Brain Connectivity

Ideally, if scanning time was not a constraint and image acquisition was carried out indefinitely, the number of recorded time observations (N) would eventually exceed the number of voxels (p) and a simple linear estimate of the association between one voxel i and the remaining gray matter voxels in the brain could be obtained by ordinary least squares (OLS). Under this theoretical scenario, the multiple regression equation would give the predicted time series for the target voxel ($\hat{Y}_i$)

$$\hat{Y}_i = \beta_0 + \beta_1 Y_1 + \ldots + \beta_{i-1} Y_{i-1} + \beta_{i+1} Y_{i+1} + \ldots + \beta_p Y_p \quad (1)$$

and a simple measure of functional connectivity for this voxel would be provided by the multiple correlation coefficient

$$Cor\left(\hat{Y}_i,\ Y_i\right) \quad (2)$$

which quantifies the degree of similarity between the expected ($\hat{Y}_i$) and observed (Y_i) time series of voxel i, and which is given by the square root of the coefficient of determination (i.e., R^2, a standard ouput from regression analyses).

However, in a real fMRI dataset the number of voxels is much larger than the number of time points (N≪p) and OLS is not feasible. This limitation may be overcome by drastically reducing the number of variables through dimensionality reduction or by considering ROIs from a brain parcellation. Here, though, there is also the alternative of using a regularization approach.

Specifically, regularization through ridge regression allows obtaining $\hat{Y}_i$ by setting a restriction on the parameter estimates of Equation 1

$$\sum_{i=1}^{p} \beta_i^2 \ < \ ct \quad (3)$$

(where *ct* stands for constant value). Such restriction may be restated as a constrained least-squares minimization regulated by a Lagrange multiplier ($\lambda \geq 0$)

$$\sum_{j=1}^{N} (y_{ij} - (\beta_0 + \beta_1 y_{1,j} + \ldots + \beta_{i-1} y_{i-1,j} + \beta_{i+1} y_{i+1,j} + \ldots + \beta_p y_{p,j}))^2 + \lambda \sum_{i=1}^{p} \beta_i^2 \quad (4)$$

where $y_{i,1}, \ldots, y_{i,N}$ stand for the individual components (time points) of Y_i.

Here, the selection of an adequate value for λ (the regularization parameter) will be important in order to achieve a good balance between bias and variance (i.e., to find a model that avoids overfitting while not being not too constrained). Furthermore, some aspects will have to be considered for the validity of ridge regression in the framework of regularized brain connectivity (RBC). Apart from the usual rescaling of variables (time series) to unit variance, λ values will have to remain fixed through all voxels and individuals, otherwise estimates of Equation 2 will not be comparable. Unfortunately, due to the lack of independence between observations in time series, the habitual cross-validation methods will not be suitable. Since there is no easy alternative to cross-validation in the current framework, we have decided to report results using a wide range of λ values (0.5, 1, 5, 10, 50, 100, and 500). All ridge regressions have been carried out with functions contained in the glmnet R library (Friedman et al., 2010).

To highlight the multivariate nature of the RBC, results obtained have been compared to those provided by simple averages of bivariate correlations. To do so, the weighted Global

TABLE 1 | Summary of demographic and clinical data.

	All patients (*N* = 148)	Matched patients (*N* = 74)	Matched controls (*N* = 74)	Statistical tests and *p*-values
Gender	97M/51F	43M/31F	43M/31F	$\chi^2 = 0$, *p*val = 1.00
Age	42.37 (10.97)	41.12 (11.83)	38.09 (13.65)	t = –1.44, *p*val = 0.15
Premorbid IQ	21.15 (4.79)	23.14 (4.34)	23.12 (4.49)	*t* = –0.02, *p*val = 0.98
Positive Syndrome	10.41 (4.61)	10.93 (5.15)		
Negative Syndrome	14.02 (6.60)	12.86 (6.41)		
Disorganization Syndrome	7.01 (2.43)	6.74 (2.27)		

Absolute frequencies for gender, and mean and standard deviations for age, Premorbid IQ (as estimated by the Word Accentuation Test) and the three Liddle Syndromes extracted from the PANSS scale are reported together with results from statistical tests comparing values for the matched samples of patients and healthy controls.

Brain Connectivity (GBC) method (Cole et al., 2010) has been also applied to the resting state images. Specifically, averages of absolute values of all bivariate correlations involving each specific voxel have been calculated. Results from the RBC have been also compared to connectivity estimates obtained through supervised principal component regressions (Bair et al., 2006; Hastie et al., 2009), a dimensionality reduction approach applied to quantify brain connectivity from fMRI images (Salvador et al., 2017).

Participants

A sample of $N = 148$ patients with a diagnosis of schizophrenia according to DSM-IV criteria (i.e. excluding patients with schizoaffective and other schizophrenia related disorders) were recruited from three hospitals from Germanes Hospitalàries located in the Province of Barcelona, Spain (Hospital Bennito Meni C.A.S.M., Hospital Sant Rafael and Hospital de la Mercè). All patients but two were taking antipsychotic medication (atypical $N = 109$, typical $N = 9$, both $N = 24$, unknown $N = 3$, equivalents of Chlorpromazine: 508.82 mg (mean), 517.55 mg (SD). A second sample of $N = 74$ healthy controls were recruited from non-medical hospital staff, their relatives and acquaintances, plus independent sources in the community.

Controls reporting a history of mental illness and/or treatment with psychotropic medication or with a psychotic first-degree relative were not included. All individuals in both samples were right handed, aged 18–65, with no history of brain trauma or neurological disease, and not having shown alcohol/substance abuse in the last 12 months. All subjects gave written informed consent before participation and the study procedures were approved by the Comité de Ética de la Investigación de FIDMAG Hermanas Hospitalarias and adhered to the Declaration of Helsinki.

Image Acquisition and Processing

Participants underwent a single MRI session in a 3.0 Tesla Philips Ingenia machine located in the Hospital Sant Joan de Déu (Barcelona, Spain) in which a resting state functional MRI (fMRI) sequence and a T1 structural image for anatomical reference were acquired. Parameters for the resting fMRI bold sequence were: TR = 2,000 ms, TE = 30 ms, flip angle = 70°, in-plane resolution = 3.5 mm × 3.5 mm, FOV = 238 mm × 245 mm, slice thickness = 3.5 mm, inter-slice gap = 0.75 mm, number of volumes = 256. Slices (32 per volume) were acquired with an interleaved order parallel to the AC-PC plane. The T1 image was acquired using a Fast Field Echo (FFE) with TR = 9.90 ms; TE = 4.60 ms; Flip angle = 8°; voxel size = 1 mm × 1 mm; slice thickness = 1 mm; slice number = 180; FOV = 240 mm). fMRI preprocessing steps included movement correction, spike scrubbing, regression of noise-independent components, non-linear normalization to the Montreal Neurological Institute space, regression of noise from ventricles and white matter, and low-frequency filtering in the 0.1–0.02 Hz interval (Salvador et al., 2017). Specifically, for the regression of noise-independent components, individual independent component analyses were previously run with Melodic, a module included in FSL (Smith et al., 2004) and those components showing clear noise patterns (most frequently edge effects due to movement) were selected. Time series of the selected components were regressed out from the time series of each voxel, and residuals were kept as the denoised time series.

Prior to the calculation of the RBC, GBC, and NRC maps a common gray matter mask was applied to the normalized fMRI images. Then, fMRI volumes were resampled to a 4 mm × 4 mm × 4 mm voxel in order to reduce computational costs. Finally, values from the individual RBC, GBC, and NRC maps where Fisher transformed before carrying out the group analyses.

Group Comparisons and Group Level Regressions

A subsample of $N = 74$ patients matched for gender, age and premorbid IQ to the sample of $N = 74$ controls was selected from the original sample of patients before carrying out group comparisons in RBC, GBC, and NRC. Premorbid IQ was estimated with the Word Accentuation Test (Del Ser et al., 1997). Positive and Negative Syndrome Scale (PANSS) scores (Kay et al., 1987) were used to calculate values of the three Liddle Syndromes (Positive, Negative, and Disorganization) (Liddle, 1987) for all $N = 148$ patients, and regressions between RBC, GBC, and NRC and clinical severity as measured by the three Syndromes were performed in this larger sample. In the regression analyses, age, gender, type of antipsychotic medication (atypical and/or typical) and dose of medication (equivalents of Chlorpromazine) were considered as nuisance covariates. In all analyses statistical significance was derived from permutation tests carried out using the randomize function included in FSL

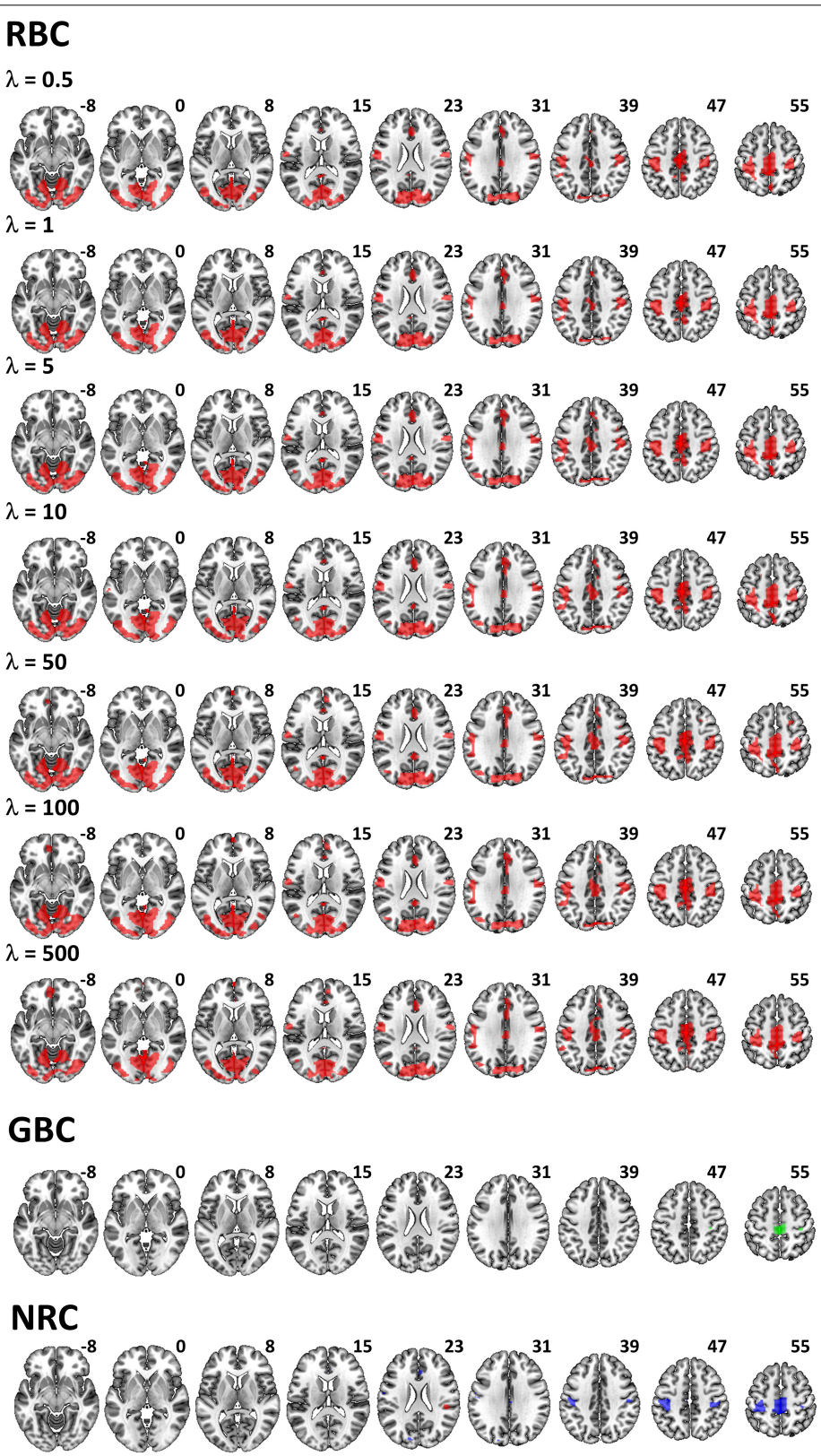

FIGURE 1 | Brain areas with significant differences in RBC, GBC and NRC between patients and healthy controls. RBC results are given for the different regularization values (λ values) applied in the ridge regressions. While for the RBC (red) and GBC (green), comparisons only included reductions in connectivity, significant disorder related reductions (blue) and increases (red) were observed with the NRC (although the later were of much smaller extent).

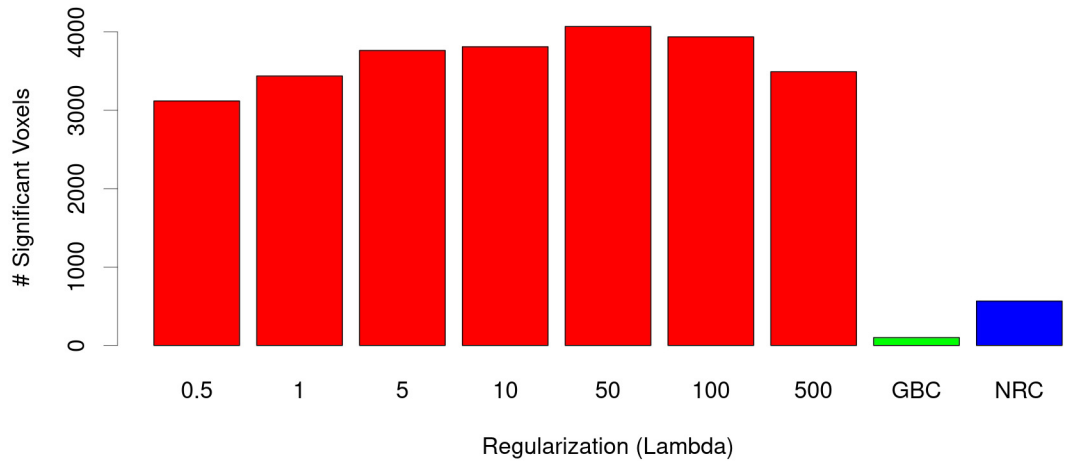

FIGURE 2 | Number of voxels with significant reductions in RBC connectivity in patients as a function of λ (red bars). Most extensive abnormalities were observed with λ = 50. In all cases these were much larger than reductions observed with the GBC (green) and the NRC (blue).

(Smith et al., 2004) and applying the Threshold-Free Cluster Enhancement (TFCE) method.

RESULTS

A summary of clinical and demographical data for the initial sample of patients with schizophrenia and for the matched samples of patients and healthy controls is provided in **Table 1**.

Group Analyses

When RBC maps from patients were compared to those of healthy controls only areas of significant reductions in connectivity were found. As shown in **Figure 1**, this pattern was consistent through all regularization values. Tests performed with λ = 50 produced the most extensive differences (**Figure 2**) including bilateral connectivity reductions in the supplementary motor area, paracentral lobule, precentral and postcentral gyri, precuneus, dorsal and anterior cingulate, ventromedial and right dorsolateral prefrontal cortex, cuneus, calcarine, lingual, lateral occipital areas and parts of the cerebellum.

All λ values applied led to much more widespread patterns of differences than those provided by both the GBC and NRC methods, which were mainly restricted to connectivity reductions in clusters of moderate size in the supplementary motor area / paracentral lobule and postcentral gyrus (**Figure 1**). As shown in **Figure 2**, though, reductions in the NRC were clearly larger than those observed with the GBC. A cluster of increased connectivity in patients was also observed in the right Rolandic operculum (**Figure 1**).

Clinical Covariates

When RBC maps were correlated with scores of the three Liddle Syndromes, a decreasing pattern of connectivity was observed for the Negative Syndrome (**Figure 3A**). This negative association involved a cluster located in the left occipital cortex (clusters shown in **Figure 3** are based on analyses using λ = 50, which led to most extensive differences in the group comparison). Another cluster of negative association with the Negative Syndrome was observed for the GBC, which was also in the occipital cortex, although with a more medial position. The GBC also showed two clusters of negative association with the Disorganization Syndrome, one of them located in the right fusiform area, and the other in the right posterior insula (**Figure 3B**). The later was also the site for the only significant cluster observed with the NRC, which was of small size and was also negatively correlated with the Disorganization Syndrome. No significant associations were found between any of the three connectivity measures and the Positive Syndrome.

DISCUSSION

As shown by the results, the RBC is much more sensitive to group differences between patients with schizophrenia and healthy controls than the GBC. The RBC and the GBC are looking at different aspects of brain connectivity. While the GBC only accounts for net differences in bivariate correlations, the RBC is a truly multivariate measure and, consequently, it may be much more sensitive to local changes in brain connectivity (changes that may go unnoticed after the averaging operation carried out by the GBC). Still, as shown by the associations found with the Liddle syndromes, the GBC may convey relevant information. Unexpectedly, the NRC, a method that is also multivariate, did not perform as sensitively as the RBC in the group comparisons, suggesting that regularization may be a better option for quantifying functional connectivity than dimensionality reduction. However, this statement may require testing through exhaustive analyses.

Results found here are, to some extent, similar to those reported in previous studies using similar methods. In a prior study on patients with schizophrenia using the GBC (Cole et al., 2011) the authors only found reduced frontal connectivity in the primary (non seed based) analyses. A similar pattern of frontal

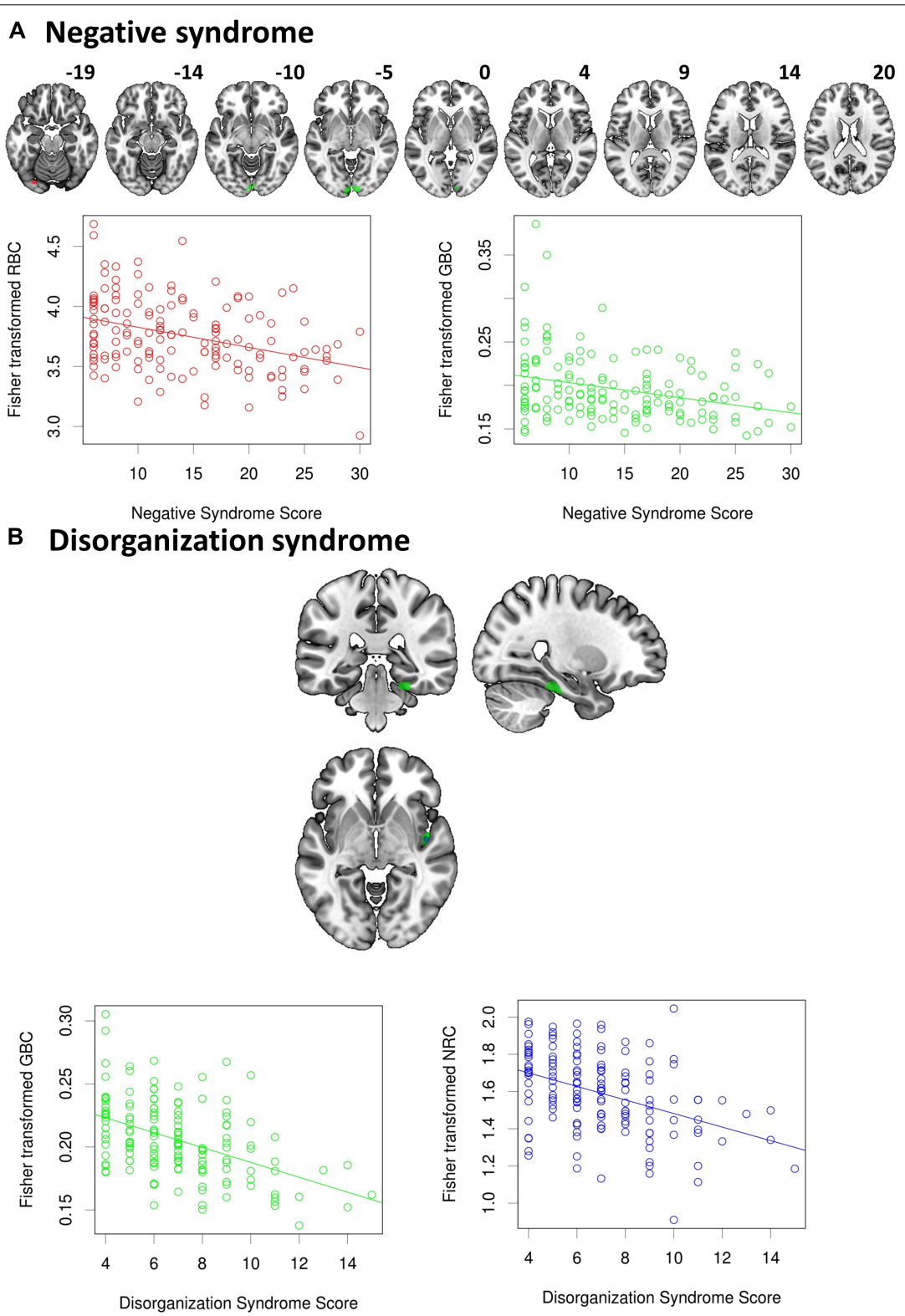

FIGURE 3 | Significant associations between scores from the Liddle syndromes and connectivity levels. While **(A)** a negative relation was observed between the Negative syndrome and both the RBC and GBC in occipital areas, **(B)** the Disorganization syndrome was negatively correlated with the GBC and the NRC, but the latter only involved a very small cluster located in the right posterior insula. No association was found with positive syndrome scores.

connectivity reduction was observed in another study using GBC in schizophrenia (Yang et al., 2014) although this pattern was reversed when the global brain signal was ignored in the pre-processing phase [regrettably, pre-processing steps may have a significant effect on resting state results (Caballero-Gaudes and Reynolds, 2017)]. Using global Functional Connectivity Density mapping (gFCD), an approach similar to GBC, based on the number of correlations above a certain threshold connecting each voxel (Tomasi and Volkow, 2010), Zhuo et al. (2017) also reported a similar pattern of disconnections in patients with schizophrenia, which included reductions in connectivity in postcentral gyri, occipital cortex, temporo-occipital conjunction, and inferior parietal lobule, although these authors also found increases in subcortical structures. On the other hand, the only study using NRC in patients with schizophrenia, which was conducted at our institution in another sample of patients and healthy controls, revealed a similar pattern of disconnection in somatosensory and occipital regions (Salvador et al., 2017), although a small cluster of increased connectivity was also found in the Caudate and no significant differences were reported for the GBC.

The dominance of reduced connectivity in these results agrees with recent meta-analyses on schizophrenia (Dong et al., 2018; Doucet et al., 2020). However, the reported abnormalities may not be restricted to schizophrenia since, although with different intensities, they have been also described in other psychotic disorders such as the bipolar disorder or major depression disorder (Xia et al., 2019). Still, they seem to be more prominent in schizophrenia (Li et al., 2021).

As previously explained in the methods, some aspects should be kept in mind in order to avoid biases and inconsistencies when applying the RBC. Most importantly λ should be kept fixed through all analyses. The selection of its value is also of relevance, as a good trade-off between variance and bias should be achieved. Unfortunately, there is no a *priori* rule for the selection of λ as its optimal value will depend on many sample specific aspects such as the number of voxels or the degree of autocorrelation and length of time series. Even so, as shown by the stability of results reported in our study using a wide range of λ values, it may be concluded that λ selection, although relevant, it does not require high accuracy.

In summary, in this study we prove that regularization, and specifically ridge regression, may be a feasible alternative to dimensionality reduction for multivariate functional connectivity estimation, even if applied at the voxel level. The regularized brain connectivity approach is able to detect a much extended set of abnormally connected regions than those detected by the global brain connectivity and the non-redundant brain connectivity methods when it is applied to a sample of patients with schizophrenia.

DATA AVAILABILITY STATEMENT

The data analyzed in this study is subject to the following licenses/restrictions: The data supporting the conclusions of this article will be made available by the authors upon sensible request. Requests to access these datasets should be directed to RS, rsalvador@fidmag.com.

ETHICS STATEMENT

The studies involving human participants were reviewed and approved by Comité de Ética de la Investigación Clínica (CEIC-CEI) FIDMAG Hermanas Hospitalarias. The patients/participants provided their written informed consent to participate in this study.

AUTHOR CONTRIBUTIONS

RS, PF-C, AV, and EP-C designed the study. PF-C, MG-L, NR, JS-V, MT, JM, PS-P, RS, and EP-C collected the data. RS, AV, and EP-C analyzed the data. RS and EP-C wrote the manuscript. All authors reviewed the written text.

FUNDING

This work was supported by several grants funded by the Instituto de Salud Carlos III and the Spanish Ministry of Science, Innovation, and Universities (co-funded by the European Regional Development Fund/European Social Fund "Investing in your future"): Miguel Servet Research Contract (CPII16/00018 to EP-C), Research Mobility programme (MV18/00054 to EP-C), Research Projects (PI18/00877 and PI21/00525 to RS, PI14/01148 to EP-C). It has also been supported by the Centro de Investigación Biomédica en Red de Salud Mental and the Generalitat de Catalunya: 2014SGR1573 to EP-C and SLT006/17/357 from the Departament de Salut to RS. Support has also been received from Secretaria d'Universitats i Recerca del Departament d'Economia i Coneixement (2017 SGR 1365) and the CERCA Programme/Generalitat de Catalunya. The study has been supported by a BITRECS project conceded to NV. BITRECS project has received funding from the European Union's Horizon 2020 Research and Innovation Programme under the Marie Skłodowska-Curie grant agreement No. 754550 and from "La Caixa" Foundation (ID 100010434), under the agreement LCF/PR/GN18/50310006.

REFERENCES

Bair, E., Hastie, T., Debashis, P., and Tibshirani, R. (2006). Prediction by supervised principal components. *J. Am. Stat. Assoc.* 473, 119–137. doi: 10.1198/016214505000000628

Bühlmann, P., and Van De Geer, S. (2011). *Statistics For High-Dimensional Data*. Berlin: Springer-Verlag.

Caballero-Gaudes, C., and Reynolds, R. C. (2017). Methods for cleaning the BOLD fMRI signal. *Neuroimage* 154, 128–149. doi: 10.1016/j.neuroimage.2016.12.018

Calhoun, V. D., Liu, J., and Adali, T. (2009). A review of group ICA for fMRI data and ICA for joint inference of imaging, genetic, and ERP data. *Neuroimage* 45, S163–S172. doi: 10.1016/j.neuroimage.2008.10.057

Cole, M. W., Anticevic, A., Repovs, G., and Barch, D. (2011). Variable global dysconnectivity and individual differences in schizophrenia. *Biol. Psychiatry* 70, 43–50. doi: 10.1016/j.biopsych.2011.02.010

Cole, M. W., Pathak, S., and Schneider, W. (2010). Identifying the brain's most globally connected regions. *Neuroimage* 49, 3132–3148. doi: 10.1016/j.neuroimage.2009.11.001

Del Ser, T., González-Montalvo, J. I., Martínez-Espinosa, S., Delgado-Villapalos, C., and Bermejo, F. (1997). Estimation of premorbid intelligence in spanish people with the word accentuation test and its application to the diagnosis of dementia. *Brain Cogn.* 33, 343–356. doi: 10.1006/brcg.1997.0877

Dong, D., Wang, Y., Chang, X., Luo, C., and Yao, D. (2018). Dysfunction of large-scale brain networks in schizophrenia: a meta-analysis of resting-state functional connectivity. *Schizophr. Bull.* 44, 168–181. doi: 10.1093/schbul/sbx034

Doucet, G. E., Janiri, D., Howard, R., O'Brien, M., Andrews-Hanna, J. R., and Frangou, S. (2020). Transdiagnostic and disease-specific abnormalities in the default-mode network hubs in psychiatric disorders: A meta-analysis of resting-state functional imaging studies. *Eur. Psychiatry* 63:e57. doi: 10.1192/j.eurpsy.2020.57

Fan, L., Li, H., Zhuo, J., Zhang, Y., Wang, J., Chen, L., et al. (2016). The human brainnetome atlas: a new brain atlas based on connectional architecture. *Cereb. Cortex* 26, 3508–3526. doi: 10.1093/cercor/bhw157

Friedman, J., Hastie, T., and Tibshirani, R. (2010). Regularization paths for generalized linear models *via* coordinate descent. *J. Stat. Softw.* 33, 1–22.

Friston, K. J., and Frith, C. D. (1995). Schizophrenia: a disconnection syndrome? *Clin. Neurosci.* 3, 89–97.

Friston, K., Brown, H. R., Siemerkus, J., and Stephan, K. E. (2016). The dysconnection hypothesis (2016). *Schizophr. Res.* 176, 83–94. doi: 10.1016/j.schres.2016.07.014

Giraldo-Chica, M., and Woodward, N. D. (2017). Review of thalamocortical resting-state fMRI studies in schizophrenia. *Schizophr. Res.* 180, 58–63. doi: 10.1016/j.schres.2016.08.005

Hastie, T., Tibshirani, R., and Friedman, J. (2009). *The Elements of Statistical Learning: Data Mining, Inference, and Prediction*. Berlin: Springer.

Kay, S. R., Fiszbein, A., and Opler, L. A. (1987). The positive and negative syndrome scale (PANSS) for schizophrenia. *Schizophr. Bull.* 13, 261–276. doi: 10.1093/schbul/13.2.261

Li, C., Dong, M., Womer, F. Y., Han, S., Yin, Y., Jiang, X., et al. (2021). Transdiagnostic time-varying dysconnectivity across major psychiatric disorders. *Hum. Brain Mapp.* 42, 1182–1196. doi: 10.1002/hbm.25285

Liddle, P. F. (1987). The symptoms of chronic schizophrenia. A re-examination of the positive-negative dichotomy. *Br. J. Psychiatry* 151, 145–151. doi: 10.1192/bjp.151.2.145

McIntosh, A. R., and Misic, B. (2013). Multivariate statistical analyses for neuroimaging data. *Annu. Rev. Psychol.* 64, 499–525. doi: 10.1146/annurev-psych-113011-143804

Salvador, R., Landin-Romero, R., Anguera, M., Canales-Rodríguez, E. J., Radua, J., Guerrero-Pedraza, A., et al. (2017). Non redundant functional brain connectivity in schizophrenia. *Brain Imaging Behav.* 11, 552–564. doi: 10.1007/s11682-016-9535-4

Salvador, R., Verdolini, N., Garcia-Ruiz, B., Jiménez, E., Sarró, S., Vilella, E., et al. (2020). Multivariate brain functional connectivity through regularized estimators. *Front. Neurosci.* 14:569540. doi: 10.3389/fnins.2020.569540

Smith, S. M., Jenkinson, M., Woolrich, M. W., Beckmann, C. F., Behrens, T. E., Johansen-Berg, H., et al. (2004). Advances in functional and structural MR image analysis and implementation as FSL. *Neuroimage* 23, S208–S219. doi: 10.1016/j.neuroimage.2004.07.051

Tomasi, D., and Volkow, N. D. (2010). Functional connectivity density mapping. *Proc. Natl. Acad. Sci. U.S.A.* 107, 9885–9890. doi: 10.1073/pnas.1001414107

Weinberger, D. R. (1993). A connectionist approach to the prefrontal cortex. *J. Neuropsychiatry Clin. Neurosci.* 5, 241–253. doi: 10.1176/jnp.5.3.241

Xia, M., Womer, F. Y., Chang, M., Zhu, Y., Zhou, Q., Edmiston, E. K., et al. (2019). Shared and distinct functional architectures of brain networks across psychiatric disorders. *Schizophr. Bull.* 45, 450–463. doi: 10.1093/schbul/sby046

Yang, G. J., Murray, J. D., Repovs, G., Cole, M. W., Savic, A., Glasser, M. F., et al. (2014). Altered global brain signal in schizophrenia. *Proc. Natl. Acad. Sci. U.S.A.* 111, 7438–7443. doi: 10.1073/pnas.1405289111

Zhou, Y., Fan, L., Qiu, C., and Jiang, T. (2015). Prefrontal cortex and the dysconnectivity hypothesis of schizophrenia. *Neurosci. Bull.* 31, 207–219. doi: 10.1007/s12264-014-1502-8

Zhuo, C., Zhu, J., Wang, C., Qu, H., Ma, X., Tian, H., et al. (2017). Brain structural and functional dissociated patterns in schizophrenia. *BMC Psychiatry* 17:45. doi: 10.1186/s12888-017-1194-5

Conflict of Interest: The authors declare that the research was conducted in the absence of any commercial or financial relationships that could be construed as a potential conflict of interest.

Publisher's Note: All claims expressed in this article are solely those of the authors and do not necessarily represent those of their affiliated organizations, or those of the publisher, the editors and the reviewers. Any product that may be evaluated in this article, or claim that may be made by its manufacturer, is not guaranteed or endorsed by the publisher.

frontiers | Frontiers in Human Neuroscience

ORIGINAL RESEARCH
published: 13 June 2022
doi: 10.3389/fnhum.2022.917270

Different Frequency of Heschl's Gyrus Duplication Patterns in Neuropsychiatric Disorders: An MRI Study in Bipolar and Major Depressive Disorders

Tsutomu Takahashi[1,2], Daiki Sasabayashi[1,2], Murat Yücel[3], Sarah Whittle[4], Valentina Lorenzetti[5], Mark Walterfang[4,6,7], Michio Suzuki[1,2], Christos Pantelis[4,7,8], Gin S. Malhi[9,10] and Nicholas B. Allen[11]*

[1] Department of Neuropsychiatry, School of Medicine, University of Toyama, Toyama, Japan, [2] Research Center for Idling Brain Science, University of Toyama, Toyama, Japan, [3] Brain Park, Turner Institute for Brain and Mental Health, School of Psychological Sciences, Monash University, Clayton, VIC, Australia, [4] Melbourne Neuropsychiatry Centre, Department of Psychiatry, The University of Melbourne and Melbourne Health, Melbourne, VIC, Australia, [5] Neuroscience of Addiction and Mental Health Program, Healthy Brain and Mind Research Centre, School of Psychology, Faculty of Health Sciences, Australian Catholic University, Melbourne, VIC, Australia, [6] Department of Neuropsychiatry, Royal Melbourne Hospital, Melbourne, VIC, Australia, [7] Florey Institute of Neuroscience and Mental Health, University of Melbourne, Melbourne, VIC, Australia, [8] North Western Mental Health, Western Hospital Sunshine, St Albans, VIC, Australia, [9] Academic Department of Psychiatry, Kolling Institute, Northern Clinical School, Faculty of Medicine and Health, The University of Sydney, Sydney, NSW, Australia, [10] CADE Clinic, Royal North Shore Hospital, Northern Sydney Local Health District, St Leonards, NSW, Australia, [11] Department of Psychology, University of Oregon, Eugene, OR, United States

OPEN ACCESS

Edited by:
Chun Meng,
University of Electronic Science and Technology of China, China

Reviewed by:
Peter Schneider,
Heidelberg University, Germany
Jing Lu,
University of Electronic Science and Technology of China, China

***Correspondence:**
Tsutomu Takahashi
tsutomu@med.u-toyama.ac.jp

Specialty section:
This article was submitted to Brain Imaging and Stimulation, a section of the journal Frontiers in Human Neuroscience

Received: 11 April 2022
Accepted: 26 May 2022
Published: 13 June 2022

Citation:
Takahashi T, Sasabayashi D, Yücel M, Whittle S, Lorenzetti V, Walterfang M, Suzuki M, Pantelis C, Malhi GS and Allen NB (2022) Different Frequency of Heschl's Gyrus Duplication Patterns in Neuropsychiatric Disorders: An MRI Study in Bipolar and Major Depressive Disorders. Front. Hum. Neurosci. 16:917270. doi: 10.3389/fnhum.2022.917270

An increased prevalence of duplicated Heschl's gyrus (HG) has been repeatedly demonstrated in various stages of schizophrenia as a potential neurodevelopmental marker, but it remains unknown whether other neuropsychiatric disorders also exhibit this macroscopic brain feature. The present magnetic resonance imaging study aimed to examine the disease specificity of the established finding of altered HG patterns in schizophrenia by examining independent cohorts of bipolar disorder (BD) and major depressive disorder (MDD). Twenty-six BD patients had a significantly higher prevalence of HG duplication bilaterally compared to 24 age- and sex-matched controls, while their clinical characteristics (e.g., onset age, number of episodes, and medication) did not relate to HG patterns. No significant difference was found for the HG patterns between 56 MDD patients and 33 age- and sex-matched controls, but the patients with a single HG were characterized by more severe depressive/anxiety symptoms compared to those with a duplicated HG. Thus, in keeping with previous findings, the present study suggests that neurodevelopmental pathology associated with gyral formation of the HG during the late gestation period partly overlaps between schizophrenia and BD, but that HG patterns may make a somewhat distinct contribution to the phenomenology of MDD.

Keywords: superior temporal gyrus, Heschl's gyrus, gyrification, major depressive disorder, bipolar disorder

INTRODUCTION

Gyrification pattern of Heschl's gyrus (HG), which includes primary auditory cortex, displays a large inter-individual variability, potentially reflecting cytoarchitectonic development during gestation (Chi et al., 1977; Armstrong et al., 1995) and/or experience-dependent structural plasticity (Zatorre et al., 2012). While functional significance of the HG gyrification patterns has not been fully elucidated, it has been demonstrated that duplicated HG is involved in the neural basis of cognitive skills, such as musicality especially for professional musicians (Schneider et al., 2005; Benner et al., 2017; Turker et al., 2017) and good (Turker et al., 2017) or poor (Leonard et al., 1993, 2001) language learning ability in non-clinical population (reviewed by Marie et al., 2016). HG duplication, which is observed in approximately 30 to 50% of healthy subjects (Leonard et al., 1998; Abdul-Kareem and Sluming, 2008; Marie et al., 2015), is thus thought to be a normal anatomical variant potentially associated with individual differences in cognitive function, but recent magnetic resonance imaging (MRI) studies have suggested that an altered HG gyrification pattern may also be associated with the pathophysiology of neuropsychiatric disorders.

Neuroimaging evidence has demonstrated an association between schizophrenia and macroscopic brain changes (Bakhshi and Chance, 2015; Takahashi and Suzuki, 2018), potentially reflecting early neurodevelopmental pathology (Weinberger, 1987; Insel, 2010). In particular, an increased prevalence of duplicated HG likely exists from the earliest stages of psychosis [e.g., high-risk status (Takahashi et al., 2021c) and at illness onset (Takahashi et al., 2021a)] and is not influenced by medication and illness chronicity (Takahashi et al., 2021b), and may underpin cognitive impairment (Takahashi et al., 2021c) and primary negative symptomatology (Takahashi et al., in submission). These HG findings implicate that altered cytoarchitectonic development of the primary auditory cortex *in utero* may contribute to early neurodevelopmental pathology of schizophrenia. However, the disease specificity of these findings in schizophrenia remains largely unknown. To our knowledge, no studies to date have specifically examined the HG duplication patterns in other neuropsychiatric disorders, such as affective disorders, that partly overlap with schizophrenia on the level of phenomenology and genetic/neurobiological findings (Prata et al., 2019; Grunze and Cetkovich-Bakmas, 2021).

While the neural underpinnings of affective disorders remain elusive, it is hypothesized that affective disorders, particularly bipolar disorder (BD), may be caused by developmentally mediated neurobiological alterations that are associated with emotion-regulation neural circuitry (Sanches et al., 2008; Phillips and Swartz, 2014). Major depressive disorder (MDD) is a phenotypically heterogeneous disorder with both biological and environmental risk factors (Slavich and Irwin, 2014; Uchida et al., 2018), in addition to which prenatal neurodevelopmental insults may also contribute to its pathophysiology (Gałecki and Talarowska, 2018; Lima-Ojeda et al., 2018). Indeed, previous MRI studies in schizophrenia (Takahashi et al., 2014b, Nishikawa et al., 2016), BD (Takahashi et al., 2014a), and MDD (Takahashi et al., 2016) have demonstrated commonly altered brain surface morphology, suggesting partly overlapping neurodevelopmental pathologies in these disorders. Further, it is notable that schizophrenia and BD patients likely exhibit similar gyrification pattern trajectories (reviewed by Sasabayashi et al., 2021) as a potential common basis of emotional dysregulation and cognitive impairments. Given that inter-individual variation in the HG gyrification pattern could affect regional neural functions and cognitive abilities (Tzourio-Mazoyer et al., 2015; Tzourio-Mazoyer and Mazoyer, 2017) and that the HG is also involved in emotional processing (Grosso et al., 2015; Concina et al., 2019), it would seem worthwhile to evaluate the potential role of HG duplication patterns on the pathophysiology of affective disorders.

The present MRI study aimed to examine the HG duplication patterns in both BD and MDD in comparison with our previous findings in schizophrenia (Takahashi et al., 2021a,b,c) to establish the common and distinct alterations in HG gyrification pattern across major psychiatric disorders. On the basis of the potential role of HG patterns in emotional processing (e.g., Tzourio-Mazoyer and Mazoyer, 2017) and previous findings of partly overlapping brain gyrification patterns in various psychiatric disorders (Sasabayashi et al., 2021), we predicted that affective disorders (especially BD) would have an increased HG duplication compared to matched healthy controls. We also explored the relationship between HG patterns and clinical characteristics in the BD and MDD groups.

MATERIALS AND METHODS

Participants

The study participants comprised 26 patients with BD, 56 with MDD, and 57 age- and sex-matched healthy controls (24 subjects matched for BD and 33 for MDD) (**Table 1**); inclusion/exclusion criteria and sample characteristics of these cohorts have been fully described elsewhere (Takahashi et al., 2014a, 2016, 2020).

Briefly, the patients fulfilling DSM-IV criteria for bipolar I disorder were recruited from the Mood Disorders Unit at the Prince of Wales Hospital, Sydney, Australia. Their diagnoses and clinical characteristics (e.g., lifetime affective episodes, medication status) were confirmed by research psychiatrists using the Structured Clinical Interview for DSM-IV patient version (SCID-IV-P) (First et al., 1998) and a detailed case note review. At the time of participation, all patients did not fulfill current manic/hypomanic or depressive episode of SCID and were considered to be under euthymic condition only with subsyndromal symptoms. Twenty-one patients were taking mood stabilizers [e.g., lithium (Li) (N = 12), valproate (VPA) (N = 12)], while the remaining 5 were not on medication at the time of scanning. Ten BD patients had a family history of affective disorders and 16 had a history of psychosis (i.e., hallucinations and/or delusions) during past affective episodes.

The MDD patients were recruited *via* local advertisement or outpatient psychiatric clinics in Melbourne, Australia. They were diagnosed by SCID-IV-P (First et al., 1998) and assessed using the Beck Depression Inventory (BDI) (Beck and Steer, 1987), Positive Affect and Negative Affect Scale (PANAS) (Watson et al.,

TABLE 1 | Sample characteristics of the study participants.

	BD cohort		MDD cohort	
	Controls (*N* = 24)	**Patients (*N* = 26)**	**Controls (*N* = 33)**	**Patients (*N* = 56)**
Age (years)	38.7 ± 11.1	38.4 ± 10.9	34.0 ± 9.9	33.8 ± 9.1
Male/female	7/17	8/18	12/21	16/40
Current IQ	115.1 ± 9.6	113.8 ± 7.1	111.1 ± 10.9	108.0 ± 9.8
Age of onset (years)	-	24.9 ± 8.4	-	23.5 ± 9.0
Illness duration (years)	-	13.5 ± 10.1	-	10.3 ± 8.1
Number of manic episodes	-	8.8 ± 10.2	-	-
Number of depressive episodes	-	11.1 ± 10.8	-	3.4 ± 3.0
Medication at scanning (yes/no)	-	21/5	-	33/19
Beck Depression Inventory	-	-	3.6 ± 4.1	23.4 ± 15.8
MASQ general distress	-	-	27.9 ± 8.3	45.8 ± 10.3
MASQ general depression	-	-	19.5 ± 7.2	41.5 ± 12.0
MASQ general anxiety	-	-	16.4 ± 6.4	28.7 ± 9.0
MASQ anxious arousal	-	-	22.0 ± 4.4	36.1 ± 12.2
MASQ high positive affect	-	-	81.1 ± 14.3	53.5 ± 16.8
MASQ loss of interest	-	-	14.7 ± 5.0	27.8 ± 7.7
PANAS positive affect	-	-	32.9 ± 7.3	25.0 ± 8.0
PANAS negative affect	-	-	11.2 ± 1.6	17.8 ± 7.7

Values represent means ± SD unless otherwise stated. BD, bipolar disorder; MASQ, Mood and Anxiety Symptom Questionnaire; MDD, major depressive disorder; PANAS, Positive and Negative Affect Schedule.

1988), and Mood and Anxiety Symptom Questionnaire (MASQ) (Watson et al., 1995) by experienced research psychologists at ORYGEN Youth Health, Melbourne. At that time, medication status in the preceding 6 months of the study was also assessed through direct interview and medical record review. At the time of scanning, 29 patients fulfilled DSM criteria of MDD (i.e., currently depressed), while 27 had a history of MDD but currently in remission. Twenty-two MDD patients (18 currently depressed and 4 remitted patients) had a comorbid diagnosis of anxiety disorders.

Participants were right-handed and were screened for head trauma, neurological illness, substance misuse, or other serious physical diseases. Age- and sex-matched healthy comparison subjects for BD (Sydney) and MDD (Melbourne) groups, screened for a personal or family history of psychiatric diseases using the SCID-IV non-patient version (First et al., 1998), were recruited through local advertisement. The study protocol was approved by the local Internal Review Boards (the Prince of Wales Hospital and University of New South Wales research ethics committees and Mental Health Research and Ethics Committee, Melbourne Health, Melbourne, Australia). The participants provided written informed consent after a complete description of the study in accordance with the Declaration of Helsinki.

Magnetic Resonance Imaging Procedures

Bipolar disorder patients and their comparison subjects were scanned using a 1.5-T GE Signa scanner at Royal Prince Alfred Hospital, Sydney, Australia, where a fast-spoiled gradient echo sequence was applied to obtain T1-weighted consecutive coronal images with a voxel size of 0.98 mm × 0.98 mm × 1.6 mm. MDD patients and their controls were scanned by a1.5T Siemens scanner (Magnetom Avanto) at Saint Vincent's Hospital Melbourne, Victoria and T1-weighted iso-voxel (1.0 mm × 1.0 mm × 1.0 mm) images were obtained in the axial orientation. Detailed imaging parameters for the BD and MDD cohorts are available elsewhere (Takahashi et al., 2014a, 2016, 2020).

For the assessment of HG gyrification patterns, brain images were realigned in three dimensions, followed by reconstruction into entire 0.98-mm (BD cohort)- or 1-mm (MDD cohort)-thick contiguous coronal images that were perpendicular to the anterior commissure-posterior commissure line using Dr. View software (Infocom, Tokyo, Japan). As fully described previously (Takahashi et al., 2021a,b,c), one experienced rater with no knowledge of the subjects' identity (TT) classified the HG gyrification into single, partly duplicated (i.e., common stem duplication; CSD), or completely duplicated (i.e., complete posterior duplication; CPD) pattern. While brain images were not corrected for inhomogeneity/artifact, anatomical landmarks for the classification were readily identified by referring to images from three directions all together (**Figure 1**). Another rater (DS), who was also experienced for HG pattern classification (Takahashi et al., 2021a,b,c), independently classified the HG patterns in a subset of randomly selected 15 brains (30 hemispheres). Intra- (TT) and inter-rater (TT and second-rater DS) reliabilities were 30/30 agreement (Cronbach's $\alpha = 1.00$) and 29/30 agreement (Cronbach's $\alpha = 0.87$), respectively.

Statistical Analysis

Group differences in the HG pattern distribution were tested by the χ^2 test or Fisher's exact test when more than 20% of cells had expected counts <5.

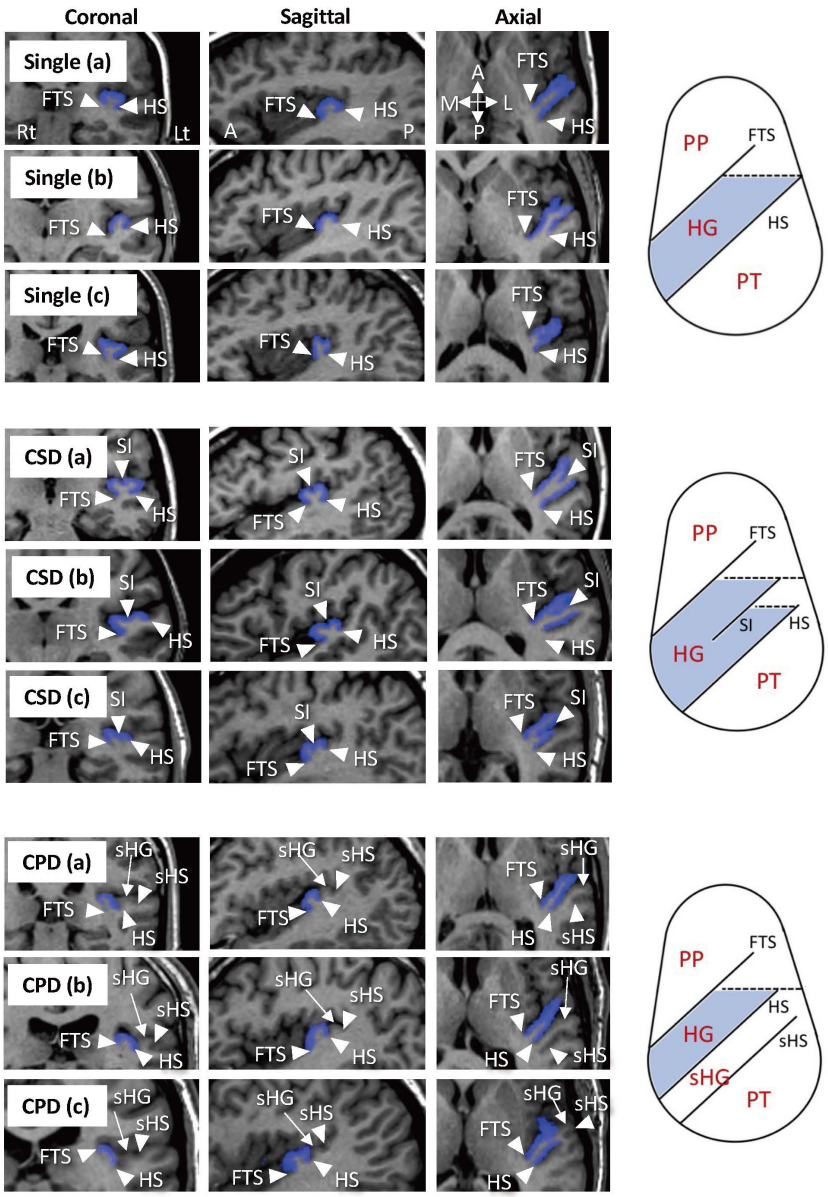

FIGURE 1 | Sample images of various Heschl's gyrus (HG) patterns and anatomical landmarks on MR images and on pattern diagrams in axial direction. The HGs on the left hemisphere are colored in blue. Subjects with a single HG pattern sometimes had a small branching at the front tip [Single (b)] (Marie et al., 2015) or a shallow cortical dimple at the crown of the HG [Single (c)]. Two hemispheres in the present study that had a separate HG posterior to the HG with partial duplication were considered to have the CSD pattern [CSD (c)]. One subject had a pattern of three separate HGs in the left hemisphere, which was classified as a variation of CPD [CPD (c)]. A, anterior; CPD, complete posterior duplication; CSD, common stem duplication; FTS, first transverse sulcus; HS, Heschl's sulcus; L, lateral; P, posterior; M, medial; PP, planum polare; PT, planum temporale; sHG, second Heschl's gyrus; sHS, second Heschl's sulcus; SI, sulcus intermedius.

Non-parametric Mann-Whitney U tests were used for assessing the relationship between the HG patterns and clinical variables, because of the non-normal distribution of most of these variables and small sample size for each HG pattern. The CSD and CPD patterns were categorized together as the 'duplicated pattern' here also due to small sample size for each pattern. Potential role of HG patterns on symptom ratings in MDD was assessed separately on the currently depressed and remitted subgroups because these subgroups were highly different in symptom severity. Statistical significance was set at p-value < 0.05.

RESULTS

Sample Characteristics

The BD and MDD groups did not differ to their controls in terms of age, sex, and intelligence (**Table 1**). Currently depressed and

remitted MDD subgroups did not differ for these demographic variables, while the currently depressed group had more severe depressive/anxiety symptoms and higher medication rates than the remitted group (Takahashi et al., 2016, 2020).

Heschl's Gyrus Pattern Distribution

The BD patients had a higher prevalence of HG duplication for both left ($\chi^2 = 6.44$, $p = 0.011$) and right ($\chi^2 = 5.51$, $p = 0.019$) hemispheres compared to controls, but there was no group difference when only the participants with duplicated HG were examined (i.e., CSD *vs.* CPD) (**Table 2** and **Figure 2**).

No significant group difference was observed between the MDD patients and matched controls irrespective of HG classification (i.e., whether CSD and CPD patterns were grouped or not) (all $p > 0.117$; **Table 3** and **Figure 2**).

The two independent control groups (24 subjects for BD and 33 for MDD) did not differ in HG pattern distribution. While sex may affect cortical folding developments (Mutlu et al., 2013), we found no significant sex difference in the HG patterns.

Relationship Between the Heschl's Gyrus Pattern and Clinical Characteristics

For both the BD and MDD patients, the HG patterns did not relate to age of onset, illness duration, number of affective episodes, or medication status (yes/no for MDD, Li-treated *vs.* non-Li-treated and VPA-treated *vs.* non-VPA-treated for BD). Also, psychotic symptoms and family history of affective disorders in the BD patients were not associated with the HG patterns.

For the currently depressed MDD patients, the patients with single HG had more severe depressive/anxiety symptoms than those with HG duplication especially for the right hemisphere (**Table 4**). However, remitted MDD patients showed no relationship between the HG patterns and these symptom ratings. For the MDD group as a whole, the patients with right single HG had a higher rate of comorbid anxiety disorder than those with right duplicated HG ($\chi^2 = 5.24$, $p = 0.022$).

For the Melbourne healthy controls, who were assessed for depressive and anxiety ratings, the subjects with right HG duplication had a higher MASQ anxious arousal score (mean = 24.1, SD = 5.5) than those with right single HG (mean = 20.0, SD = 1.5) (U=185.5, $p = 0.008$).

DISCUSSION

This MRI study in affective disorders (BD and MDD) examined the disease specificity of the HG gyrification patterns in comparison with previous findings in schizophrenia, because these major neuropsychiatric disorders exhibit partly common phenomenology (e.g., depressive symptoms in BD and MDD, executive dysfunction in BD and schizophrenia) and brain characteristics associated with gyrification pattern (reviewed by Sasabayashi et al., 2021). One of the strengths of this study is that it includes both MDD and BD cohorts, as differences/similarities of brain morphology between these affective disorders have not been well explored. Our results demonstrated that the BD patients had an increased prevalence of HG duplication bilaterally, which was similar to our previous findings in schizophrenia (Takahashi et al., 2021a,b,c). While the main objective of this study was to show the prevalence of HG duplication in affective disorders, we also explored potential contribution of HG patterns on clinical characteristics. The MDD patients did not differ in the prevalence of HG duplication compared to healthy controls, but their HG patterns were significantly associated with symptom severity during a depressive episode. These findings suggest partly overlapping neurodevelopmental origins between BD and schizophrenia, while the neurodevelopmental process associated with embryonic gyral formation may also contribute to certain clinical aspects of MDD. While we have previously reported a reduced normal leftward volumetric asymmetry of the planum temporale, which locates directly posterior to HG, in both BD (Takahashi et al., 2010a) and MDD (Takahashi et al., 2010b) groups as a common gross morphologic feature, the present results suggest the specific role of HG patterns as a distinct marker between these affective disorders.

The present finding of increased prevalence of duplicated HG in the BD patients is in line with the notion of common neurobiological substrates for BD and schizophrenia (Goodkind et al., 2015), a hypothesis that has been supported by a wide range of similarities in genetic (Lichtenstein et al., 2009; Bipolar Disorder and Schizophrenia Working Group of the Psychiatric Genomics Consortium, 2018; Brainstorm et al., 2018), neuroimaging (Hanford et al., 2016; Koshiyama et al., 2020), and neuropsychological (Bora, 2015) findings. The inter-individual variations in the HG gyrification are formed during late gestation along with neural development (Chi et al., 1977; Van Essen, 1997) and its duplication may lead to learning disability after birth (Leonard et al., 1993, 2001), and regional dysfunction in adulthood (Tzourio-Mazoyer et al., 2015). The HG is a part of the primary auditory cortex (Rademacher et al., 1993; Da Costa et al., 2011) but it also plays a crucial role in emotional processing (Grosso et al., 2015; Concina et al., 2019). Interestingly, recent neuroimaging studies have demonstrated shared glutamatergic abnormalities (Atagün et al., 2015), reduced cortical thickness (Mørch-Johnsen et al., 2018), and reduced functional connectivity (Wei et al., 2018) in BD and schizophrenia patients in the HG region. Taken together with these findings, our results likely support the hypothesis that BD and schizophrenia patients exhibit shared hyper-gyrification and compromised neural connectivity in the cortical regions as a consequence of pre/perinatal neurodevelopmental insult, which later underpin common clinical manifestations such as emotional dysregulation and executive dysfunction (Sasabayashi et al., 2021). Our results further revealed no relationship between the HG patterns and illness stages and medication status in the BD patients, supporting its role as a stable trait marker.

In contrast to the findings in BD and schizophrenia (Takahashi et al., 2021a,b,c), the HG patterns in the MDD patients did not differ significantly from those of healthy controls, suggesting a less prominent neurodevelopmental pathology. Previous transdiagnostic studies in brain gyrification of temporal region (Sasabayashi et al., 2021) and white matter microstructure in the

TABLE 2 | Gyrification pattern of Heschl's gyrus (HG) for both hemispheres in the bipolar disorder (BD) cohort.

		Right HG pattern [*N* (%)]			
		Single	**CSD**	**CPD**	**Total**
Healthy controls					
Left HG pattern [*N* (%)]	Single	8 (33.3)	4 (16.7)	4 (16.7)	16 (66.7)
	CSD	0 (0)	3 (12.5)	1 (4.2)	4 (16.7)
	CPD	3 (12.5)	1 (4.2)	0 (0.0)	4 (16.7)
	Total	11 (45.8)	8 (33.3)	5 (20.8)	24 (100.0)
BD					
Left HG pattern [*N* (%)]	Single	2 (7.7)	2 (7.7)	4 (15.4)	8 (30.8)
	CSD	2 (7.7)	9 (34.6)	3 (11.5)	14 (53.8)
	CPD	0 (0)	2 (7.7)	2 (7.7)	4 (15.4)
	Total	4 (15.4)	13 (50.0)	9 (34.6)	26 (100.0)

CSD, common stem duplication; CPD, complete posterior duplication.

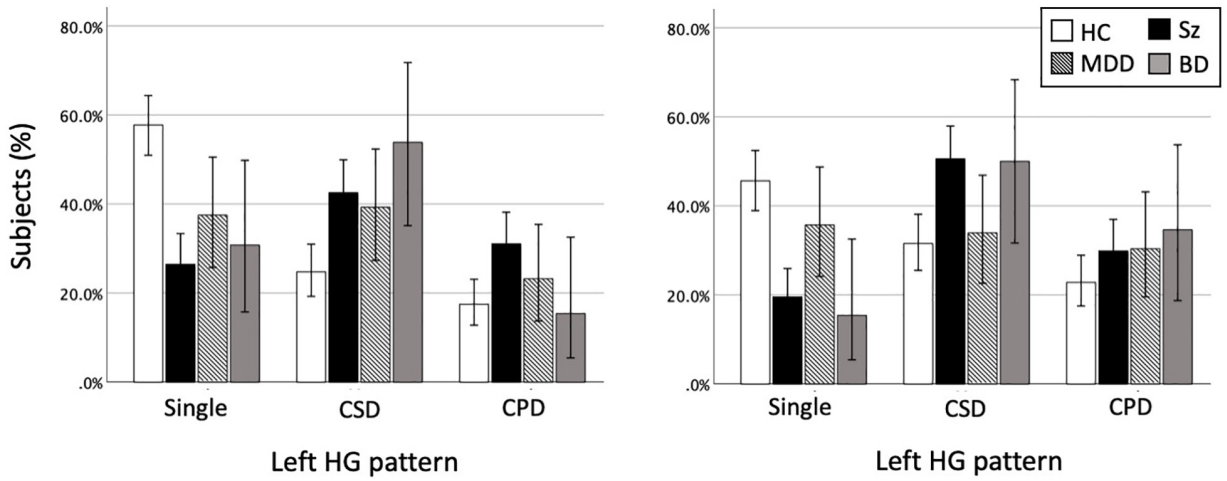

FIGURE 2 | Heschl's gyrus (HG) gyrification patterns in healthy controls (HC), schizophrenia (Sz), major depressive disorder (MDD), and bipolar disorder (BD). The present study examined the HG patterns in MDD and BD cohorts, but the data of 174 patients with Sz (Takahashi et al., 2021a,b,c) are also presented here for the purpose of comparison. The results of the HC group (*N* = 206) reflect all data from the present and our previous (Takahashi et al., 2021a,b,c) studies. Direct comparisons between the disorders showed that the MDD patients had a lower prevalence of right HG duplication compared to Sz ($\chi^2 = 6.17$, $p = 0.013$) and BD ($\chi^2 = 3.55$, $p = 0.060$) patients. However, there was no group difference between the BD and Sz. Error bars show 95% confidence intervals. CPD, complete posterior duplication; CSD, common stem duplication.

limbic system (Koshiyama et al., 2020) also demonstrated near-normal findings only in the MDD among these disorders. On the other hand, we found a significant relationship between the single HG pattern and severe depressive/anxiety symptoms in the MDD patients under an active depressive state. This relationship was somewhat unexpected because the HG duplication, which may relate to regional dysfunction (Tzourio-Mazoyer et al., 2015), contributed to anxiety tendencies in healthy subjects in this study. However, a recent MRI study in MDD also suggested potential contribution of hypo-gyrification to depressive symptomatology in various regions of the brain (Schmitgen et al., 2019). Since this structural MRI study cannot address the functional significance of the HG patterns on depression symptomatology, potential mechanisms of different contribution of HG patterns on anxiety between non-clinical population and pathological status remains unknown and should be examined in future studies exploring this relationship. Normal or even higher prevalence of single HG in the tinnitus patients compared to controls (Schneider et al., 2009) may also support a complex relationship between the HG patterns and regional functioning. Nevertheless, the present study suggested that embryonic neurodevelopmental processes associated with gyral formation of HG may play a role in the phenomenology of MDD in later life potentially by interacting with environmental factors in the epigenetic mechanisms (Gałecki and Talarowska, 2018).

It should be noted that HG duplication itself is observed in healthy subjects and is associated with their cognitive abilities (Marie et al., 2016). In particular, musical ability in subjects without neuropsychiatric disorders seems to be associated with larger HG (Schneider et al., 2002; Seither-Preisler et al., 2014; Wengenroth et al., 2014; Dalboni da Rocha et al., 2020) and higher percentage of HG duplications (Schneider et al., 2005;

TABLE 3 | Gyrification pattern of Heschl's gyrus (HG) for both hemispheres in the major depressive disorder (MDD) cohort.

		Right HG pattern [*N* (%)]			
		Single	**CSD**	**CPD**	**Total**
Healthy controls					
Left HG pattern [*N* (%)]	Single	9 (27.3)	6 (18.2)	3 (9.1)	18 (54.5)
	CSD	4 (12.1)	1 (3.0)	2 (6.1)	7 (21.2)
	CPD	4 (12.1)	1 (3.0)	3 (9.1)	8 (24.2)
	Total	17 (51.5)	8 (24.2)	8 (24.2)	33 (100.0)
cMDD					
Left HG pattern [*N* (%)]	Single	5 (17.2)	1 (3.4)	4 (13.8)	10 (34.5)
	CSD	5 (17.2)	4 (13.8)	1 (3.4)	10 (34.5)
	CPD	1 (3.4)	4 (13.8)	4 (13.8)	9 (31.0)
	Total	11 (37.9)	9 (31.0)	9 (31.0)	29 (100.0)
rMDD					
Left HG pattern [*N* (%)]	Single	3 (11.1)	4 (14.8)	4 (14.8)	11 (40.7)
	CSD	3 (11.1)	6 (22.2)	3 (11.1)	12 (44.4)
	CPD	3 (11.1)	0 (0.0)	1 (3.7)	4 (14.8)
	Total	9 (33.3)	10 (37.0)	8 (29.6)	27 (100.0)

cMDD, currently depressed patients; CSD, common stem duplication; CPD, complete posterior duplication; rMDD, remitted depressed patients.

TABLE 4 | Symptom ratings of the currently depressed patients with different Heschl's gyrus (HG) patterns.

	Left hemisphere			**Right hemisphere**		
	Single HG (*N* = 10)	**Duplicated HG (*N* = 19)**	**Mann-Whitney tests**	**Single HG (*N* = 11)**	**Duplicated HG (*N* = 18)**	**Mann-Whitney tests**
Beck Depression Inventory	41.5 ± 8.2	34.4 ± 8.5	$U = 53.0$, $p = 0.056$	41.6 ± 6.2	33.9 ± 9.2	$U = 44.0$, $p = 0.012$
MASQ general distress	50.9 ± 6.2	50.3 ± 8.7	$U = 87.5$, $p = 0.906$	55.7 ± 5.4	47.1 ± 7.3	$U = 31.5$, $p = 0.002$[a]
MASQ general depression	53.3 ± 5.7	44.0 ± 9.2	$U = 37.5$, $p = 0.010$	51.6 ± 6.8	44.5 ± 9.6	$U = 46.0$, $p = 0.025$
MASQ general anxiety	31.8 ± 6.9	32.4 ± 9.8	$U = 95.0$, $p = 0.832$	40.0 ± 5.2	27.1 ± 6.5	$U = 10.5$, $p < 0.001$[a]
MASQ anxious arousal	41.9 ± 7.8	42.1 ± 14.2	$U = 92.0$, $p = 0.944$	49.7 ± 11.5	37.0 ± 10.0	$U = 38.0$, $p = 0.008$
MASQ high positive affect	34.5 ± 5.8	48.6 ± 14.0	$U = 146.0$, $p = 0.006$	41.6 ± 10.1	44.9 ± 15.4	$U = 101.5$, $p = 0.711$
MASQ loss of interest	34.7 ± 7.3	29.9 ± 5.2	$U = 39.5$, $p = 0.014$	35.0 ± 5.2	29.4 ± 6.2	$U = 46.0$, $p = 0.025$
PANAS positive affect	19.8 ± 5.6	22.5 ± 6.8	$U = 107.0$, $p = 0.308$	20.3 ± 6.6	22.5 ± 6.4	$U = 117.5$, $p = 0.264$
PANAS negative affect	23.1 ± 9.6	20.3 ± 8.0	$U = 71.0$, $p = 0.498$	28.4 ± 7.8	16.6 ± 5.1	$U = 22.0$, $p < 0.001$[a]

Values represent means ± SD. MASQ, Mood and Anxiety Symptom Questionnaire; PANAS, Positive and Negative Affect Schedule.
[a] *Significant even after Bonferroni's correction for multiple comparisons [18 comparisons; $p < 0.00278$ (0.05/18)].*

Benner et al., 2017) especially on the right hemisphere. Because individuals with William Beuron syndrome, a rare genetic disorder with characteristic musicality, likely exhibit larger HG and increased HG duplication predominantly on the left hemisphere (Wengenroth et al., 2010), it may be hypothesized that changes in the right and left HGs associated with musicality may be mainly attributable to the amount of training and genetic factors, respectively. It is currently unknown whether increased HG duplication in the neuropsychiatric disorders has different mechanisms from inter-individual HG variation in healthy subjects, but the former probably reflects their early neurodevelopmental pathology. Given that right HG generally develops 1 to 2 weeks earlier than left HG during mid-to-late gestation (Chi et al., 1977), our results of bilateral changes in HG pattern in schizophrenia (Takahashi et al., 2021a,b,c) and BD may support severe and prolonged neurodevelopmental abnormalities in these disorders. Further, schizophrenia (Takahashi et al., 2021a) and BD (Takahashi et al., 2010a) groups have an increased HG duplication with marked HG 'atrophy,' suggesting different mechanisms between normal variation in the HG morphology and HG changes in these neuropsychiatric disorders.

Several potential confounding factors in this study should be noted. First, different MR settings (e.g., scanners, parameters) used for the BD and MDD patients limited the comparability of our data (Pøibil et al., 2019). We therefore used the control groups matched for demographic background and MR setting for each patient group. Further, it is unlikely that different scanning condition significantly affected our conclusion, because the anatomical landmarks for HG classification (**Figure 1**) could be readily identified in all of the study participants. In this study, we referred to our previous results in schizophrenia (Takahashi et al., 2021a,b,c) to interpretate the current findings in affective disorders. However, these previous data were assessed in different racial/ethnic population (Toyama, Japan) from the current Australian cohorts, which might affect the results (Brickman et al., 2008; Rao et al., 2017). Although we

found no significant differences in HG pattern distribution at least between three control groups with different MR settings and populations (Sydney, Melbourne, and Toyama), future transdiagnostic studies with more homogeneous conditions (i.e., on a single MRI scanner) are required. Second, the sample size of both disease groups and healthy controls was relatively small, which may have contributed to the lower statistical power. While the MDD patients showed no significant difference in HG patterns compared to controls, they were characterized by a somewhat higher duplication rate especially on the left hemisphere (**Figure 2**). Because the HG may also participate in learning and memory processing (Weinberger, 2015), it may be possible that future study in a larger MDD cohort will detect an altered HG pattern as a common neural underpinning of memory deficits observed in MDD, BD, and schizophrenia (Marazziti et al., 2010; Esan et al., 2020). Finally, it was not possible to examine the relationship between the HG patterns and symptom severity in our BD cohort because they were under remission state at the time of scanning. Further, despite potential contribution of HG gyrification patterns to cognitive function for both non-clinical population (Tzourio-Mazoyer et al., 2015) and schizophrenia (Takahashi et al., 2021c), the current BD and MDD patients were not systematically assessed for their cognitive impairment. Thus, the potential role of HG patterns on the phenomenology of affective disorders (especially symptom severity and cognitive function in BD) and its disease specificity requires further exploration.

In conclusion, the present study demonstrated that patients with BD have a common macroscopic brain characteristic of increased HG duplication with those who have schizophrenia, which may partly underlie common clinical manifestations between these disorders. Conversely, the distribution of HG patterns in the MDD patients was similar to healthy controls and distinctively different from these disorders. While replication studies in a larger transdiagnostic cohort will be clearly required, our results of distinct HG patterns between the BD and MDD patients may contribute to imaging-based differential diagnosis and prediction of clinical course (e.g., later manic episode) at early stages in patients with depressive symptoms.

DATA AVAILABILITY STATEMENT

The raw data supporting the conclusion of this article will be made available by the authors, without undue reservation.

ETHICS STATEMENT

The studies involving human participants were reviewed and approved by the Prince of Wales Hospital and University of New South Wales Research Ethics Committees and Mental Health Research and Ethics Committee, Melbourne Health, Melbourne, Australia. The patients/participants provided their written informed consent to participate in this study.

AUTHOR CONTRIBUTIONS

MY, MS, CP, GM, and NA conceived the concept for and methodology of the study and contributed to the writing and editing of the manuscript. TT conducted statistical analyses and wrote the manuscript. MY, SW, VL, MW, GM, and NA recruited subjects and were involved in clinical and diagnostic assessments. TT and DS analyzed MRI data. All authors contributed to and have approved the final manuscript.

FUNDING

This work was supported in part by JSPS KAKENHI Grant Numbers JP18K07550 to TT, JP18K15509 to DS, and JP20H03598 to MS, and by Health and Labour Sciences Research Grants for Comprehensive Research on Persons with Disabilities from the Japan Agency for Medical Research and Development (AMED) Grant Number JP19dk0307029 to MS. CP was supported by a National Health and Medical Research Council (NHMRC) L3 Investigator Grant (1196508) and a NHMRC Program Grant (ID: 1150083).

REFERENCES

Abdul-Kareem, I. A., and Sluming, V. (2008). Heschl gyrus and its included primary auditory cortex: structural MRI studies in healthy and diseased subjects. *J. Magn. Reson. Imag.* 28, 287–299. doi: 10.1002/jmri.21445

Armstrong, E., Schleicher, A., Omran, H., Curtis, M., and Zilles, K. (1995). The ontogeny of human gyrification. *Cereb. Cortex.* 5, 56–63. doi: 10.1093/cercor/5.1.56

Atagün, M. I., Şıkoğlu, E. M., Can, S. S., Karakaş-Uğurlu, G., Ulusoy-Kaymak, S., Çayköylü, A., et al. (2015). Investigation of Heschl's gyrus and planum temporale in patients with schizophrenia and bipolar disorder: a proton magnetic resonance spectroscopy study. *Schizophr. Res.* 161, 202–209. doi: 10.1016/j.schres.2014.11.012

Bakhshi, K., and Chance, S. A. (2015). The neuropathology of schizophrenia: A selective review of past studies and emerging themes in brain structure and cytoarchitecture. *Neuroscience* 303, 82–102. doi: 10.1016/j.neuroscience.2015.06.028

Beck, A. T., and Steer, R. T. (1987). *Beck Depression Inventory Manual*. San Antonio: Harcourt Brace Jovanovich.

Benner, J., Wengenroth, M., Reinhardt, J., Stippich, C., Schneider, P., and Blatow, M. (2017). Prevalence and function of Heschl's gyrus morphotypes in musicians. *Brain Struct. Funct.* 222, 3587–3603. doi: 10.1007/s00429-017-1419-x

Bipolar Disorder and Schizophrenia Working Group of the Psychiatric Genomics Consortium (2018). Genomic dissection of bipolar disorder and schizophrenia, including 28 subphenotypes. *Cell* 173, 1705–1715. doi: 10.1016/j.cell.2018.05.046

Bora, E. (2015). Developmental trajectory of cognitive impairment in bipolar disorder: comparison with schizophrenia. *Eur. Neuropsychopharmacol.* 25, 158–168. doi: 10.1016/j.euroneuro.2014.09.007

Brainstorm, C., Anttila, V., BulikSullivan, B., Finucane, H. K., Walters, R. K., Bras, J., et al. (2018). Analysis of shared heritability in common disorders of the brain. *Science* 360:eaa8757. doi: 10.1126/science.aap8757

Brickman, A. M., Schupf, N., Manly, J. J., Luchsinger, J. A., Andrews, H., Tang, M. X., et al. (2008). Brain morphology in older African Americans, Caribbean

Hispanics, and whites from northern Manhattan. *Arch. Neurol.* 65, 1053–1061. doi: 10.1001/archneur.65.8.1053

Chi, J. G., Dooling, E. C., and Gilles, F. H. (1977). Gyral development of the human brain. *Ann. Neurol.* 1, 86–93. doi: 10.1002/ana.410010109

Concina, G., Renna, A., Grosso, A., and Sacchetti, B. (2019). The auditory cortex and the emotional valence of sounds. *Neurosci. Biobehav. Rev.* 98, 256–264. doi: 10.1016/j.neubiorev.2019.01.018

Da Costa, S., van der Zwaag, W., Marques, J. P., Frackowiak, R. S., Clarke, S., and Saenz, M. (2011). Human primary auditory cortex follows the shape of Heschl's gyrus. *J. Neurosci.* 31, 14067–14075. doi: 10.1523/JNEUROSCI.2000-11.2011

Dalboni da Rocha, J. L., Schneider, P., Benner, J., Santoro, R., Atanasova, T., VanDeVille, D., et al. (2020). TASH: toolbox for the automated segmentation of Heschl's gyrus. *Sci. Rep.* 10:3887. doi: 10.1038/s41598-020-60609-y

Esan, O., Oladele, O., Adediran, K. I., and Abiona, T. O. (2020). Neurocognitive Impairments (NCI) in bipolar disorder: comparison with schizophrenia and healthy controls. *J. Affect. Disord.* 277, 175–181. doi: 10.1016/j.jad.2020.08.015

First, M. B., Spitzer, R. L., Gibbon, M., and Williams, J. B. W. (1998). *Structured Clinical Interview for DSM-IV*. Washington, DC: American Psychiatric Press.

Gałecki, P., and Talarowska, M. (2018). Neurodevelopmental theory of depression. *Prog. Neuropsychopharmacol. Biol. Psychiatry* 80, 267–272. doi: 10.1016/j.pnpbp.2017.05.023

Goodkind, M., Eickhoff, S. B., Oathes, D. J., Jiang, Y., Chang, A., Jones-Hagata, L. B., et al. (2015). Identification of a common neurobiological substrate for mental illness. *JAMA Psychiatry* 72, 305–315. doi: 10.1001/jamapsychiatry.2014.2206

Grosso, A., Cambiaghi, M., Concina, G., Sacco, T., and Sacchetti, B. (2015). Auditory cortex involvement in emotional learning and memory. *Neuroscience* 299, 45–55. doi: 10.1016/j.neuroscience.2015.04.068

Grunze, H., and Cetkovich-Bakmas, M. (2021). Apples and pears are similar, but still different things." Bipolar disorder and schizophrenia- discrete disorders or just dimensions? *J. Affect. Disord.* 290, 178–187. doi: 10.1016/j.jad.2021.04.064

Hanford, L. C., Nazarov, A., Hall, G. B., and Sassi, R. B. (2016). Cortical thickness in bipolar disorder: a systematic review. *Bipolar. Disord.* 18, 4–18. doi: 10.1111/bdi.12362

Insel, T. R. (2010). Rethinking schizophrenia. *Nature* 468, 187–193. doi: 10.1038/nature09552

Koshiyama, D., Fukunaga, M., Okada, N., Morita, K., Nemoto, K., Usui, K., et al. (2020). White matter microstructural alterations across four major psychiatric disorders: mega-analysis study in 2937 individuals. *Mol. Psychiatry* 25, 883–895. doi: 10.1038/s41380-019-0553-7

Leonard, C. M., Eckert, M. A., Lombardino, L. J., Oakland, T., Kranzler, J., Mohr, C. M., et al. (2001). Anatomical risk factors for phonological dyslexia. *Cereb. Cortex.* 11, 148–157. doi: 10.1093/cercor/11.2.148

Leonard, C. M., Puranik, C., Kuldau, J. M., and Lombardino, L. J. (1998). Normal variation in the frequency and location of human auditory cortex landmarks. Heschl's gyrus: where is it? *Cereb. Cortex.* 8, 397–406. doi: 10.1093/cercor/8.5.397

Leonard, C. M., Voeller, K. K., Lombardino, L. J., Morris, M. K., Hynd, G. W., Alexander, A. W., et al. (1993). Anomalous cerebral structure in dyslexia revealed with magnetic resonance imaging. *Arch. Neurol.* 50, 461–469. doi: 10.1001/archneur.1993.00540050013008

Lichtenstein, P., Yip, B. H., Björk, C., Pawitan, Y., Cannon, T. D., Sullivan, P. F., et al. (2009). Common genetic determinants of schizophrenia and bipolar disorder in Swedish families: a population-based study. *Lancet* 373, 234–239. doi: 10.1016/S0140-6736(09)60072-6

Lima-Ojeda, J. M., Rupprecht, R., and Baghai, T. C. (2018). Neurobiology of depression: a neurodevelopmental approach. *World J. Biol. Psychiatry* 19, 349–359. doi: 10.1080/15622975.2017.1289240

Marazziti, D., Consoli, G., Picchetti, M., Carlini, M., and Faravelli, L. (2010). Cognitive impairment in major depression. *Eur. J. Pharmacol.* 626, 83–86. doi: 10.1016/j.ejphar.2009.08.046

Marie, D., Jobard, G., Crivello, F., Perchey, G., Petit, L., Mellet, E., et al. (2015). Descriptive anatomy of Heschl's gyri in 430 healthy volunteers, including 198 left-handers. *Brain Struct. Funct.* 220, 729–743. doi: 10.1007/s00429-013-0680-x

Marie, D., Maingault, S., Crivello, F., Mazoyer, B., and Tzourio-Mazoyer, N. (2016). Surface-based morphometry of cortical thickness and surface area associated with heschl's gyri duplications in 430 healthy volunteers. *Front. Hum. Neurosci.* 10:69. doi: 10.3389/fnhum.2016.00069

Mørch-Johnsen, L., Nerland, S., Jørgensen, K. N., Osnes, K., Hartberg, C. B., Andreassen, O. A., et al. (2018). Cortical thickness abnormalities in bipolar disorder patients with a lifetime history of auditory hallucinations. *Bipolar. Disord.* 20, 647–657. doi: 10.1111/bdi.12627

Mutlu, A. K., Schneider, M., Debbane, M., Badoud, D., Eliez, S., and Schaer, M. (2013). Sex differences in thickness, and folding developments throughout the cortex. *NeuroImage* 82, 200–207. doi: 10.1016/j.neuroimage.2013.05.076

Nishikawa, Y., Takahashi, T., Takayanagi, Y., Furuichi, A., Kido, M., Nakamura, M., et al. (2016). Orbitofrontal sulcogyral pattern and olfactory sulcus depth in the schizophrenia spectrum. *Eur. Arch. Psychiatry Clin. Neurosci.* 266, 15–23. doi: 10.1007/s00406-015-0587-z

Phillips, M. L., and Swartz, H. A. A. (2014). critical appraisal of neuroimaging studies of bipolar disorder: toward a new conceptualization of underlying neural circuitry and a road map for future research. *Am. J. Psychiatry* 171, 829–843. doi: 10.1176/appi.ajp.2014.13081008

Prata, D. P., Costa-Neves, B., Cosme, G., and Vassos, E. (2019). Unravelling the genetic basis of schizophrenia and bipolar disorder with GWAS: a systematic review. *J. Psychiatr. Res.* 114, 178–207. doi: 10.1016/j.jpsychires.2019.04.007

Pøibil, J., Pøibilová, A., and Frollo, I. (2019). Analysis of the influence of different settings of scan sequence parameters on vibration and noise generated in the open-air MRI scanning area. *Sensors* 19:4198. doi: 10.3390/s19194198

Rademacher, J., Caviness, V. S. Jr., Steinmetz, H., and Galaburda, A. M. (1993). Topographical variation of the human primary cortices: implications for neuroimaging, brain mapping, and neurobiology. *Cereb. Cortex.* 3, 313–329. doi: 10.1093/cercor/3.4.313

Rao, N. P., Jeelani, H., Achalia, R., Achalia, G., Jacob, A., Bharath, R. D., et al. (2017). Population differences in brain morphology: need for population specific brain template. *Psychiatry Res. Neuroimag.* 265, 1–8. doi: 10.1016/j.pscychresns.2017.03.018

Sanches, M., Keshavan, M. S., Brambilla, P., and Soares, J. C. (2008). Neurodevelopmental basis of bipolar disorder: a critical appraisal. *Prog. Neuropsychopharmacol. Biol. Psychiatry* 32, 1617–1627. doi: 10.1016/j.pnpbp.2008.04.017

Sasabayashi, D., Takahashi, T., Takayanagi, Y., and Suzuki, M. (2021). Anomalous brain gyrification patterns in major psychiatric disorders: a systematic review and transdiagnostic integration. *Transl. Psychiatry* 11:176. doi: 10.1038/s41398-021-01297-8

Schmitgen, M. M., Depping, M. S., Bach, C., Wolf, N. D., Kubera, K. M., Vasic, N., et al. (2019). Aberrant cortical neurodevelopment in major depressive disorder. *J. Affect. Disord.* 243, 340–347. doi: 10.1016/j.jad.2018.09.021

Schneider, P., Andermann, M., Wengenroth, M., Goebel, R., Flor, H., Rupp, A., et al. (2009). Reduced volume of Heschl's gyrus in tinnitus. *Neuroimage* 45, 927–939. doi: 10.1016/j.neuroimage.2008.12.045

Schneider, P., Scherg, M., Dosch, H. G., Specht, H. J., Gutschalk, A., and Rupp, A. (2002). Morphology of Heschl's gyrus reflects enhanced activation in the auditory cortex of musicians. *Nat. Neurosci.* 5, 688–694. doi: 10.1038/nn871

Schneider, P., Sluming, V., Roberts, N., Scherg, M., Goebel, R., Specht, H. J., et al. (2005). Structural and functional asymmetry of lateral Heschl's gyrus reflects pitch perception preference. *Nat. Neurosci.* 8, 1241–1247. doi: 10.1038/nn1530

Seither-Preisler, A., Parncutt, R., and Schneider, P. (2014). Size and synchronization of auditory cortex promotes musical, literacy, and attentional skills in children. *J. Neurosci.* 34, 10937–10949. doi: 10.1523/JNEUROSCI.5315-13.2014

Slavich, G. M., and Irwin, M. R. (2014). From stress to inflammation and major depressive disorder: a social signal transduction theory of depression. *Psychol. Bull.* 140, 774–815. doi: 10.1037/a0035302

Takahashi, T., and Suzuki, M. (2018). Brain morphologic changes in early stages of psychosis: implications for clinical application and early intervention. *Psychiatry Clin. Neurosci.* 72, 556–571. doi: 10.1111/pcn.12670

Takahashi, T., Malhi, G. S., Nakamura, Y., Suzuki, M., and Pantelis, C. (2014a). Olfactory sulcus morphology in established bipolar affective disorder. *Psychiatry Res. Neuroimag.* 222, 114–117. doi: 10.1016/j.pscychresns.2014.02.005

Takahashi, T., Malhi, G. S., Wood, S. J., Yücel, M., Walterfang, M., Kawasaki, Y., et al. (2010a). Gray matter reduction of the superior temporal gyrus in patients with established bipolar I disorder. *J. Affect. Disord.* 123, 276–282. doi: 10.1016/j.jad.2009.08.022

Takahashi, T., Nishikawa, Y., Yücel, M., Whittle, S., Lorenzetti, V., Walterfang, M., et al. (2016). Olfactory sulcus morphology in patients with current and past major depression. *Psychiatry Res. Neuroimag.* 255, 60–65. doi: 10.1016/j.pscychresns.2016.07.008

Takahashi, T., Sasabayashi, D., Takayanagi, Y., Furuichi, A., Kido, M., Nakamura, M., et al. (2021a). Altered Heschl's gyrus duplication pattern in first-episode schizophrenia. *Schizophr. Res.* 237, 174–181. doi: 10.1016/j.schres.2021.09.011

Takahashi, T., Sasabayashi, D., Takayanagi, Y., Furuichi, A., Kido, M., Pham, T. V., et al. (2021b). Increased Heschl's gyrus duplication in schizophrenia spectrum disorders: a cross-sectional MRI study. *J. Pers. Med.* 11:40. doi: 10.3390/jpm11010040

Takahashi, T., Sasabayashi, D., Takayanagi, Y., Higuchi, Y., Mizukami, Y., Nishiyama, S., et al. (2021c). Heschl's gyrus duplication pattern in individuals at risk of developing psychosis and patients with schizophrenia. *Front. Behav. Neurosci.* 15:647069. doi: 10.3389/fnbeh.2021.647069

Takahashi, T., Sasabayashi, D., Yücel, M., Whittle, S., Lorenzetti, V., Walterfang, M., et al. (2020). Pineal gland volume in major depressive and bipolar disorders. *Front. Psychiatry* 11:450. doi: 10.3389/fpsyt.2020.00450

Takahashi, T., Wood, S. J., Yung, A. R., Nelson, B., Lin, A., Yücel, M., et al. (2014b). Altered depth of the olfactory sulcus in ultra high-risk individuals and patients with psychotic disorders. *Schizophr. Res.* 153, 18–24. doi: 10.1016/j.schres.2014.01.041

Takahashi, T., Yücel, M., Lorenzetti, V., Walterfang, M., Kawasaki, Y., Whittle, S., et al. (2010b). An MRI study of the superior temporal subregions in patients with current and past major depression. *Prog. Neuropsychopharmacol. Biol. Psychiatry* 34, 98–103. doi: 10.1016/j.pnpbp.2009.10.005

Turker, S., Reiterer, S. M., Seither-Preisler, A., and Schneider, P. (2017). "When music speaks": auditory cortex morphology as a neuroanatomical marker of language aptitude and musicality. *Front. Psychol.* 8, 2096. doi: 10.3389/fpsyg.2017.02096

Tzourio-Mazoyer, N., and Mazoyer, B. (2017). Variations of planum temporale asymmetries with Heschl's Gyri duplications and association with cognitive abilities: MRI investigation of 428 healthy volunteers. *Brain Struct. Funct.* 222, 2711–2726. doi: 10.1007/s00429-017-1367-5

Tzourio-Mazoyer, N., Marie, D., Zago, L., Jobard, G., Perchey, G., Leroux, G., et al. (2015). Heschl's gyrification pattern is related to speech-listening hemispheric lateralization: FMRI investigation in 281 healthy volunteers. *Brain Struct. Funct.* 220, 1585–1599. doi: 10.1007/s00429-014-0746-4

Uchida, S., Yamagata, H., Seki, T., and Watanabe, Y. (2018). Epigenetic mechanisms of major depression: targeting neuronal plasticity. *Psychiatry Clin. Neurosci.* 72, 212–227. doi: 10.1111/pcn.12621

Van Essen, D. C. A. (1997). tension-based theory of morphogenesis and compact wiring in the central nervous system. *Nature* 385, 313–318. doi: 10.1038/385313a0

Watson, D., Clark, L., and Tellegen, A. (1988). Development and validation of brief measures of positive and negative affect: the PANAS scales. *J. Pers. Soc. Psychol.* 54, 1063–1070.

Watson, D., Clark, L., Weber, K., Assenheimer, J., Strauss, M., and McCormick, R. (1995). Testing a tripartite model: I. Evaluating the convergent and discriminant validity of anxiety and depression symptom scales. *J. Abnorm. Psychol.* 104, 3–14.

Wei, Y., Chang, M., Womer, F. Y., Zhou, Q., Yin, Z., Wei, S., et al. (2018). Local functional connectivity alterations in schizophrenia, bipolar disorder, and major depressive disorder. *J. Affect. Disord.* 236, 266–273. doi: 10.1016/j.jad.2018.04.069

Weinberger, D. R. (1987). Implications of normal brain development for the pathogenesis of schizophrenia. *Arch. Gen. Psychiatry* 44, 660–669. doi: 10.1001/archpsyc.1987.01800190080012

Weinberger, N. M. (2015). New perspectives on the auditory cortex: learning and memory. *Handb. Clin. Neurol.* 129, 117–147. doi: 10.1016/B978-0-444-62630-1.00007-X

Wengenroth, M., Blatow, M., Bendszus, M., and Schneider, P. (2010). Leftward lateralization of auditory cortex underlies holistic sound perception in Williams syndrome. *PLoS One* 5:e12326. doi: 10.1371/journal.pone.0012326

Wengenroth, M., Blatow, M., Heinecke, A., Reinhardt, J., Stippich, C., Hofmann, E., et al. (2014). Increased volume and function of right auditory cortex as a marker for absolute pitch. *Cereb. Cortex.* 24, 1127–1137. doi: 10.1093/cercor/bhs391

Zatorre, R. J., Fields, R. D., and Johansen-Berg, H. (2012). Plasticity in gray and white: neuroimaging changes in brain structure during learning. *Nat. Neurosci.* 15, 528–536. doi: 10.1038/nn.3045

Conflict of Interest: The authors declare that the research was conducted in the absence of any commercial or financial relationships that could be construed as a potential conflict of interest.

Publisher's Note: All claims expressed in this article are solely those of the authors and do not necessarily represent those of their affiliated organizations, or those of the publisher, the editors and the reviewers. Any product that may be evaluated in this article, or claim that may be made by its manufacturer, is not guaranteed or endorsed by the publisher.

frontiers | Frontiers in Human Neuroscience

ORIGINAL RESEARCH
published: 13 June 2022
doi: 10.3389/fnhum.2022.877461

Effect of Season of Birth on Hippocampus Volume in a Transdiagnostic Sample of Patients With Depression and Schizophrenia

Nora Schaub[1†], Nina Ammann[1†], Frauke Conring[1], Thomas Müller[1], Andrea Federspiel[1], Roland Wiest[2], Robert Hoepner[3], Katharina Stegmayer[1‡] and Sebastian Walther[1‡]*

[1] Translational Research Center, University Hospital of Psychiatry and Psychotherapy, Bern, Switzerland, [2] Support Center of Advanced Neuroimaging (SCAN), Inselspital, University Institute of Diagnostic and Interventional Neuroradiology, Bern, Switzerland, [3] Department of Neurology, Inselspital, University Hospital and University of Bern, Bern, Switzerland

OPEN ACCESS

Edited by:
Felix Brandl, Technical University of Munich, Germany

Reviewed by:
Jeffrey S. Bedwell, University of Central Florida, United States
Ting-Yat Wong, University of Pennsylvania, United States

***Correspondence:**
Katharina Stegmayer
katharina.stegmayer@upd.unibe.ch

[†]*These authors share first authorship*

[‡]*These authors have contributed equally to this work and share senior authorship*

Specialty section:
This article was submitted to Brain Imaging and Stimulation, a section of the journal Frontiers in Human Neuroscience

Received: *16 February 2022*
Accepted: *17 May 2022*
Published: *13 June 2022*

Citation:
Schaub N, Ammann N, Conring F, Müller T, Federspiel A, Wiest R, Hoepner R, Stegmayer K and Walther S (2022) Effect of Season of Birth on Hippocampus Volume in a Transdiagnostic Sample of Patients With Depression and Schizophrenia. Front. Hum. Neurosci. 16:877461. doi: 10.3389/fnhum.2022.877461

Psychiatric disorders share an excess of seasonal birth in winter and spring, suggesting an increase of neurodevelopmental risks. Evidence suggests season of birth can serve as a proxy of harmful environmental factors. Given that prenatal exposure of these factors may trigger pathologic processes in the neurodevelopment, they may consequently lead to brain volume alterations. Here we tested the effects of season of birth on gray matter volume in a transdiagnostic sample of patients with schizophrenia and depression compared to healthy controls (n = 192). We found a significant effect of season of birth on gray matter volume with reduced right hippocampal volume in summer-born compared to winter-born patients with depression. In addition, the volume of the right hippocampus was reduced independent from season of birth in schizophrenia. Our results support the potential impact of season of birth on hippocampal volume in depression.

Keywords: depression, schizophrenia, season of birth, structural neuroimaging, hippocampus, gray matter

INTRODUCTION

Severe mental illness is associated with shared antenatal and early neurodevelopmental risk, while later on, distinct trajectories convey heterotypic risk for disorders such as schizophrenia or depression (Damme et al., 2022). Epidemiological studies indicate that individuals who are winter- and spring-born have an increased risk of up to 8% to develop schizophrenia (Torrey et al., 1997). In fact, except for known infectious diseases, for no other diseases seasonal birth excesses was described as clearly as those for schizophrenia and bipolar disorder (Torrey et al., 1997). Likewise, an excess of up to 5.5% of depression cases was shown in spring- born subjects (Torrey et al., 1996; Disanto et al., 2012). In addition, one study demonstrated that spring-born individuals had a higher risk of suicidality (Joiner et al., 2002) pointing to an effect of season of birth on this severe and disabling symptom. Although a seasonal birth-excess in psychiatric disorders has been repeatedly reported, the reason for this excess is unclear.

Season of birth acts as a valuable proxy, to study the impact of harmful environmental factors during fetal maturation. Because most infectious agents have seasonal shifts in their incidence, they form a possible explanation for the winter- and spring birth excess in psychiatric disorders. In fact,

incidences of prenatal bacterial and viral infections change throughout the year, with a rise during the fall and winter months and decline during spring and summer. Moreover, prenatal infections and inflammation are associated with an elevated risk for psychiatric disorders (Al-Haddad et al., 2019a,b). Early research focused primarily on the identification of pathogens such as toxoplasma gondii, rubella virus, cytomegalovirus, and herpes simplex as possible explanations for the winter–spring birth excess in psychiatric disorders. However, accumulating evidence now suggests that a wide variety of viral and bacterial infections—possibly including COVID-19 (Zaigham and Andersson, 2020; Pantelis et al., 2021) can lead to an increase of psychiatric disorders (see 7 for review). These findings are also in line with the neurodevelopmental hypothesis of schizophrenia (Fatemi and Folsom, 2009) and the fetal-origin hypothesis of mood disorder (Barker, 1998) respectively, suggesting prenatal inflammation to act as a first hit leading to neurodevelopmental abnormalities, which will hamper adaptive brain development and thus increase the risk for major psychiatric disorders.

Depression as well as schizophrenia go along with significant (Shah et al., 2017; Brandl et al., 2019; Hellewell et al., 2019; Huang et al., 2021; Liloia et al., 2021; Serra-Blasco et al., 2021; Gutman et al., 2022), progressive (Vita et al., 2012) transdiagnostic (Goodkind et al., 2015) as well as diagnosis and symptom specific (Horn et al., 2010; Stegmayer et al., 2014, 2016; Walther et al., 2017; Viher et al., 2018; Kindler et al., 2019; Schoretsanitis et al., 2019; Dean et al., 2020; Mertse et al., 2022) patterns of gray matter loss which may represent a hallmark of both disorders. Given the evidence for winter– and spring-birth excesses for schizophrenia, and major depression, and, as already mentioned, the suggested link with neurodevelopmental abnormalities, the question arises as to whether this seasonal birth pattern is associated with alterations in the brain. In fact, animal studies using mouse models of schizophrenia or depression point to alterations in particular within the hippocampus, frontal cortex and the cerebellum following prenatal infections and inflammation (Cotter et al., 1995; Fatemi et al., 1998a,b, 1999, 2002a,b, 2008; Meyer et al., 2008; Ratnayake et al., 2012). This is consistent with the fact that reduced hippocampus volume was confirmed, and alterations within the hippocampus have been largely suggested as relevant for the development of schizophrenia (Nelson et al., 1998; Wright et al., 2000; Heckers, 2001; Honea et al., 2005; Steen et al., 2006; Vita et al., 2006; Heckers and Konradi, 2010; Tamminga et al., 2010) and depression (Sheline et al., 2002; Campbell and MacQueen, 2004; Videbech, 2004; Koolschijn et al., 2009; McKinnon et al., 2009; Cole et al., 2011; Kempton et al., 2011; Bora et al., 2012a,b; Du et al., 2012, 2014; Sacher et al., 2012; Lai, 2013; Sexton et al., 2013; Zhao et al., 2014; Schmaal et al., 2016; Zhang et al., 2016). Effects of season of birth on brain structure were shown in both, depression and schizophrenia. Patients with schizophrenia and depression who are winter-born show a decrease in brain volume, and altered white matter connectivity compared to summer-born patients. In detail, studies confirm ventricular enlargements for winter- and spring-births in schizophrenia (Sacchetti et al., 1987, 1992; Zipursky and Schulz, 1987; Degreef et al., 1988; d'Amato et al., 1994), with some conflicting results (Wilms et al., 1992; Roy et al., 1995). Contrary, summer-born schizophrenia patients had significantly lower fractional anisotropy in widespread white matter regions (i.e., the corpus callosum, internal and external capsule, corona radiata, posterior thalamic radiation, sagittal stratum, and superior longitudinal fasciculus) compared to patients born in the remainder of the year (Giezendanner et al., 2013). Likewise, winter-born patients with bipolar affective depression had more subcortical and periventricular white matter lesions compared to summer-born patients (Moore et al., 2001). Thus, there is evidence of structural alterations in the brain associated with season of birth and schizophrenia as well as depression. However, the distribution of brain alterations as effect of season of birth and whether summer-born or winter-born patients show alterations in brain structure is still unclear. So far, no study assessed transdiagnostic differences in gray matter volume associated with season of birth.

Here we therefore aim to detect effects of season of birth on gray matter volume in a transdiagnostic sample of patients with schizophrenia and depression, compared to healthy controls. Specifically, we hypothesized a relationship between gray matter volume and season of birth in patients with depression as well as patients with schizophrenia and that this association would not be observed in healthy controls. In particular, we suggest decreased volume within the hippocampus in winter-born patients.

MATERIALS AND METHODS

Participants

In total, we included 192 participants, 87 patients with schizophrenia (SZ; 53 winter-born: WB, 34 summer-born: SB), 39 patients with depression (DP; 19 WB; 20 SB), and 66 healthy controls (HC; 42 WB, 24 SB). To stratify participants into seasonal groups, we applied the same cut-off criterion used in previous studies (i.e., winter-born: November through May; summer-born: June through October; Giezendanner et al., 2013). We recruited in- and outpatients at the University Hospital of Psychiatry and Psychotherapy in Bern and healthy controls *via* advertisement and among staff. Patients and controls were the same as in our previous reports (Horn et al., 2010; Walther et al., 2011, Walther et al., 2012a,b; Orosz et al., 2012; Stegmayer et al., 2013, 2014, 2016; Cantisani et al., 2016). Patients were diagnosed according to DSM-IV criteria, while current symptom severity was assessed with the Beck Depression Inventory (Beck, 1961), the Hamilton Depression Inventory (Hamilton, 1986) and the Positive and Negative Syndrome Scale (Kay et al., 1987). Additionally, all participants completed the Mini International Neuropsychiatric Interview (MINI; Sheehan et al., 1998).

Exclusion criteria were substance abuse or dependence (except nicotine), history of head trauma with concurrent loss of consciousness, history of electroconvulsive treatment, a severe medical condition or left-handedness (according to the Edinburgh handedness inventory; Oldfield, 1971). Additional exclusion criteria for controls were history of any psychiatric disorder or a first-degree relative with a schizophrenia spectrum disorder or depression. The local ethics committee (Kantonale

Ethikkommission Bern: KEK Bern) approved the study protocol and all participants provided written informed consent.

Neuroimaging

For structural imaging, a 3D-T1-weighted Modified Driven Equilibrium Fourier Transform Pulse (MDEFT) Sequence (Deichmann et al., 2004) was acquired on a 3-T Siemens Magnetom TrioTim Scanner System, equipped with a standard 12-channel radio frequency head coil (Siemens Vision, Erlangen, Germany). This sequence provided 176 sagittal slices with 256 × 256 matrix points, a 256 × 256 field of view (FOV), and a nominal isotopic resolution of 1 mm × 1 mm × 1 mm. Further scan parameters were 7.92 ms repetition time (TR), 2.48 ms echo time (TE) and a flip angle (FA) of 16°. We preprocessed all resulting high-resolution images with the SPM 12 (Ashburner and Friston, 2000; Wellcome Trust Center for Neuroimaging, London[1]). All preprocessing steps were conducted using standard procedures as implemented in SPM 12, in particular the voxel-based morphometry (VBM) toolbox. Default settings were used. The images have been normalized and modulated. Structural images were bias-corrected, tissue-classified and normalized to Montreal Neurological Institute space using linear (12-parameter affine) and non-linear transformations. Gray matter volume per voxel was calculated by applying an absolute threshold masking of 0.1 and modulating the normalized segmented images with a non-linear only warping. For quality check of the procedures, the normalized, bias-corrected images were visually inspected. MRI images with artifacts, anatomical abnormalities as well as neurodegenerative changes were excluded. Finally the normalized, segmented and modulated volumes were smoothed with an 8 mm full width at half maximum (FWHM) Gaussian kernel (Honea et al., 2005).

Statistical Analyses

We analyzed structural images with SPM 12 (Wellcome Trust Centre for NeuroImaging, University College London, United Kingdom) and demographic and clinical data with SPSS for windows (IBM, version 26.0). Univariate analyses, two-sample *t*-tests and chi-square tests (χ^2) were used, respectively.

Our main investigative interest was the effect of patient status (SZ, DP, HC) and season of birth (WB, SB) on whole brain gray matter volume. We therefore performed a one-way analysis of covariation (ANCOVA) over six groups (SZ_{WB}, SZ_{SB}, DP_{WB}, DP_{SB}, HC_{WB}, and HC_{SB}). To control for trend-level gender differences between summer- and winter-born subjects as well as variability in head sizes, we added total gray matter volume and gender as covariates into the main model. We then performed an outlier-analyses of the ANCOVA over the six groups extracting gray matter values of the significant clusters. We considered a value to be an outlier, if it lied either below or above the following ranges: The 1st quartile—1.5 × interquartile range, or the 3rd quartile + 1.5 × interquartile range. Three potential outlier were identified and subsequently removed from all further analyses—two within the schizophrenia- summer-born group and one within the healthy control summer-born group. No outlier were identified within either of the depression groups. Furthermore, as patient groups differed in education and age, we provide the results of the whole-brain ANCOVA with education and age as additional covariates of no interest in the **Supplementary Material**.

In addition, we plotted extracted mean gray matter values for the six groups and performed *post hoc* comparisons of extracted GM values between patient groups and summer- and winter-born subjects applying univariate analyses and *t*-tests, respectively. To examine a group × season interaction effect on hippocampal volume, we calculated a two-way ANOVA on hippocampal volume [with factors season of birth (SB vs WB) and patient status (SZ vs HC vs DP)] (**Supplementary Table 4** and **Supplementary Figure 3**). We corrected *post hoc* group comparisons with Sidak-correction for multiple testing.

Finally, we assessed the season-of-birth effect on whole brain GM volume for the patient status groups separately (DP, SZ and HC). We therefore performed *t*-tests within the ANCOVA, comparing mean gray matter values of WB and SB individuals within SZ, DP and HC participants, respectively. We report imaging results yielding significance at $p < 0.05$ (FWE-corrected). For illustration purposes, all images are displayed at a threshold of $p < 0.001$, cluster sizes $k > 50$ voxels, uncorrected. To provide additional information, we show the results of the whole brain contrasts at a lower threshold ($p < 0.001$ uncorrected, cluster sizes $k > 50$ voxels) in the **Supplementary Material**. We calculated effect sizes for *F*-tests: η_p^2 (eta^2), based on *F*-value, df-1 and df-2, for *t*-tests: *d* (Cohen's D), based on *t*-value and df and for χ^2-test: φ (phi) calculated based on χ^2-value, and sample size.

RESULTS

WB patients with schizophrenia and depression, as well as WB healthy controls, did not differ in age, gender and education from their SB counterparts. Likewise, WB subjects over all groups did not differ significantly in age and education from SB individuals. As expected, patients with schizophrenia included more male and patients with depression more female participants. In addition, patients with depression were older than patients with schizophrenia. Demographic and clinical variables are provided in **Table 1**.

Lower Hippocampal Volume in Summer-Born Patients With Depression

The whole-brain analysis revealed a group effect within the right hippocampus, pFWE-corr = 0.015; F (Joiner et al., 2002) = 8.47; η_p^2 = 0.190; k = 11 voxels; x = 26, y = −24, z = −12 (**Figure 1**). Lowering the threshold ($p < 0.001$, cluster sizes: $k > 50$ voxels; uncorrected) revealed additional frontal and orbital clusters (see **Supplementary Material Supplementary Figure 1** and **Supplementary Table 1**). Including education and age as additional covariates yielded substantially the same results (see **Supplementary Table 2**).

Post hoc comparisons of extracted gray-matter values showed a decrease of right hippocampal volume in summer-born

[1]http://www.fil.ion.ucl.ac.uk/spm

TABLE 1 | Demographic and clinical variables.

Schizophrenia	**WB (*n* = 53)**	**SB (*n* = 34)**	***df***	***t*/*X*²**	***p***	***d*/φ**
Age (M/SD)	37.6 (11.1)	34.9 (11.4)	85	1.086	0.281	0.235
Gender (male%)	30 (56.6%)	23 (67.6%)	1	1.061	0.303	0.112
Education (M/SD)	13.2 (3.8)	13.0 (3.0)	85	0.244	0.808	0.053
Nr. of episodes (M/SD)	4.8 (5.2)	6.5 (7.9)	85	−1.230	0.222	−0.267
PANSS total (M/SD)	64.4 (18.3)	68.2 (18.4)	85	−0.950	0.345	−0.206
PANSS pos (M/SD)	15.9 (6.5)	17.7 (6.6)	85	−1.281	0.204	−0.277
PANSS neg (M/SD)	16.5 (6.3)	16.8 (5.8)	85	−0.198	0.843	−0.043
CPZ (M/SD)	429.5 (342.5)	416.4 (347.0)	85	0.173	0.863	0.038
Depression	**WB (*n* = 19)**	**SB (*n* = 20)**	***df***	***t*/*X*²**	***p***	***d*/φ**
Age (M/SD)	44.4 (11.4)	43.5 (14.5)	37	0.207	0.837	0.068
Gender (male%)	6 (31.6%)	10 (50.0%)	1	1.367	0.242	0.189
Education (M/SD)	15.5 (5.5)	13.6 (2.5)	37	1.373	0.178	0.451
Nr. of episodes (M/SD)	8.3 (9.1)	12.2 (22.3)	37	−0.716	0.479	−0.235
HAMD total (M/SD)	22.6 (7.4)	24.3 (5.6)	37	−0.765	0.450	−0.251
BDI total (M/SD)	22.0 (11.1)	27.2 (10.9)	37	−1.425	0.163	−0.469
Healthy Controls	**WB (*n* = 42)**	**SB (*n* = 24)**	**df**	***t*/*X*²**	**p**	***d*/φ**
Age (M/SD)	40.3 (15.2)	37.3 (12.9)	64	0.802	0.426	0.201
Gender (male%)	21 (50.0%)	16 (66.7%)	1	1.722	0.189	0.160
Education (M/SD)	14.8 (3.3)	14.0 (2.8)	64	0.960	0.341	0.240
All subjects	**WB (*n* = 114)**	**SB (*n* = 78)**	***df***	***t*/*X*²**	***p***	***d*/φ**
Age	39.7 (12.9)	37.9 (13.0)	190	0.975	0.331	0.143
Gender (male%)	57 (50.0%)	49 (62.8%)	1	3.078	0.079	0.127
Education	14.2 (4.0)	13.5 (2.8)	190	1.308	0.192	0.190
Patient Status Groups	**SZ (*n* = 87)**	**DP (*n* = 39)**	**HC (*n* = 66)**	***df***	***F*/*X*²**	***p***	***d*/φ**
Age	36.57 (11.25)	43.92 (12.91)	39.21 (14.35)	2	4.508	0.012	0.046
Gender (male%)	53 (60.9%)	16 (41.0%)	37 (56.1%)	2	4.339	0.114	0.150
Education	13.14 (3.5)	14.51 (4.3)	14.48 (3.1)	2	3.467	0.033	0.035

WB = winter-born; SB = summer-born; SZ = schizophrenia; DP = depression; HC = healthy controls; PANSS = Positive and Negative Syndrome Scale; pos = positive symptoms; neg = negative symptoms; HAMD = Hamilton rating scale for depression; BDI = Beck Depression Inventory; CPZ = Chlorpromazine equivalent dosage; df = degrees of freedom; M = Mean; SD = Standard deviation; IQR = interquartile range; X^2 = Chi-squared test.

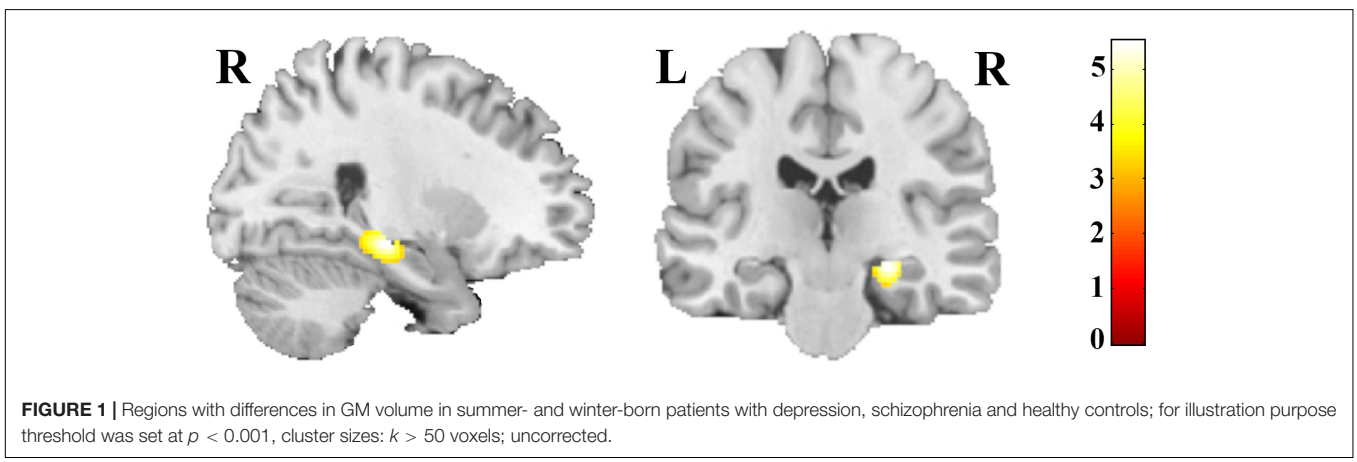

FIGURE 1 | Regions with differences in GM volume in summer- and winter-born patients with depression, schizophrenia and healthy controls; for illustration purpose threshold was set at $p < 0.001$, cluster sizes: $k > 50$ voxels; uncorrected.

DP, when compared to winter-born DP. Furthermore, SZ patients had a decreased hippocampal volume compared to HC participants and DP patients, independent of season of birth (**Figure 2**). Finally, summer-born subjects, independent of group showed lower hippocampal volume compared to winter-born subjects.

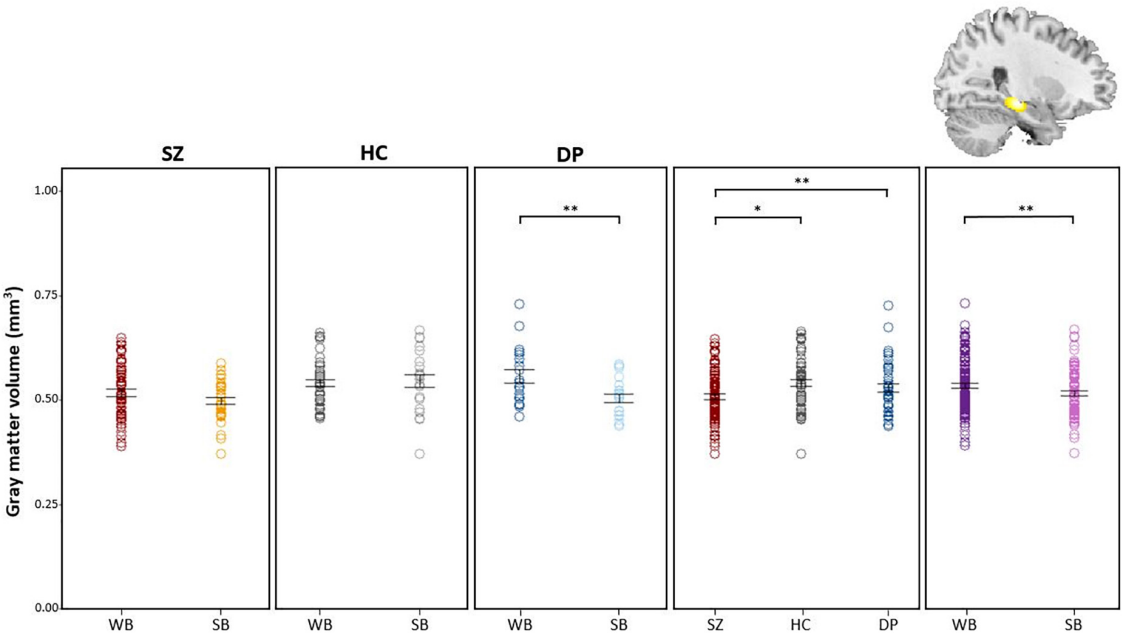

FIGURE 2 | *Post hoc* comparisons of extracted GM values show decreased volume of the hippocampus in DP_{SB} vs. DP_{WB} patients, in SZ patients vs. HC participants, in SZ patients vs DP patients and in WB vs SB individuals. *WB* = Winter-born; *SB* = Summer-born; *SZ* = Schizophrenia; *DP* = Depression; *HC* = Healthy Control; $^{**}p < 0.01$, $^{*}p < 0.05$.

Likewise whole brain *t*-tests within the ANCOVA revealed a decreased volume within the hippocampus in DP_{SB} ($_{pFWE-corr}$ = 0.003; t = 5.48; x = 26, y = −22, z = −12) (**Supplementary Figure 2** and **Supplementary Table 3**). We detected no significant differences comparing SZ_{SB} and SZ_{WB} patients.

DISCUSSION

Here we test the effect of season of birth on gray matter volume in a large transdiagnostic sample of 192 subjects with depression, schizophrenia and healthy controls. As hypothesized, we demonstrate a significant effect of season of birth on gray matter volume. In particular, we found an association of season of birth and right hippocampal volume in depression. However, contrary to our hypothesis summer-born patients showed decreased hippocampal volume compared to winter-born patients with depression. No effect of season of birth was present in schizophrenia. In contrast, schizophrenia patients had a right hippocampal volume reduction independent of season of birth.

Volumetric changes shown with VBM cannot offer direct information about the underlying cellular mechanism relevant for the effects. Therefore, deductive reasoning from volumetric changes to functional changes remains speculative. However, it has been suggested that volumetric changes seen with VBM are the result of a multifactorial process including multiple cellular modifications, for example cell density, cell size, myelination and vascularization affecting relaxation times and voxel intensities on a T1-weighted image (Zatorre et al., 2012). Given that season of birth can serve as a proxy of harmful environmental factors, our results argue for such environmental factors leading to hippocampal volume reduction in summer-born depression.

As stated in the introduction, a birth excess in winter-born patients with depression has repeatedly been found. In fact, harmful environmental factors are thought to affect neurodevelopment in perinatal stages and thus increase the risk to develop the disorder. Importantly previous reports suggest harmful effects of season of birth in depression. According to these observations we expected a decreased gray matter volume, in particular within the hippocampus in winter-born patients. Previous reports show alterations in hippocampal development leading to reduction in gray matter within the hippocampus following prenatal infection. For instance, reduced cell density in pyramidal and non-pyramidal cells as well as signs of atrophy (e.g., Fatemi et al., 1999, 2002a, 2008) were demonstrated. These alterations were associated with inflammation-induced depressive-like behavior in mice such as decrease of exploratory behavior (Shi et al., 2003; Meyer, 2006; Samuelsson et al., 2006; Fortier et al., 2007; Meyer et al., 2008; Li et al., 2009; Spini et al., 2021). On the contrary, here we show gray matter reduction in the hippocampus in summer-born compared to winter-born patients. Therefore, we have to conclude that the described seasonal birth excess in winter is not related to hippocampal volume reduction in depression.

The hippocampus is one of the most studied brain regions in the context of depression. In fact, bilateral hippocampal volume reductions form the most reliable regional gray matter abnormalities identified in depression (Koolschijn et al., 2009;

McKinnon et al., 2009; Cole et al., 2011; Kempton et al., 2011; Bora et al., 2012a,b; Du et al., 2012, 2014; Sacher et al., 2012; Arnone et al., 2013; Lai, 2013; Sexton et al., 2013; Stratmann et al., 2014; Zhao et al., 2014; Schmaal et al., 2016; Zhang et al., 2016; Yüksel et al., 2018) and subjects with subclinical symptoms (Besteher et al., 2020). The hippocampus is a brain region specifically sensitive to infectious agents (Green and Nolan, 2014), is important for stress regulation for instance *via* its inhibitory control over HPA-axis activity, and is more broadly involved in cognitive and affective processing *via* its widespread connections with prefrontal and limbic brain regions (Duman and Monteggia, 2006). Furthermore, antidepressant action may be accomplished through the prevention of cell apoptosis in the hippocampus (McKernan et al., 2009; Chen et al., 2017). Likewise, modern models of depression suggest hippocampal atrophy in humans as key in the development of the disease. In fact, lower hippocampal volume has been suggested as a risk marker of depression (Chen et al., 2010; Rao et al., 2010; Cole et al., 2011). Reduced hippocampal volume has been consistently shown to be about 5% smaller in depression (for meta-analyses see Koolschijn et al., 2009; McKinnon et al., 2009; Cole et al., 2011; Kempton et al., 2011; Bora et al., 2012a,b; Du et al., 2012, 2014; Sacher et al., 2012; Arnone et al., 2013; Lai, 2013; Sexton et al., 2013; Zhao et al., 2014; Schmaal et al., 2016; Zhang et al., 2016). Importantly, reductions in hippocampal volume are not only explained as consequence of medication (Zhao et al., 2014) or psychiatric comorbidities (Du et al., 2012) and have been shown throughout the lifespan (Sexton et al., 2013). Thus, reductions in hippocampal volume are a robust structural marker observed in depression. Our finding of reduced hippocampal volume in summer-born patients with depression add to this evidence and suggesting a key role of environmental factors as perinatal events in the disturbance of hippocampal development as risk factor for depression leastwise in a subgroup of patients. Importantly although previously alterations associated with season of birth in summer-born patients were not shown in depression, this effect was seen in schizophrenia and healthy subjects with psychotic experiences. In detail, summer-born schizophrenia patients had significantly lower fractional anisotropy in widespread white matter regions (i.e., the corpus callosum, internal and external capsule, corona radiata, posterior thalamic radiation, sagittal stratum, and superior longitudinal fasciculus) compared to patients born in the remainder of the year (Kempton et al., 2011), and cortical cortical thinning was detected in summer-born healthy individuals with subthreshold psychosis symptoms (Koolschijn et al., 2009).

To the best of our knowledge, this is the first study to investigate the effect of season of birth on gray matter volume in a transdiagnostic sample of patients, in particular including depression. The mechanisms that account for the detected reduced hippocampal volume in depressed summer-born patients are beyond the scope of this study and understanding the pathophysiological mechanisms by which infection, inflammation, and depression are linked is complex. It was hypothesized that several factors (for instance increased oxidative stress, hypothalamic–pituitary–adrenal axis dysfunction, neurotransmitter insufficiency or reductions in growth factors) or a combination of these factors may lead to a possible final pathway of decreases in neuropil, immunoreactivity, and dendritic spine density or neuronal apoptosis that may underlay gray matter loss in the hippocampus. However, several other factors such as unhealthy lifestyle in patients may also contribute to our finding. Still, the present finding of a relationship between season of birth and right hippocampal volume support the hypothesis of perinatal events involving a seasonal factor and subsequent pathologic brain development in depression.

Turning to schizophrenia, we show a general reduction of hippocampal volume irrespective of season of birth. This fact may hamper to detect specific effects of season of birth within the hippocampus. However, our finding is in line with previous reports showing hippocampal volume reduction in schizophrenia (Nelson et al., 1998; Heckers and Konradi, 2010; Adriano et al., 2012), even at the onset of the disorder in the first episode (Adriano et al., 2012; McHugo et al., 2020), as well as in ad risk subjects who later develop the disorder (Harrisberger et al., 2016). Contrary, and as mentioned in the introduction, previous reports have observed alterations in the brain structure associated with season of birth, which was not the case in our report. In particular, ventricular enlargement in winter-born compared to summer-born patients with schizophrenia was shown (Sacchetti et al., 1987, 1992; Zipursky and Schulz, 1987; Degreef et al., 1988; d'Amato et al., 1994). In addition, one DTI study displayed structural white matter impairments in patients born in summer relative to patients born in winter (Giezendanner et al., 2013).

We have to point out limitations of our report. First, all but seven patients were on psychotropic medication. We cannot rule out that medication had an effect on hippocampal volume. In particular, medication may hamper to detect an effect of volume reduction in schizophrenia. However, SB and WB schizophrenia patients did not differ in CPZ equivalents as a proxy of antipsychotic dosage. In addition, previous reports detected alterations in brain structure in medicated schizophrenia patients (Sacchetti et al., 1987, 1992; Zipursky and Schulz, 1987; Degreef et al., 1988; d'Amato et al., 1994; Giezendanner et al., 2013). Furthermore meta-analytic evidence suggests that hippocampal volume reduction in depression is not solely explained as a medication effect (Zhao et al., 2014). Second, we do not have information of possible infections or other complications during the prenatal period or birth as well as birth weight or whether it was preterm birth in our subjects. Thus, the seasonal birth pattern is associated with alterations in the brain but we cannot conclude on the causes. Third, sample size was not balanced over the groups leading to smaller sample size of patients with depression (n = 39). Finally, several factors have been suggested that may moderate the association between depression and hippocampal volume including depression severity and state (Arnone et al., 2013) or age-of-onset of the first depressive episode (Schmaal et al., 2016). However, in our study winter- and summer-born patients with depression did not differ in depression severity and age of onset.

In conclusion, our results demonstrate that seasonal birth pattern may contribute to hippocampal volume reduction in depression. Additionally, we demonstrate that schizophrenia patients show a hippocampal volume reduction independent

of season of birth. The finding of a relationship between season of birth and hippocampal volume in depression support the hypothesis of a harmful perinatal event and subsequent pathologic brain development in depression, at least in a subgroup of patients.

DATA AVAILABILITY STATEMENT

The raw data supporting the conclusions of this article will be made available by the authors, without undue reservation.

ETHICS STATEMENT

The studies involving human participants were reviewed and approved by Ethics Commission of the Canton of Bern [Kantonale Ethikkomission Bern (KEK)], Switzerland. The patients/participants provided their written informed consent to participate in this study.

AUTHOR CONTRIBUTIONS

SW designed the study, wrote the protocol, acquired the funding, and supervised the data acquisition. KS analyzed the data and wrote the first draft of the manuscript. NS, NA, and FC recruited the subjects and conducted the assessments. All authors discussed findings and edited the manuscript.

FUNDING

This study received funding from the Swiss National Science Foundation (Grant Nos. 320030_129668/1, and 152619/1), as well as the Bangerter-Rhyner Foundation (to SW).

SUPPLEMENTARY MATERIAL

The Supplementary Material for this article can be found online at: https://www.frontiersin.org/articles/10.3389/fnhum.2022.877461/full#supplementary-material

REFERENCES

Adriano, F., Caltagirone, C., and Spalletta, G. (2012). Hippocampal volume reduction in first-episode and chronic schizophrenia: a review and meta-analysis. *Neuroscientist* 18, 180–200. doi: 10.1177/1073858410395147

Al-Haddad, B. J. S., Jacobsson, B., Chabra, S., Modzelewska, D., Olson, E. M., Bernier, R., et al. (2019a). Long-term risk of neuropsychiatric disease after exposure to infection in utero. *JAMA Psychiatry*. 76:594. doi: 10.1001/jamapsychiatry.2019.0029

Al-Haddad, B. J. S., Oler, E., Armistead, B., Elsayed, N. A., Weinberger, D. R., Bernier, R., et al. (2019b). The fetal origins of mental illness. *Am. J. Obstet Gynecol.* 221, 549–562. doi: 10.1016/j.ajog.2019.06.013

Arnone, D., McKie, S., Elliott, R., Juhasz, G., Thomas, E. J., Downey, D., et al. (2013). State-dependent changes in hippocampal grey matter in depression. *Mol. Psychiatry* 18, 1265–1272. doi: 10.1038/mp.2012.150

Ashburner, J., and Friston, K. J. (2000). Voxel-based morphometry–the methods. *Neuroimage* 11, 805–821. doi: 10.1006/nimg.2000.0582

Barker, D. (1998). *Mothers, Babies and Health in Later Life*. Edinburgh: Churchhill Livingstone.

Beck, A. T. (1961). An inventory for measuring depression. *Arch. Gen. Psychiatry.* 4:561. doi: 10.1001/archpsyc.1961.01710120031004

Besteher, B., Gaser, C., and Nenadić, I. (2020). Brain structure and subclinical symptoms: a dimensional perspective of psychopathology in the depression and anxiety spectrum. *Neuropsychobiology* 79, 270–283. doi: 10.1159/000501024

Bora, E., Fornito, A., Pantelis, C., and Yücel, M. (2012a). Gray matter abnormalities in major depressive disorder: a meta-analysis of voxel based morphometry studies. *J. Affect. Disord.* 138, 9–18. doi: 10.1016/j.jad.2011.03.049

Bora, E., Harrison, B. J., Davey, C. G., Yücel, M., and Pantelis, C. (2012b). Meta-analysis of volumetric abnormalities in cortico-striatal-pallidal-thalamic circuits in major depressive disorder. *Psychol. Med.* 42, 671–681. doi: 10.1017/s0033291711001668

Brandl, F., Avram, M., Weise, B., Shang, J., Simões, B., Bertram, T., et al. (2019). Specific substantial dysconnectivity in schizophrenia: a transdiagnostic multimodal meta-analysis of resting-state functional and structural magnetic resonance imaging studies. *Biol. Psychiatry* 85, 573–583. doi: 10.1016/j.biopsych.2018.12.003

Campbell, S., and MacQueen, G. (2004). The role of the hippocampus in the pathophysiology of major depression. *J. Psychiatry Neurosci.* 29, 417–426.

Cantisani, A., Stegmayer, K., Bracht, T., Federspiel, A., Wiest, R., Horn, H., et al. (2016). Distinct resting−state perfusion patterns underlie psychomotor retardation in unipolar vs. bipolar depression. *Acta Psychiatr Scand.* 134, 329–338. doi: 10.1111/acps.12625

Chen, M. C., Hamilton, J. P., and Gotlib, I. H. (2010). Decreased hippocampal volume in healthy girls at risk of depression. *Arch. Gen. Psychiatry* 67, 270–276. doi: 10.1001/archgenpsychiatry.2009.202

Chen, W. J., Du, J. K., Hu, X., Yu, Q., Li, D. X., Wang, C. N., et al. (2017). Protective effects of resveratrol on mitochondrial function in the hippocampus improves inflammation-induced depressive-like behavior. *Physiol. Behav.* 182, 54–61. doi: 10.1016/j.physbeh.2017.09.024

Cole, J., Costafreda, S. G., McGuffin, P., and Fu, C. H. Y. (2011). Hippocampal atrophy in first episode depression: a meta-analysis of magnetic resonance imaging studies. *J. Affect. Disord.* 134, 483–487. doi: 10.1016/j.jad.2011.05.057

Cotter, D., Takei, N., Farrell, M., Sham, P., Quinn, P., Larkin, C., et al. (1995). Does prenatal exposure to influenza in mice induce pyramidal cell disarray in the dorsal hippocampus? *Schizophr Res.* 16, 233–241. doi: 10.1016/0920-9964(94)E0082-I

d'Amato, T., Rochet, T., Daléry, J., Chauchat, J. H., Martin, J. P., and Marie-Cardine, M. (1994). Seasonality of birth and ventricular enlargement in chronic schizophrenia. *Psychiatry Res. Neuroimaging.* 55, 65–73. doi: 10.1016/0925-4927(94)90001-9

Damme, K. S. F., Park, J. S., Walther, S., Vargas, T., Shankman, S. A., and Mittal, V. A. (2022). Depression and psychosis risk shared vulnerability for motor signs across development, symptom dimensions, and familial risk. *Schizophr. Bull.* sbab133. doi: 10.1093/schbul/sbab133

Dean, D. J., Woodward, N., Walther, S., McHugo, M., Armstrong, K., and Heckers, S. (2020). Cognitive motor impairments and brain structure in schizophrenia spectrum disorder patients with a history of catatonia. *Schizophr Res.* 222, 335–341. doi: 10.1016/j.schres.2020.05.012

Degreef, G., Mukherjee, S., Bilder, R., and Schnur, D. (1988). Season of birth and CT scan findings in schizophrenic patients. *Biol. Psychiatry* 24, 461–464. doi: 10.1016/0006-3223(88)90186-2

Deichmann, R., Schwarzbauer, C., and Turner, R. (2004). Optimisation of the 3D MDEFT sequence for anatomical brain imaging: technical implications at 1.5 and 3 T. *Neuroimage* 21, 757–767. doi: 10.1016/j.neuroimage.2003.09.062

Disanto, G., Morahan, J. M., Lacey, M. V., Deluca, G. C., Giovannoni, G., Ebers, G. C., et al. (2012). Seasonal distribution of psychiatric births in England. *PLoS One* 7:e34866. doi: 10.1371/journal.pone.0034866

Du, M. Y., Liu, J., Chen, Z., Huang, X., Li, J., Kuang, W., et al. (2014). Brain grey matter volume alterations in late-life depression. *J. Psychiatry Neurosci.* 39, 397–406. doi: 10.1503/jpn.130275

Du, M. Y., Wu, Q. Z., Yue, Q., Li, J., Liao, Y., Kuang, W. H., et al. (2012). Voxelwise meta-analysis of gray matter reduction in major depressive disorder. *Prog. Neuropsychopharmacol. Biol. Psychiatry* 36, 11–16. doi: 10.1016/j.pnpbp.2011.09.014

Duman, R. S., and Monteggia, L. M. (2006). A neurotrophic model for stress-related mood disorders. *Biol. Psychiatry.* 59, 1116–1127. doi: 10.1016/j.biopsych.2006.02.013

Fatemi, S. H., Earle, J., Kanodia, R., Kist, D., Emamian, E. S., Patterson, P. H., et al. (2002a). Prenatal viral infection leads to pyramidal cell atrophy and macrocephaly in adulthood: implications for genesis of autism and schizophrenia. *Cell. Mol. Neurobiol.* 22, 25–33. doi: 10.1023/a:1015337611258

Fatemi, S. H., Emamian, E. S., Kist, D., Sidwell, R. W., Nakajima, K., Akhter, P., et al. (1999). Defective corticogenesis and reduction in Reelin immunoreactivity in cortex and hippocampus of prenatally infected neonatal mice. *Mol. Psychiatry* 4, 145–154. doi: 10.1038/sj.mp.4000520

Fatemi, S. H., Emamian, E. S., Sidwell, R. W., Kist, D. A., Stary, J. M., Earle, J. A., et al. (2002b). Human influenza viral infection in utero alters glial fibrillary acidic protein immunoreactivity in the developing brains of neonatal mice. *Mol. Psychiatry* 7, 633–640. doi: 10.1038/sj.mp.4001046

Fatemi, S. H., and Folsom, T. D. (2009). The neurodevelopmental hypothesis of schizophrenia. *Revisited Schizophr. Bull.* 35, 528–548. doi: 10.1093/schbul/sbn187

Fatemi, S. H., Reutiman, T. J., Folsom, T. D., Huang, H., Oishi, K., Mori, S., et al. (2008). Maternal infection leads to abnormal gene regulation and brain atrophy in mouse offspring: implications for genesis of neurodevelopmental disorders. *Schizophr. Res.* 99, 56–70. doi: 10.1016/j.schres.2007.11.018

Fatemi, S. H., Sidwell, R., Akhter, P., Sedgewick, J., Thuras, P., Bailey, K., et al. (1998a). Human influenza viral infection in utero increases nNOS expression in hippocampi of neonatal mice. *Synapse* 29, 84–88. doi: 10.1002/(SICI)1098-2396(199805)29:1<84::AID-SYN8<3.0.CO

Fatemi, S. H., Sidwell, R., Kist, D., Akhter, P., Meltzer, H. Y., Bailey, K., et al. (1998b). Differential expression of synaptosome-associated protein 25 kDa [SNAP-25] in hippocampi of neonatal mice following exposure to human influenza virus in utero. *Brain Res.* 800, 1–9. doi: 10.1016/s0006-8993(98)00450-8

Fortier, M. E., Luheshi, G. N., and Boksa, P. (2007). Effects of prenatal infection on prepulse inhibition in the rat depend on the nature of the infectious agent and the stage of pregnancy. *Behav. Brain Res.* 181, 270–277. doi: 10.1016/j.bbr.2007.04.016

Giezendanner, S., Walther, S., Razavi, N., Van Swam, C., Fisler, M. S., Soravia, L. M., et al. (2013). Alterations of white matter integrity related to the season of birth in schizophrenia: a DTI study. *PLoS One* 8:e75508. doi: 10.1371/journal.pone.0075508

Goodkind, M., Eickhoff, S. B., Oathes, D. J., Jiang, Y., Chang, A., Jones-Hagata, L. B., et al. (2015). Identification of a common neurobiological substrate for mental illness. *JAMA Psychiatry* 72, 305–315. doi: 10.1001/jamapsychiatry.2014.2206

Green, H. F., and Nolan, Y. M. (2014). Inflammation and the developing brain: consequences for hippocampal neurogenesis and behavior. *Neurosci. Biobehav. Rev.* 40, 20–34. doi: 10.1016/j.neubiorev.2014.01.004

Gutman, B. A., van Erp, T. G., Alpert, K., Ching, C. R., Isaev, D., Ragothaman, A., et al. (2022). A meta−analysis of deep brain structural shape and asymmetry abnormalities in 2,833 individuals with schizophrenia compared with 3,929 healthy volunteers via the ENIGMA consortium. *Hum. Brain Mapp.* 43, 352–372. doi: 10.1002/hbm.25625

Hamilton, M. (1986). *The Hamilton Rating Scale for Depression. Assessment of Depression*. Berlin: Springer, 143–152.

Harrisberger, F., Buechler, R., Smieskova, R., Lenz, C., Walter, A., Egloff, L., et al. (2016). Alterations in the hippocampus and thalamus in individuals at high risk for psychosis. *NPJ Schizophr.* 2:16033. doi: 10.1038/npjschz.2016.33

Heckers, S. (2001). Neuroimaging studies of the hippocampus in schizophrenia. *Hippocampus* 11, 520–528. doi: 10.1002/hipo.1068

Heckers, S., and Konradi, C. (2010). *Hippocampal Pathology in Schizophrenia. Behavioral Neurobiology of Schizophrenia and Its Treatment*. Berlin: Springer, 529–553.

Hellewell, S. C., Welton, T., Maller, J. J., Lyon, M., Korgaonkar, M. S., Koslow, S. H., et al. (2019). Profound and reproducible patterns of reduced regional gray matter characterize major depressive disorder. *Transl. Psychiatry* 9, 1–8. doi: 10.1038/s41398-019-0512-8

Honea, R., Crow, T. J., Passingham, D., and Mackay, C. E. (2005). Regional deficits in brain volume in schizophrenia: a meta-analysis of voxel-based morphometry studies. *Am. J. Psychiatry* 162, 2233–2245. doi: 10.1176/appi.ajp.162.12.2233

Horn, H., Federspiel, A., Wirth, M., Müller, T. J., Wiest, R., Walther, S., et al. (2010). Gray matter volume differences specific to formal thought disorder in schizophrenia. *Psychiatry Res. Neuroimaging* 182, 183–186. doi: 10.1016/j.pscychresns.2010.01.016

Huang, K., Kang, Y., Wu, Z., Wang, Y., Cai, S., and Huang, L. (2021). Asymmetrical alterations of grey matter among psychiatric disorders: a systematic analysis by voxel-based activation likelihood estimation. *Prog. Neuropsychopharmacol. Biol. Psychiatry* 110:110322. doi: 10.1016/j.pnpbp.2021.110322

Joiner, T. E., Pfaff, J. J., Acres, J. G., and Johnson, F. (2002). Birth month and suicidal and depressive symptoms in Australians born in the Southern vs. the Northern hemisphere. *Psychiatry Res.* 112, 89–92. doi: 10.1016/S0165-1781(02)00183-X

Kay, S. R., Fiszbein, A., and Opler, L. A. (1987). The positive and negative syndrome scale (PANSS) for schizophrenia. *Schizophr. Bull.* 13, 261–276. doi: 10.1093/schbul/13.2.261

Kempton, M. J., Salvador, Z., Munafò, M. R., Geddes, J. R., Simmons, A., Frangou, S., et al. (2011). Structural neuroimaging studies in major depressive disorder: meta-analysis and comparison with bipolar disorder. *Arch. Gen. Psychiatry* 68:675. doi: 10.1001/archgenpsychiatry.2011.60

Kindler, J., Michel, C., Schultze-Lutter, F., Felber, G., Hauf, M., Schimmelmann, B. G., et al. (2019). Functional and structural correlates of abnormal involuntary movements in psychosis risk and first episode psychosis. *Schizophr. Res.* 212, 196–203. doi: 10.1016/j.schres.2019.07.032

Koolschijn, P. C. M. P., Van Haren, N. E. M., Lensvelt-Mulders, G. J. L. M., Hulshoff Pol, H. E., and Kahn, R. S. (2009). Brain volume abnormalities in major depressive disorder: a meta-analysis of magnetic resonance imaging studies. *Hum. Brain Mapp.* 30, 3719–3735. doi: 10.1002/hbm.20801

Lai, C. H. (2013). Gray matter volume in major depressive disorder: a meta-analysis of voxel-based morphometry studies. *Psychiatry Res. Neuroimaging* 211, 37–46. doi: 10.1016/j.pscychresns.2012.06.006

Li, Q., Cheung, C., Wei, R., Hui, E. S., Feldon, J., Meyer, U., et al. (2009). Prenatal immune challenge is an environmental risk factor for brain and behavior change relevant to schizophrenia: evidence from mri in a mouse model. *PLoS One* 4:e6354. doi: 10.1371/journal.pone.0006354

Liloia, D., Brasso, C., Cauda, F., Mancuso, L., Nani, A., Manuello, J., et al. (2021). Updating and characterizing neuroanatomical markers in high-risk subjects, recently diagnosed and chronic patients with schizophrenia: a revised coordinate-based meta-analysis. *Neurosci. Biobehav. Rev.* 123, 83–103. doi: 10.1016/j.neubiorev.2021.01.010

McHugo, M., Armstrong, K., Roeske, M. J., Woodward, N. D., Blackford, J. U., and Heckers, S. (2020). Hippocampal volume in early psychosis: a 2-year longitudinal study. *Transl. Psychiatry.* 10, 1–10. doi: 10.1038/s41398-020-00985-1

McKernan, D. P., Dinan, T. G., and Cryan, J. F. (2009). "Killing the blues": a role for cellular suicide (apoptosis) in depression and the antidepressant response? *Prog. Neurobiol.* 88, 246–263. doi: 10.1016/j.pneurobio.2009.04.006

McKinnon, M. C., Yucel, K., Nazarov, A., and MacQueen, G. M. (2009). A meta-analysis examining clinical predictors of hippocampal volume in patients with major depressive disorder. *J. Psychiatry Neurosci.* 34:41.

Mertse, N., Denier, N., Walther, S., Breit, S., Grosskurth, E., Federspiel, A., et al. (2022). Associations between anterior cingulate thickness, cingulum bundle microstructure, melancholia and depression severity in unipolar depression. *J. Affect. Disord.* 301, 437–444. doi: 10.1016/j.jad.2022.01.035

Meyer, U. (2006). The time of prenatal immune challenge determines the specificity of inflammation-mediated brain and behavioral pathology. *J. Neurosci.* 26, 4752–4762. doi: 10.1523/jneurosci.0099-06.2006

Meyer, U., Nyffeler, M., Yee, B. K., Knuesel, I., and Feldon, J. (2008). Adult brain and behavioral pathological markers of prenatal immune challenge during early/middle and late fetal development in mice. *Brain Behav. Immun.* 22, 469–486. doi: 10.1016/j.bbi.2007.09.012

Moore, P. B., El-Badri, S. M., Cousins, D., Shepherd, D. J., Young, A. H., McAllister, V. L., et al. (2001). White matter lesions and season of birth of patients with bipolar affective disorder. *Am. J. Psychiatry* 158, 1521–1524. doi: 10.1176/appi.ajp.158.9.1521

Nelson, M. D., Saykin, A. J., Flashman, L. A., and Riordan, H. J. (1998). Hippocampal volume reduction in schizophrenia as assessed by magnetic resonance imaging. *Arch. Gen. Psychiatry* 55:433. doi: 10.1001/archpsyc.55.5.433

Oldfield, R. C. (1971). The assessment and analysis of handedness: the Edinburgh inventory. *Neuropsychologia* 9, 97–113. doi: 10.1016/0028-3932(71)90067-4

Orosz, A., Jann, K., Federspiel, A., Horn, H., Höfle, O., Dierks, T., et al. (2012). Reduced cerebral blood flow within the default-mode network and within total gray matter in major depression. *Brain Connect* 2, 303–310. doi: 10.1089/brain.2012.0101

Pantelis, C., Jayaram, M., Hannan, A. J., Wesselingh, R., Nithianantharajah, J., Wannan, C. M., et al. (2021). Neurological, neuropsychiatric and neurodevelopmental complications of COVID-19. *Aust. N Z J. Psychiatry* 55, 750–762. doi: 10.1177/0004867420961472

Rao, U., Chen, L. A., Bidesi, A. S., Shad, M. U., Thomas, M. A., and Hammen, C. L. (2010). Hippocampal changes associated with early-life adversity and vulnerability to depression. *Biol. Psychiatry* 67, 357–364. doi: 10.1016/j.biopsych.2009.10.017

Ratnayake, U., Quinn, T. A., Castillo-Melendez, M., Dickinson, H., and Walker, D. W. (2012). Behaviour and hippocampus-specific changes in spiny mouse neonates after treatment of the mother with the viral-mimetic Poly I:C at mid-pregnancy. *Brain Behav. Immun.* 26, 1288–1299. doi: 10.1016/j.bbi.2012.08.011

Roy, M., Flaum, M., and Andreasen, N. (1995). No difference found between winter- and non-winter-born schizophrenic cases. *Schizophr. Res.* 17, 241–248. doi: 10.1016/0920-9964(95)00010-0

Sacchetti, E., Calzeroni, A., Vita, A., Terzi, A., Pollastro, F., and Cazzullo, C. L. (1992). The brain damage hypothesis of the seasonality of births in schizophrenia and major affective disorders: evidence from computerised tomography. *Br. J. Psychiatry* 160, 390–397. doi: 10.1192/bjp.160.3.390

Sacchetti, E., Vita, A., Battaglia, M., Calzeroni, A., Conte, G., Invernizzi, G., et al. (1987). "Season of birth and cerebral ventricular enlargement in schizophrenia," in *Etiopathogenetic Hypotheses of Schizophrenia: The Impact of Epidemiological, Biochemical and Neuromorphological Studies*, eds C. L. Cazzullo, G. Invernizzi, E. Sacchetti, and A. Vita (Dordrecht: Springer Netherlands), 93–98.

Sacher, J., Neumann, J., Fünfstück, T., Soliman, A., Villringer, A., and Schroeter, M. L. (2012). Mapping the depressed brain: a meta-analysis of structural and functional alterations in major depressive disorder. *J. Affect. Disord.* 140, 142–148. doi: 10.1016/j.jad.2011.08.001

Samuelsson, A. M., Jennische, E., Hansson, H. A., and Holmäng, A. (2006). Prenatal exposure to interleukin-6 results in inflammatory neurodegeneration in hippocampus with NMDA/GABAA dysregulation and impaired spatial learning. *Am. J. Physiol. Regul. Integr. Comp. Physiol.* 290, R1345–R1356. doi: 10.1152/ajpregu.00268.2005

Schmaal, L., Veltman, D. J., Van Erp, T. G. M., Sämann, P. G., Frodl, T., Jahanshad, N., et al. (2016). Subcortical brain alterations in major depressive disorder: findings from the ENIGMA major depressive disorder working group. *Mol. Psychiatry* 21, 806–812. doi: 10.1038/mp.2015.69

Schoretsanitis, G., Stegmayer, K., Razavi, N., Federspiel, A., Müller, T. J., Horn, H., et al. (2019). Inferior frontal gyrus gray matter volume is associated with aggressive behavior in schizophrenia spectrum disorders. *Psychiatry Res. Neuroimaging* 290, 14–21. doi: 10.1016/j.pscychresns.2019.06.003

Serra-Blasco, M., Radua, J., Soriano-Mas, C., Gómez-Benlloch, A., Porta-Casteràs, D., Carulla-Roig, M., et al. (2021). Structural brain correlates in major depression, anxiety disorders and post-traumatic stress disorder: a voxel-based morphometry meta-analysis. *Neurosci. Biobehav. Rev.* 129, 269–281. doi: 10.1016/j.neubiorev.2021.07.002

Sexton, C. E., Mackay, C. E., and Ebmeier, K. P. (2013). A systematic review and meta-analysis of magnetic resonance imaging studies in late-life depression. *Am. J. Geriatr. Psychiatry* 21, 184–195. doi: 10.1016/j.jagp.2012.10.019

Shah, C., Zhang, W., Xiao, Y., Yao, L., Zhao, Y., Gao, X., et al. (2017). Common pattern of gray-matter abnormalities in drug-naive and medicated first-episode schizophrenia: a multimodal meta-analysis. *Psychol. Med.* 47, 401–413. doi: 10.1017/S0033291716002683

Sheehan, D. V., Lecrubier, Y., Sheehan, K. H., Amorim, P., Janavs, J., Weiller, E., et al. (1998). The mini-international neuropsychiatric interview (MINI): the development and validation of a structured diagnostic psychiatric interview for DSM-IV and ICD-10. *J. Clin. Psychiatry* 59, 22–33.

Sheline, Y. I., Mittler, B. L., and Mintun, M. A. (2002). The hippocampus and depression. *Eur. Psychiatry* 17, 300s–305s. doi: 10.1016/S0924-9338(02)00655-7

Shi, L., Fatemi, S. H., Sidwell, R. W., and Patterson, P. H. (2003). Maternal influenza infection causes marked behavioral and pharmacological changes in the offspring. *J. Neurosci.* 23, 297–302. doi: 10.1523/jneurosci.23-01-00297.2003

Spini, V. B. M. G., Ferreira, F. R., Gomes, A. O., Duarte, R. M. F., Oliveira, V. H. S., Costa, N. B., et al. (2021). Maternal immune activation with H1N1 or toxoplasma gondii antigens induces behavioral impairments associated with mood disorders in rodents. *Neuropsychobiology* 80, 234–241. doi: 10.1159/000510791

Steen, R. G., Mull, C., McClure, R., Hamer, R. M., and Lieberman, J. A. (2006). Brain volume in first-episode schizophrenia. *Br. J. Psychiatry* 188, 510–518. doi: 10.1192/bjp.188.6.510

Stegmayer, K., Bohlhalter, S., Vanbellingen, T., Federspiel, A., Moor, J., Wiest, R., et al. (2016). Structural brain correlates of defective gesture performance in schizophrenia. *Cortex* 78, 125–137. doi: 10.1016/j.cortex.2016.02.014

Stegmayer, K., Horn, H., Federspiel, A., Razavi, N., Bracht, T., Laimböck, K., et al. (2014). Ventral striatum gray matter density reduction in patients with schizophrenia and psychotic emotional dysregulation. *NeuroImage Clin.* 4, 232–239. doi: 10.1016/j.nicl.2013.12.007

Stegmayer, K., Horn, H. J., Federspiel, A., Razavi, N., Laimböck, K., Bracht, T., et al. (2013). Supplementary motor area (SMA) volume correlates with psychotic symptoms associated with dysregulation of the motor system: a voxel-based morphometry (VBM) study. *Eur. Arch. Psychiatry Clin. Neurosci.* 263, S66–S67.

Stratmann, M., Konrad, C., Kugel, H., Krug, A., Schöning, S., Ohrmann, P., et al. (2014). Insular and hippocampal gray matter volume reductions in patients with major depressive disorder. *PLoS One* 9:e102692. doi: 10.1371/journal.pone.0102692

Tamminga, C. A., Stan, A. D., and Wagner, A. D. (2010). The hippocampal formation in schizophrenia. *Am. J. Psychiatry* 167, 1178–1193. doi: 10.1176/appi.ajp.2010.09081187

Torrey, E. F., Miller, J., Rawlings, R., and Yolken, R. H. (1997). Seasonality of births in schizophrenia and bipolar disorder: a review of the literature. *Schizophr. Res.* 28, 1–38. doi: 10.1016/s0920-9964(97)00092-3

Torrey, E. F., Rawlings, R. R., Ennis, J. M., Merrill, D. D., and Flores, D. S. (1996). Birth seasonality in bipolar disorder, schizophrenia, schizoaffective disorder and stillbirths. *Schizophr. Res.* 21, 141–149. doi: 10.1016/0920-9964(96)00022-9

Videbech, P. (2004). Hippocampal volume and depression: a meta-analysis of MRI studies. *Am. J. Psychiatry* 161, 1957–1966. doi: 10.1176/appi.ajp.161.11.1957

Viher, P. V., Stegmayer, K., Kubicki, M., Karmacharya, S., Lyall, A. E., Federspiel, A., et al. (2018). The cortical signature of impaired gesturing: findings from schizophrenia. *NeuroImage Clin.* 17, 213–221. doi: 10.1016/j.nicl.2017.10.017

Vita, A., De Peri, L., Deste, G., and Sacchetti, E. (2012). Progressive loss of cortical gray matter in schizophrenia: a meta-analysis and meta-regression of longitudinal MRI studies. *Transl. Psychiatry* 2, e190–e. doi: 10.1038/tp.2012.116

Vita, A., De Peri, L., Silenzi, C., and Dieci, M. (2006). Brain morphology in first-episode schizophrenia: a meta-analysis of quantitative magnetic resonance imaging studies. *Schizophr. Res.* 82, 75–88. doi: 10.1016/j.schres.2005.11.004

Walther, S., Federspiel, A., Horn, H., Razavi, N., Wiest, R., Dierks, T., et al. (2011). Alterations of white matter integrity related to motor activity in schizophrenia. *Neurobiol. Dis.* 42, 276–283. doi: 10.1016/j.nbd.2011.01.017

Walther, S., Höfle, O., Federspiel, A., Horn, H., Hügli, S., Wiest, R., et al. (2012a). Neural correlates of disbalanced motor control in major depression. *J. Affect. Disord.* 136, 124–133. doi: 10.1016/j.jad.2011.08.020

Walther, S., Hügli, S., Höfle, O., Federspiel, A., Horn, H., Bracht, T., et al. (2012b). Frontal white matter integrity is related to psychomotor retardation in major depression. *Neurobiol. Dis.* 47, 13–19. doi: 10.1016/j.nbd.2012.03.019

Walther, S., Schäppi, L., Federspiel, A., Bohlhalter, S., Wiest, R., Strik, W., et al. (2017). Resting-state hyperperfusion of the supplementary motor area in catatonia. *Schizophr. Bull.* 43, 972–981. doi: 10.1093/schbul/sbw140

Wilms, G., Van Ongeval, C., Baert, A. L., Claus, A., Bollen, J., De Cuyper, H., et al. (1992). Ventricular enlargement, clinical correlates and treatment outcome in chronic schizophrenic inpatients. *Acta Psychiatr. Scand.* 85, 306–312. doi: 10.1111/j.1600-0447.1992.tb01474.x

Wright, I. C., Rabe-Hesketh, S., Woodruff, P. W. R., David, A. S., Murray, R. M., and Bullmore, E. T. (2000). Meta-analysis of regional brain

volumes in schizophrenia. *Am. J. Psychiatry* 157, 16–25. doi: 10.1176/ajp.157.1.16

Yüksel, D., Engelen, J., Schuster, V., Dietsche, B., Konrad, C., Jansen, A., et al. (2018). Longitudinal brain volume changes in major depressive disorder. *J. Neural. Transm.* 125, 1433–1447. doi: 10.1007/s00702-018-1919-8

Zaigham, M., and Andersson, O. (2020). Maternal and perinatal outcomes with COVID−19: a systematic review of 108 pregnancies. *Acta Obstet. Gynecol. Scand.* 99, 823–829. doi: 10.1111/aogs.13867

Zatorre, R. J., Fields, R. D., and Johansen-Berg, H. (2012). Plasticity in gray and white: neuroimaging changes in brain structure during learning. *Nat. Neurosci.* 15, 528–536. doi: 10.1038/nn.3045

Zhang, H., Li, L., Wu, M., Chen, Z., Hu, X., Chen, Y., et al. (2016). Brain gray matter alterations in first episodes of depression: a meta-analysis of whole-brain studies. *Neurosci. Biobehav. Rev.* 60, 43–50. doi: 10.1016/j.neubiorev.2015.10.011

Zhao, Y. J., Du, M. Y., Huang, X. Q., Lui, S., Chen, Z. Q., Liu, J., et al. (2014). Brain grey matter abnormalities in medication-free patients with major depressive disorder: a meta-analysis. *Psychol. Med.* 44, 2927–2937. doi: 10.1017/s0033291714000518

Zipursky, R. B., and Schulz, S. C. (1987). Seasonality of birth and CT findings in schizophrenia. *Biol. Psychiatry.* 22, 1288–1292. doi: 10.1016/0006-3223(87)90040-0

Conflict of Interest: SW received honoraria from Janssen, Lundbeck, Mepha, Neurolite, Otsuka and Sunovion, and served on advisory boards for Lundbeck and Sunovion in 2019. KS received honoraria from Janssen, Lundbeck, Mepha, and Sunovion. RH received speaker/advisor honorary from Merck, Novartis, Roche, Biogen, Alexion, Sanofi, Janssen, Bristol-Myers Squibb, and Almirall, and received research support within the last 5 years from Roche, Merck, Sanofi, Biogen, Chiesi, and Bristol-Myers Squibb, and also received research grants from the Swiss MS Society, and also serves as associated editor for Journal of Central Nervous System disease.

The remaining authors declare that the research was conducted in the absence of any commercial or financial relationships that could be construed as a potential conflict of interest.

Publisher's Note: All claims expressed in this article are solely those of the authors and do not necessarily represent those of their affiliated organizations, or those of the publisher, the editors and the reviewers. Any product that may be evaluated in this article, or claim that may be made by its manufacturer, is not guaranteed or endorsed by the publisher.

frontiers | Frontiers in Human Neuroscience

TYPE Original Research
PUBLISHED 05 August 2022
DOI 10.3389/fnhum.2022.954898

OPEN ACCESS

EDITED BY
Franziska Knolle,
Technical University of Munich,
Germany

REVIEWED BY
Jakob André Kaminski,
Charité University Medicine Berlin,
Germany
Wei Deng,
Affiliated Mental Health Center
and Hangzhou Seventh People's
Hospital, China
Uzma Zahid,
University of Oxford, United Kingdom

*CORRESPONDENCE
Lena Palaniyappan
lena.palaniyappan@mcgill.ca

†These authors share first authorship

SPECIALTY SECTION
This article was submitted to
Brain Imaging and Stimulation,
a section of the journal
Frontiers in Human Neuroscience

RECEIVED 27 May 2022
ACCEPTED 19 July 2022
PUBLISHED 05 August 2022

CITATION
Liang L, Silva AM, Jeon P, Ford SD, MacKinley M, Théberge J and Palaniyappan L (2022) Widespread cortical thinning, excessive glutamate and impaired linguistic functioning in schizophrenia: A cluster analytic approach.
Front. Hum. Neurosci. 16:954898.
doi: 10.3389/fnhum.2022.954898

Widespread cortical thinning, excessive glutamate and impaired linguistic functioning in schizophrenia: A cluster analytic approach

Liangbing Liang[1,2†], Angélica M. Silva[2†], Peter Jeon[3], Sabrina D. Ford[2,4], Michael MacKinley[2,5], Jean Théberge[3,5,6] and Lena Palaniyappan[2,3,5,6,7*]

[1]Graduate Program in Neuroscience, Western University, London, ON, Canada, [2]Robarts Research Institute, Western University, London, ON, Canada, [3]Department of Medical Biophysics, Western University, London, ON, Canada, [4]London Health Sciences Centre, Victoria Hospital, London, ON, Canada, [5]Lawson Health Research Institute, London, ON, Canada, [6]Department of Psychiatry, Western University, London, ON, Canada, [7]Department of Psychiatry, Douglas Mental Health University Institute, McGill University, Montreal, QC, Canada

Introduction: Symptoms of schizophrenia are closely related to aberrant language comprehension and production. Macroscopic brain changes seen in some patients with schizophrenia are suspected to relate to impaired language production, but this is yet to be reliably characterized. Since heterogeneity in language dysfunctions, as well as brain structure, is suspected in schizophrenia, we aimed to first seek patient subgroups with different neurobiological signatures and then quantify linguistic indices that capture the symptoms of "negative formal thought disorder" (i.e., fluency, cohesion, and complexity of language production).

Methods: Atlas-based cortical thickness values (obtained with a 7T MRI scanner) of 66 patients with first-episode psychosis and 36 healthy controls were analyzed with hierarchical clustering algorithms to produce neuroanatomical subtypes. We then examined the generated subtypes and investigated the quantitative differences in MRS-based glutamate levels [in the dorsal anterior cingulate cortex (dACC)] as well as in three aspects of language production features: fluency, syntactic complexity, and lexical cohesion.

Results: Two neuroanatomical subtypes among patients were observed, one with near-normal cortical thickness patterns while the other with widespread cortical thinning. Compared to the subgroup of patients with relatively normal cortical thickness patterns, the subgroup with widespread cortical thinning was older, with higher glutamate concentration in dACC and produced speech with reduced mean length of T-units (complexity) and lower repeats of content words (lexical cohesion), despite being equally fluent (number of words).

Conclusion: We characterized a patient subgroup with thinner cortex in first-episode psychosis. This subgroup, identifiable through macroscopic changes, is also distinguishable in terms of neurochemistry (frontal glutamate) and language behavior (complexity and cohesion of speech). This study supports the hypothesis that glutamate-mediated cortical thinning may contribute to a phenotype that is detectable using the tools of computational linguistics in schizophrenia.

KEYWORDS

thickness, spectroscopy, computational linguistics, first-episode psychosis, natural language processing, formal thought disorder

Introduction

Schizophrenia is a disorder that affects how language is employed in everyday use during social interactions (Covington et al., 2005; Kuperberg, 2010; Wible, 2012). Based on the Diagnostic and Statistical Manual of Mental Disorders 5th edition (DSM-5) (American Psychiatric Association, 2013), all of the 5 symptom criteria for diagnosing schizophrenia involve speech and language in one form or another (American Psychiatric Association, 2013). For example, hallucinations are often voices that speak (Alderson-Day et al., 2021); negative symptoms are characterized by "alogia" or reduced speech fluency; thought disorder is expressed as deviations in speech; catatonic features often include mutism (lack of speech production) (Oyebode, 2021); delusions often include an element of misinterpretation of social conversations or deficits in the use of propositional language (Zimmerer et al., 2017). Despite this strong linguistic dependency of the construct of schizophrenia, not every patient diagnosed with this illness displays a detectable speech disturbance (Roche et al., 2015; Kircher et al., 2018; Oomen et al., 2022). It is important to identify patients who are most likely to be afflicted in the language domain, as speech disturbances directly affect the educational and occupational success (Palaniyappan et al., 2019), interpersonal (Tan et al., 2014) and social functioning (Marggraf et al., 2020) as well as endured stigma (Penn et al., 2000). Identification of this subgroup may assist in prognostication in schizophrenia, as well as making early and targeted interventions for a group that may have higher educational and vocational needs possible, before they manifest significant deficits in these domains.

The heterogeneity of linguistic deficits may stem from the presence of a subgroup of patients who do not display the expected language anomalies (Oomen et al., 2022). Alternatively, conventional measures of "formal thought disorder (FTD)" that seek to examine overt communication difficulties may miss the subtle aspects of this deficit, thus introducing an apparent heterogeneity (Mikesell and Bromley, 2016). We need sensitive and objective measures of language indices to study this issue in detail (see Elvevåg et al., 2010; Foltz et al., 2016; Holmlund et al., 2020 for more explanations). One of these tools is natural language processing (NLP) in computational linguistics (Ratana et al., 2019; Corcoran and Cecchi, 2020; Corcoran et al., 2020; Hitczenko et al., 2021). NLP tools use computer algorithms to understand and analyze written text or speech. NLP is a branch of artificial intelligence that uses real-world language as input, and processes it using linguistic rules or patterns identified through statistics, to allow machines to make sense of our language. Such NLP tools do not rely on a clinician's inferential skill to assess the cognitive-linguistic health status (Voleti et al., 2020) of patients from early stages of psychosis (Delvecchio et al., 2019) and are able to predict psychosis onset in individuals at clinical high-risk (CHR) (Bedi et al., 2015). These approaches have broadly focused on syntactic (Thomas et al., 1990; Thomas, 1996; Covington et al., 2005; Delvecchio et al., 2019) and semantic indices (Corcoran et al., 2018; Bar et al., 2019; Alonso-Sánchez et al., 2022; Parola et al., 2022) as the affected domains in psychosis.

Prior studies that focused on quantitative analysis of language have established the following dysfunctions in patients with schizophrenia. First, patients display syntactic simplification [(Morice and Ingram, 1982, 1983; Fraser et al., 1986; Morice and McNicol, 1986; King et al., 1990; DeLisi, 2001; Bilgrami et al., 2022) i.e., they use simple constructions with minimal clause dependencies and also with a limited richness of content]. Secondly, patients show patterns of reduced cohesion (Crider, 1997), for example, lacking prior reference when invoking a description (Chaika and Lambe, 1989) or insufficient lexical repetitions (Gupta et al., 2018) needed to generate cohesion during a discursive discourse (Crossley et al., 2016). Reduced syntactic complexity and cohesion can lead to aberrant word graphs (Mota et al., 2012) and a reduction in number of words spoken (reduced fluency) (Allen et al., 1993; DeLisi, 2001; Morgan et al., 2021).

While some of these features have been linked to the presence of clinically detected FTD, the rating-scale measures of FTD have been poor predictors of linguistic dysfunction *per se* (Mackinley et al., 2021; Tang et al., 2021). Furthermore, as symptom measures fluctuate over time (state-like), they have limited utility in identifying stable subgroups (Jablensky, 2006). Even among speech characteristics, those that relate to "positive symptoms" appear to be more state-related, while those relating to negative symptoms [or Impoverishment of Thinking (Liddle et al., 2002)] appear to be more pervasive. More trait-like measures, e.g., those derived from brain anatomy or genetic composition, that map on to emerging biological insights [e.g., implicating the glutamatergic synapses (Iyegbe and O'Reilly, 2022; Trubetskoy et al., 2022)], may be required to see if specific subgroups of patients have linguistic deficits. Furthermore, as antipsychotics themselves can induce language impairment (de Boer et al., 2020), recruitment of patients with first-episode psychosis with minimal exposure to antipsychotic medications is necessary to identify subgroups with language dysfunction from illness onset.

In the current study, we first identify subgroups of patients with first-episode schizophrenia using the neuroanatomical measure of MRI-derived cortical thickness. Structural neuroanatomical features are considered to be more stable than symptom rating and physiological recordings, which can vary on a day-to-day basis. In addition, MRI-derived thickness is quantified objectively in an automatized manner with minimal manual intervention in the quantification process. Thus, brain structure can provide more stable and reliable clustering solutions. Further, aberrant cortical thickness has been reported in various illness stages of schizophrenia (Zhao et al., 2022), and has been found to track the inter-individual

TABLE 1 Demographic, clinical, neurobiological, and linguistic data of patients with first-episode psychosis and healthy controls.

	FEP	HC	Pearson's chi-squared test or Welch *t*-tests	
N	66	36	–	
Demographics				
Age (years)	22.82 (4.77)	21.53 (3.32)	$t(94.043) = 1.6005$, $p = 0.1128$	
Female/male	12/54	12/24	X-squared (1) = 2.1896, $p = 0.1389$	
Education scale (1/2/3/4)	15/18/20/13	5/3/14/13	X-squared (3) = 8.0131, $p = 0.04574$	*
Clinical				
PANSS-8 (total)	25.18 (6.72)	–	–	
PANSS-8 positive	11.62 (3.48)	–	–	
PANSS-8 negative	6.97 (4.41)	–	–	
PANSS-8 general	5.18 (2.46)			
DUP (weeks) [median (IQR)]	11.0 (4, 24)	–	–	
DDD lifetime exposure [median (IQR)]	0.5 (0, 2.99)	–	–	
Antipsychotic naïve (%)	42%			
Functional				
SOFAS	40.96 (12.40)	–		
NEET status: yes/no	24/29	0/31	X-squared (1) = 17.497, $p < 0.0001$	***
Neurobiological				
Glutamate (mM)	6.79 (1.16)	6.51 (1.35)	$t(53.766) = 0.99493$, $p = 0.3242$	
Mean cortical thickness (mm)	2.45 (0.12)	2.48 (0.096)	$t(94) = 1.90350$, $p = 0.0600$	
Language variables				
TLI (Total)	1.48 (1.41)	0.29 (0.39)	$t(81.668) = 6.4188$, $p < 0.00001$	***
TLI impoverishment	0.57 (0.72)	0.14 (0.25)	$t(87.397) = 4.3669$, $p < 0.0001$	***
TLI disorganization	0.91 (1.21)	0.15 (0.26)	$t(75.114) = 4.9033$, $p < 0.00001$	***
Average total number of words	119.18 (38.85)	141.34 (29.83)	$t(88.706) = -3.1775$, $p = 0.002045$	**
MLS	14.37 (4.58)	14.21 (2.74)	$t(96.753) = 0.20899$, $p = 0.8349$	
MLT	12.21 (3.00)	12.49 (2.08)	$t(93.295) = -0.56025$, $p = 0.5767$	
MLC	7.73 (1.20)	8.19 (1.18)	$t(73.659) = -1.8858$, $p = 0.06327$	
Repeated contents lemmas	0.229 (0.047)	0.247 (0.033)	$t(89.792) = -2.1269$, $p = 0.03617$	*

Values are reported as "Mean (SD)" unless specified otherwise.
IQR, Interquartile range; FEP, first episode psychosis; HC, healthy controls; PANSS, Positive and Negative Symptoms Scale; DUP, duration of untreated psychosis; DDD, Defined Daily Dose; SOFAS, Social and Occupational Functioning Assessment Scale; NEET, not in employment, education and training; TLI, Thought and Language Index; MLS, mean length of sentences; MLT, mean length of T-units; MLC, mean length of clauses.
*p < 0.05, **p < 0.01, ***p < 0.001.

differences in psychotic symptoms (Oertel-Knöchel et al., 2013) and Thought and Language Disorder scores in schizophrenia (Palaniyappan et al., 2020). Prior cluster analytic studies have uncovered a consistent cluster of patients with generalized reduction in cortical thickness (Dwyer et al., 2018; Chand et al., 2020; Liang et al., 2022). We use similar methods and then we examine if these subgroups have a meaningful neurochemical basis for their differences, by examining the MRS-derived glutamate levels measured from their frontal cortex, extending our recent work (Liang et al., 2022) to a larger sample.

Abnormal cortical thickness in schizophrenia has been previously linked to dysregulated glutamate levels (Plitman et al., 2014, 2016; Shah et al., 2020) and glutamatergic dysfunction had been considered to contribute to the "FTD" burden in schizophrenia (Kircher et al., 2018). We select dACC as our region of interest for glutamate measurement as it constitutes the core hub of the large-scale brain network called the Salience Network that appears to play a key role in the neurocognitive dysfunction in schizophrenia (Palaniyappan, 2021). Finally, we used a picture description task to study computational linguistic measures that are reflective of a "negative" FTD, first described by Fish (Casey and Kelly, 2019) and later reported by Andreasen (1979) and others (Kircher et al., 2018) as being more characteristic of established schizophrenia. Negative FTD is characterized by reduced quantity and quality of speech output; in a linguistically impoverished subgroup, this will be reflected in (i) reduced fluency (number of words spoken), (ii) reduced cohesion (measured by counting instances of content with prior reference, i.e., repeat content lemmas, e.g., run, running, and ran), and (iii) reduced syntactic complexity [mean length of sentences (MLS), clauses and minimal terminable units T-units, the smallest word group that could be considered a grammatical sentence, often composed of a main clause and subordinate clauses attached to it (Hunt, 1970)].

While there are numerous quantitative linguistic measures reported to be different in case-control comparisons, we chose items that predominantly map onto the negative symptom domain of schizophrenia (Tan et al., 2021; Bilgrami et al., 2022), independent of corpus-based distributional probabilities [which has limitations in understanding compositionality (Lenci, 2018)—a crucial locus of dysfunction in schizophrenia (Chaika, 1974)] and are readily interpretable [e.g., we did not use referential cohesion measure which is conflated in the presence of perseveration (Lundin et al., 2020)]. The features we selected are also intuitive in their link to known clinical features [reduced word count relates to alogia; lack of cohesion and simplified syntax relates to the poverty of content (Bedi et al., 2015; Corcoran et al., 2018; Minor et al., 2019)]. Furthermore, compared to other aspects of communication disturbances, the features of reduced fluency and richness of content (negative factor) selectively relate to poor response to treatment (Peralta et al., 1992). A neuroanatomically defined subgroup high in these "negative FTD type" linguistic features can be expected to be of prognostic relevance in schizophrenia.

Considering previous structural imaging-based cluster analytic studies, our primary hypothesis is that patient subgroups with distinct cortical thickness patterns can be identified in first-episode schizophrenia. In particular, a subgroup with widespread cortical thinning would emerge. Considering the association between cortical thinning, dysregulated glutamate levels and FTD burden, our secondary hypotheses are as follows: (i) The subgroup with deviant cortical thickness patterns also has abnormal glutamate levels measured in dACC; (ii) This subgroup displays impairments (negative FTD-type) in language production features, such as syntactic simplicity, reduced speech output and lower speech cohesion.

Materials and methods

Participants

We recruited 76 patients with first-episode psychosis from the Prevention and Early Intervention for Psychosis Program at the London Health Sciences Centre in London, Ontario, Canada from 2017 to 2021. Since 10 patients were unable to go through magnetic resonance imaging (MRI) scanning, we included data collected for 66 patients in this study. Inclusion criteria for patients include (1) having less than 14 days of lifetime exposure to antipsychotic medications, and (2) being at their first clinical presentation of psychotic symptoms. We followed up with patients for over 6 months to determine the validity of a diagnosis of first-episode schizophrenia prospectively. We also recruited 36 healthy volunteers, group-matched for age, sex, and parental socioeconomic status, who had no personal history of mental illnesses and no family history of psychotic disorders. All participants had no significant head injury, drug/alcohol dependence, or major medical illnesses, were fluent in English, and provided written informed consent to participate in the study. The work reported here is part of a longitudinal study registered on clinicaltrials.gov (Identifier: NCT02882204) and approved by the Western University Health Sciences Research Ethics Board, London, Ontario, Canada.

Measures and instruments

Psychiatric symptoms

Symptom severity was measured by the 8-item Positive and Negative Syndrome Scale (PANSS) (Lin et al., 2018) through interviews conducted by two research psychiatrists. Functional outcome was indexed by the Social and Occupational Functional Assessment Scale (SOFAS) (Morosini et al., 2000). The duration of untreated psychosis was calculated using the first report of positive symptoms as the starting point. We

also obtained patients' NEET (Not in Education, Employment, and Training) status. We converted participants' level of education into an ordinal scale (1: incomplete high school diploma; 2: completed high school diploma; 3: some post-secondary study; 4: completed post-secondary study or higher). Lifetime antipsychotic medication exposure was calculated by multiplying the number of days taking antipsychotics and prescribed Defined Daily Dose (DDD) values according to the World Health Organization (World Health Organization [WHO], 2022).

Thought and Language Index

Data was collected using Thought and Language Index (TLI) (Liddle et al., 2002) to reflect the two dimensions of language disorders in schizophrenia, impoverishment and disorganization. We used a picture-speech task that induced participants to elaborate 1-min spontaneous speech (oral soliloquies) in response to three images from the Thematic Apperception Test (Murray, 1943) after hearing specific instructions: "I am going to show you some pictures, one at a time. When I put each picture in front of you, I want you to describe the picture to me, as fully as you can. Tell me what you see in the picture, describe what you see in this image, and what you think might be happening." Responses were recorded, transcribed, and scored. Impoverishment score was the sum of scores for these 3 dimensions: poverty of speech, weakening of goal and preservation of ideas, while disorganization score was indexed by 5 dimensions: looseness, peculiar use of words, peculiar sentences, peculiar logic, and distractibility.

Language assessment

The same transcribed speech samples also underwent automatic analysis to measure both syntactic complexity and cohesion at the semantic level.

Tool for the automatic analysis of syntactic complexity and sophistication

The automatic analysis of syntactic complexity and sophistication (TAASSC) is an open-source[1] used in wide-ranging languages and grammatical frameworks with recent improvements in machine-learning approaches and NLP. This tool is complemented by a syntactic complexity analyzer (SCA)—a package with an accuracy of around 90% in part of speech (POS) tagging. The package includes a traditional and large measure of syntactic complexity following the taxonomy in Lu (2010): mean length of sentences (MLS), mean length of T-units (MLT), and mean length of clauses (MLC), word counts, and Terminal Units (T-unit) defined as the main clause with its attached subordinate clause(s) indicating speech cohesion as well as logical flow in the given information (see **Supplementary material** for more detailed descriptions).

Tool for the automatic analysis of cohesion

Tool for the automatic analysis of cohesion (TAACO 2.0)[2] (Crossley et al., 2016) is a freely available text analysis tool which incorporates a wide-ranging of global indices—over 150 classic and recently developed indices related to text cohesion—local, global, and overall text cohesion can significantly predict both text cohesion and speaking quality whether the speaking samples show greater semantic overlap incorporating automated semantic analysis (Crossley et al., 2019). TAACO includes 194 indices of cohesion in seven main categories: Type token ratio (TTR) and density, lexical overlap (sentences), lexical overlap (paragraphs), semantic overlap, connectives, givenness, and source text similarity. Of this, we focus on the givenness index as we analyze speech rather than written text. Givenness, as opposed to newness in a discourse transcript, indicates whether information occurring in a segment has already occurred in an earlier segment. Repeat content words or lemmas (e.g., nouns, verbs, adjectives, etc.) are calculated as a proportion of the total number of words spoken within each 1-min picture description.

Magnetic resonance imaging and magnetic resonance spectroscopy acquisition and processing

A total of 66 participants underwent neuroanatomy and spectroscopy scanning with an ultra-high-resolution 7-Tesla MRI scanner (8-channel transmit and 32-channel receive head-only coil) at Centre for Functional and Metabolic Mapping (CFMM), Western University, London, Canada. Structural images were obtained by a T1-weighted 0.75 mm isotropic MP2RAGE sequence with the following parameters: Repetition Time (TR) = 6,000 ms, Time to Echo (TE) = 2.83 ms, Inversion Time $(TI)_1$ = 800 ms, TI_2 = 2,700 ms, flip-angle 1 (α_1) = 4°, flip-angle 2 (α_2) = 5°, Field of View (FOV) = 350 mm × 263 mm × 350 mm, T_{acq} = 9 min 38 s, $iPAT_{PE}$ = 3 and 6/8 partial k-space, slice thickness = 0.75 mm. Freesurfer (version 6.0.0) (FreeSurfer Software Suite, 2021) was used to preprocess the obtained T1-weighted images. FreeSurfer provides automated brain image processing steps including intensity normalization, tissue segmentation and cortical parcellation (recon-all Free Surfer Wiki, 2022). Visual inspections of errors such as surface location misplacement were carried out according to the troubleshooting guide provided by FreeSurfer team (FsTutorial/TroubleshootingData, 2022). We acquired the cortical thickness values based on the Destrieux parcellation atlas (Destrieux et al., 2010). Magnetic resonance spectroscopy (MRS) signal was measured on a voxel placed in the dorsal anterior cingulate cortex (dACC; MNI coordinates:

1 https://www.linguisticanalysistools.org/taassc.html

2 https://www.linguisticanalysistools.org/taaco.html

TABLE 2 Demographic, clinical, neurobiological, and linguistic data of subgroups.

	Subgroup 1 patients	Subgroup 2 patients	Patient subgroup comparison	Subgroup 1 healthy controls
N	46	20		33
Demographics			**Pearson's Chi-squared test or Welch *t*-tests**	
Age (years)	21.37 (3.72)	26.15 (5.31)	$t(27.433) = -3.6527$, $p = 0.001081$ *	21.15 (3.08)
Female/male	10/36	2/18	X-squared (1) = 0.62274, $p = 0.43$	12/21
Education scale (1/2/3/4)	9/14/16/7	6/4/4/6	X-squared (3) = 3.7761, $p = 0.2867$	5/3/14/10
Clinical			**Welch *t*-tests**	
PANSS-8 (total)	25.76 (7.02)	23.85 (5.91)	$t(42.677) = 1.1376$, $p = 0.2616$	–
PANSS-8 positive	11.67 (3.46)	11.50 (3.64)	$t(34.519) = 0.18146$, $p = 0.8571$	–
PANSS-8 negative	7.48 (4.46)	5.80 (4.15)	$t(38.757) = 1.4755$, $p = 0.1481$	–
PANSS-8 general	5.22 (2.41)	5.10 (2.63)	$t(33.503) = 0.17063$, $p = 0.8655$	
DUP (weeks) [median (IQR)]	13 (4, 26)	8.5 (5.75, 16.5)	$t(23.362) = -0.53167$, $p = 0.6027$	–
DDD lifetime exposure [median (IQR)]	0 (0, 2.54)	1.25 (0, 3.9)	$t(20.156) = -1.6477$, $p = 0.1149$	–
Functional			**Pearson's Chi-squared test or Welch *t*-tests**	
SOFAS	40.98 (13.19)	40.90 (10.67)	$t(44.354) = 0.025424$, $p = 0.9798$	–
NEET status: yes/no	19/19	5/10	X-squared (1) = 0.62686, $p = 0.4285$	–
Neurobiological			**ANOVA with age as a covariate**	
Glutamate (mM)	6.57 (1.03)	7.28 (1.30)	$F(1) = 5.10$, $p = 0.028$, *Age effect: $p = 0.13$	6.50 (1.40)
Mean cortical thickness (mm)	2.50 (0.068)	2.32 (0.057)	$F(1) = 126.225$, $p < 0.000$, ***Age effect: $p = 0.12$	2.49 (0.061)
Language variables			**Welch *t*-tests**	
TLI (total)	1.28 (1.28)	1.93 (1.64)	$t(29.517) = -1.5629$, $p = 0.1287$	0.28 (0.40)
TLI impoverishment	0.48 (0.61)	0.79 (0.92)	$t(26.725) = -1.3843$, $p = 0.1777$	0.13 (0.23)
TLI disorganization	0.82 (1.14)	1.14 (1.37)	$t(30.974) = -0.92366$, $p = 0.3628$	0.16 (0.26)
Average total number of words	119.47 (35.45)	118.43 (47.46)	$t(24.954) = 0.084721$, $p = 0.9332$	141.53 (31.15)
MLS	14.58 (4.01)	13.91 (5.89)	$t(23.59) = 0.4227$, $p = 0.6763$	14.03 (2.67)
MLT	12.79 (3.09)	10.75 (2.20)	$t(43.928) = 2.9509$, $p = 0.005066$ **	12.45 (2.13)
MLC	7.90 (1.25)	7.30 (0.96)	$t(40.658) = 2.0284$, $p = 0.04911$ *	8.24 (1.21)
Repeated contents lemmas	0.240 (0.044)	0.204 (0.047)	$t(28.741) = 2.6991$, $p = 0.01152$ *	0.249 (0.034)

Values are reported as "Mean (SD)" unless specified otherwise.
IQR, Interquartile range; FEP, first episode psychosis; HC, healthy controls; PANSS, Positive and Negative Symptoms Scale; DUP, duration of untreated psychosis; DDD, Defined Daily Dose; SOFAS, Social and Occupational Functioning Assessment Scale; NEET, not in employment, education and training; TLI, Thought and Language Index; MLS, mean length of sentences; MLT, mean length of T-units; MLC, mean length of clauses.
*$p < 0.05$, **$p < 0.01$, ***$p < 0.001$.

1, 16, 38). The details of MRS acquisition and analysis have been previously described (see **Supplementary material**) and a subset of this sample has been reported in prior works (Jeon et al., 2021; Liang et al., 2022).

Statistical analyses

We applied agglomerative hierarchical clustering with Ward's method and Euclidean distance to 148 cortical thickness values [based on Destrieux parcellation atlas (Destrieux et al., 2010) output using FreeSurfer] of all 102 participants including 66 patients and 36 healthy controls. Agglomerative hierarchical clustering starts with calculating the distance (e.g., Euclidean distance) between all pairs of data objects and putting the most similar data objects into the same cluster. The newly formed clusters are then again grouped with one another based on a linkage function (e.g., Ward's method), until all data objects merge into one single cluster. The optimal number of clusters was determined by the consensus votes from 16 clustering validity indices using NbClust (Charrad et al., 2014) in R (version 4.0.3). Pearson's chi-squared tests (with Yate's continuity correction) were used to compare categorical variables, while Welch *t*-tests were used to compare continuous variables. If the obtained subgroups showed difference(s) in confounding variables (e.g., age or gender), ANCOVA was used to show effects between subgroups while accounting for effects of the covariates. We used FreeSurfer to find (1) between-cluster differences in vertex-by-vertex cortical thickness while regressing out the effect of age using a general linear model, and to locate (2) cortical regionals that correlated with glutamatergic metabolic levels. The thickness values at each vertex were mapped to the surface of an average brain template, and the cortical

map was smoothed with a Gaussian kernel of 10 mm full width at half-maximum. We used Monte Carlo simulations with 1,000 permutations and a cluster-forming threshold of $P = 0.05$ (two-tailed) to correct for multiple comparisons as implemented in FreeSurfer.

Results

Demographic, clinical, linguistic, and neurobiological measurements are provided in **Table 1** and **Supplementary material**.

The cluster validity procedure of hierarchical clustering of 148 cortical thickness values of 66 patients with first-episode psychosis and 36 healthy controls suggested that a two-cluster solution is optimal (9/16 cluster validity indices). Results of clustering only patients are shown in **Supplementary material**. Proceeding with a two-cluster solution, around 70% of patients ($n = 46$) with first-episode psychosis were clustered with the majority of the healthy controls ($n = 33$) in Cluster 1, while the remaining 30% of patients ($n = 20$) were in Cluster 2 which only included 3 healthy individuals. Demographic, clinical, neurometabolite, and language functioning information of the three subgroups (Cluster 1 patients, Cluster 2 patients, and Cluster 1 healthy controls) is summarized in **Table 2** and **Supplementary Table 1**. Overall, compared to Cluster 1 patients, Cluster 2 patients have significantly older age, lower mean cortical thickens (non-significant age effect), higher glutamate concentration in dACC (non-significant age effect) as well as lower MLT (complexity) and repeated contents lemmas (cohesion) despite a preserved number of words within the given time frame (fluency). There is no significant difference between the two clusters in duration of untreated psychosis, lifetime exposure to antipsychotics, PANSS, and SOFAS scores.

Comparisons of cortical thickness between patients from the two subgroups (adjusted for age) are shown in **Figure 1**. After multiple testing corrections, patients in Cluster 1 had significantly lower thickness in 8 clusters (average area size = 410.44 mm^2) in the left hemisphere and right hemisphere, respectively (see **Supplementary Table 2** and **Figure 1** for details). Comparisons of cortical thickness between the patients and controls from Cluster 1 (adjusted for age and corrected for multiple comparisons) revealed no regional differences in thickness values, indicating that this subgroup of patients had a "healthy" cortical morphological pattern.

Multiple cortical regions were correlated with dACC glutamate levels in patients (**Figure 2**), but these correlations were not significant after multiple testing corrections. Correlation matrices of other variables of interest are presented in **Supplementary material**.

In summary, patients from Cluster 1 had similar neuroanatomical patterns to healthy controls, while patients from Cluster 2 were a distinct subgroup with widespread cortical thinning, higher glutamate concentration, and exhibited and reduced syntactic complexity and cohesion. This subgroup was thus impoverished in cortical structure as well as linguistic features.

Discussion

In the current study, we identified a subgroup of 30% of patients with first-episode schizophrenia who are distinguishable on the basis of their MRI-derived cortical thickness profiles—displaying a generalized reduction in thickness (referred to as "Subgroup 2") compared to the other group (70%) who have an unimpaired thickness profile similar to most healthy control subjects (referred to as "Subgroup 1"). Subgroup 2 is older in age at the time of the first presentation, has higher MRS-derived glutamate levels in the dorsal ACC and showed a pattern of linguistic impoverishment characterized by reduced fluency, syntactic simplicity, and repetitiveness. Taken together, these observations indicate a distinct subtype of schizophrenia that shows a pattern of cortical impoverishment along with linguistic impoverishment in the presence of higher prefrontal (dACC) glutamate levels at first presentation.

The emergence of a cortical impoverishment group showing a distributed reduction in cortical thickness compared to the other subgroup of patients and healthy controls is now a well-established feature of cluster analytical studies in schizophrenia. In a prior work where we studied two independent groups of patients with established schizophrenia as well as a part of the sample reported here, we observed a reliably identifiable subgroup of patients with cortical impoverishment (Liang et al., 2022), who did not differ from other patients in the cognitive or clinical severity. Similar findings also reported a "cortical impoverishment subgroup" at various illness stages (Sugihara et al., 2017; Dwyer et al., 2018; Chand et al., 2020; Pan et al., 2020), supporting the stability of this subtype. While the mechanistic processes underlying this structural deviation are still circumspect, based on the higher glutamate levels noted in this subgroup using 7T MRS from a dorsal ACC voxel, a putative link to excitotoxicity (Plitman et al., 2014) (or E/I dysfunction Limongi et al., 2020) can be drawn.

According to the NMDA hypofunction or glutamatergic dysregulation models of schizophrenia, higher glutamate transmission may relate to excitation-inhibition imbalance (Limongi et al., 2020) and if unchecked, may result in synaptic and neuronal loss (Wang and Qin, 2010). These cellular mechanisms have been hypothesized to underlie structural deficits in schizophrenia (Plitman et al., 2014). Multilevel genetic and physiological studies are needed to further pursue this observation. We now provide an important lead in this pursuit by identifying language dysfunction in this subgroup of schizophrenia. Additionally, we want to highlight the implications of dissecting neurobiological

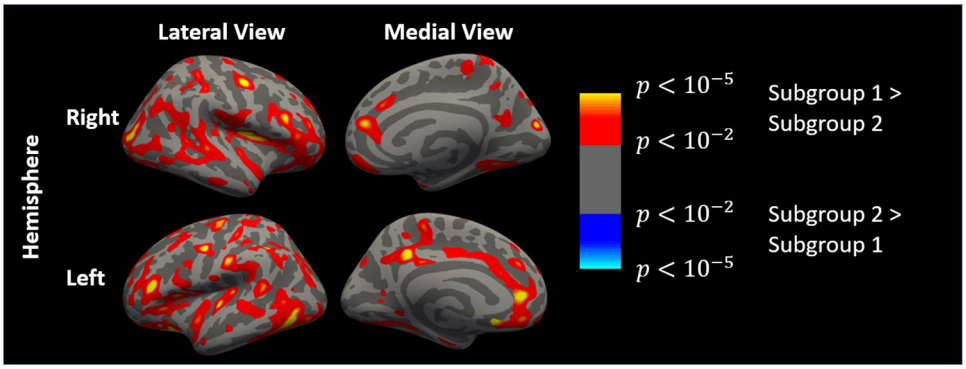

FIGURE 1
Cortical thickness map of differences between patients from Subgroup 1 and Subgroup 2 generated by FreeSurfer (regressing out age effect with a general linear model, uncorrected). Left hemisphere and right hemisphere in lateral and medial view, respectively.

heterogeneity in schizophrenia. In our study, despite displaying similar symptom severity and social functioning, the two patient subgroups have distinct neurobiological underpinnings, and may represent different pathophysiological pathways of developing schizophrenia.

Through a parts-of-speech (POS) tagging approach in NLP, we studied "poverty of content" at 3 components of grammatical structures: mean length of sentences, clauses and T-units. All are large syntactic complexity indices used as a proxy of cognitive parameters because producing a T-unit is a more complex process than producing coordinated clauses (Szmrecsanyi, 2004). T-units serve as an informative index to distinguish the amount of independent clausal coordination in the expressed idea. Moreover, T-units provided the rule-based identification process considering the selecting word for subordination (e.g., using "because") or coordination (e.g., using "and") (Beaman, 1984). Therefore, a reduction in coordinated T-units demonstrates notable syntactic simplicity in our Subgroup 2. These results are congruent with Bilgrami and colleagues' works (Bilgrami et al., 2022) who also reported lower POS syntactic complexity in those patients who had negative symptoms. The authors found that reduced sentence length and decreased use of words that introduce dependent clauses (e.g., using complementizer or determiner pronouns such as "that" and "which") are associated with negative thought disorder (Bilgrami et al., 2022). Additionally, our observations raise the question of whether patients with higher developmental disruption form the subgroup with cortical and linguistic impoverishment since syntactic complexity is a phenomenon that develops during childhood (Givon, 2009; Frizelle et al., 2018) and reaches a plateau around the age of 20 (Nippold et al., 2014). If developmental disturbances during childhood and adolescence lie in the pathogenesis of schizophrenia and can be detected using NLP tools (*via* progressive aberrations in syntactic complexity; see Silva et al., 2022), this may provide a promising avenue for early identification.

In clinical settings, linguistic dysfunction in schizophrenia relies on a standardized rating scale (PANSS and TLI) to define speech impairment as one sign of FTD (Elvevåg et al., 2007; Iter et al., 2018). The two patient subgroups did not differ in TLI or PANSS scores even though the diagnostic group of FES differed from healthy subjects in TLI rating score as expected. This observation speaks to the ability of automated quantitative processes to parse the subtler aspects of language dysfunction, an issue that has been discussed at length in several recent works based on the NLP approach (Corcoran and Cecchi, 2020; Hitczenko et al., 2021). We observed a reduction of repeated content lemma (e.g., nouns, verbs, adjectives) in our Subgroup 2. This index traditionally characterizes the systematic relationship—explicit or implicit—between lexical items, i.e., cohesive cues, placed at the text surface (Sanders and Maat, 1976). For example, if two adjacent ideas (sentence-to-sentence, clause-to-clause) comprise the same noun (e.g., woman), the lexical repetition will explicitly help connect both ideas. However, if the first clause contains the word "bridge" and the second contains the word "iron," the connection weakens even though it is logical. Therefore, in this work, we quantify cohesion (Halliday and Hasan, 1976; Graesser et al., 2004) through a lexical approach applied to how speech has been produced, without any assumption about how it is understood by listeners or readers (i.e., lexical cohesion as distinct from semantic coherence) (Just et al., 2020).

The linguistic phenomenon of reduced content word-lemmas relating to cortical thinning can be understood in several ways (Crossley et al., 2016). Firstly, reduced repetition of content-lemmas directly negatively influences the givenness of the generated speech. Givenness refers to the distribution of the given/known information or ideas as opposed to the new/unknown information. A "cortically impoverished" patient may build ideas as small clauses with little relationship between them. Secondly, a decline in the use of repeated content lemma makes it difficult to recover the

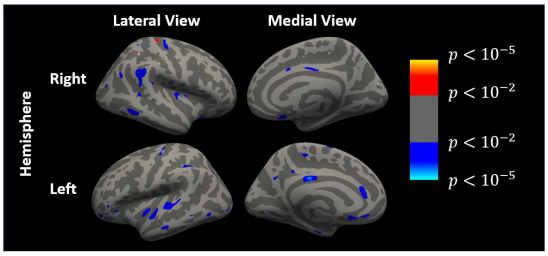

FIGURE 2
Cortical regions that are correlated with dACC glutamate levels (uncorrected) generated by FreeSurfer. Left and right hemispheres in lateral and medial view, respectively. Blue/cyan colors indicate negative correlations while red/yellow colors indicate positive correlations.

meaningful information from the preceding passage, generating a sense of empty speech (i.e., poverty of content) with reduced informative value to the listener.

Our study has several strengths: We were able to overcome the difficulty of collecting speech data in an acute, untreated state of psychosis, and determine their diagnosis of first-episode schizophrenia. Furthermore, we ensured transcribers, as well as speech analysts, were blind to diagnosis. We employed ultra-high field strength MRS whereby the glutamate quantification from MS-spectra had a high specificity. Finally, we used multiple clustering procedures and derived a two-cluster solution based on a majority-based consensus, adding to the stability of the observed subtype. Nevertheless, several limitations need consideration. We had a limited number of female participants which limits generalizability; we did not see a statistical effect of sex between the groups, but our small numbers preclude a stratified analysis. Second, thickness-based clustering resulted in age differences between the subgroups; however, we included age as a covariate in downstream analyses for glutamate and regional thickness to ensure this confound did not affect the inferences we make. Nevertheless, the non-linear influence of age on these variables cannot be ruled out. Third, we did not assess IQ formally. In our recent study where we examined the influence of cognition on thickness-based clustering in greater detail, the effect of individual differences in cognitive performance in the thickness profile was minimal among patients (Liang et al., 2022). Thus, while we can be confident that the reported thickness reduction and language dysfunction in a subgroup is not due to low extreme distributions of IQ as a result, we cannot exclude that an undetermined proportion of variance in these variables could be explained by cognitive differences. Finally, our speech samples were restricted to one language (English) and were based on a single discursive discourse (picture description) and single modality (oral soliloquies-monolog) elicited in the context of a research interview. The effect of contextual differences, language as well as types and duration of elicitation task on our linguistic observations needs further examination.

In sum, we can link the putative excitotoxicity (glutamate excess) to reduced gray matter thickness (cortical impoverishment) and the objectively computed negative phenomenology of language (or linguistic impoverishment) in first-episode schizophrenia. This finding supports the presence of detectable neurobiological subtypes of schizophrenia. Connecting the cellular/synaptic processes (glutamate) with objectively quantified language behaviors through macroscopic brain changes (thickness) may facilitate more consistent brain-behaviors mapping in schizophrenia.

Data availability statement

The authors agree to make data and codes supporting the results presented in their paper available upon reasonable request, within the stipulations laid by the ethics committee. Requests to access the datasets should be directed to the corresponding author.

Ethics statement

The studies involving human participants were reviewed and approved by the Western University Health Sciences Research Ethics Board. The patients/participants provided their written informed consent to participate in this study.

Author contributions

LP supervised and planned the study. SF and MM recruited patients and collected the data. LL and MM conducted MRI data analysis. JT designed spectroscopy protocol, and supervised PJ for MRS data acquisition and analysis. AMS analyzed the speech sample data. LL designed and conducted the statistical analyses. LL and AMS created the original draft under supervision of LP. All authors contributed to and approved the final manuscript.

Funding

The TOPSY study was funded by the Canadian Institutes of Health Research (CIHR) Foundation Grant (Grant no. 375104/2017) to LP with data acquisition supported by the Canada First Excellence Research Fund to BrainSCAN, Western University (Imaging Core). LP acknowledged salary support from the Tanna Schulich Chair of Neuroscience and Mental

Health. LL was funded by a studentship from the Canada First Excellence Research Fund to BrainSCAN, Western University. PJ was funded by the Jonathan and Joshua Graduate Scholarship and Ontario Graduate Scholarship and NSERC Discovery (Grant no. RGPIN/05055-2016) to JT. AMS's position was funded by a Project Grant from the Canadian Institutes of Health Research (Grant no. FRN 391348). SF was partly supported by a grant from the Children's Health Foundation, London, ON to the PROSPECT clinic at the Programme for Early Intervention and Prevention in Psychosis (PEPP-London). MM was supported by the Jonathan and Joshua Memorial Scholarship from Schulich School of Medicine, Western University.

Acknowledgments

We acknowledge Ali Khan for their assistance in data acquisition in the TOPSY study. We acknowledge Cassandra Branco for their assistance in clinical recruitment. We acknowledge Kara Dempster, Julie Richard, Raj Harricharan, Priya Subramanian, and Hooman Ganjavi for diagnostic consensus and symptom assessments.

Conflict of interest

LP reported personal fees from Janssen Canada, Otsuka Canada, SPMM Course Limited, United Kingdom, Canadian Psychiatric Association; book royalties from Oxford University Press; investigator-initiated educational grants from Janssen Canada, Sunovion and Otsuka Canada outside the submitted work. LP is the convenor of DISCOURSE in Psychosis, an international consortium of researchers interested in the study of language in psychosis.

The remaining authors declare that the research was conducted in the absence of any commercial or financial relationships that could be construed as a potential conflict of interest.

Publisher's note

Supplementary material

The Supplementary Material for this article can be found online at: https://www.frontiersin.org/articles/10.3389/fnhum.2022.954898/full#supplementary-material

References

Alderson-Day, B., Woods, A., Moseley, P., Common, S., Deamer, F., Dodgson, G., et al. (2021). Voice-Hearing and Personification: Characterizing Social Qualities of Auditory Verbal Hallucinations in Early Psychosis. *Schizophr. Bull.* 47, 228–236. doi: 10.1093/schbul/sbaa095

Allen, H. A., Liddle, P. F., and Frith, C. D. (1993). Negative Features, Retrieval Processes and Verbal Fluency in Schizophrenia. *Br. J. Psychiatry* 163, 769–775. doi: 10.1192/bjp.163.6.769

Alonso-Sánchez, M. F., Ford, S. D., MacKinley, M., Silva, A., Limongi, R., and Palaniyappan, L. (2022). Progressive changes in descriptive discourse in First Episode Schizophrenia: A longitudinal computational semantics study. *Schizophrenia* 8:36. doi: 10.1038/s41537-022-00246-8

American Psychiatric Association (2013). *Diagnostic and Statistical Manual of Mental Disorders (DSM–5)*. Virginia, US: American Psychiatric Association. doi: 10.1176/appi.books.9780890425596

Andreasen, N. C. (1979). Thought, language, and communication disorders. II. Diagnostic significance. *Arch. Gen. Psychiatry* 36, 1325–1330. doi: 10.1001/archpsyc.1979.01780120055007

Bar, K., Zilberstein, V., Ziv, I., Baram, H., Dershowitz, N., Itzikowitz, S., et al. (2019). "Semantic Characteristics of Schizophrenic Speech," in *Proceedings of the Sixth Workshop on Computational Linguistics and Clinical Psychology*, (Minneapolis: Association for Computational Linguistics), 84–93. doi: 10.18653/v1/W19-3010

Beaman, K. (1984). "Coordination and subordination revisited: Syntactic complexity in spoken and written narrative discourse," in *Coherence in Spoken and Written Discourse*, ed. D. Tannen (Norwood, NJ: Ablex), 45–80.

Bedi, G., Carrillo, F., Cecchi, G. A., Slezak, D. F., Sigman, M., Mota, N. B., et al. (2015). Automated analysis of free speech predicts psychosis onset in high-risk youths. *NPJ Schizophr.* 1:15030. doi: 10.1038/npjschz.2015.30

Bilgrami, Z. R., Sarac, C., Srivastava, A., Herrera, S. N., Azis, M., Haas, S. S., et al. (2022). Construct validity for computational linguistic metrics in individuals at clinical risk for psychosis: Associations with clinical ratings. *Schizophr. Res.* 245, 90–96. doi: 10.1016/j.schres.2022.01.019

Casey, P., and Kelly, B. (2019). *Fish's Clinical Psychopathology Mental Health, Psychiatry and Clinical Psychology .4th Ed.* Cambridge: Cambridge University Press.

Chaika, E. (1974). A linguist looks at "schizophrenic" language. *Brain Lang.* 1, 257–276. doi: 10.1016/0093-934X(74)90040-6

Chaika, E., and Lambe, R. A. (1989). Cohesion in schizophrenic narratives, revisited. *J. Commun. Disord.* 22, 407–421. doi: 10.1016/0021-9924(89)90034-8

Chand, G. B., Dwyer, D. B., Erus, G., Sotiras, A., Varol, E., Srinivasan, D., et al. (2020). Two distinct neuroanatomical subtypes of schizophrenia revealed using machine learning. *Brain* 143, 1027–1038. doi: 10.1093/brain/awaa025

Charrad, M., Ghazzali, N., Boiteau, V., and Niknafs, A. (2014). NbClust: An R Package for Determining the Relevant Number of Clusters in a Data Set. *J. Stat. Softw.* 61, 1–36. doi: 10.18637/jss.v061.i06

Corcoran, C. M., and Cecchi, G. A. (2020). Using Language Processing and Speech Analysis for the Identification of Psychosis and Other Disorders. *Biol. Psychiatry Cogn. Neurosci. Neuroimaging* 5, 770–779. doi: 10.1016/j.bpsc.2020.06.004

Corcoran, C. M., Carrillo, F., Fernández-Slezak, D., Bedi, G., Klim, C., Javitt, D. C., et al. (2018). Prediction of psychosis across protocols and risk cohorts using automated language analysis. *World Psychiatry* 17, 67–75. doi: 10.1002/wps.20491

Corcoran, C. M., Mittal, V. A., Bearden, C. E., E Gur, R., Hitczenko, K., and Bilgrami, Z. (2020). Language as a biomarker for psychosis: A natural language processing approach. *Schizophr. Res.* 226, 158–166. doi: 10.1016/j.schres.2020.04.032

Covington, M. A., He, C., Brown, C., Naçi, L., McClain, J. T., Fjordbak, B. S., et al. (2005). Schizophrenia and the structure of language: The linguist's view. *Schizophr. Res.* 77, 85–98. doi: 10.1016/j.schres.2005.01.016

Crider, A. (1997). Perseveration in schizophrenia. *Schizophr. Bull.* 23, 63–74. doi: 10.1093/schbul/23.1.63

Crossley, S. A., Kyle, K., and Dascalu, M. (2019). The Tool for the Automatic Analysis of Cohesion 2.0: Integrating semantic similarity and text overlap. *Behav. Res. Methods* 51, 14–27. doi: 10.3758/s13428-018-1142-4

Crossley, S. A., Kyle, K., and McNamara, D. S. (2016). The tool for the automatic analysis of text cohesion (TAACO): Automatic assessment of local, global, and text cohesion. *Behav. Res. Methods* 48, 1227–1237. doi: 10.3758/s13428-015-0651-7

de Boer, J. N., Voppel, A. E., Brederoo, S. G., Wijnen, F. N. K., and Sommer, I. E. C. (2020). Language disturbances in schizophrenia: The relation with antipsychotic medication. *NPJ Schizophr.* 6:24. doi: 10.1038/s41537-020-00114-3

DeLisi, L. E. (2001). Speech disorder in schizophrenia: Review of the literature and exploration of its relation to the uniquely human capacity for language. *Schizophr. Bull.* 27, 481–496. doi: 10.1093/oxfordjournals.schbul.a006889

Delvecchio, G., Caletti, E., Perlini, C., Siri, F. M., Andreella, A., Finos, L., et al. (2019). Altered syntactic abilities in first episode patients: An inner phenomenon characterizing psychosis. *Eur. Psychiatry* 61, 119–126. doi: 10.1016/j.eurpsy.2019.08.001

Destrieux, C., Fischl, B., Dale, A., and Halgren, E. (2010). Automatic parcellation of human cortical gyri and sulci using standard anatomical nomenclature. *NeuroImage* 53, 1–15. doi: 10.1016/j.neuroimage.2010.06.010

Dwyer, D. B., Cabral, C., Kambeitz-Ilankovic, L., Sanfelici, R., Kambeitz, J., Calhoun, V., et al. (2018). Brain Subtyping Enhances The Neuroanatomical Discrimination of Schizophrenia. *Schizophr. Bull.* 44, 1060–1069. doi: 10.1093/schbul/sby008

Elvevåg, B., Foltz, P. W., Rosenstein, M., and DeLisi, L. E. (2010). An automated method to analyze language use in patients with schizophrenia and their first-degree relatives. *J. Neurolinguist.* 23, 270–284. doi: 10.1016/j.jneuroling.2009.05.002

Elvevåg, B., Foltz, P. W., Weinberger, D. R., and Goldberg, T. E. (2007). Quantifying incoherence in speech: An automated methodology and novel application to schizophrenia. *Schizophr. Res.* 93, 304–316. doi: 10.1016/j.schres.2007.03.001

Foltz, P. W., Rosenstein, M., and Elvevag, B. (2016). Detecting clinically significant events through automated language analysis: Quo imus?. *NPJ Schizophr.* 2:15054. doi: 10.1038/npjschz.2015.54

Fraser, W. I., King, K. M., Thomas, P., and Kendell, R. E. (1986). The Diagnosis of Schizophrenia by Language Analysis. *Br. J. Psychiatry* 148, 275–278. doi: 10.1192/bjp.148.3.275

FreeSurfer Software Suite (2021). Available online at: http://surfer.nmr.mgh.harvard.edu/ (accessed May 20, 2022).

Frizelle, P., Thompson, P. A., Mcdonald, D., and Bishop, D. V. M. (2018). Growth in syntactic complexity between four years and adulthood: Evidence from a narrative task. *J. Child Lang.* 45, 1174–1197. doi: 10.1017/S0305000918000144

FsTutorial/TroubleshootingData (2022). *Free Surfer Wiki*. Available online at: https://surfer.nmr.mgh.harvard.edu/fswiki/FsTutorial/TroubleshootingData

Givon, T. (2009). *The Genesis of Syntactic Complexity*. Amsterdam: John Benjamins Publishing Company.

Graesser, A. C., McNamara, D. S., Louwerse, M. M., and Cai, Z. (2004). Coh-Metrix: Analysis of text on cohesion and language. *Behav. Res. Methods Instrum. Comput.* 36, 193–202. doi: 10.3758/BF03195564

Gupta, T., Hespos, S. J., Horton, W. S., and Mittal, V. A. (2018). Automated analysis of written narratives reveals abnormalities in referential cohesion in youth at ultra high risk for psychosis. *Schizophr. Res.* 192, 82–88. doi: 10.1016/j.schres.2017.04.025

Halliday, M. A. K., and Hasan, R. (1976). *Cohesion in English. English Language Series*. London: Longman.

Hitczenko, K., Mittal, V. A., and Goldrick, M. (2021). Understanding Language Abnormalities and Associated Clinical Markers in Psychosis: The Promise of Computational Methods. *Schizophr. Bull.* 47, 344–362. doi: 10.1093/schbul/sbaa141

Holmlund, T. B., Fedechko, T. L., Elvevag, B., and Cohen, A. S. (2020). "Tracking language in real time in psychosis," in *A Clinical Introduction to Psychosis: Foundations for Clinical Psychologists and Neuropsychologists*, eds J. C. Badcock and G. Paulik (San Diego, CA: Elsevier Academic Press), 663–685. doi: 10.1016/B978-0-12-815012-2.00028-6

Hunt, K. W. (1970). Syntactic Maturity in Schoolchildren and Adults. *Monogr. Soc. Res. Child Dev.* 35, 1–67. doi: 10.2307/1165818

Iter, D., Yoon, J., and Jurafsky, D. (2018). "Automatic Detection of Incoherent Speech for Diagnosing Schizophrenia," in *Proceedings of the Fifth Workshop on Computational Linguistics and Clinical Psychology: From Keyboard to Clinic*, (New Orleans, LA: Association for Computational Linguistics), 136–146. doi: 10.18653/v1/W18-0615

Iyegbe, C. O., and O'Reilly, P. F. (2022). Genetic origins of schizophrenia find common ground. *Nature* 604, 433–435. doi: 10.1038/d41586-022-00773-5

Jablensky, A. (2006). Subtyping schizophrenia: Implications for genetic research. *Mol. Psychiatry* 11, 815–836. doi: 10.1038/sj.mp.4001857

Jeon, P., Limongi, R., Ford, S. D., Mackinley, M., Dempster, K., Théberge, J., et al. (2021). Progressive Changes in Glutamate Concentration in Early Stages of Schizophrenia: A Longitudinal 7-Tesla MRS Study. *Schizophr. Bull. Open* 2:sgaa072. doi: 10.1093/schizbullopen/sgaa072

Just, S. A., Haegert, E., Koøánová, N., Bröcker, A. L., Nenchev, I., Funcke, J., et al. (2020). Modeling Incoherent Discourse in Non-Affective Psychosis. *Front. Psychiatry* 11:846. doi: 10.3389/fpsyt.2020.00846

King, K., Fraser, W. I., Thomas, P., and Kendell, R. E. (1990). Re-examination of the Language of Psychotic Subjects. *Br. J. Psychiatry* 156, 211–215. doi: 10.1192/bjp.156.2.211

Kircher, T., Bröhl, H., Meier, F., and Engelen, J. (2018). Formal thought disorders: From phenomenology to neurobiology. *Lancet Psychiatry* 5, 515–526. doi: 10.1016/S2215-0366(18)30059-2

Kuperberg, G. R. (2010). Language in schizophrenia Part 1: An Introduction. *Lang. Linguist. Compass* 4, 576–589. doi: 10.1111/j.1749-818X.2010.00216.x

Lenci, A. (2018). Distributional Models of Word Meaning. *Annu. Rev. Linguist.* 4, 151–171. doi: 10.1146/annurev-linguistics-030514-125254

Liang, L., Heinrichs, R. W., Liddle, P. F., Jeon, P., Théberge, J., and Palaniyappan, L. (2022). Cortical impoverishment in a stable subgroup of schizophrenia: Validation across various stages of psychosis. *Schizophr. Res.* [Epub ahead of print]. doi: 10.1016/j.schres.2022.05.013

Liddle, P. F., Ngan, E. T. C., Caissie, S. L., Anderson, C. M., Bates, A. T., Quested, D. J., et al. (2002). Thought and Language Index: An instrument for assessing thought and language in schizophrenia. *Br. J. Psychiatry* 181, 326–330. doi: 10.1192/bjp.181.4.326

Limongi, R., Jeon, P., Mackinley, M., Das, T., Dempster, K., Théberge, J., et al. (2020). Glutamate and Dysconnection in the Salience Network: Neurochemical, Effective Connectivity, and Computational Evidence in Schizophrenia. *Biol. Psychiatry* 88, 273–281. doi: 10.1016/j.biopsych.2020.01.021

Lin, C. H., Lin, H. S., Lin, S. C., Kuo, C. C., Wang, F. C., and Huang, Y. H. (2018). Early improvement in PANSS-30, PANSS-8, and PANSS-6 scores predicts ultimate response and remission during acute treatment of schizophrenia. *Acta Psychiatr. Scand.* 137, 98–108. doi: 10.1111/acps.12849

Lu, X. (2010). Automatic analysis of syntactic complexity in second language writing. *Int. J. Corpus Linguist.* 15, 474–496. doi: 10.1075/ijcl.15.4.02lu

Lundin, N. B., Hochheiser, J., Minor, K. S., Hetrick, W. P., and Lysaker, P. H. (2020). Piecing together fragments: Linguistic cohesion mediates the relationship between executive function and metacognition in schizophrenia. *Schizophr. Res.* 215, 54–60. doi: 10.1016/j.schres.2019.11.032

Mackinley, M., Chan, J., Ke, H., Dempster, K., and Palaniyappan, L. (2021). Linguistic determinants of formal thought disorder in first episode psychosis. *Early Interv. Psychiatry* 15, 344–351. doi: 10.1111/eip.12948

Marggraf, M. P., Lysaker, P. H., Salyers, M. P., and Minor, K. S. (2020). The link between formal thought disorder and social functioning in schizophrenia: A meta-analysis. *Eur. Psychiatry* 63:e34. doi: 10.1192/j.eurpsy.2020.30

Mikesell, L., and Bromley, E. (2016). "Exploring the Heterogeneity of 'Schizophrenic Speech," in *The Palgrave Handbook of Adult Mental Health: Discourse and Conversation Studies*, eds M. O'Reilly and J. N. Lester (London: Palgrave Macmillan), 329–351. doi: 10.1057/9781137496850_18

Minor, K. S., Willits, J. A., Marggraf, M. P., Jones, M. N., and Lysaker, P. H. (2019). Measuring disorganized speech in schizophrenia: Automated analysis explains variance in cognitive deficits beyond clinician-rated scales. *Psychol. Med.* 49, 440–448. doi: 10.1017/S0033291718001046

Morgan, S. E., Diederen, K., Vértes, P. E., Ip, S. H. Y., Wang, B., Thompson, B., et al. (2021). Natural Language Processing markers in first episode psychosis and people at clinical high-risk. *Transl. Psychiatry* 11:630. doi: 10.1038/s41398-021-01722-y

Morice, R. D., and Ingram, J. C. (1982). Language analysis in schizophrenia: Diagnostic implications. *Aust. N. Z. J. Psychiatry* 16, 11–21. doi: 10.3109/00048678209161186

Morice, R. D., and Ingram, J. C. L. (1983). Language complexity and age of onset of schizophrenia. *Psychiatry Res.* 9, 233–242. doi: 10.1016/0165-1781(83)90048-3

Morice, R., and McNicol, D. (1986). Language Changes in Schizophrenia: A Limited Replication. *Schizophr. Bull.* 12, 239–251. doi: 10.1093/schbul/12.2.239

Morosini, P. L., Magliano, L., Brambilla, L., Ugolini, S., and Pioli, R. (2000). Development, reliability and acceptability of a new version of the DSM-IV Social and Occupational Functioning Assessment Scale (SOFAS) to assess routine social functioning. *Acta Psychiatr. Scand.* 101, 323–329. doi: 10.1111/j.1600-0447.2000.tb10933.x

Mota, N. B., Vasconcelos, N. A. P., Lemos, N., Pieretti, A. C., Kinouchi, O., Cecchi, G. A., et al. (2012). Speech Graphs Provide a Quantitative Measure of Thought Disorder in Psychosis. *PLoS One* 7:e34928. doi: 10.1371/journal.pone.0034928

Murray, H. A. (1943). *Thematic Apperception Test*. Cambridge, MA: Harvard University Press.

Nippold, M. A., Cramond, P. M., and Hayward-Mayhew, C. (2014). Spoken language production in adults: Examining age-related differences in syntactic complexity. *Clin. Linguist. Phon.* 28, 195–207. doi: 10.3109/02699206.2013.841292

Oertel-Knöchel, V., Knöchel, C., Rotarska-Jagiela, A., Reinke, B., Prvulovic, D., Haenschel, C., et al. (2013). Association between Psychotic Symptoms and Cortical Thickness Reduction across the Schizophrenia Spectrum. *Cereb. Cortex* 23, 61–70. doi: 10.1093/cercor/bhr380

Oomen, P. P., de Boer, J. N., Brederoo, S. G., Voppel, A. E., Brand, B. A., Wijnen, F. N. K., et al. (2022). Characterizing speech heterogeneity in schizophrenia-spectrum disorders. *J. Psychopathol. Clin. Sci.* 131, 172–181. doi: 10.1037/abn0000736

Oyebode, F. (2021). *Sims' Symptoms in the Mind: Textbook of Descriptive Psychopathology - 7th Edition*. Amsterdam: Elsevier.

Palaniyappan, L. (2021). Dissecting the neurobiology of linguistic disorganisation and impoverishment in schizophrenia. *Semin. Cell Dev. Biol.* doi: 10.1016/j.semcdb.2021.08.015 [Epub ahead of print].

Palaniyappan, L., Al-Radaideh, A., Gowland, P. A., and Liddle, P. F. (2020). Cortical thickness and formal thought disorder in schizophrenia: An ultra high-field network-based morphometry study. *Prog. Neuropsychopharmacol. Biol. Psychiatry* 101:109911. doi: 10.1016/j.pnpbp.2020.109911

Palaniyappan, L., Mota, N. B., Oowise, S., Balain, V., Copelli, M., Ribeiro, S., et al. (2019). Speech structure links the neural and socio-behavioural correlates of psychotic disorders. *Prog. Neuropsychopharmacol. Biol. Psychiatry* 88, 112–120. doi: 10.1016/j.pnpbp.2018.07.007

Pan, Y., Pu, W., Chen, X., Huang, X., Cai, Y., Tao, H., et al. (2020). Morphological Profiling of Schizophrenia: Cluster Analysis of MRI-Based Cortical Thickness Data. *Schizophr. Bull.* 46, 623–632. doi: 10.1093/schbul/sbz112

Parola, A., Lin, J. M., Simonsen, A., Bliksted, V., Zhou, Y., Wang, H., et al. (2022). Speech disturbances in schizophrenia: Assessing cross-linguistic generalizability of NLP automated measures of coherence. *medRxiv* [Preprint]. doi: 10.1101/2022.03.28.22272995

Penn, D. L., Kohlmaier, J. R., and Corrigan, P. W. (2000). Interpersonal factors contributing to the stigma of schizophrenia: Social skills, perceived attractiveness, and symptoms. *Schizophr. Res.* 45, 37–45. doi: 10.1016/S0920-9964(99)00213-3

Peralta, V., Cuesta, M. J., and de Leon, J. (1992). Formal thought disorder in schizophrenia: A factor analytic study. *Compr. Psychiatry* 33, 105–110. doi: 10.1016/0010-440X(92)90005-B

Plitman, E., Nakajima, S., de la Fuente-Sandoval, C., Gerretsen, P., Chakravarty, M. M., and Kobylianskii, J. (2014). Glutamate-mediated excitotoxicity in schizophrenia: A review. *Eur. Neuropsychopharmacol.* 24, 1591–1605. doi: 10.1016/j.euroneuro.2014.07.015

Plitman, E., Patel, R., Chung, J. K., Pipitone, J., Chavez, S., Reyes-Madrigal, F., et al. (2016). Glutamatergic Metabolites, Volume and Cortical Thickness in Antipsychotic-Naive Patients with First-Episode Psychosis: Implications for Excitotoxicity. *Neuropsychopharmacoloy* 41, 2606–2613. doi: 10.1038/npp.2016.84

Ratana, R., Sharifzadeh, H., Krishnan, J., and Pang, S. A. (2019). Comprehensive Review of Computational Methods for Automatic Prediction of Schizophrenia With Insight Into Indigenous Populations. *Front. Psychiatry* 10:659. doi: 10.3389/fpsyt.2019.00659

recon-all Free Surfer Wiki (2022). Available online at: https://surfer.nmr.mgh.harvard.edu/fswiki/recon-all (accessed May 20, 2022).

Roche, E., Creed, L., MacMahon, D., Brennan, D., and Clarke, M. (2015). The Epidemiology and Associated Phenomenology of Formal Thought Disorder: A Systematic Review. *Schizophr. Bull.* 41, 951–962. doi: 10.1093/schbul/sbu129

Sanders, T., and Maat, H. P. (1976). *Cohesion and Coherence: Linguistic Approaches*. Available online at: https://coek.info/pdf-cohesion-and-coherence-linguistic-approaches-.html (accessed May 20, 2022).

Shah, P., Plitman, E., Iwata, Y., Kim, J., Nakajima, S., Chan, N., et al. (2020). Glutamatergic neurometabolites and cortical thickness in treatment-resistant schizophrenia: Implications for glutamate-mediated excitotoxicity. *J. Psychiatr. Res.* 124, 151–158. doi: 10.1016/j.jpsychires.2020.02.032

Silva, A. M., Limongi, R., MacKinley, M., Ford, S. D., Alonso-Sánchez, M. F., and Palaniyappan, L. (2022). Syntactic complexity of spoken language in the diagnosis of schizophrenia: A probabilistic Bayes network model. *Schizophr. Res.* [Epub ahead of print]. doi: 10.1016/j.schres.2022.06.011

Sugihara, G., Oishi, N., Son, S., Kubota, M., Takahashi, H., and Murai, T. (2017). Distinct Patterns of Cerebral Cortical Thinning in Schizophrenia: A Neuroimaging Data-Driven Approach. *Schizophr. Bull.* 43, 900–906. doi: 10.1093/schbul/sbw176

Szmrecsanyi, B. (2004). "On operationalizing syntactic complexity," in *Le poids des mots Proceedings of the 7th International Conference on Textual Data Statistical Analysis*, eds P. Gérard, F. Cédrick, and D. Anne (Louvain-la-Neuve: Presses universitaires de Louvain), 1032–1039.

Tan, E. J., Meyer, D., Neill, E., and Rossell, S. L. (2021). Investigating the diagnostic utility of speech patterns in schizophrenia and their symptom associations. *Schizophr. Res.* 238, 91–98. doi: 10.1016/j.schres.2021.10.003

Tan, E. J., Thomas, N., and Rossell, S. L. (2014). Speech disturbances and quality of life in schizophrenia: Differential impacts on functioning and life satisfaction. *Compr. Psychiatry* 55, 693–698. doi: 10.1016/j.comppsych.2013.10.016

Tang, S. X., Kriz, R., Cho, S., Park, S. J., Harowitz, J., Gur, R. E., et al. (2021). Natural language processing methods are sensitive to sub-clinical linguistic differences in schizophrenia spectrum disorders. *NPJ Schizophr.* 7:630. doi: 10.1038/s41537-021-00154-3

Thomas, P. (1996). Syntactic Complexity and Negative Symptoms in First Onset Schizophrenia. *Cogn. Neuropsychiatry* 1, 191–200. doi: 10.1080/135468096396497

Thomas, P., King, K., Fraser, W. I., and Kendell, R. E. (1990). Linguistic Performance in Schizophrenia: A Comparison of Acute and Chronic Patients. *Br. J. Psychiatry* 156, 204–210. doi: 10.1192/bjp.156.2.204

Trubetskoy, V., Pardiñas, A. F., Qi, T., Panagiotaropoulou, G., Awasthi, S., Bigdeli, T. B., et al. (2022). Mapping genomic loci implicates genes and synaptic biology in schizophrenia. *Nature* 604, 502–508. doi: 10.1038/s41586-022-04434-5

Voleti, R., Liss, J. M., and Berisha, V. A. (2020). Review of Automated Speech and Language Features for Assessment of Cognitive and Thought Disorders. *IEEE J. Sel. Top. Signal. Process.* 14, 282–298.

Wang, Y., and Qin, Z. H. (2010). Molecular and cellular mechanisms of excitotoxic neuronal death. *Apoptosis* 15, 1382–1402. doi: 10.1007/s10495-010-0481-0

Wible, C. G. (2012). Schizophrenia as a Disorder of Social Communication. *Schizophr. Res. Treat.* 2012:920485. doi: 10.1155/2012/920485

World Health Organization [WHO] (2022). *Defined Daily Dose (DDD)*. Available online at: https://www.who.int/tools/atc-ddd-toolkit/about-ddd (accessed May 20, 2022).

Zhao, Y., Zhang, Q., Shah, C., Li, Q., Sweeney, J. A., Li, F., et al. (2022). Cortical Thickness Abnormalities at Different Stages of the Illness Course in Schizophrenia: A Systematic Review and Meta-analysis. *JAMA Psychiatry* 79, 560–570. doi: 10.1001/jamapsychiatry.2022.0799

Zimmerer, V. C., Watson, S., Turkington, D., Ferrier, I. N., and Hinzen, W. (2017). Deictic and Propositional Meaning—New Perspectives on Language in Schizophrenia. *Front. Psychiatry* 8:17. doi: 10.3389/fpsyt.2017.00017

frontiers | Frontiers in Human Neuroscience

TYPE Methods
PUBLISHED 23 September 2022
DOI 10.3389/fnhum.2022.958706

OPEN ACCESS

EDITED BY
Chun Meng,
University of Electronic Science and Technology of China, China

REVIEWED BY
Ashkan Faghiri,
Georgia State University, United States
Victor Manuel Vergara,
Georgia State University, United States

*CORRESPONDENCE
David Sutherland Blair
davidsutherland.blair@upf.edu

SPECIALTY SECTION
This article was submitted to Brain Imaging and Stimulation, a section of the journal Frontiers in Human Neuroscience

RECEIVED 31 May 2022
ACCEPTED 03 August 2022
PUBLISHED 23 September 2022

CITATION
Blair DS, Soriano-Mas C, Cabral J, Moreira P, Morgado P and Deco G (2022) Complexity changes in functional state dynamics suggest focal connectivity reductions. *Front. Hum. Neurosci.* 16:958706. doi: 10.3389/fnhum.2022.958706

Complexity changes in functional state dynamics suggest focal connectivity reductions

David Sutherland Blair [1]*, Carles Soriano-Mas [2,3,4], Joana Cabral [5], Pedro Moreira [5,6,7], Pedro Morgado [5,6,8] and Gustavo Deco [1,9,10,11]

[1]Facultad de Comunicación, Universitat Pompeu Fabra, Barcelona, Spain, [2]Psychiatry and Mental Health Group, Neuroscience Program, Institut d'Investigació Biomèdica de Bellvitge, Barcelona, Spain, [3]Network Center for Biomedical Research on Mental Health, Carlos III Health Institute, Madrid, Spain, [4]Department of Social Psychology and Quantitative Psychology, Universitat de Barcelona, Barcelona, Spain, [5]Life and Health Sciences Research Institute, School of Medicine, University of Minho, Braga, Portugal, [6]ICVS/3B's, PT Government Associate Laboratory, Braga, Portugal, [7]Psychological Neuroscience Lab, CIPsi, School of Psychology, University of Minho, Braga, Portugal, [8]Clinical Academic Center—Braga, Braga, Portugal, [9]Institució Catalana de Recerca i Estudis Avançats, Barcelona, Spain, [10]Department of Neuropsychology, Max Planck Institute for Human Cognitive and Brain Sciences, Leipzig, Germany, [11]School of Psychological Sciences, Monash University, Clayton, VIC, Australia

The past two decades have seen an explosion in the methods and directions of neuroscience research. Along with many others, complexity research has rapidly gained traction as both an independent research field and a valuable subdiscipline in computational neuroscience. In the past decade alone, several studies have suggested that psychiatric disorders affect the spatiotemporal complexity of both global and region-specific brain activity (Liu et al., 2013; Adhikari et al., 2017; Li et al., 2018). However, many of these studies have not accounted for the distributed nature of cognition in either the global or regional complexity estimates, which may lead to erroneous interpretations of both global and region-specific entropy estimates. To alleviate this concern, we propose a novel method for estimating complexity. This method relies upon projecting dynamic functional connectivity into a low-dimensional space which captures the distributed nature of brain activity. Dimension-specific entropy may be estimated within this space, which in turn allows for a rapid estimate of global signal complexity. Testing this method on a recently acquired obsessive-compulsive disorder dataset reveals substantial increases in the complexity of both global and dimension-specific activity versus healthy controls, suggesting that obsessive-compulsive patients may experience increased disorder in cognition. To probe the potential causes of this alteration, we estimate subject-level effective connectivity *via* a Hopf oscillator-based model dynamic model, the results of which suggest that

obsessive-compulsive patients may experience abnormally high connectivity across a broad network in the cortex. These findings are broadly in line with results from previous studies, suggesting that this method is both robust and sensitive to group-level complexity alterations.

KEYWORDS

LEiDA, Hopf bifurcation, whole-brain model, obsessive-compulsive disorder, independent component analysis, eigendecomposition, Shannon entropy, network-based statistic

Introduction

Revolution has rocked the field of neuroimaging for the past two decades. Technological development has led to previously unattainable combinations of spatial and temporal resolution, even as the discovery of organized resting state activity (Biswal et al., 1996, 1997a,b, 1998; Biswal, 2012) has opened an entire new area of study. These developments have complemented one another in many lines of study, but perhaps the most notable is in the study of psychiatric disorders, where ethical concerns can make task-based or symptom provocation studies difficult (DuVal, 2004). The ability to study functional connectivity dynamics without the practical or ethical complications of symptom provocation has allowed psychiatric data collection in enormous quantity and quality. Indeed, so much data is now available that analysis has surpassed collection as the biggest challenge in neuroscience (Burns et al., 2013; Furcila et al., 2019).

Increasingly, neuroscientists have turned to mathematics and computational tools to interpret this data. The nature of neural data and the mixed backgrounds of many neuroscientists have led to the use of tools from a wide variety of mathematical fields, including statistics (Friston et al., 2006), econometrics (Friston, 2011), network analysis (Bullmore and Sporns, 2009), statistical physics (Deco et al., 2008), information theory (Pincus, 1991; Richman and Moorman, 2000), and dynamical systems (Rolls et al., 2008). The use of such tools has led to dramatic conceptual advances in the study of brain function, such as the use of network analysis to quantify structure in brain activity (Meunier et al., 2009; Shen et al., 2010) and the discovery that cognition is a distributed, rather than localized, phenomenon (Hillebrand et al., 2016; Atasoy et al., 2018). However, to paraphrase Dr. John Archibald Wheeler, as our island of knowledge grows, so too does the shoreline which surrounds it. The advances of the past two decades have revealed as many questions as answers.

One longstanding question in neuroscience and neuropsychiatry is how to quantify the complexity of the brain's functional dynamics. While microarray studies of functional complexity are not new (Paninski, 2003; Pereda et al., 2005; Quian Quiroga and Panzeri, 2009), the whole-brain level presents two serious problems. First, even coarse neuroimaging parcellations have more than $N = 60$ regions of interest (ROIs) (Hagmann et al., 2008), and connectivity matrices have at least $\frac{N(N-1)}{2}$ elements (assuming symmetry and neglecting the main diagonal). The curse of dimensionality makes meaningful results difficult to find in such a high-dimensional space. Second, these regions are not generally statistically independent in time. Indeed, functional connectivity analysis relies on such interregional dependence. While these dependencies have revealed much about brain function, they also invalidate the most natural measure of functional complexity—namely the Shannon joint entropy (Shannon, 1949)—as its calculation requires statistical independence of the constituent signals. Several authors have attempted to compare the functional complexity of groups and subjects by other means (Ostwald and Bagshaw, 2011; Liu et al., 2013; McIntosh et al., 2014; Grieder et al., 2018; Zheng et al., 2020; Xin et al., 2021), but they may overlook interregional statistical dependencies and thus risk erroneous estimates of region-specific complexity. A rigorous means of quantifying the functional complexity alterations which characterize psychiatric disorders remains elusive.

In this paper, we propose a novel analysis pipeline aimed at solving these problems. We begin by adapting the Leading Eigenvector Dynamics Analysis (LEiDA) framework (Cabral et al., 2017; Figueroa et al., 2019; Lord et al., 2019) to identify a low-dimensional space which captures the temporal dynamics and complexity of functional connectivity. This requires two important innovations to the LEiDA framework. First, we develop a data-based method to estimate the state space dimensionality *a priori*. Previous studies have treated the number of dimensions as a free parameter and relied on *post facto* comparisons to determine an appropriate threshold (Cabral et al., 2017; Gu et al., 2018; Shappell et al., 2019; Vergara et al., 2020). While these methods have proven effective, they require leaving the number of groups as a free parameter. This requires multiple runs of a clustering algorithm to determine which setting is most effective. Such runs are computationally expensive, adding both time and cost to the analysis. Further, such trial-and-error approaches offer no guarantee of selecting the true number of meaningful groups. Thus, this development

may improve both the precision and the efficiency of future analyses.

The use of independent component analysis represents the second major innovation to the LEiDA pipeline. Previous LEiDA analyses have used a *k*-means clustering algorithm to isolate connectivity state centroids and assign state labels to each time point. While this allows a characterization of state transition mechanics (Cabral et al., 2017; Lord et al., 2019; Vohryzek et al., 2020), *k*-means clustering suffers from two serious shortcomings which render it unsuitable for our purposes. First, *k*-means clusters generally display temporal dependencies, which make the calculation of statistical complexity extremely complex. Independent component analysis' minimization of such dependencies (Calhoun et al., 2013) drastically simplifies these calculations. Second, most (although not all) *k*-means clustering algorithms assign only a single state to each time point. This enforces a binary, on-off image of state activity which discards much of the signal's complexity—entirely incompatible with an algorithm designed to measure that complexity.

To alleviate these concerns, we replace the *k*-means clustering algorithm of LEiDA with independent component analysis (ICA) (Hyvärinen and Oja, 2000). ICA has been shown to maximize the temporal independence of its components (Calhoun et al., 2013) and so avoids dependencies between components. In addition, ICA does not assign a single active state to each time point, but instead estimates the activity of each state across the entire dataset. This provides a far more detailed view of how functional activity evolves in the space which these independent components define. A similar method has been proven highly effective in the context of neural spike trains (Lopes-dos-Santos et al., 2013).

These two innovations produce a space with the minimum number of independent dimensions necessary to capture meaningful patterns. Such a space makes calculating and comparing temporal complexity (as measured by the Shannon entropy) of each subject simple. Given the critical nature of ICA, we have named our analysis pipeline LEICA (Leading Eigenvector Independent Component Analysis) to differentiate it from the LEiDA framework on which it is based.

We elected to test this pipeline on a dataset (Moreira et al., 2017) consisting of obsessive-compulsive disorder (OCD) patients and number of age-, gender-, and education-matched controls (N_{OCD} = 40, $N_{control}$ = 39). The wide prevalence and severe effects of OCD factored into this choice of dataset; with some 2.1% of the population affected each year (DuPont et al., 1995), it is a widespread, yet poorly understood disorder that causes its victims great distress. Obsessive thoughts and compulsive behaviors often hinder victims' ability to concentrate, with predictable effects on learning and productivity (Piacentini et al., 2003; Weidle et al., 2014). These factors contribute to a high societal cost of illness (DuPont et al., 1995; Lenhard et al., 2021) and reduced quality of life for patients. Despite its prevalence, the disorder's functional dynamics remain poorly understood; in particular, we have been unable to find any attempts to examine the functional complexity of OCD patients. In this study, we demonstrate that the obsessive-compulsive group displays elevated joint entropies compared to healthy controls. Indeed, not only can we identify which group has higher joint entropy, but also along which dimension the entropy changes.

Finally, in order to inform hypotheses on possible causes of this altered complexity, we implemented a coupled Hopf oscillator network model (Kuznetsov, 1998; Freyer et al., 2011, 2012; Deco et al., 2017b). The model estimates subject-level connectivity by fitting observed entropies. Notably, this requires the model to be trained in component space rather than the parcellation space, as the joint entropy can only be reliably calculated in this low-dimensional space. The trained model suggests that patients express enhanced connectivity in a brain-wide network, while having reduced connectivity in several small networks. It must be emphasized that link-level model results should be considered a hypothesis rather than a conclusion, as the high dimensionality of the model space makes drawing such small-scale conclusions premature. Nonetheless, the finding of general cortical hyperconnectivity coupled with targeted hypoconnectivity is consistent, and link-level results provide targets for future research. Overall, model results suggest that the LEICA method can extract alterations invisible in other spaces.

Materials and methods

Participants

This paper uses a dataset from a previous study at the Universidad do Minho, Portugal (Moreira et al., 2017). A detailed description may be found in that paper, but a summary is included here for completeness.

Eighty right-handed subjects (40 patients with OCD, 40 controls) participated in this study. Recruitment ensured that controls matched patients in age, sex, education, and ethnic origin. Both patients and controls were screened to remove subjects with comorbid mental health, neurological or major medical disorders (except nicotine use or dependence). Patients were all confirmed to have been using stable doses of medication for three months prior to the study. Specifically, 72.2% used selective serotonin reuptake inhibitors (SSRIs), 11.1% tricyclic antidepressants (TCA), and 16.7% a combination of these medications.

Image acquisition occurred in a 1.5 T Siemens Magnetom Avanto MRI scanner (Siemens, Erlangen, Germany) with a standard 12-channel receiver coil. Images were visually examined for artifacts and the functional data preprocessed using FSL. Slice-timing correction used the first slice as a reference, a rigid-body spatial transformation aligned the volumes of each subject with the mean volume, and motion

scrubbing identified time points contaminated by significant motion. Participants with more than 20 such time points were removed from analysis. Images were then non-linearly normalized to MNI standard space and linear regression used to remove motion-related variance and signals from white matter and cerebrospinal fluid. Acquisitions were filtered with a Gaussian spatial smoothing kernel (8 mm FWHM) and a temporal band-pass filter (0.01–0.08 Hz). This frequency band has demonstrated greater reliability and functional relevance in fMRI compared to others (Biswal et al., 1995; Achard et al., 2006; Buckner et al., 2009; Glerean et al., 2012). This low frequency band has the additional advantage of averaging out physiological noise and hemodynamic response functions, as these signals have frequencies above 0.08 Hz and thus fall outside the passband of this filter. Finally, following the preprocessing, Moreira et al. (2017) extracted the mean BOLD time series of the 116 cortical, subcortical, and cerebellar regions of the Anatomical Automatic Labeling atlas (Tzourio-Mazoyer et al., 2002). As our study focuses on cortical and subcortical regions, the 26 cerebellar regions of the Anatomical Automatic Labeling (AAL) atlas were removed. A complete and ordered list of regions in this study may be viewed in **Table 1**.

TABLE 1 Table displays the 90 cortical and subcortical regions of the standard 116-region AAL parcellation (Tzourio-Mazoyer et al., 2002) in symmetrical, left-first order.

R Precentral Gyrus
R Superior Frontal Gyrus, Dorsolateral
R Superior Frontal Gyrus, Orbital Part
R Middle Frontal Gyrus
R Middle Frontal Gyrus, Orbital Part
R Inferior Frontal Gyrus, Opercular Part
R Inferior Frontal Gyrus, Triangular Part
R Inferior Frontal Gyrus, Orbital Part
R Rolandic Operculum
R Supplementary Motor Area
R Olfactory Cortex
R Superior Frontal Gyrus, Medial
R Superior Frontal Gyrus, Medial Orbital
R Gyrus Rectus
R Insula
R Anterior Cingulate and Paracingulate Gyri
R Median Cingulate and Paracingulate Gyri
R Posterior Cingulate Gyrus
R Hippocampus
R Parahippocampal Gyrus
R Amygdala
R Calcarine Fissure
R Cuneus
R Lingual Gyrus
R Superior Occipital Gyrus
R Middle Occipital Gyrus
R Inferior Occipital Gyrus
R Fusiform Gyrus
R Postcentral Gyrus
R Superior Parietal Gyrus
R Inferior Parietal Gyri
R Supramarginal Gyrus
R Angular Gyrus
R Precuneus
R Paracentral Lobule
R Caudate Nucleus
R Lenticular Nucleus, Putamen
R Lenticular Nucleus, Pallidum
R Thalamus
R Heschl Gyrus
R Superior Temporal Gyrus
R Temporal Pole: Superior Temporal Gyrus
R Middle Temporal Gyrus
R Temporal Pole: Middle Temporal Gyrus
R Inferior Temporal Gyrus
L Inferior Temporal Gyrus
L Temporal Pole: Middle Temporal Gyrus
L Middle Temporal Gyrus
L Temporal Pole: Superior Temporal Gyrus

(Continued)

Functional connectivity

Dynamic functional connectivity

This study uses Coherence Connectivity Dynamics (Deco et al., 2017a) to compute the dynamic functional connectivity (dFC) (**Figure 1A**). The remaining 90 cortical and subcortical time series were demeaned, detrended, and underwent a Hilbert transform to produce a phase time series θ, such that θ(n,t) represents the phase of region n at time t (**Figure 1C**). Upon computing θ, the phase coherence between regions *m* and *n* at time *t* $\left(\mathrm{dFC}\left(\mathrm{m},\mathrm{n},\mathrm{t}\right)\right)$ is computed using Equation 1:

$$\mathbf{dFC}\left(\mathbf{m},\mathbf{n},\mathbf{t}\right)=\mathbf{cos}\left(\boldsymbol{\theta}\left(\mathbf{m},\mathbf{t}\right)-\boldsymbol{\theta}\left(\mathbf{n},\mathbf{t}\right)\right)$$

where cos is the cosine function. Thus, $\mathrm{dFC}\left(\mathrm{m},\mathrm{n},\mathrm{t}\right)=1$ if the regions m and n are in phase at time t $\left(\theta\left(\mathrm{m},\mathrm{t}\right)-\theta\left(\mathrm{n},\mathrm{t}\right)=0,\pm2\pi\right)$, and $\mathrm{dFC}\left(\mathrm{m},\mathrm{n},\mathrm{t}\right)=0$ if the regions are perfectly out of phase at time t $\left(\theta\left(\mathrm{m},\mathrm{t}\right)-\theta\left(\mathrm{n},\mathrm{t}\right)=\pm\pi\right)$. This produces a dFC array with dimensions N × N × T, where N is the number of ROIs and T represents the number of time points. Since cos (θ) is an even function, each N × N matrix dFC (t) is symmetric.

Leading eigenvector analysis: Theoretical basis

The fundamental goal of the LEiDA process is to project the dominant spatial connectivity pattern dynamics into a lower-dimensional space for ease of analysis. Identifying this dominant pattern at each time point is greatly simplified by the symmetry and realness of individual dFC matrices. As symmetric and real

TABLE 1 (Continued)

L Superior Temporal Gyrus
L Heschl Gyrus
L Thalamus
L Lenticular Nucleus, Pallidum
L Lenticular Nucleus, Putamen
L Caudate Nucleus
L Paracentral Lobule
L Precuneus
L Angular Gyrus
L Supramarginal Gyrus
L Inferior Parietal Gyri
L Superior Parietal Gyrus
L Postcentral Gyrus
L Fusiform Gyrus
L Inferior Occipital Gyrus
L Middle Occipital Gyrus
L Superior Occipital Gyrus
L Lingual Gyrus
L Cuneus
L Calcarine Fissure
L Amygdala
L Parahippocampal Gyrus
L Hippocampus
L Posterior Cingulate Gyrus
L Median Cingulate and Paracingulate Gyri
L Anterior Cingulate and Paracingulate Gyri
L Insula
L Gyrus Rectus
L Superior Frontal Gyrus, Medial Orbital
L Superior Frontal Gyrus, Medial
L Olfactory Cortex
L Supplementary Motor Area
L Rolandic Operculum
L Inferior Frontal Gyrus, Orbital Part
L Inferior Frontal Gyrus, Triangular Part
L Inferior Frontal Gyrus, Opercular Part
L Middle Frontal Gyrus, Orbital Part
L Middle Frontal Gyrus
L Superior Frontal Gyrus, Orbital Part
L Superior Frontal Gyrus, Dorsolateral
L Precentral Gyrus

Unless otherwise noted, all figures in this study sort brain regions identically to this table. Due to space constraints, figures do not generally contain all 90 regional labels.

matrices are always diagonalizable, the dFC at any time point t can be decomposed into

$$\mathrm{dFC}\,(t) = VDV^{-1}$$

with V being the eigenvectors of dFC (t) and D the diagonal matrix of eigenvalues. As the eigenvectors of a symmetric matrix must be orthogonal, $V^{-1} = V^T$; thus,

$$\mathrm{dFC}\,(t) = VDV^T$$

which may be equivalently written as

$$\mathrm{dFC}\,(t) = VDV^T = \sum_n \lambda_n v_n v_n^T$$

where v_n is the n^{th} eigenvector and λ_n the n^{th} eigenvalue of dFC (t). At each time point, the instantaneous FC matrix may be decomposed into a weighted sum of eigenvector outer products $v_n v_n^T$ weighted according to the respective eigenvalue λ_n. Thus, finding the dominant spatial pattern at any time point simply involves finding the eigenvector with the largest eigenvalue at that time point. In addition, one may easily compute the proportion of variance which this pattern captures simply by dividing the leading eigenvalue by the sum of all eigenvalues:

$$\rho = \frac{\lambda_l}{\sum_n \lambda_n}$$

Previous work demonstrates that the leading eigenvector consistently represents more than 50% of data variance (Cabral et al., 2017; Lord et al., 2019), a finding confirmed in the present study. Further, experiments with the use of additional eigenvectors demonstrated no improvement in performance or clinical interpretability. The authors thus believe that a single eigenvector is sufficient to represent functional connectivity dynamics.

This compression has three distinct advantages for further signal analysis. First, by compressing each N × N dFC (t) matrix to an N × 1 vector p_l, this method reduces sample dimensionality from $\frac{N(N-1)}{2}$ to N. Second, the primary connectivity pattern should contain virtually no noise, as noise components generally appear in trailing eigenvectors. Finally, previous work in spectral community detection (Newman, 2006; Leicht and Newman, 2008) has demonstrated that the leading eigenvector p_l (t) can separate brain regions into communities based on the sign of each region r ∈ p_l (t), with the magnitude of r indicating that assignment's "strength". Thus, transforming the dFC (t) matrix to p_l (t) converts interregional phase-locking values into regional community assignment values. Put another way, the leading eigenvector of an FC matrix naturally separates network nodes into two mutually opposing communities.

Leading eigenvector analysis: Application

We adapt the LEiDA (Cabral et al., 2017; Figueroa et al., 2019; Lord et al., 2019) by examining only the leading eigenvector $\mathbf{v}_l$ (t) of each $N \times N$ **dFC** (t) matrix. At each time point, the leading eigenvector of the $N \times N$ **dFC** (t) is extracted (**Figure 1D**); once the leading eigenvectors of all time points have been extracted, they are concatenated horizontally to form a space-time matrix **E** (**Figure 1E**). Each row r of **E** represents one brain region r, and each column t contains the leading eigenvector $\mathbf{v}_l$ (t) for time t. The laws of linear algebra render

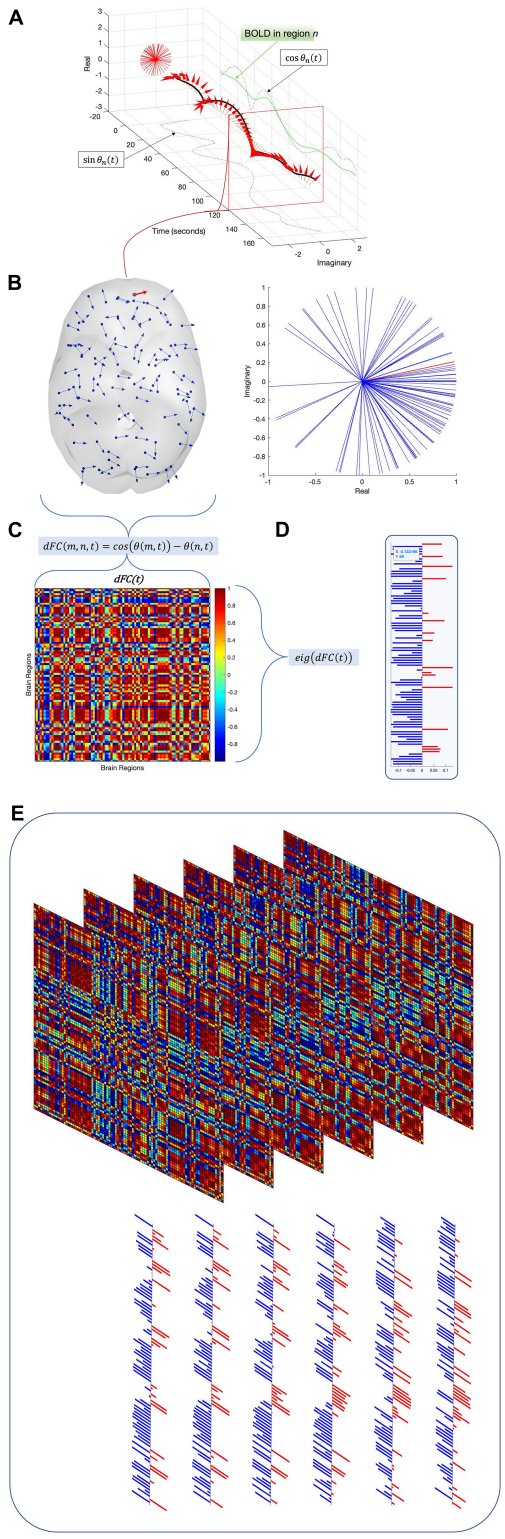

FIGURE 1
To compute time-resolved functional connectivity (dynamic functional connectivity, or dFC), each regional time series (green trace) is converted into an analytic signal using the Hilbert transform. Euler's formula converts this analytic signal into a

(Continued)

FIGURE 1 (Continued)
time-resolved phase signal **(A)** with both real and imaginary parts (dashed black traces). For each time point, the phase signals of all regions are sampled **(B)** and the cosine distance between each pair of regions is computed to produce an instantaneous functional connectivity matrix **(C)**. The leading eigenvector V_1 of this functional connectivity matrix is then isolated **(D)**. Repeating this process for all time points and subjects across the dataset results in a 2-D array E of leading eigenvectors **(E)**. Running an eigendecomposition on E's autocorrelation matrix and counting the number of eigenvalues greater than the upper bound of the Marčenko–Pastur distribution reveals the number of dimensions necessary to describe the nonrandom activity in panel **(E)**.

$\mathbf{v_l}$ (t) and $-\mathbf{v_l}$ (t) equivalent, so we follow the convention that most elements in each eigenvector should be negative (Figueroa et al., 2019).

Component detection

To find the communities that recur above chance, we must determine a significance threshold for regional co-activation. Although surrogate methods, e.g., a permutation test, can establish such a threshold, they are slow and computationally intensive. We propose a far cheaper and more elegant method based on autocorrelation matrix eigenvalues (Peyrache et al., 2009, 2010). It has been established for several decades that if an $m \times n$ matrix $\mathbf{M}$ has statistically independent rows (as would be expected for uncoupled noisy oscillators), the eigenvalues of its autocorrelation matrix follow the Marčenko–Pastur distribution (Marčenko and Pastur, 1967). Crucially, this distribution has analytically tractable limits

$$\lambda_{min}^{max} = \sigma^2\left(1 \pm \sqrt{\frac{1}{q}}\right)^2$$

where σ is the standard deviation of $\mathbf{M}$ and $q \equiv \frac{n}{m} \geq 1$. Thus, if communities do not recur over time, the eigenvalues of $\mathbf{E}$'s correlation matrix should lie within the limits imposed by λ_{min}^{max}. Conversely, should any communities of $\mathbf{E}$ recur at a rate significantly above chance, a corresponding number of eigenvalues of the correlation matrix of $\mathbf{E}$ should exceed the upper limit λ_{max}. This method has been validated in the spike activity context (Lopes-dos-Santos et al., 2011, 2013) and in a previously published fMRI study (Deco et al., 2019). In the present dataset, it detects 12 components (**Figure 4A**).

Component extraction

Upon finding the total number of recurrent communities with the Marčenko–Pastur distribution, we utilize the fastICA algorithm (Laubach et al., 1999; Hyvärinen and Oja, 2000) to extract these communities and their activity time courses from the matrix E. Since the fastICA algorithm requires the user to manually specify the number of independent components, the Marčenko–Pastur distribution threshold is crucial to providing an objective, data-driven metric for the number of components.

After computing **E**′s covariance matrix, 12 eigenvalues were found to surpass the Marčenko–Pastur upper bound. ICA was then run to extract these 12 distinct and temporally independent components (**Figure 4A**). As fastICA can only extract the magnitude of an independent component, not its sign, the spatial map's positive and negative signs should be understood to represent relative orientations rather than absolute weights.

Entropy analysis

Independent component analysis was selected as a clustering algorithm because, by definition, it minimizes the statistical dependencies between components. This should completely—or at least almost completely—prevent the temporal dependencies between components. If this is the case, then the joint entropy over all components is simply the sum of the individual components' Shannon entropies (Cover and Thomas, 2005):

$$H(C_1, \ldots, C_N) = \sum_{j=1}^{N} H(C_j)$$

It is possible to compute the joint entropy of each subject by computing the Shannon entropy of each component's activation time series and summing them. This allows the construction of a distribution of subject joint entropies, which can then be analyzed for group-level differences.

Group comparisons

We search for group-level differences using a difference-of-means permutation test (Krol, 2021) with 10,000 permutations, and provide multiple-comparison correction *via* the false discovery rate (Benjamini and Hochberg, 1995). The Bonferroni (1935) and Sidak (1967) thresholds verify these results.

Effective connectivity

Brain network model

The brain network consists of the 90 cortical and subcortical nodes (regions) of the AAL parcellation, coupled according to the standard 90-region AAL connectivity template **C**. Internal node dynamics are modeled as the normal form of a supercritical Hopf oscillator (Deco et al., 2017b). This produces

$$\frac{dx_j}{dt} = x_j\left(\alpha_j - x_j^2 - y_j^2\right) - \omega_j y_j + G\sum_i C_{ij}\left(x_i - x_j\right) + \beta\eta_j(t)$$

$$\frac{dy_j}{dt} = y_j\left(\alpha_j - x_j^2 - y_j^2\right) - \omega_j x_j + G\sum_i C_{ij}\left(y_i - y_j\right) + \beta\eta_j(t)$$

where C_{ij} is the connection strength from j to i and G represents global coupling efficiency. ω_j is estimated directly from the BOLD time series by extracting the dominant frequency of node j within the band of 0.01 to 0.08 Hz. α and G are set to the initial values of $\alpha = 0$ and $G = 0.2$, in line with previous work (Deco and Kringelbach, 2016; Deco et al., 2017b).

Particle swarm optimization

The connection strengths $\mathbf{C}_{ij}$ are optimized using the population swarm algorithm (Kennedy and Eberhart, 1995; Erik et al., 2010; Mezura-Montes et al., 2011). This algorithm simulates a population of individual particles moving in random directions within an N-dimensional space, where N is the number of free parameters. At each optimization step, each particle can continue exploring the space, move to its optimal prior position, or move to the global optimal prior position. The model is then tested using the new positions of each particle as parameters, and the individual and global optima are updated as necessary.

Cost function

The particle swarm algorithm seeks to minimize the difference between simulated and empirical data distributions. We quantify this difference as the Euclidean distance between entropy distributions:

$$d(S, E)\sqrt{\sum_{j=1}^{N}\left(S(j) - E(j)\right)^2}$$

After simulating a BOLD signal, this simulated signal is separated into components using the mixing matrix W, and the Shannon entropy of each component is computed. The Euclidean distance between the simulated entropy distribution and its empirical counterpart is used as the optimization cost function, which guides the particle swarm algorithm's estimates for optimal model parameters. Pre-fit and post-fit cost function distributions are shown in **Figure 2**.

Network analysis

Our study's goal is to find network-level connectivity changes in obsessive compulsive disorder patients. To this end, we apply two group-level analyses to the connectivity estimates obtained in the previous section.

Network-based statistic

The network-based statistic (NBS) is a component detection approach (Zalesky et al., 2010) with substantially greater power than traditional family-wise error (FWE) correction. Unlike traditional FWE correction, the NBS tests the significance of an effect's size rather than its magnitude. This drastically reduces the multiple-comparison correction and allows the estimation of an empirical null distribution *via* a permutation test.

Upon estimating the effective connectivity of each subject, we run a group-level comparison with the NBS to search for significant connectivity changes in obsessive compulsive disorder. As control parameters, we used a significance threshold of $t = 4.5$ and a standard case-comparison contrast. Additional significance thresholds of $t = 4$, 5, and 5.5 were

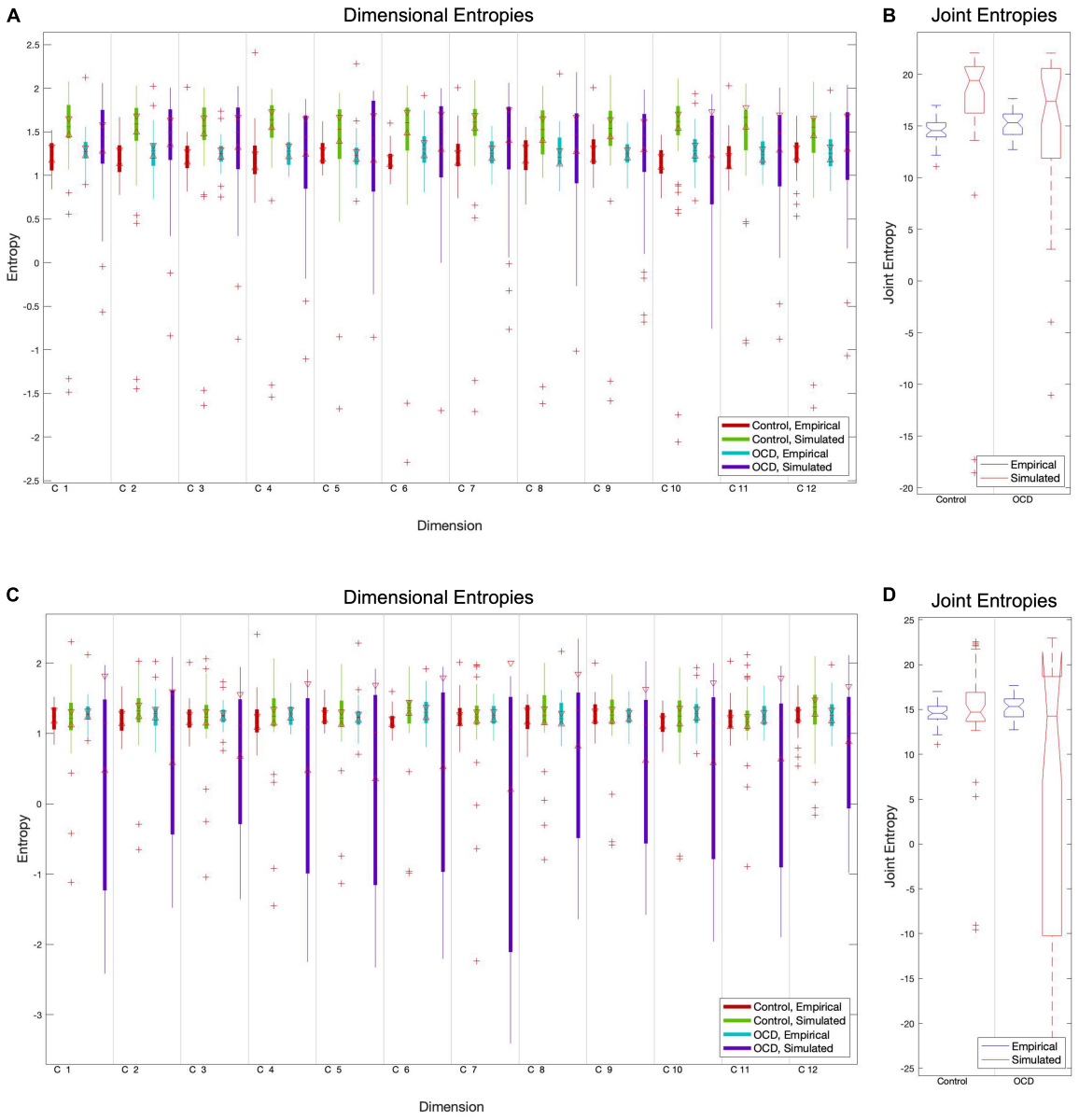

FIGURE 2
The particle swarm fitting algorithm, like most optimization algorithms, minimizes a cost function to determine how well the model predicts real data. We chose the Euclidean distance between empirical and simulated entropy vectors as a cost function due to its conceptual simplicity and confirmed its superiority versus absolute maximum distance. Comparisons of component-level entropy distributions pre-fit **(A)** and post-fit **(C)** demonstrate that this method does improve the model for controls. Comparisons of pre-fit **(B)** and post-fit **(D)** joint entropy confirm this. While optimization brings the mean entropies of patient models closer to those of empirical subjects, its performance is quite inconsistent in this group. This is reflected in the extremely high variance in post-optimization dimensional and joint entropies **(C,D)**.

also tested, the results of which results may be viewed in the **Supplementary Figures**.

Degree strength analysis

In addition to the NBS, we run a group-level comparison of the node strengths. Specifically, we test for differences in strength between groups for each node in the effective connectivity network. The directed nature of effective connectivity required that both in- and out-strength be examined.

Comparison analyses

To compare LEICA's efficacy to more familiar methods, we repeated the above analyses with two other versions of the dynamic functional connectivity array. The first such

comparison simply consists of the vectorized upper triangle of each **dFC** (t), concatenated to form a space-time array $\left(\frac{N(N-1)}{2} \times T\right)$. The second comparison consists of the spatial average of each **dFC** (t), likewise concatenated to form a space-time array ($N \times T$). Pre- and post-eigendecomposition steps are identical for all inputs.

Results

Functional analysis

Dynamic functional connectivity

Both control and patient time series are parcellated according to the AAL atlas (Tzourio-Mazoyer et al., 2002). Each subject's dynamic functional connectivity is computed using Coherence Connectivity Dynamics (Deco et al., 2017a). Analysis is restricted to the cortical and subcortical regions; as such, the 26 cerebellar regions of the AAL atlas are discarded. The resultant three-dimensional array must be converted into two dimensions for further analysis. Three methods are tested. In the first method, we extract the leading eigenvector (90×1) of each time point's connectivity matrix. The eigenvectors of all time point are then concatenated to form a subject-level 90×175 eigenvector time series **E**. In the second method, each time point's connectivity matrix is averaged horizontally, and the resulting average coherence vectors (90×1) are concatenated to form a subject-level 90×175 mean coherence time series **M**. Finally, each time point's connectivity matrix is vectorized to form a 4005×1 connectivity vector, and these vectors are again concatenated to form a subject-level 4005×175 **dFC** time series (as each connectivity matrix is symmetric and the main diagonal neglected, only the upper triangle is vectorized).

Functional dimensions

To determine the number of dimensions necessary, all subjects' time series are concatenated and the autocorrelation matrix of this global time series array calculated. The number of significant dimensions is then the number of eigenvalues in the autocorrelation matrix which exceed the upper bound of the Marčenko–Pastur distribution (Marčenko and Pastur, 1967). Applying this method to the eigenvector time series **E** identifies 12 independent dimensions across the resting state of all subjects (**Figure 4A**). ICA can then convert the 90-dimensional eigenvector time series **E** into its 12-dimensional representation $\mathbf{T}_E$ (Lopes-dos-Santos et al., 2011, 2013) (**Figure 4B**). Repeating this process for the vectorized **dFC** produces the 347-dimensional representation $\mathbf{T}_F$, and the spatially averaged **M** produces the 11-dimensional representation $\mathbf{T}_M$.

Joint entropy

Since each time series in the low-dimensional space is statistically independent, each dimension's Shannon entropy may be calculated (Singh et al., 2003; Delattre and Fournier, 2017) independent of the others'. Computing the subject-level Shannon entropy of each substate's time series results in a $D \times S$ array of entropy values for patients and controls, where S is the number of dimensions and S the number of subjects per group. This format means that computing the subject-level joint entropy simply requires summing along

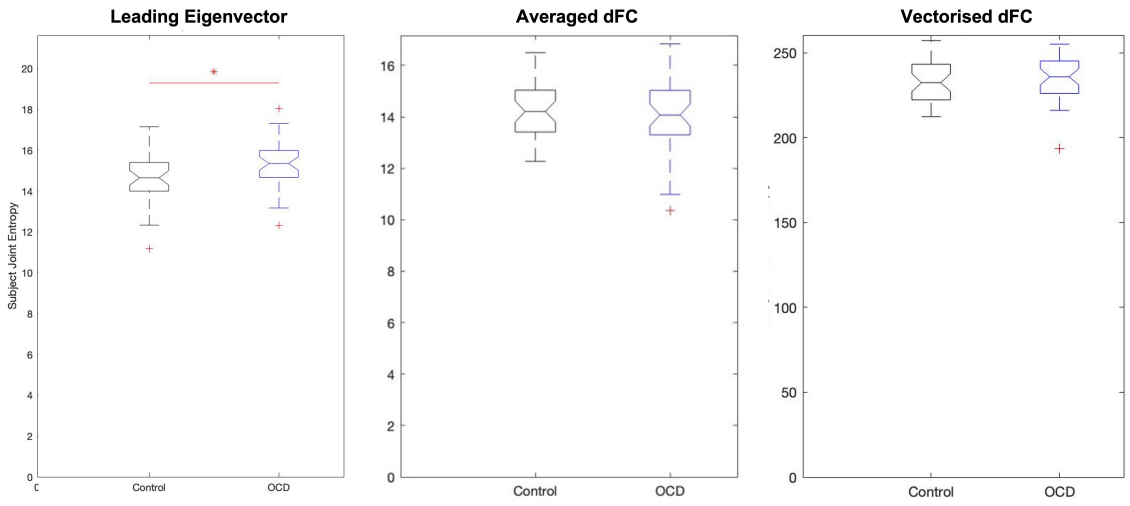

FIGURE 3
Analysis of eigenvector-based component time series (T_E) shows that obsessive-compulsive patients display substantially higher joint entropy than age-, gender-, and education-matched controls. On average, controls display a joint entropy of 14.5695±1.2473, while patients display a mean joint entropy of 15.2214±1.1535. Neither spatial average-based components nor vectorized dFC-based components display group-level changes.

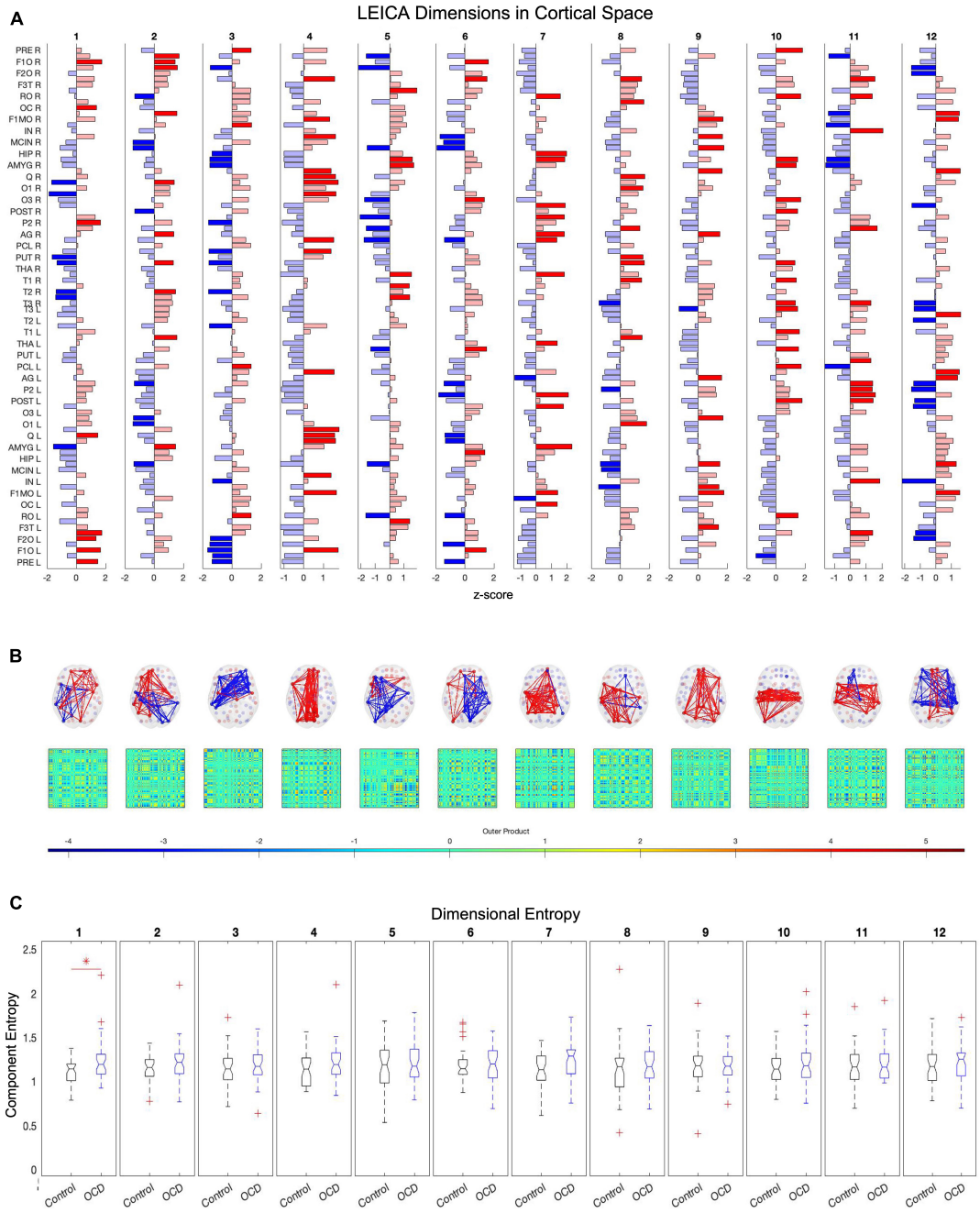

FIGURE 4
Twelve of the eigenvalues of E's autocorrelation matrix exceed the upper limit of the Marčenko-Pastur distribution, suggesting that 12 dimensions are necessary to capture E's activity. Independent component analysis reveals how these dimensions map to brain regions **(A)**. Map weights have been converted into z-scores for this figure and regions with a weight $z < 1.3$ are depicted in faded color. Plotting these mapping vectors in the brain and as connectivity **(B)** reveals that the trailing dimensions (9, 10, 11, and 12) display notable homotopic symmetry, while leading dimensions are strongly asymmetric. Finally, group-level entropy analysis shows that the first dimension displays significantly higher entropy in obsessive-compulsive patients than in controls **(C)**. Note that dimensions are ordered according to average activity level across the dataset.

this array's first dimension. This produces two $1 \times S$ joint entropy distributions, which can be compared with any standard statistical test. Applying this process to eigenvector-based entropy scores again shows elevated entropy in patients relative to controls (p = 0.0119, Hodges' G = −0.5833) (Figure 3). However, the joint entropy distributions of $\mathbf{T}_F$ and of $\mathbf{T}_M$ display no significant group-level differences. Eigenvector-based analysis thus appears to preserve the information of the full

signal while reducing dimensionality almost 30-fold—a crucial consideration, as the curse of dimensionality states that patterns become exponentially harder to detect as dimensionality increases.

Dimension-specific entropy

To determine whether alterations in entropy concentrate in specific dimensions, we started with the same $D \times S$ patient and control arrays of entropy values as the previous section. Each row of these arrays was compared and corrected with the false discovery rate. As above, this analysis was run for all three compression methods: $\mathbf{T}_E$ (eigenvectors), $\mathbf{T}_F$ (uuncompressed), and $\mathbf{T}_M$ (spatial average). Only the eigenvector-based representation ($\mathbf{T}_E$) detects a significant alteration along any dimension, specifically the first (ordered according to mean activity). This dimension consists of paired anticorrelated communities and both display significantly higher entropy in patients than in age-, gender-, and education-matched controls (Figure 4C).

In component space, we find that one LEICA component displays higher entropy in patients than in controls (1.1818 ± 0.1401, 1.3075 ± 0.2276, $p = 0.0020$, Hedges' $g - 0.6634$). This substate consists of two opposing communities, with the sign of each brain region denoting to which community that region belongs and the magnitude of that region's weight denoting the strength of its association with that community (see Table 2 for a list of implicated regions). We opted to concentrate on regions with absolute z-scores above 1.3 ($|\mathbf{z}| > 1.3$) (Figure 4A). Under these constraints, the first community contains the left precentral gyrus, left and right frontal superior cortex (orbital), left middle frontal gyrus (orbital), the left inferior frontal gyrus (opercular), left cuneus, right olfactory bulb, and right inferior parietal gyrus. Its opposite number includes the right lingual gyrus, right occipital medial gyrus, right putamen, right pallidum, left amygdala, right middle temporal gyrus, and right temporal pole of the middle temporal gyrus (Figure 4). This result survives both the false discovery rate and the Sidak multiple comparison correction.

TABLE 2 Table displays the regions of the first dimension with absolute z-scores exceeding 1.3 ($|z| > 1.3$).

Component 1 ($z > 1.3$)

Positive	Negative
L Precentral Gyrus	L Amygdala
L Superior Frontal Gyrus, Orbital Part	R Temporal Pole: Middle Temporal Gyrus
L Middle Frontal Gyrus, Orbital Part	R Middle Temporal Gyrus
L Inferior Frontal Gyrus, Opercular Part	R Lenticular Nucleus, Pallidum
L Cuneus	R Lenticular Nucleus, Putamen
R Inferior Parietal Gyri	R Middle Occipital Gyrus
R Olfactory Cortex	R Lingual Gyrus
R Superior Frontal Gyrus, Orbital Part	

The sign of each regional weight indicates to which of two communities it belongs, with the magnitude of its weight indicating its centrality to that community. Regions with absolute z-scores exceeding 1.3 ($|z| > 1.3$) can be considered core nodes in a more distributed network which covers the entirety of the brain space.

Connectivity model

Network-based statistic

In order to hypothesize on causes for these shifts in dynamical richness, we fit a networked Hopf model (Deco et al., 2017b) to each subject's entropy profile. After obtaining subject-level effective connectivity profiles from these models, we applied the network-based statistic (NBS) (Zalesky et al., 2010) to determine which, if any, connections display significant group-level alterations. In addition, we examined the in-strength and out-strength of each node for significant alterations between groups. Only the eigenvector-based decomposition produced a generative model which displays significant group-level alterations in network connectivity; the spatially averaged and uncompressed decompositions failed to find meaningful results.

Results from the network-based statistic depend upon the t-statistic chosen at the thresholding step. Unfortunately, no data-driven method for determining an optimal threshold has yet been developed, nor has such a threshold been established experimentally. As such, it must be treated as a free parameter. A threshold of 4.5 reveals a single large hyperconnected component and 11 small hypoconnected components in the patient population (Figure 5). These hypoconnected components consist of

1. Left superior frontal gyrus (orbital), left superior frontal gyrus (medial orbital), and left lenticular nucleus (putamen)
2. Left middle frontal gyrus and left caudate nucleus
3. Left Rolandic operculum, left insula, left supramarginal gyrus, left superior temporal gyrus, left middle temporal gyrus, and left temporal pole (middle temporal gyrus)
4. Left middle occipital gyrus, left superior frontal gyrus (medial), left middle occipital gyrus, left inferior occipital gyrus, left and right precuneus, left superior parietal gyrus, and right superior occipital gyrus
5. Left calcarine fissure, left fusiform gyrus, left cuneus, left and right posterior cingulate gyrus, and left superior occipital gyrus
6. Right temporal pole (superior temporal gyrus), right inferior temporal gyrus, and right middle frontal gyrus (orbital)
7. Right middle temporal gyrus and right inferior frontal gyrus (orbital)
8. Right supplementary motor area and right paracentral lobule
9. Right amygdala and right fusiform gyrus

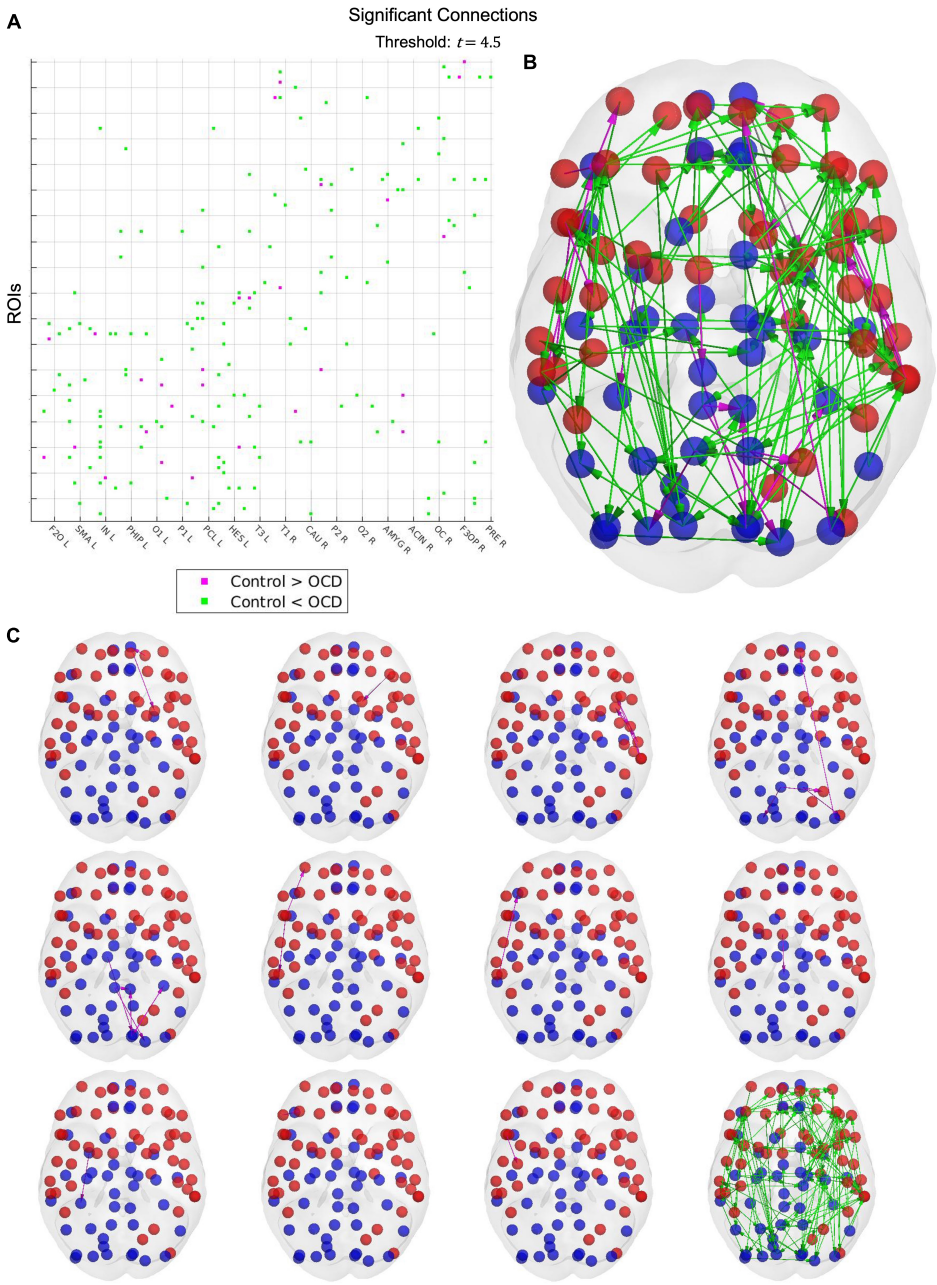

FIGURE 5
Results from the network-based statistic. A t-statistic threshold of 4.5 returns 12 connected components **(C)**, visualized together as a connectivity matrix **(A)** and in cortical space **(B)**. Cyan links indicate that the connection is stronger in OCD patients than in healthy controls, while magenta links indicate the converse. Although only one connected component displays increased strength in patients, this component includes 87 of the 90 cortical nodes in the AAL parcellation, suggesting that obsessive-compulsive disorder may be characterized by widespread cortical hyperconnectivity. The 11 control-biased components, by contrast, consist of between one to six links, with larger components tending to concentrate in small topographical areas. Notably, many regions displaying depressed connectivity in patients are known to be involved in top-down control and impulse inhibition. OCD may thus be characterized by localized disruptions in top-down inhibitory activity, which may explain the widespread hyperconnectivity observed in patients.

10. Right inferior frontal gyrus (triangular) and right middle frontal gyrus
11. Right inferior frontal gyrus (opercular) and right precentral gyrus

However, it should be emphasized that other settings of the t-statistic threshold will produce slightly different results. For example, raising the threshold to $t = 5$ causes the hyperconnected network to fragment into a single

large component and two small ones (see **Supplementary material**). Similarly, one could expect that hypoconnected components would consolidate into fewer, larger networks at lower thresholds.

Discussion

Summary

The replacement of *k*-means clustering with ICA and *post hoc* goodness-of-fit metrics with data-driven estimates of dimensionality allowed us to directly quantify and compare whole-brain functional complexity between groups. Independent component analysis has, of course, been used in neuroimaging research for several decades. Thus, one must ask whether LEICA provides an advantage over independent component analysis on the unmodified dynamic functional connectivity array. Of the three low-dimensional spaces evaluated in this study, only the eigenvector-based space captured any differences between patient and control groups. In addition to finding group-level joint entropy alterations, this eigenvector-based space could isolate the dimensions responsible for this increase. Training a model in this space allowed us to capture several connectivity alterations which are well-supported in the neurophysiological literature. This substantial improvement in sensitivity suggests that LEICA will prove a useful tool for future research into functional complexity and dimensionality.

Phenomenological considerations

Perhaps the greatest advantage of ICA compared to alternative clustering methods, such as *k*-means, is the ability to use metrics which depend on statistical independence. It is probable that this improved resolution will lend itself to other information-theoretic metrics such as functional complexity (Zamora-López et al., 2016) or Granger causality. Such direct comparisons of activity complexity may lead to a deeper understanding of the pathophysiological bases of psychiatric disorders and other neurobehavioral phenomena.

At the phenomenological level, analysis of both leading eigenvectors and unmodified dFC showed higher average entropy in patients than controls. This is in contrast to previous reports of decreased entropy in obsessive-compulsive patients (Aydin et al., 2015), although reports of adolescents with OCD have found increased entropy in networks of cortical and subcortical nodes in the cortico-striatal-thalamo-cortical (CSTC) circuit (Sen et al., 2020). How this apparent increase in complexity—which, in information-theoretic terms, is equivalent to randomness—maps to the well-established tendency of obsessive-compulsive patients to become "stuck" in stereotyped, repetitive patterns will be an interesting topic for future research. It may be that these stereotyped patterns represent a coping mechanism, intended to reduce the randomness of brain activity by imposing control of inputs and responses.

Such a hypothesis receives some support in the fact that the dimension found to increase patient entropy maps to two anticorrelated networks which roughly separate prefrontal-parietal regions vs. subcortical-temporal nodes. Prefrontal and parietal regions exert a top-down inhibitory control on striatal and limbic regions, which has been related to emotion regulation and cognitive control capacities (Ochsner et al., 2012; Etkin et al., 2015). Alterations in such interregional interactions have been associated with mood and anxiety disorders, including OCD (Etkin and Wager, 2007; Picó-Pérez et al., 2017). Decreased order within this network may disrupt top-down inhibition and thus affect emotion regulation and cognitive control, both of which are affected in the context of CSTC dysfunction in OCD (van den Heuvel et al., 2016). Stereotyped, repetitive behaviors—i.e. compulsions—may thus act as a compensatory mechanism by which the brain attempts to impose order on its surroundings.

Interestingly, the affected dimension also contains several occipital nodes. Although the occipital cortex has not typically been considered a core part of neurobiological models of OCD, previous research has shown that such regions and their projections to limbic cortices may play an important role in the induction of increased anxiety levels in patients with contamination obsessions induced by actual or mental images (i.e., intrusive thoughts) of dirt (Göttlich et al., 2014; Moreira et al., 2017). In future research, it may be worth examining whether the patient's entropic alterations along this dimension correlates with anxiety or compulsive behavior, which could be as measured by e.g. the Hamilton Anxiety Rating Scale (HAM-A) (Hamilton, 1959) or the Yale-Brown Obsessive-Compulsive Scale (Y-BOCS) (Goodman et al., 1989).

Mechanistic considerations

Regarding the mechanistic analyses, we observe that the generative model recovers a broad network of hyperconnected regions in the patient population. This network includes most nodes in the 90-region AAL atlas and is evident up to a to t-statistic threshold of 4.5. OCD may then be characterized by hyperconnectivity across much of the cortex and subcortical regions. Such a hypothesis would contrast OCD with disorders such as schizophrenia or autism, which appear to be characterized by long-range hypoconnectivity (Friston et al., 2016; Hull et al., 2017); however, previous studies have shown cortical hyperexcitability in patient populations (Cano et al., 2018; Rolls et al., 2020). It is possible that, in keeping with phenomenological results, the

hypoconnected components represent regulatory regions whose underperformance encourages hyperactivity. The pallidum, for instance, as part of the CSTC circuitry, is the major inhibitory output from the striatum to the thalamus and the subthalamus, and an increased inhibitory output the from the external globus pallidum to the subthalamus may result in the thalamic and cortical hyperexcitability that has been shown to characterize patients with OCD (Cano et al., 2018). Alterations in the Rolandic operculum, on the other hand, have been related to the impulsive nature of the so-called autogenous obsessions and compulsions in a subgroup of patients with OCD (Subirà et al., 2013), as well as with the premonitory urges associated with tic behaviors and sensory phenomena (Wang et al., 2011) that are observed in a large proportion of patients with OCD (Rosario et al., 2009).

Limitations and future steps

Three cautionary notes must be added. First, the LEICA method is, by necessity, agnostic as to the true orientation of its communities. Since eigendecomposition and ICA can determine only the orientation of communities relative to each other, not relative to the data itself, LEICA cannot determine which community is "positive" or "negative" in any absolute sense. This may be established by a parallel analysis observing which community is more or less active at any given time; such an analysis is unnecessary for the present purposes.

Second, the Hopf network model should not be considered predictive at the level of individual links. It has been able to replicate known phenomena and mechanisms in past studies (Jobst et al., 2017) and brain-level results, e.g., the widespread cortical hyperconnectivity in obsessive-compulsive patients, appear robust. However, the Hopf oscillator remains an idealized simplification of neural dynamics. To predict neurobiological mechanisms would require both more detailed data and a more sophisticated model, e.g., a model incorporating transmission delays and neuromodulation. Link-level model results in this paper should thus be considered starting points for future research rather than forming hard conclusions themselves.

Finally, while the network-based statistic (NBS) is a well-established method, its results remain dependent on the choice of t-statistic threshold employed. This does not affect the power of the results, only the effect size of the results reported. Unfortunately, no data-driven method has yet been established for determining an appropriate threshold. However, studying which connections survive the different thresholds allows us to partially quantify the group-level effect size.

In addition to these general concerns, the present model fits the control group considerably better than the patient group. It is not immediately clear to the authors why this is the case, as both groups undergo identical procedures. That the model returns meaningful results despite this poor performance suggests that improving the fitting procedure's performance may yield entirely novel insights. The question of model optimization will be of major interest in future studies.

The widespread alterations in cortical connectivity likely affect activity propagation and organization. While such alterations were outside the scope of this study, they are of great interest to the understanding of OCD's functionality. Leveraging established network analyses frameworks, such as community detection or node centrality measures, may provide further insights into the cortical activity adaptations of OCD, and potentially in related disorders such as anxiety and depression.

Conclusion

The search for a natural low-dimensional space for the analysis of functional connectivity dynamics remains an active area of research. We present a novel method based on established theory to map functional activity to such a space. The resulting space ensures interdimensional statistical independence, which allows the quantification and direct comparison of information content (randomness) between groups and subjects. Comparisons with classic independent component analysis shows that LEICA preserves functional complexity while increasing sensitivity and power. This increased power allows LEICA to recover evidence supporting several extant hypotheses on the causes of obsessive-compulsive disorder, most notably the importance of top-down control as exerted by prefrontal and parietal regions on the limbic system. Training a generative model in this space similarly recovers known functional characteristics of OCD, e.g., broad cortical hyperconnectivity, and highlights specific connections as targets for future studies. Given these results and its novel ability to directly compare information content, we anticipate that the LEICA framework and its extensions will become a crucial tool in the ongoing efforts to quantify and explain the connectivity substates of the brain in both human and nonhuman studies.

Data availability statement

The raw data supporting the conclusions of this article will be made available by the authors, without undue reservation. The code used in this study is available online at https://github.com/decolab/LEICA, https://github.com/decolab/Functions and https://github.com/decolab/Effective-Connectivity--Hopf.

Ethics statement

The studies involving human participants were reviewed and approved by Ethics Committee of the Hospital de Braga,

Portugal. The patients/participants provided their written informed consent to participate in this study.

Author contributions

DB developed and executed the analysis, wrote the manuscript, and generated all figures in this report. CS-M provided neurobiological and physiological analysis for this report. JC provided the code and explanation for the LEiDA algorithm, which the primary author developed into the methods described in this article. PMore and PMorg collected the data analyzed in this report, as detailed in the methods section. GD, proposed this study to the primary author and supervised the course of this research. All authors contributed to the article and approved the submitted version.

Funding

This work was funded by ICVS Scientific Microscopy Platform, member of the National infrastructure PPBI–Portuguese Platform of Bioimaging (PPBI-POCI-01-0145-FEDER-022122); by National funds, through the Foundation for Science and Technology (FCT)–project UIDB/50026/2020 and UIDP/50026/2020; and by the project NORTE-01-0145-FEDER-000039, supported by Norte Portugal Regional Operational Programme (NORTE 2020), under the PORTUGAL 2020 Partnership Agreement, through the European Regional Development Fund (ERDF).

Acknowledgments

We wish to thank Ane Lopez-Gonzalez for her advice and reviews of this manuscript.

Conflict of interest

PMore has received in the past 3 years grants, CME-related honoraria, or consulting fees from Angelini, AstraZeneca, Bial, Biogen, DGS-Portugal, FCT, FLAD, Janssen-Cilag, Gulbenkian Foundation, Lundbeck, Springer Healthcare, Tecnimede, Viatris, and 2CA-Braga. During data collection, PMorg was supported by the FCT fellowship grant with the number PDE/BDE/113601/2015 from the PhD-iHES program. PMore was funded by the Fundaccão Calouste Gulbenkian [Contract Grant Number: P-139977; project "Better mental health during ageing based on temporal prediction of individual brain ageing trajectories (TEMPO)"].

The remaining authors declare that the research was conducted in the absence of any commercial or financial relationships that could be construed as a potential conflict of interest.

Publisher's note

Supplementary material

The Supplementary Material for this article can be found online at: https://www.frontiersin.org/articles/10.3389/fnhum.2022.958706/full#supplementary-material

SUPPLEMENTARY FIGURE 1
To compute time-resolved functional connectivity (dynamic functional connectivity, or dFC), each bandpass-filtered regional time series is converted into an analytic signal using the Hilbert transform. Euler's formula converts this analytic signal into a time-resolved phase signal **(A)**. For each time point, the phase signals of all regions are sampled **(B)** and the cosine distance between each pair of regions is computed to produce an instantaneous functional connectivity matrix **(C)**. The leading eigenvector $\mathbf{V}_1$ of this functional connectivity matrix is then isolated **(D)**. Repeating this process for all time points and subjects across the dataset results in a 2-D array **E** of leading eigenvectors **(E)**. Running an eigendecomposition on **E**'s autocorrelation matrix and counting the number of eigenvalues greater than the upper bound of the Marčenko-Pastur distribution reveals the number of dimensions necessary to describe the nonrandom activity in **E**. This figure displays all regions with a z-score higher than z = 1 in full color.

SUPPLEMENTARY FIGURE 2
Results from the network-based statistic. A t-statistic threshold of 4.0 returns six connected components **(C)**, visualized together as a connectivity matrix **(A)** and in cortical space **(B)**. Cyan links indicate that the connection is stronger in OCD patients than in healthy controls, while magenta links indicate the converse. Although only one connected component displays increased strength in patients, this component includes all 90 of the cortical nodes in the AAL parcellation, suggesting that obsessive-compulsive disorder may be characterized by widespread cortical hyperconnectivity. Control-biased components, by contrast, consist of between three to nine links, with larger components tending to concentrate in small topographical areas. Notably, many regions displaying depressed connectivity in patients are known to be involved in top-down control and impulse inhibition. OCD may thus be characterized by localized disruptions in top-down inhibitory activity, which may explain the widespread hyperconnectivity observed in patients.

SUPPLEMENTARY FIGURE 3
Results from the network-based statistic. A t-statistic threshold of 5.0 returns 11 connected components **(C)**, visualized together as a connectivity matrix **(A)** and in cortical space **(B)**. Cyan links indicate that the connection is stronger in OCD patients than in healthy controls, while magenta links indicate the converse. At this threshold, the connected component displaying increased strength in patients breaks into three sections, with the largest containing 78 of the 90 nodes in the

AAL parcellation. This is considerably larger than the other two control-biased components, which have one and two links respectively. The eight surviving control-biased components consist of up to three links.

SUPPLEMENTARY FIGURE 4
Results from the network-based statistic. A t-statistic threshold of 5.5 returns 16 connected components **(C)**, visualized together as a connectivity matrix **(A)** and in cortical space **(B)**. Cyan links indicate that the connection is stronger in OCD patients than in healthy controls, while magenta links indicate the converse. At this threshold, the connected component displaying increased strength in patients breaks into 10 sections, with the largest containing 33 of the 90 regions of the AAL. The six control-biased components consist of up to two links. The fall in number of control-based components with increasing t-threshold further indicates that OCD is characterized by excessive connectivity across the cortex.

SUPPLEMENTARY FIGURE 5
Results from the network-based statistic. A t-statistic threshold of 6.0 returns 17 connected components **(C)**, visualized together as a connectivity matrix **(A)** and in cortical space **(B)**. Cyan links indicate that the connection is stronger in OCD patients than in healthy controls, while magenta links indicate the converse. At this threshold, the connected component displaying increased strength in patients breaks into 14 sections. Most of these consist of only one or two links. The two largest consist of a 14-region and nine-region chain, respectively. Only three control-biased components survive, neither of which exceeds a single link in size. It thus appears that OCD is characterized by excessive connectivity in patients.

References

Achard, S., Salvador, R., Whitcher, B., Suckling, J., and Bullmore, E. T. (2006). A resilient, low-frequency, small-world human brain functional network with highly connected association cortical hubs. *J. Neurosci.* 26, 63–72. doi: 10.1523/JNEUROSCI.3874-05.2006

Adhikari, M. H., Hacker, C. D., Siegel, J. S., Griffa, A., Hagmann, P., Deco, G., et al. (2017). Decreased integration and information capacity in stroke measured by whole brain models of resting state activity. *Brain* 140, 1068–1085. doi: 10.1093/brain/awx021

Atasoy, S., Deco, G., Kringelbach, M. L., and Pearson, J. (2018). Harmonic brain modes: A unifying framework for linking space and time in brain dynamics. *Neuroscientist* 24, 277–293. doi: 10.1177/1073858417728032

Aydin, S., Arica, N., Ergul, E., and Tan, O. (2015). Classification of obsessive compulsive disorder by EEG complexity and hemispheric dependency measurements. *Int. J. Neural Syst.* 25:1550010. doi: 10.1142/S0129065715500100

Benjamini, Y., and Hochberg, Y. (1995). Controlling the false discovery rate : a practical and powerful approach to multiple testing. *J. R. Statist. Soc. Seri. B (Methodological)* 57, 289–300.

Biswal, B. B. (2012). Resting state FMRI: A personal history. *NeuroImage* 62, 938–944. doi: 10.1016/j.neuroimage.2012.01.090

Biswal, B. B., DeYoe, E. A., and Hyde, J. S. (1996). Reduction of physiological fluctuations in FMRI using digital filters. *Magn. Res. Med.* 35, 107–113. doi: 10.1002/mrm.1910350114

Biswal, B. B., Hudetz, A. G., Yetkin, F. Z., Haughton, V. M., and Hyde, J. S. (1997a). Hypercapnia reversibly suppresses low-frequency fluctuations in the human motor cortex during rest using echo-planar MRI. *J. Cerebral Blood Flow Metab.* 17, 301–308. doi: 10.1097/00004647-199703000-00007

Biswal, B. B., Van Kylen, J., and Hyde, J. S. (1997b). Simultaneous assessment of flow and BOLD signals in resting-state functional connectivity maps. *NMR Biomed.* 10, 165–170. doi: 10.1002/(SICI)1099-1492(199706/08)10:4/5<165::AID-NBM454<3.0.CO;2-7

Biswal, B. B., Ulmer, J. L., Krippendorf, R. L., Harsch, H. H., Daniels, D. L., Hyde, J. S., et al. (1998). Abnormal cerebral activation associated with a motor task in tourette syndrome. *Am. J. Neuroradiol.* 19, 1509–1512.

Biswal, B. B., Yetkin, F. Z., Haughton, V. M., Hyde, J. S., Yetkin, F. Z., Haughton, V. M., et al. (1995). Functional connectivity in the motor cortex of resting human brain using echo-planar mri. *Magn. Res. Med.* 34, 537–541. doi: 10.1002/mrm.1910340409

Bonferroni, C. E. (1936). Teoria statistica delle classi e calcolo delle probabilita. *Pubbl. R Istit. Superiore Sci. Econ. Commer. DiFirenze* 8, 3–62.

Buckner, R. L., Sepulcre, J., Talukdar, T., Krienen, F. M., Liu, H., Hedden, T., et al. (2009). Cortical hubs revealed by intrinsic functional connectivity: mapping, assessment of stability, and relation to Alzheimer's disease. *J. Neurosci.* 29, 1860–1873. doi: 10.1523/JNEUROSCI.5062-08.2009

Bullmore, E. T., and Sporns, O. (2009). Complex brain networks: graph theoretical analysis of structural and functional systems. *Nat. Rev. Neurosci.* 10, 186–198. doi: 10.1038/nrn2575

Burns, R., Roncal, W. G., Kleissas, D., Lillaney, K., Manavalan, P., Perlman, E., et al. (2013). "The open connectome project data cluster: scalable analysis and vision for high-throughput neuroscience," in *Proceedings of the 25th international conference on scientific and statistical database management (SSDBM)*, Vol. 27, (New York, NY: Association for Computing Machinery), 1–11. doi: 10.1145/2484838.2484870

Cabral, J. R. B., Vidaurre, D., Marques, P., Magalhães, R., Moreira, P. S., Soares, J. M., et al. (2017). Cognitive performance in healthy older adults relates to spontaneous switching between states of functional connectivity during rest. *Sci. Rep.* 7:5135. doi: 10.1038/s41598-017-05425-7

Calhoun, V. D., Potluru, V. K., Phlypo, R., Silva, R. F., Pearlmutter, B. A., Caprihan, A., et al. (2013). Independent component analysis for brain FMRI does indeed select for maximal independence. *PLoS One* 8:e73309. doi: 10.1371/journal.pone.0073309

Cano, M., Alonso, P., Martínez-Zalacaín, I., Subirà, M., Real, E., Segalàs, C., et al. (2018). Altered functional connectivity of the subthalamus and the bed nucleus of the stria terminalis in obsessive-compulsive disorder. *Psychol. Med.* 48, 919–928. doi: 10.1017/S0033291717002288

Cover, T. M., and Thomas, J. A. (2006). *Elements of information theory*, 2nd Edn. Hoboken, NJ: John Wiley & Sons, Ltd. doi: 10.1002/047174882X

Deco, G., Cabral, J. R. B., Woolrich, M. W., Stevner, A. B. A., van Hartevelt, T. J., and Kringelbach, M. L. (2017a). Single or multiple frequency generators in on-going brain activity: A mechanistic whole-brain model of empirical MEG data. *NeuroImage* 152, 538–550. doi: 10.1016/j.neuroimage.2017.03.023

Deco, G., Kringelbach, M. L., Jirsa, V. K., and Ritter, P. (2017b). The dynamics of resting fluctuations in the brain: Metastability and its dynamical cortical core. *Sci. Rep.* 7:3095. doi: 10.1038/s41598-017-03073-5

Deco, G., Cruzat, J., and Kringelbach, M. L. (2019). Brain songs framework used for discovering the relevant timescale of the human brain. *Nat. Commun.* 10, 1–13. doi: 10.1038/s41467-018-08186-7

Deco, G., Jirsa, V. K., Robinson, P. A., Breakspear, M., and Friston, K. J. (2008). The dynamic brain: from spiking neurons to neural masses and cortical fields. *PLoS Comput. Biol.* 4:1–35. doi: 10.1371/journal.pcbi.1000092

Deco, G., and Kringelbach, M. L. (2016). Metastability and coherence: Extending the communication through coherence hypothesis using a whole-brain computational perspective. *Trends Neurosci.* 39, 125–135. doi: 10.1016/j.tins.2016.01.001

Delattre, S., and Fournier, N. (2017). On the kozachenko–leonenko entropy estimator. *J. Statist. Plan. Infer.* 185, 69–93. doi: 10.1016/j.jspi.2017.01.004

DuPont, R. L., Rice, D. P., Shiraki, S., and Rowland, C. R. (1995). Economic costs of obsessive-compulsive disorder. *Med. Int.* 8, 102–109.

DuVal, G. (2004). Ethics in psychiatric research: Study design issues. *Can. J. Psychiatry* 49, 55–59. doi: 10.1177/070674370404900109

Erik, M., Pedersen, H., and Pedersen, M. E. H. (2010). Good parameters for particle swarm optimization. *Techn. Rep.* 2010, 1–12.

Etkin, A., Büchel, C., and Gross, J. J. (2015). The neural bases of emotion regulation. *Nat. Rev. Neurosci.* 16, 693–700. doi: 10.1038/nrn4044

Etkin, A., and Wager, T. D. (2007). Functional neuroimaging of anxiety: A meta-analysis of emotional processing in PTSD, social anxiety disorder, and specific phobia. *Am. J. Psychiatry* 164, 1476–1488. doi: 10.1176/appi.ajp.2007.07030504

Figueroa, C. A., Cabral, J. R. B., Mocking, R. J. T., Rapuano, K. M., van Hartevelt, T. J., Deco, G., et al. (2019). Altered ability to access a clinically relevant control

network in patients remitted from major depressive disorder. *Hum. Brain Mapp.* 40, 2771–2786. doi: 10.1002/hbm.24559

Freyer, F., Roberts, J. A., Becker, R., Robinson, P. A., Ritter, P., and Breakspear, M. (2011). Biophysical mechanisms of multistability in resting-state cortical rhythms. *J. Neurosci.* 31, 6353–6361. doi: 10.1523/JNEUROSCI.6693-10.2011

Freyer, F., Roberts, J. A., Ritter, P., and Breakspear, M. (2012). A canonical model of multistability and scale-invariance in biological systems. *PLoS Comput. Biol.* 8:e1002634. doi: 10.1371/journal.pcbi.1002634

Friston, K. J. (2011). Functional and effective connectivity: A review. *Brain Connect.* 1, 13–36. doi: 10.1089/brain.2011.0008

Friston, K. J., Brown, H. R., Siemerkus, J., and Stephan, K. E. (2016). The dysconnection hypothesis (2016). *Schizophr. Res.* 176, 83–94.

Friston, K. J., Kilner, J., and Harrison, L. (2006). A free energy principle for the brain. *J. Physiol. Paris* 100, 70–87. doi: 10.1016/J.JPHYSPARIS.2006.10.001

Furcila, D., García, M., Toader, C., Morales, J., LaTorre, A., Rodríguez, Á, et al. (2019). Intool explorer: An interactive exploratory analysis tool for versatile visualizations of neuroscientific data. *Front. Neuroanat.* 13:1–17. doi: 10.3389/fnana.2019.00028

Glerean, E., Salmi, J., Lahnakoski, J. M., Jääskeläinen, P., and Sams, M. (2012). Functional magnetic resonance imaging phase synchronization as a measure of dynamic functional connectivity. *Brain Connect.* 2, 91–101. doi: 10.1089/brain.2011.0068

Goodman, W. K., Price, L. H., Rasmussen, S. A., Mazure, C., Fleischmann, R. L., Hill, C. L., et al. (1989). The yale-brown obsessive compulsive scale: I. development, use, and reliability. *Arch. General Psychiatry* doi: 10.1001/archpsyc.1989.01810110048007.

Göttlich, M., Krämer, U. M., Kordon, A., Hohagen, F., and Zurowski, B. (2014). Decreased limbic and increased fronto-parietal connectivity in unmedicated patients with obsessive-compulsive disorder. *Hum. Brain Mapp.* 35, 5617–5632. doi: 10.1002/hbm.22574

Grieder, M., Wang, D. J. J., Dierks, T., Wahlund, L. O., and Jann, K. (2018). Default mode network complexity and cognitive decline in mild Alzheimer's disease. *Front. Neurosci.* 12:770. doi: 10.3389/fnins.2018.00770

Gu, S., Cieslak, M., Baird, B., Muldoon, S. F., Grafton, S. T., Pasqualetti, F., et al. (2018). The energy landscape of neurophysiological activity implicit in brain network structure. *Sci. Rep.* 8:2507. doi: 10.1038/s41598-018-20123-8

Hagmann, P., Cammoun, L., Gigandet, X., Meuli, R., Honey, C. J., Wedeen, V. J., et al. (2008). Mapping the structural core of human cerebral cortex. *PLoS Biol.* 6:e159. doi: 10.1371/journal.pbio.0060159

Hamilton, M. (1959). The assessment of anxiety states by rating. *Br. J. Med. Psychol.* 32, 50–55. doi: 10.1111/j.2044-8341.1959.tb00467.x

van den Heuvel, O. A., van Wingen, G., Soriano-Mas, C., Alonso, P., Chamberlain, S. R., Nakamae, T., et al. (2016). Brain circuitry of compulsivity. *Eur. Neuropsychopharmacol.* 26, 810–827. doi: 10.1016/j.euroneuro.2015.12.005

Hillebrand, A., Tewarie, P. K., van Dellen, E., Yu, M., Carbo, E. W. S., Douw, L., et al. (2016). Direction of information flow in large-scale resting-state networks is frequency-dependent. *Proc. Natl. Acad. Sci. U.S.A.* 113, 3867–3872. doi: 10.1073/pnas.1515657113

Hull, J. V., Dokovna, L. B., Jacokes, Z. J., Torgerson, C. M., Irimia, A., and Van Horn, J. D. (2017). Resting-state functional connectivity in autism spectrum disorders: A review. *Front. Psychiatry* 7:205. doi: 10.3389/fpsyt.2016.00205

Hyvärinen, A., and Oja, E. (2000). Independent component analysis: Algorithms and applications. *Neural Networks* 13:6080. doi: 10.1016/S0893-6080(00)00026-5

Jobst, B. M., Hindriks, R., Laufs, H., Tagliazucchi, E., Hahn, G., Ponce-Alvarez, A., et al. (2017). Increased stability and breakdown of brain effective connectivity during slow-wave sleep: Mechanistic insights from whole-brain computational modelling. *Sci. Rep.* 7:4634. doi: 10.1038/s41598-017-04522-x

Kennedy, J., and Eberhart, R. (1995). "Particle swarm optimization," in *Proceedings of the ICNN'95 - International Conference on Neural Networks*, (IEEE), doi: 10.1109/ICNN.1995.488968

Krol, L. R. (2021). *Permutation Test*. Berlin: GitHub.

Kuznetsov, Y. A. (1998). *Elements of Applied Bifurcation Theory. Elements of Applied Bifurcation Theory*. New York, NY: Springer, doi: 10.1007/b98848

Laubach, M., Shuler, M., and Nicolelis, M. A. L. (1999). Independent component analyses for quantifying neuronal ensemble interactions. *J. Neurosci. Methods* 94, 141–154. doi: 10.1016/S0165-0270(99)00131-4

Leicht, E. A., and Newman, E. J. (2008). Community structure in directed networks. *Phys. Rev. Lett.* 100, 1–4. doi: 10.1103/PhysRevLett.100.118703

Lenhard, F., Aspvall, K., Andersson, E., Ahlen, J., Serlachius, E., Lavner, M., et al. (2021). The cost of obsessive–compulsive disorder in swedish youth. *Child Psychiatry Hum. Dev.* doi: 10.1007/s10578-021-01261-z [Epub ahead of print].

Li, X., Zhu, Z., Zhao, W., Sun, Y., Wen, D., Xie, Y., et al. (2018). Decreased resting-state brain signal complexity in patients with mild cognitive impairment and Alzheimer's disease: A multi-scale entropy analysis. *Biomed. Optics Exp.* 9:1916. doi: 10.1364/BOE.9.001916

Liu, C. Y., Krishnan, A. P., Yan, L., Smith, R. X., Kilroy, E., Alger, J. R., et al. (2013). Complexity and synchronicity of resting state blood oxygenation level-dependent (BOLD) functional MRI in normal aging and cognitive decline. *J. Magn. Res. Imag.* 38, 36–45. doi: 10.1002/jmri.23961

Lopes-dos-Santos, V., Conde-Ocazionez, S., Nicolelis, M. A. L., Ribeiro, S. T., and Tort, A. B. L. (2011). Neuronal assembly detection and cell membership specification by principal component analysis. *PLoS One* 6:20996. doi: 10.1371/journal.pone.0020996

Lopes-dos-Santos, V., Ribeiro, S. T., and Tort, A. B. L. (2013). Detecting cell assemblies in large neuronal populations. *J. Neurosci. Methods* 220, 149–166. doi: 10.1016/j.jneumeth.2013.04.010

Lord, L. D., Expert, P., Atasoy, S., Roseman, L., Rapuano, K., Lambiotte, R., et al. (2019). Dynamical exploration of the repertoire of brain networks at rest is modulated by psilocybin. *NeuroImage* 199, 127–142. doi: 10.1016/j.neuroimage.2019.05.060

Marčenko, V. A., and Pastur, L. A. (1967). Distribution of eigenvalues for some sets of random matrices. *Mathemat. USSR Sbornik* 1, 457–483. doi: 10.1070/SM1967v001n04ABEH001994

McIntosh, A. R., Vakorin, V., Kovacevic, N., Wang, H., Diaconescu, A., and Protzner, A. B. (2014). Spatiotemporal dependency of age-related changes in brain signal variability. *Cerebral Cortex* 24, 1806–1817. doi: 10.1093/cercor/bht030

Meunier, D., Lambiotte, R., Fornito, A., Ersche, K. D., and Bullmore, E. T. (2009). Hierarchical modularity in human brain functional networks. *Front. Hum. Neurosci.* 3:1–12. doi: 10.3389/neuro.11.037

Mezura-Montes, E., Coello, C., Mezura, E., and Coello, C. (2011). Constraint-handling in nature-inspired numerical optimization: Past, present and future. *Swarm Evol. Comput.* 1, 173–194. doi: 10.1016/j.swevo.2011.10.001

Moreira, P., Marques, P., Soriano-Mas, C., Magalhães, R., Sousa, N., Soares, J., et al. (2017). The neural correlates of obsessive-compulsive disorder: A multimodal perspective. *Trans. Psychiatry* 7:e1224. doi: 10.1038/tp.2017.189

Newman, M. E. J. (2006). Modularity and community structure in networks. *Proc. Natl. Acad. Sci. U.S.A.* 103, 8577–8582. doi: 10.1073/pnas.0601602103

Ochsner, K. N., Silvers, J. A., and Buhle, J. T. (2012). Functional imaging studies of emotion regulation: A synthetic review and evolving model of the cognitive control of emotion. *Ann. N.Y. Acad. Sci.* 1251, E1–E24. doi: 10.1111/j.1749-6632.2012.06751.x

Ostwald, D., and Bagshaw, A. P. (2011). Information theoretic approaches to functional neuroimaging. *Magn. Res. Imag.* 29, 1417–1428. doi: 10.1016/j.mri.2011.07.013

Paninski, L. (2003). Estimation of entropy and mutual information. *Neural Comput.* 15, 1191–1253. doi: 10.1162/089976603321780272

Pereda, E., Quiroga, R. Q., and Bhattacharya, J. (2005). Nonlinear multivariate analysis of neurophysiological signals. *Prog. Neurobiol.* 77, 1–37.

Peyrache, A., Benchenane, K., Khamassi, M., Wiener, S. I., and Battaglia, F. P. (2010). Principal component analysis of ensemble recordings reveals cell assemblies at high temporal resolution. *J. Comput. Neurosci.* 29, 309–325. doi: 10.1007/s10827-009-0154-6

Peyrache, A., Khamassi, M., Benchenane, K., Wiener, S. I., and Battaglia, F. P. (2009). Replay of rule-learning related neural patterns in the prefrontal cortex during sleep. *Nat. Neurosci.* 12, 919–926. doi: 10.1038/nn.2337

Piacentini, J., Bergman, R. L., Keller, M., and McCracken, J. (2003). Functional impairment in children and adolescents with obsessive-compulsive disorder. *J. Child Adoles. Psychopharmacol.* 13, 61–69. doi: 10.1089/104454603322126359

Picó-Pérez, M., Radua, J., Steward, T., Menchón, J. M., and Soriano-Mas, C. (2017). Emotion regulation in mood and anxiety disorders: A meta-analysis of FMRI cognitive reappraisal studies. *Prog. Neuro Psychopharmacol. Biol. Psychiatry* 79, 96–104. doi: 10.1016/j.pnpbp.2017.06.001

Pincus, S. M. (1991). Approximate entropy as a measure of system complexity. *Proc. Natl. Acad. Sci. U.S.A.* 88, 2297–2301. doi: 10.1073/pnas.88.6.2297

Quian Quiroga, R., and Panzeri, S. (2009). Extracting information from neuronal populations: information theory and decoding approaches. *Nat. Rev. Neurosci.* 10, 173–185. doi: 10.1038/NRN2578

Richman, J. S., and Moorman, J. R. (2000). Physiological time-series analysis using approximate entropy and sample entropy. *Am. J. Physiol. Heart Circ. Physiol.* 278, H2039–H2049. doi: 10.1152/ajpheart.2000.278.6.H2039

Rolls, E. T., Cheng, W., Gilson, M., Gong, W., Deco, G., Lo, C. Y. Z., et al. (2020). Beyond the disconnectivity hypothesis of schizophrenia. *Cerebral Cortex* 30, 1213–1233. doi: 10.1093/cercor/bhz161

Rolls, E. T., Loh, M., and Deco, G. (2008). An attractor hypothesis of obsessive-compulsive disorder. *Eur. J. Neurosci.* 28, 782–793. doi: 10.1111/j.1460-9568.2008.06379.x

Rosario, M. C., Prado, H. S., Borcato, S., Diniz, J. B., Shavitt, R. G., Hounie, A. G., et al. (2009). Validation of the university of São Paulo sensory phenomena scale: initial psychometric properties. *CNS Spectr.* 14, 315–323. doi: 10.1017/S1092852900020319

Sen, B., Bernstein, G. A., Mueller, B. A., Cullen, K. R., and Parhi, K. K. (2020). Sub-graph entropy based network approaches for classifying adolescent obsessive-compulsive disorder from resting-state functional MRI. *Neuro. Clin.* 26:102208. doi: 10.1016/j.nicl.2020.102208

Shannon, C. E. (1949). A mathematical theory of communication. *Math. Theory Commun.* 1924, 1–54.

Shappell, H. M., Caffo, B. S., Pekar, J. J., and Lindquist, M. A. (2019). Improved state change estimation in dynamic functional connectivity using hidden semi-markov models. *NeuroImage* 191, 243–257. doi: 10.1016/j.neuroimage.2019.02.013

Shen, X., Papademetris, X., and Constable, R. T. (2010). Graph-theory based parcellation of functional subunits in the brain from resting-state FMRI data. *NeuroImage* 50, 1027–1035. doi: 10.1016/j.neuroimage.2009.12.119

Sidak, Z. (1967). Rectangular confidence regions for the means of multivariate normal distributions. *J. Am. Stat. Assoc.* 62, 626–633.

Singh, H., Misra, N., Hnizdo, V., Fedorowicz, A., and Demchuk, E. (2003). Nearest neighbor estimates of entropy. *Am. J. Math. Manage. Sci.* 23, 301–321. doi: 10.1080/01966324.2003.10737616

Subirà, M., Alonso, P., Segalàs, C., Real, E., ópez-Solà, C. L., Pujol, J., et al. (2013). Brain structural alterations in obsessive-compulsive disorder patients with autogenous and reactive obsessions. *PLoS One* 8:e75273. doi: 10.1371/journal.pone.0075273

Tzourio-Mazoyer, N., Landeau, B., Papathanassiou, D., Crivello, F., Etard, O., Delcroix, N., et al. (2002). Automated anatomical labeling of activations in SPM using a macroscopic anatomical parcellation of the MNI MRI single-subject brain. *NeuroImage* 15, 273–289. doi: 10.1006/nimg.2001.0978

Vergara, V. M., Salman, M., Abrol, A., Espinoza, F. A., and Calhoun, V. D. (2020). Determining the number of states in dynamic functional connectivity using cluster validity indexes. *J. Neurosci. Methods* 337:108651. doi: 10.1016/j.jneumeth.2020.108651

Vohryzek, J., Deco, G., Cessac, B., Kringelbach, M. L., and Cabral, J. R. B. (2020). Ghost attractors in spontaneous brain activity: Recurrent excursions into functionally-relevant BOLD phase-locking states. *Front. Syst. Neurosci.* 14:1–15. doi: 10.3389/fnsys.2020.00020

Wang, Z., Maia, T. V., Marsh, R., Colibazzi, T., Gerber, A., and Peterson, B. S. (2011). The neural circuits that generate tics in tourette's syndrome. *Am. J. Psychiatry* 168, 1326–1337. doi: 10.1176/appi.ajp.2011.09111692

Weidle, B., Jozefiak, T., Ivarsson, T., and Thomsen, P. H. (2014). Quality of life in children with OCD with and without comorbidity. *Health Quality Life Out.* 12, 1–12. doi: 10.1186/s12955-014-0152-x

Xin, X., Long, S., Sun, M., and Gao, X. (2021). The application of complexity analysis in brain blood-oxygen signal. *Brain Sci.* 11:1415. doi: 10.3390/brainsci11111415

Zalesky, A., Fornito, A., and Bullmore, E. T. (2010). Network-based statistic: identifying differences in brain networks. *NeuroImage* 53, 1197–1207. doi: 10.1016/j.neuroimage.2010.06.041

Zamora-López, G., Chen, Y., Deco, G., Kringelbach, M. L., and Zhou, C. (2016). Functional complexity emerging from anatomical constraints in the brain: The Significance of network modularity and rich-clubs. *Sci. Rep.* 6, 1–18. doi: 10.1038/srep38424

Zheng, H., Onoda, K., Nagai, A., and Yamaguchi, S. (2020). Reduced dynamic complexity of BOLD signals differentiates mild cognitive impairment from normal aging. *Front. Aging Neurosci.* 12:90. doi: 10.3389/fnagi.2020.00090

frontiers | Frontiers in Human Neuroscience

TYPE Original Research
PUBLISHED 28 October 2022
DOI 10.3389/fnhum.2022.1029149

OPEN ACCESS

EDITED BY
Stefan Borgwardt,
University of Lübeck, Germany

REVIEWED BY
Arcady A. Putilov,
Federal Research Center of Fundamental and Translational Medicine, Russia
Alexandra Korda,
University Medical Center Schleswig-Holstein, Germany

*CORRESPONDENCE
Tina D. Kristensen
tina.dam.kristensen@regionh.dk

†These authors share senior authorship

SPECIALTY SECTION
This article was submitted to Brain Imaging and Stimulation, a section of the journal Frontiers in Human Neuroscience

RECEIVED 26 August 2022
ACCEPTED 07 October 2022
PUBLISHED 28 October 2022

CITATION
Rasmussen JØ, Nordholm D, Glenthøj LB, Jensen MA, Garde AH, Ragahava JM, Jennum PJ, Glenthøj BY, Nordentoft M, Baandrup L, Ebdrup BH and Kristensen TD (2022) White matter microstructure and sleep-wake disturbances in individuals at ultra-high risk of psychosis. *Front. Hum. Neurosci.* 16:1029149. doi: 10.3389/fnhum.2022.1029149

White matter microstructure and sleep-wake disturbances in individuals at ultra-high risk of psychosis

Jesper Ø. Rasmussen[1], Dorte Nordholm[2], Louise B. Glenthøj[2,3], Marie A. Jensen[4], Anne H. Garde[4,5], Jayachandra M. Ragahava[1,6], Poul J. Jennum[7,8], Birte Y. Glenthøj[1,8], Merete Nordentoft[2,8], Lone Baandrup[1,8,9], Bjørn H. Ebdrup[1,8†] and Tina D. Kristensen[1*†]

[1]Centre for Neuropsychiatric Schizophrenia Research, Mental Health Centre Glostrup, Copenhagen University Hospital – Mental Health Services CPH, Copenhagen, Denmark, [2]Copenhagen Research Centre for Mental Health, Mental Health Centre Copenhagen, Copenhagen University Hospital – Mental Health Services CPH, Copenhagen, Denmark, [3]Department of Psychology, Faculty of Social Sciences, University of Copenhagen, Copenhagen, Denmark, [4]The National Research Centre for the Working Environment, Copenhagen, Denmark, [5]Department of Public Health, University of Copenhagen, Copenhagen, Denmark, [6]Functional Imaging Unit, Department of Clinical Physiology, Nuclear Medicine and PET, Copenhagen University Hospital, Rigshospitalet, Copenhagen, Denmark, [7]Danish Centre for Sleep Medicine, Department of Clinical Neurophysiology, Copenhagen University Hospital, Rigshospitalet, Copenhagen, Denmark, [8]Department of Clinical Medicine, Faculty of Health and Medical Sciences, University of Copenhagen, Copenhagen, Denmark, [9]Mental Health Centre Copenhagen, Copenhagen University Hospital – Mental Health Services CPH, Copenhagen, Denmark

Aim: White matter changes in individuals at ultra-high risk for psychosis (UHR) may be involved in the transition to psychosis. Sleep-wake disturbances commonly precede the first psychotic episode and predict development of psychosis. We examined associations between white matter microstructure and sleep-wake disturbances in UHR individuals compared to healthy controls (HC), as well as explored the confounding effect of medication, substance use, and level of psychopathology.

Methods: Sixty-four UHR individuals and 35 HC underwent clinical interviews and diffusion weighted imaging. Group differences on global and callosal mean fractional anisotropy (FA) was tested using general linear modeling. Sleep-wake disturbances were evaluated using the subjective measures disturbed sleep index (DSI) and disturbed awakening index (AWI) from the Karolinska Sleep Questionnaire, supported by objective sleep measures from one-night actigraphy. The primary analyses comprised partial correlation analyses between global FA/callosal FA and sleep-wake measures. Secondary analyses investigated multivariate patterns of covariance between measures of sleep-wake disturbances and FA in 48 white matter regions of interest using partial least square correlations.

Results: Ultra-high risk for psychosis individuals displayed lower global FA (F = 14.56, $p < 0.001$) and lower callosal FA (F = 11.34, p = 0.001) compared to HC. Subjective sleep-wake disturbances were significantly higher among the UHR individuals (DSI: F = 27.59, $p < 0.001$, AWI: F = 36.42, $p < 0.001$). Lower callosal FA was correlated with increased wake after sleep onset (r = −0.34, p = 0.011) and increased sleep fragmentation index (r = −0.31, p = 0.019) in UHR individuals. Multivariate analyses identified a pattern of covariance in regional FA which were associated with DSI and AWI in UHR individuals (p = 0.028), but not in HC. Substance use, sleep medication and antipsychotic medication did not significantly confound these associations. The association with objective sleep-wake measures was sustained when controlling for level of depressive and UHR symptoms, but symptom level confounded the covariation between FA and subjective sleep-wake measures in the multivariate analyses.

Conclusion: Compromised callosal microstructure in UHR individuals was related to objectively observed disruptions in sleep-wake functioning. Lower FA in ventrally located regions was associated with subjectively measured sleep-wake disturbances and was partly explained by psychopathology. These findings call for further investigation of sleep disturbances as a potential treatment target.

KEYWORDS

ultra-high risk of psychosis, white matter, diffusion weighted imaging, sleep, substance use, psychopathology

Introduction

The ultra-high risk state of psychosis (UHR) designates a putative prodromal phase of psychosis (Yung et al., 2005) and is defined by criteria of attenuated psychotic symptoms, brief limited intermittent psychotic symptoms, and/or a diagnosis of schizotypal personality disorder or a genetic risk, along with a functional decline. A recent meta-analysis found a transition rate to psychosis of 25% within the first 3 years (Salazar De Pablo et al., 2021). Multiple risk factors for transitioning has been identified, including severity of attenuated psychotic symptoms, negative symptoms, substance use, physical inactivity, unemployment and male sex (Fusar-Poli et al., 2020). Considering the potential detrimental effects of psychosis, research on modifiable risk factors of disease progression is critical for early intervention (Pantelis et al., 2005; Bora et al., 2009).

The influence of sleep-wake disturbances on the development of psychopathology has increasingly been acknowledged. Sleep-wake disturbances can be evaluated using self-report questionnaires regarding a specific period (e.g., last night or last month), but they are vulnerable to recall-bias (Lunsford-Avery et al., 2015; Aili et al., 2017). Objective methods are polysomnography (the gold standard) and actigraphy, the latter less invasive and more convenient (Aili et al., 2017). Due to a well-described discrepancy between subjective and objective sleep measures, a combination of approaches is preferred (Trimmel et al., 2021). Sleep-wake disturbances are common in individuals diagnosed with schizophrenia (Waite et al., 2020) and commonly precede the first psychotic episode (Yung and Nelson, 2011; Zaks et al., 2022), and have predicted psychotic symptoms in a high-risk sample (Lunsford-Avery et al., 2015). According to a recent systematic review and meta-analysis (Clarke et al., 2021), sleep-wake disturbances are more present in UHR individuals compared to HC, and it applies both to self-reported (e.g., sleep quality and fragmented sleep) and objective sleep-wake measures (e.g., sleep latency, daytime napping, and movement during sleep). However, few studies with objective sleep measures such as actigraphy or polysomnography have been reported, and only four studies were identified and included in the meta-analysis (Clarke et al., 2021).

Cerebral white matter (WM) changes have been shown to be implicated in the pathophysiology of psychotic disorders (Vitolo et al., 2017; Zhao et al., 2022) including UHR individuals, although the changes appear more subtle than in patients with an established psychotic disorder (Peters et al., 2010; Pettersson-Yeo et al., 2011; Karlsgodt et al., 2012; Samartzis et al., 2014;

Wheeler and Voineskos, 2014; Canu et al., 2015). The most applied white matter index is fractional anisotropy (FA). Lower FA is often interpreted as impaired WM microstructure (Jones et al., 2013) and have been associated with loss of axonal coherence, demyelination, or neurodegeneration (Song et al., 2002; Alexander et al., 2007, 2011; Pasternak et al., 2009). Lower FA has been reported in UHR individuals compared to HC in widespread WM regions (Carletti et al., 2012; Lagopoulos et al., 2013), such as the major association tracts interconnecting frontal regions with temporal and limbic regions (Clemm Von Hohenberg et al., 2014; Rigucci et al., 2016; Vijayakumar et al., 2016), as well as the large projection tracts connecting the cortical and subcortical structures (Katagiri et al., 2015; Saito et al., 2017). Cross-sectional studies have found regional lower FA to be associated with more severe attenuated psychotic symptoms (Nägele et al., 2020). In a previous independent cross-sectional study in UHR individuals we reported WM alterations in UHR individuals which were associated with positive and negative symptoms as well as level of functioning (Krakauer et al., 2017). In a study population partly overlapping with the current sample we found that global FA at baseline predicted transition to psychosis after one year (Kristensen et al., 2021a), and that changes in negative symptoms were linked to white matter changes in superior longitudinal fasciculus (Kristensen et al., 2021b).

Psychosis has been conceptualized as a global brain disorder of dysconnectivity (Friston, 1998). Global WM studies have identified associations between WM microstructure and sleep-wake measures, such as sleep duration in healthy adults (Khalsa et al., 2017; Grumbach et al., 2020) and in adolescents (Telzer et al., 2015), as well as sleep quality in an aging populations (Kocevska et al., 2019), patients with depression (Sexton et al., 2017), and patients with mild traumatic brain injury (Raikes et al., 2018). However, the participants of these studies are heterogeneous including clinical and non-clinical samples, aging or adolescents, as well as neurologically afflicted populations. Hence the results and localization of the associations are mixed (Zitser et al., 2020). To our knowledge, no studies to date have examined associations between WM and sleep-wake disturbances in UHR individuals.

Global approaches may conceal information derived from informed hypotheses on associations between specific symptoms and predefined WM regions of interest (ROIs). The main commissural tract in the brain is corpus callosum (CC), which is critical for the interhemispheric information transfer and coordination of functional activity (Mancuso et al., 2019). CC has together with neuronal populations located to the brainstem been hypothesized to be involved in a complex synchronization of interhemispheric activity, regulating the timing and duration of rapid eye movement (REM) (Nielsen et al., 1992). Indeed, different aspects of sleep quality have been linked to CC, such as sleep oscillations (Piantoni et al., 2013), sleep efficiency, total sleep time (Altendahl et al., 2020), REM as well as non-REM sleep (Avvenuti et al., 2019; Bernardi et al., 2021). One study found that WM metrics of CC mediated associations between poor sleep quality and symptomatology in patients with depression (Li et al., 2020). Hence, investigating associations between predefined ROIs such as CC and predefined measures of sleep, as well as exploring associations to all WM regions may be optimal.

Substance use disorder is significantly more common in UHR individuals (Carney et al., 2017) and patients suffering from schizophrenia (Hunt et al., 2018) than in the general population. Substance use is known to affect both WM microstructure (Murray et al., 2017; Hampton et al., 2019) and sleep (Huhn et al., 2022), as well as the risk of developing psychosis (Murray et al., 2017; Murrie et al., 2020; Hjorthøj et al., 2021). A meta-analysis found lower FA in CC in individuals with a substance use disorder, however, it appeared dependent on the type of substance (Hampton et al., 2019). Studies have demonstrated that substance use worsens both the subjective experience of sleep quality and objective sleep-wake measures, including reduced total sleep time (TST) and increased Wake After Sleep Onset (WASO) (Huhn et al., 2022). It is well-known that substance use can induce transient and dose dependent psychotic symptoms. A recent meta-analysis reported an overall transition rate of 25% from any substance induced psychosis to schizophrenia with the most elevated transition rate of 34% found in patients with a cannabis-induced psychosis (Murrie et al., 2020).

A study from our group showed that antipsychotic medication affected WM microstructure in frontal fasciculi in antipsychotic naïve patients with first episode psychosis (Ebdrup et al., 2015). Additionally, changes in WM microstructure have been reported in patients with affective disorders (Jenkins et al., 2016; Cui et al., 2020). Hence, the potential confounding effects of both antipsychotic medication, sleep medication, as well as depressive symptoms being markedly prevalent in UHR individuals may be important to explore.

In this study, we examine the association between global and regional WM microstructure and sleep-wake disturbances in UHR individuals compared to HC. We hypothesize, that lower mean global FA as well as lower FA in CC are associated with more severe sleep-wake disturbances. Secondly, we investigate potential covariation between FA in all ROIs and sleep-wake disturbances. Finally, we exploratively investigate if these potential associations may be explained by substance use, medication (antipsychotics and sleep medicine), and psychopathology (depressive symptoms and UHR symptoms).

Materials and methods

Cross-sectional data were derived from The FOCUS-trial (Glenthøj et al., 2015). The main trial design and primary outcomes have been reported elsewhere (Glenthøj et al., 2015,

2020). After initiation, the main trial was extended with several add-on studies at a later timepoint. Hence, sample size was reduced for the current subset of UHR individuals selected from the main trial (Flow chart in **Supplementary Figure 1**). Participants were recruited from psychiatric inpatient and outpatient facilities in Copenhagen, Denmark, between April 2014 and December 2017. The trial protocol was approved by the Committee on Health Research Ethics of the Capital Region in Denmark (H-6-2013-015). All participants provided written informed consent prior to inclusion.

Participants

Data for the current study was collected at baseline from help-seeking individuals meeting at least one of the three UHR-criteria according to the Comprehensive Assessment of At-Risk Mental States (CAARMS) (Yung et al., 2005): attenuated psychotic symptoms, and/or brief limited intermittent psychotic symptoms, and/or trait and vulnerability state along with a significant drop or sustained low functioning for the past year. Exclusion criteria were a history of a psychotic episode of more than one week duration; psychiatric symptoms explained by a physical illness with psychotropic effect (e.g., delirium) or acute intoxication from any substance; a diagnosis of a serious developmental disorder (e.g., Asperger's syndrome or IQ < 70); or current treatment with methylphenidate. HC were recruited by web based advertising or via advertisements at local educational institutions. HC had no current or previous psychiatric diagnosis, substance use or dependency, and no first-degree relatives with a psychotic disorder. In the main trial HC were concurrently included and matched to the UHR individuals on age, sex, ethnicity, and parental socioeconomic status.

Assessments

Clinical assessments

Axis I and selected Axis II diagnoses (schizotypal-, paranoid-, and borderline personality disorder) were examined using the Structured Clinical Interview for DSM-IV (SCID) (First et al., 1997). To examine whether a participant met the UHR criteria, the semi-structured interview Comprehensive Assessment of At-Risk Mental States (CAARMS) (Morrison et al., 2011) was used. CAARMS is rated with an intensity score and a frequency score in four different domains of positive UHR symptoms (unusual thought content, non-bizarre ideas, disorganized speech, or perceptual abnormalities). Based on these scores it is determined if the patient meets UHR-criteria. If the intensity exceeds cut-off for psychosis and does not resolve spontaneously within the duration of one week, the UHR state is exceeded. Furthermore, UHR criteria of trait and vulnerability is met with a schizotypal personality disorder or a psychotic illness in a first degree relative, along with a decline in functioning ($\geq$30% drop for at least a month) or a sustained low functioning ($\leq$50 for at least a year) assessed with the Social and Occupational Functioning Assessment Scale (SOFAS) (Morosini et al., 2000). Here, we used the CAARMS composite score, which is calculated from the four different domains of positive UHR symptoms by multiplication of the intensity score and the frequency score within each domain, and next adding the scores from the 4 domains. Depressive symptomatology was assessed using the Montgomery-Åsberg Depression Rating Scale (MADRS) (Montgomery and Asberg, 1979), which is a 10 items interview based questionnaire related to depressive symptoms. The Alcohol Smoking and Substance Involvement Screening Test (ASSIST) (Ali et al., 2002) was used to assess the occurrence and extent of substance use. ASSIST is a short interview based questionnaire, consisting of eight questions aiming to examine both present (last three month) and lifetime use of different substances (alcohol, tobacco, cannabis, cocaine, amphetamines, inhalants, sedatives, hallucinogens, opiates, and other drugs). For each substance ever used, frequency was rated on a 5-point Likert scale, (0 = never, 1 = once or twice, 2 = monthly, 3 = weekly and 4 = daily or almost daily). Use of antipsychotics and sleep medicine (including benzodiazepines, antihistamines, and melatonin) was self-reported, both prescribed medicine for daily use and for use "as needed" were registered, and if the medicine was ingested during the 24-h of actigraphy.

All clinical assessments were conducted by experienced psychologists and medical doctors with comprehensive training in the assessment instruments. Inter-rater reliability was assessed in the main trial using intra-class correlations for clinical outcomes, revealing excellent inter-rater reliability (Glenthøj et al., 2020).

Sleep assessments

The subjectively experienced sleep quality was assessed with a modified version of the Karolinska Sleep Questionnaire (Åkerstedt et al., 2002) both during the past night and during the past four weeks. Seven items about sleep disturbances were covered: (a) difficulties falling asleep, (b) disturbed/restless sleep, (c) repeated awakenings, (d) premature awakenings, (e) difficulties waking up, (f) non-refreshing sleep, and (g) exhaustion at awakening. All scores ranking from 1 to 5 (1 = never, 2 = seldom, 3 = sometimes/several times per month, 4 = mostly/several days per week, 5 = always), higher scores indicating less refreshing sleep. The Disturbed Sleep Index (DSI) was calculated as the sum of the four items, (a), (b), (c), and (d), ranking from 4 to 20. The Disturbed Awakening Index (AWI) was calculated as the sum of the three items (e), (f), and (g), ranking from 3 to 15. Individuals with missing data on single items were excluded from the analyses.

The objective sleep-wake measures were obtained using an actigraph. An actiwatch (ActiGraph wGT3X-BT from

ActiGraph FL, USA) was worn on the non-dominant wrist for 24 h. Data were collected with a sampling rate of 30 Hz and 1-min epochs were used to score wake and sleep pattern. Data were analyzed with ActiGraph Sleep Analysis (ActiGraph, FL, USA). The actigraph measures applied in this study were: total sleep time (TST), wake after sleep onset (WASO) (minutes spend awake after sleep had occurred), sleep efficiency (SE) (the ratio between TST and total time in bed), and sleep fragmentation index (SFI) (index of restlessness during the sleep period expressed as a percentage, higher score indicating more disrupted sleep). The actigraph was accompanied by a sleep diary reporting bedtime, awakening time, and medicine intake.

The subjective sleep measures are regarded as primary in the analyses as they cover the last four weeks and must be considered more representative than one-night actigraphy. In our analyses we include both the subjective and the objective sleep-wake measures and consider whether the objective measures support the findings of the subjective measures.

Image acquisition and processing

The details of image acquisition and processing have been described elsewhere (Kristensen et al., 2019). Briefly, we acquired the MRI scans on a 3T scanner (Philips Healthcare, Best, Netherlands). Two diffusion-weighted images using single shot spin-echo echoplanar imaging sequence with 30 non-collinear diffusion-weighted (b = 1.000 s/mm^2) directions and one non-diffusion weighted (b = 0 s/mm^2) in opposite phase encoding directions were acquired, enabling correction for susceptibility distortions (Andersson et al., 2003). Tools from the FSL software library v5.0.10 (Jenkinson et al., 2012) and MRtrix3[1] was used for image processing. DWI data were denoised (Dhollander et al., 2016; Veraart et al., 2016b,a), and images were corrected for B1 field inhomogeneity (Zhang et al., 2001; Smith et al., 2004). Eddy current and susceptibility artifact correction (Andersson and Sotiropoulos, 2016) was performed, and absolute and relative head motion parameters were extracted. Tract-based spatial statistics (TBSS) (Smith et al., 2004, 2006) was used to align FA data into the FMRIN58 template using the non-linear image registration tool (FNIRT) (Andersson et al., 2007a,b). The mean FA image (threshold of 0.2) was thinned to create mean study-specific FA skeleton maps (Smith et al., 2006). Using the John Hopkins University WM tractography atlas labels (Mori and Van Zijl, 2007; Hua et al., 2008), we calculated mean FA for the 48 ROIs for each UHR individual. Mean global FA was calculated as the average of the weighted FA in the 48 ROIs from skeletonized data. FA for CC was calculated as the summed mean FA for the 3 callosal segments (genu + body + splenium)/3 (**Supplementary Figure 2** and **Supplementary Text 1** for further details).

MRI quality metrics were assessed by visual inspection, and MRI quality metrics from each subject was calculated using a quality assessment method described by Roalf et al. (2016) [Range between "Good" and "Excellent" quality, details are reported elsewhere (Kristensen et al., 2019)].

Statistical analyses

Univariate analyses

All univariate analyses were performed using Statistical Package for the Social Sciences (SPSS) version 25.0, (IBM, Armonk, NY, USA). Descriptive variables were reported as percent, means, and standard deviations. Chi-square tests and general linear modelling (GLM) were used to compare UHR individuals to HC on descriptive variables. Effect of group on mean global FA and callosal FA were tested using GLM with age, sex, relative and absolute motion in scanner as covariates.

Partial correlation analyses were performed in SPSS to test covariation between mean FA in the CC and the subjective and objective measures of sleep-wake disturbances, including age, sex, relative and absolute motion in scanner as covariates. Primary analyses tested the effect of group with ANOVA (UHR individuals vs. HC). All tests were corrected for multiple comparisons using the Benjamin–Hochberg procedure with an FDR of $p < 0.05$.

Post-hoc, we tested the potential effect of substance use, medication, and psychopathology by including each substance as well as a composite score for substance use, medication (antipsychotics and sleep medicine yes/no), and measure of psychopathology [depressive (MADRS score) or UHR-symptoms (CAARMS composite score)] as covariates, along with age, sex, relative and absolute motion in scanner in the partial correlation model. *Post-hoc* tests were uncorrected for multiplicity.

Multivariate analyses

Group differences on the 48 ROIs were tested with multivariate GLM using the MATLAB software (version 2021a) including age, sex, relative and absolute motion as covariates.

The partial least square-correlation (PLS-C) analysis (McIntosh and Lobaugh, 2004; Kovacevic et al., 2013) was performed using the MATLAB software (version 2021a). We included two subjective and four objective sleep-wake measures and mean FA values of 48 WM-regions, co-varied for age, sex, and relative and absolute motion in scanner. In brief, PLS-C is used to identify latent variables (LVs), which express maximum covariance between patterns of regional FA associated with sleep-wake disturbances. Both the significance level of the omnibus test (Reisfeld and Mayeno, 2013) and of the individual LVs were assessed using permutation testing (100,000 permutations) to obtain a p-value based on non-rotated sampling distribution of singular values (Kovacevic et al., 2013). For the omnibus test, the Inertia index that was calculated as the sum of all singular values of all the LVs

1 www.mrtrix.org

identified by PLS-C, was used for permutations testing (Abdi and Williams, 2013). LVs with a $p < 0.05$ were considered significant. Only LVs with a cross-block covariance larger than 5% were reported (Grigg and Grady, 2010). The reliability of saliences was assessed using bootstrapping (100,000 bootstraps with procrustean rotation) to obtain 95% confidence intervals. Confidence intervals of the saliences that did not cross zero were considered reliable (Krishnan et al., 2011). Details on PLS-C are provided in **Supplementary Text 2**.

In planned exploratory analyses, we entered substance use, medication (antipsychotics and sleep medication), and psychopathology [level of depressive symptoms (MADRS score), and level of UHR-symptoms (CAARMS composite score)] as covariates in the multivariate PLS-C. In addition, we performed sensitivity analyses on a reduced sample of antipsychotic free UHR individuals ($n = 45$). Finally, *post-hoc* analyses explored a potential mediation effects of levels of psychopathology on significant associations between regional FA and sleep-wake measures using Process for SPSS by Hayes (2017).

Results

Characteristics of participants are reported in **Table 1**. No differences were found between UHR individuals and HC on the sociodemographic variables of age, sex or estimated premorbid IQ (See further details in **Table 1**). As well, no differences were found when comparing characteristics of UHR individuals in antipsychotic medication with UHR individuals with no antipsychotic medication (see further details in **Supplementary Table 1**).

White matter

UHR individuals had significantly lower global FA ($F = 14.06$, $p < 0.001$), and lower FA in CC ($F = 12.86$, $p < 0.001$) when compared to HC (**Table 1**).

Furthermore, the multivariate test including all 48 ROIs showed significant lower FA in UHR individuals (omnibus test $p < 0.001$). The significant pattern indicated that 22/48 ROIs contributed reliably with lower FA in UHR individuals ($p = 0.001$) bilaterally: middle cerebellar peduncle; genu, body, and splenium of CC; posterior limb of internal capsule; superior corona radiata; posterior thalamic radiation; external capsule; and superior longitudinal fasciculus. Left hemisphere: retrolenticular part of internal capsule; posterior corona radiata; sagittal stratum; cingulum; and tapetum. Right hemisphere: cerebral peduncle; anterior corona radiata; and cingulum hippocampus (**Figure 1**).

Sleep

We found a significant difference between groups on the subjective sleep-wake measures (**Table 2**, **Figure 2**, and **Supplementary Figure 3**). The UHR individuals had significantly higher DSI (i.e., more disturbed sleep), both the preceding night ($F = 18.41$, $p < 0.001$) and across the last four weeks ($F = 27.59$, $p < 0.001$). The AWI was significantly higher (i.e., less refreshed at awakening) in the UHR-group, both the preceding night ($F = 19.03$, $p < 0.001$) and across the last four weeks ($F = 36.42$, $p < 0.001$).

Overall, we found no significant differences between groups on the objective sleep-wake measures from the actigraph. Among female participants we found significantly higher SE ($F = 12.83$, $p = 0.001$) and TST ($F = 6.76$, $p = 0.011$) and significantly lower WASO ($F = 8.37$, $p = 0.005$) and SFI ($F = 4.45$, $p = 0.038$) (**Supplementary Table 2**).

Substance use, psychopathology, and medication

Among the UHR individuals, two had a history and one had a current diagnosis of substance use disorder. Six UHR individuals had an earlier and none had a current diagnosis of dependence, which was in accordance with the eligibility criteria.

UHR individuals had a significantly higher use of nicotine (χ^2 18.07, $p = 0.001$) compared to HC, and a significantly lower consumption of alcohol (χ^2 9.67, $p = 0.046$). Although not significant, we noticed that three UHR individuals had a daily or almost daily use of cannabis, compared to no HC. Likewise, no HC had ever used simulants (amphetamine, ecstasy, amphetamine, etc.), where three UHR individuals had tried it, and one had a monthly use (**Supplementary Table 3**).

The UHR individuals comprised a heterogenous sample with a majority of $n = 38$ (59.4%) diagnosed with an affective disorder, $n = 37$ (57.8%) with an anxiety disorder, and $n = 21$ (32.4%) diagnosed with a personality disorder (**Table 1**). The mean baseline score on MADRS was equivalent to a mild depression, which is in accordance with the high incidence of affective disorders.

Thirty-eight (59.4%) of the sample were antipsychotic-naïve and $n = 19$ (29.7%) reported current use of antipsychotic medication in low dosages. Of other medications which may affect sleep, one UHR individual reported current treatment of a benzodiazepine, 6 melatonin, and 15 reported current use of antidepressants (**Table 1**).

TABLE 1 Sociodemographic and clinical data at baseline for individuals at ultra-high risk and healthy controls.

Variable Mean (S.D.)/Percent	UHR (N = 64)	Healthy controls (N = 35)	Significance
Age Mean (SD)	23.6 (3.9)	23.7 (2.7)	$p = 0.87$
Sex			$p = 0.07$, χ^2 2.87
Male	57.8%	40.0%	
Female	42.2%	60.0%	
Premorbid IQ (DART)	21.2 (7.2)	22.7 (6.9)	$p = 0.32$
Years of education	**13.7 (2.4)**	**16.4 (2.0)**	**$p < 0.01$**
Parental SES			**$p = 0.03$, χ^2 7.39**
Low	7.8%	0.0%	
Medium	45.3%	23.1%	
High	46.9%	76.9%	
Function (SOFAS)	**54.1 (9.9)**	**87.7 (6.8)**	**$p < 0.01$, $F = 322.1$**
Activity-level[#]	**14.9 (17.3)**	**42.7 (8.0)**	**$p < 0.01$, $F = 71.96$**
White matter			
Global, mean FA (SD)	0.599 (0.016)	0.612 (0.012)	**$p < 0.001$, $F = 14.56$**
Corpus Callosum, mean FA (SD)	0.739 (0.021)	0.753 (0.015)	**$p = 0.001$, $F = 11.34$**
Absolute motion in scanner	1.262 (0.346)	1.227 (0.373)	$p = 0.646$, $F = 0.21$
Relative motion in scanner	0.178 (0.083)	0.159 (0.063)	$p = 0.250$, $F = 1.34$
Diagnoses			
Affective disorder	59.4% (38)	–	
Anxiety disorder	57.8% (37)	–	
Personality disorder	32.4% (21)	–	
Other diagnoses	21.9% (14)	–	
Diagnose of lifetime[†] abuse	3.1% (2)	–	
Diagnose of lifetime[†] dependency	9.4% (6)	–	
Diagnose of current[†] abuse	1.6% (1)	–	
Diagnose of current[†] dependency	0.0% (0)	–	
Medication			
Antipsychotic-naïve	59.4% (38)	–	
Current[†] antipsychotics	29.7% (19)	–	
Current[†] antidepressants	23.4% (15)	–	
Current[†] benzodiazepines	1.6% (1)	–	
Current[†] melatonin	9.4% (6)	–	
Clinical symptoms			
CAARMS composite score	49.91 (15.71)	–	
MADRS total	15.86 (7.31)	–	

[#]Activity-level is hours per week spend on work and education. Significant difference between UHR individuals and healthy controls are marked in bold.
CAARMS, comprehensive assessment of at-risk mental state; DART, Danish adult reading list; FA, fractional anisotropy; IQ, intelligence quotient; MADRS, Montgomery-Åsberg Depression Rating Scale, No., number; SD, standard deviation; SES, socio-economic status; SOFAS, social and occupational function assessment scale; TS, trait and state; UHR, ultra-high risk.

Partial correlations between callosal fractional anisotropy and sleep-wake measures

We identified significant negative correlations between callosal FA and WASO ($p = 0.011$, $r = -0.337$) as well as with SFI ($p = 0.019$, $r = -0.313$) in UHR individuals (Table 3). When including all participants, significant correlations between callosal FA and AWI ($p = 0.029$, $r = -0.230$), SE ($p = 0.020$, $r = 0.243$), WASO ($p = 0.007$, $r = -0.283$), and SFI ($p = 0.032$, $r = -0.225$) remained significant after controlling for multiplicity. However, in the within-group analyses we could not confirm the significant correlation between callosal FA, AWI and SE among the UHR individuals, and no significant correlations between global or callosal mean FA were identified in HC. The partial correlation analyses were also performed on the reduced sample of antipsychotic free UHR individuals

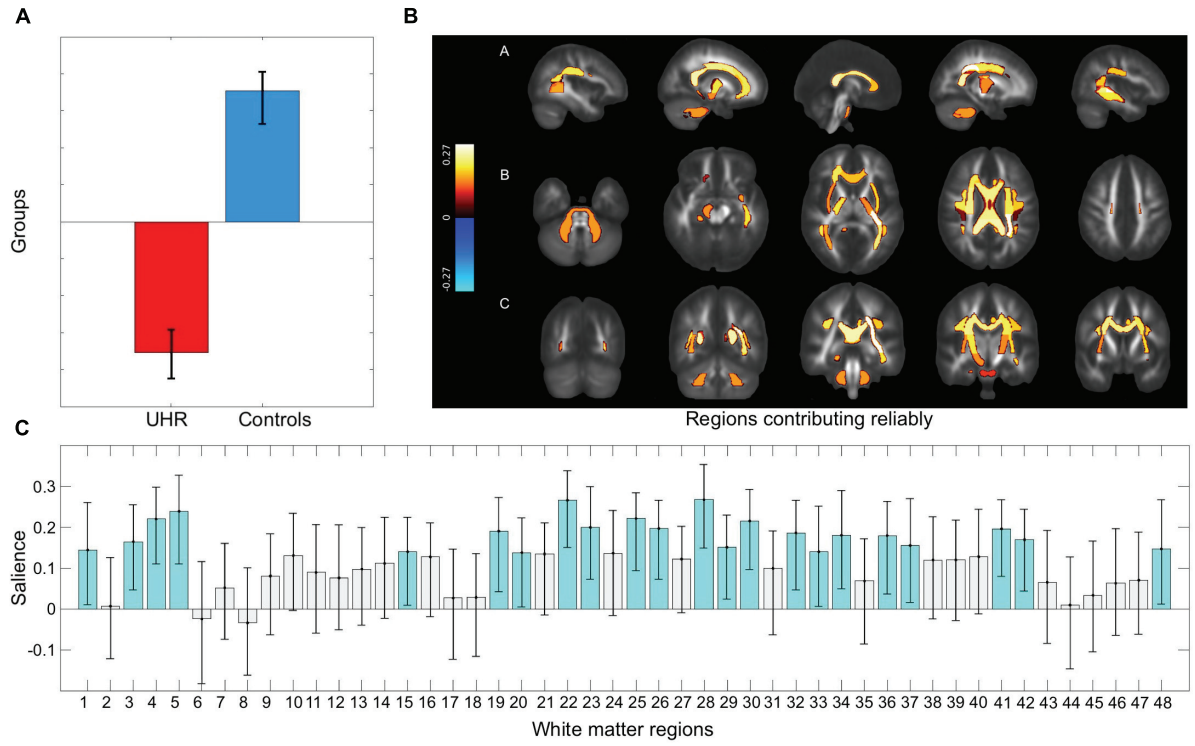

FIGURE 1
Group difference on 48 white matter regions. Figure displays the results from the multivariate GLM testing group difference between UHR individuals and healthy controls on fractional anisotropy (FA) in 48 regions of interest. **(A)** The significant group difference shows lower fractional anisotropy in UHR individuals compared to healthy controls in the 48 regions of interest (ROIs). **(B)** The ROIs which contributes reliably are visualized using JHU white matter atlas. Reliably contributing regions are bilaterally: middle cerebellar peduncle; genu, body, and splenium of corpus callosum; posterior limb of internal capsule; superior corona radiata; posterior thalamic radiation; external capsule; and superior longitudinal fasciculus. Left hemisphere: retrolenticular part of internal capsule; posterior corona radiata; sagittal stratum; cingulum; and tapetum. Right hemisphere: cerebral peduncle; anterior corona radiata; and cingulum hippocampus. **(C)** The pattern of covariance in all 48 ROIs, with the regions contributing reliably marked in turquoise. A list linking the numbers to the regions are displayed in the **Supplementary Text 3**. A, anterior; L, left; P, posterior; R, right; UHR, ultra-high risk.

(n = 45), which showed identical results (**Supplementary Table 4**).

Multivariate covariance between fractional anisotropy and sleep-wake disturbances

The PLS-C interaction analysis on all participants revealed a trend level significant association between patterns of regional FA and sleep-wake disturbances comparing UHR individuals to HCs (omnibus test p = 0.078). *Post-hoc* sensitivity analyses including all HC and a subsample of antipsychotic free UHR individuals showed a strong association (omnibus test p = 0.031) between a pattern of disturbed sleep-wake measures (lower SE, higher WASO, SFI, and AWI) and widespread lower FA in 24/48 WM regions explaining 69.89% of the covariance (LV1 p = 0.032) (see **Supplementary Figure 4A** for details). The next step within group PLS-C analysis identified an association between a pattern of regional FA and sleep-wake measures in UHR individuals (omnibus test p = 0.028) but not in HC (omnibus test p = 0.290). In UHR individuals, one significant latent variable (LV) was identified: LV3 explained 15% of the covariance (p = 0.013). LV3 comprised a pattern where higher FA in fornix, along with lower FA in left and right corticospinal tract, left cerebral peduncle, left medial lemniscus, and left cingulum (hippocampus) contributed reliably. This pattern of regional FA was associated with a pattern of more severely disturbed sleep (DSI) and awakening (AWI) contributing reliably (See **Figure 3** for details).

Confounding effects of substance use, medication, and psychopathology

Non-parametric tests of correlations between single substances as well as composite substance score and sleep-wake measures in all participants revealed nicotine use to be positively correlated to scores on 5/6 measures of sleep-wake disturbances: DSI (p = 0.003, r = 0.292), AWI (p < 0.001,

TABLE 2 Sleep at baseline.

Variable Mean (SD)/percent	UHR individuals (*N* = 64)	Healthy controls (*N* = 35)	Significance
Karolinska Sleep Questionnaire			
The last 4 weeks			
Disturbed Sleep Index (DSI)[1]	12.09 (3.56)	8.46 (2.71)	**$p < 0.001$, F = 27.59**
Disturbed Awakening Index (AWI)[2]	11.20 (2.75)	7.86 (2.42)	**$p < 0.001$, $F = 36.42$**
The last night			
Disturbed Sleep Index (DSI)[1]	10.66 (3.48)	7.68 (2.83)	**$p < 0.001$, $F = 18.41$**
Disturbed Awakening Index (AWI)[2]	9.44 (2.51)	7.34 (1.81)	**$p < 0.001$, $F = 19.03$**
Actigraphy measures (last night)			
Total Sleep Time (TST, h/min)[3]	6/39.51 (1/43.01)	6/33.97 (1/5.01)	$p = 0.775$, $F = 0.08$
Sleep Efficiency (SE)[4]	84.90 (9.32)	86.42 (8.42)	$p = 0.427$, $F = 0.64$
Sleep Fragmentation Index (SFI)[5]	27.41 (15.41)	25.07 (13.22)	$p = 0.453$, $F = 0.57$
Wake After Sleep Onset (WASO, min)[6]	59.55 (39.71)	55.74 (42.64)	$p = 0.662$, $F = 0.19$

Table displays the subjective data on disturbed sleep from Karolinska Sleep Questionnaire and objective measures from one-night Actigraphy in ultra-high-risk individuals compared with healthy controls.
[1]Disturbed sleep index (DSI) was computed as the sum of four items [(a)–(d), ranging 1–5, higher scores represented a more disturbed sleep]: (a) difficulties falling asleep, (b) disturbed/restless sleep, (c) repeated awakenings, and (d) premature awakening.
[2]Disturbed awakening index (AWI) was computed as the sum of three items [(e)–(g), all ranging 1–5, higher scores represented poorer sleep (= less refreshing sleep)]: (e) ease of awakening, (f) refreshing sleep, and (g) the degree of exhaustion at awakening.
[3]Total Sleep Time (TST) – The total number of minutes labeled as "asleep" during nighttime using the automatized algorithm from ActiGraph wGT3X-BT.
[4]Sleep Efficiency (SE) – Number of sleep minutes divided by the total number of minutes the subject was in bed.
[5]Sleep Fragmentation Index (SFI) restlessness during the sleep period expressed as sum of Movement Index (MI = The total of scored awake minutes divided by Total time in bed in hours × 100) and Fragmentation Index (FI = The percentage of one minute periods of sleep vs. all periods of sleep in the sleep period.
[6]Wake after Sleep Onset (WASO): The total number of minutes the subject was awake after sleep onset occurred.
Significant difference between UHR individuals and healthy controls are marked in bold.

$r = 0.578$), SE ($p = 0.025$, $r = -0.229$), WASO ($p = 0.013$, $r = 0.252$), and SFI ($p = 0.016$, $r = 0.245$) (uncorrected). No other substances were correlated to sleep-wake measures (**Supplementary Table 5**). We did not observe confounding effect of use of single substances or the substance use composite score on the correlation between callosal FA and sleep-wake measures (**Supplementary Table 6**).

Sleep-wake disturbances were positively associated with psychopathology in UHR individuals: DSI to depressive symptoms ($p < 0.001$, $r = 0.433$) and AWI to UHR-symptoms ($p = 0.020$, $r = 0.290$) (**Supplementary Table 7**). When *post-hoc* entering psychopathology as well as use of antipsychotics and sleep medication as covariates along with age, sex, relative and absolute motion in scanner in the partial correlation model, we found that the significant negative association between callosal FA and WASO, as well as SFI sustained including antipsychotics (WASO: $p = 0.011$, $r = -0.337$; SFI: $p = 0.019$, $r = -0.312$), sleep medication (WASO: $p = 0.011$, $r = -0.338$; SFI: $p = 0.020$, $r = -0.310$), UHR-symptoms (WASO: $p = 0.016$, $r = -0.319$; SFI: $p = 0.033$, $r = -0.286$), and depressive symptoms (WASO: $p = 0.010$, $r = -0.339$; SFI: $p = 0.020$, $r = -0.310$) as covariates (**Supplementary Table 6**).

In the multivariate PLS-C, we found no effect of entering substance use, antipsychotic medication, and sleep medication as covariates on the overall result (**Supplementary Table 8**). However, in the *post-hoc* sensitivity analyses on a reduced sample of antipsychotic free UHR individuals we found a borderline significant association between a pattern of disturbed sleep-wake measures (lower TST, higher DSI) and lower FA in 7/48 WM regions explaining 11.38% of the covariance (omnibus test $p = 0.033$, LV3 $p = 0.082$) (see **Supplementary Figure 4B** for details). Furthermore, the omnibus test was only significant at trend level when psychopathology was included in the model (UHR-symptoms omnibus test $p = 0.052$. LV3 $p = 0.005$, cross-block covariance 15.97%; Depressive symptoms omnibus test $p = 0.087$, no significant LVs).

Discussion

To the best of our knowledge, this is the first study in individuals at UHR investigating associations between WM microstructure and subjective and objective sleep-wake measures and how common clinical confounders may affect this association.

As expected, UHR individuals presented with lower FA compared to HC at a global as well as at a regional level in CC. This result was supported in the multivariate test including all 48 ROIs. The finding is in accordance with the majority of studies in UHR individuals reporting subtle and widespread

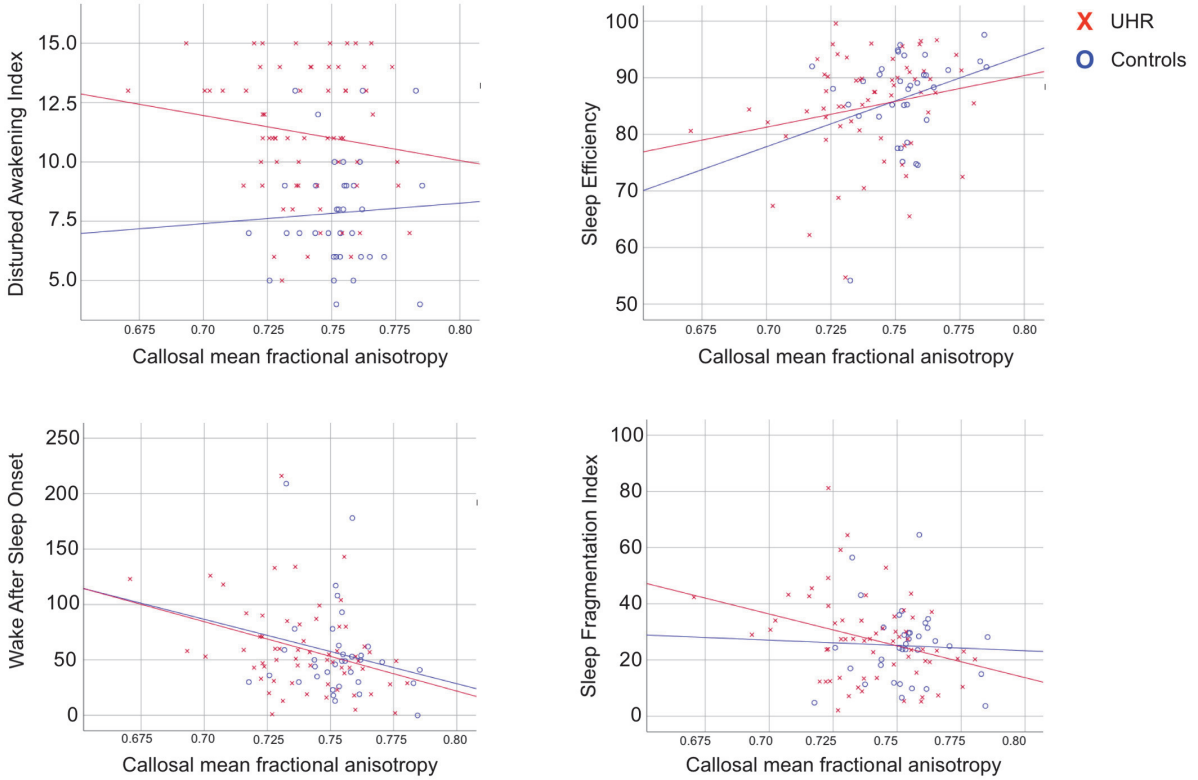

FIGURE 2
Relations between callosal fractional anisotropy and sleep measures. Scatterplots illustrating the significant relations between mean callosal fractional anisotropy and sleep parameters. UHR, individuals at ultra-high risk for psychosis.

TABLE 3 Sleep parameters associated with global and callosal fractional anisotropy.

	Global mean FA			Corpus callosum FA		
	UHR	HC	ALL	UHR	HC	ALL
Karolinska Sleep Questionnaire (the last 4 weeks)						
DSI	$r = 0.133$ $p = 0.328$	$r = 0.296$ $p = 0.106$	$r = -0.031$ $p = 0.774$	$r = 0.156$ $p = 0.250$	$r = 0.319$ $p = 0.080$	$r = -0.015$ $p = 0.887$
AWI	$r = -0.111$ $p = 0.415$	$r = 0.095$ $p = 0.610$	**$r = -0.216$** **$p = 0.040$**	$r = -0.173$ $p = 0.203$	$r = 0.231$ $p = 0.211$	**$r = -0.230$** **$p = 0.029$***
Actigraphy (last night)						
SE	$r = 0.166$ $p = 0.221$	$r = 0.212$ $p = 0.251$	$r = 0.186$ $p = 0.078$	$r = 0.225$ $p = 0.096$	$r = 0.303$ $p = 0.097$	**$r = 0.243$** **$p = 0.020$***
TST	$r = -0.100$ $p = 0.464$	$r = 0.275$ $p = 0.134$	$r = -0.029$ $p = 0.788$	$r = -0.113$ $p = 0.407$	$r = 0.253$ $p = 0.169$	$r = -0.041$ $p = 0.702$
WASO	**$r = -0.295$** **$p = 0.027$**	$r = 0.016$ $p = 0.932$	**$r = -0.215$** **$p = 0.041$**	**$r = -0.337$** **$p = 0.011$***	$r = -0.165$ $p = 0.376$	**$r = -0.283$** **$p = 0.007$***
SFI	**$r = -0.274$** **$p = 0.041$**	$r = 0.231$ $p = 0.212$	$r = -0.187$ $p = 0.076$	**$r = -0.313$** **$p = 0.019$***	$r = 0.173$ $p = 0.352$	**$r = -0.225$** **$p = 0.032$***

Table displays results from the partial correlation-analyses between mean global and callosal fractional anisotropy (FA) and sleep parameters, covaried for age, sex, and relative and absolute motion in scanner. Pearson's correlation tests were two-tailed. Bootstrapping (×1,000) was performed to provide confidence intervals.
Significance level under $p < 0.05$ are marked in bold. *Indicates significant correlation $p < 0.05$ after FDR correction for multiple comparisons according to the Benjamin-Hochberg procedure.
AWI, Disturbed awakening index; CI, confidence interval, DSI, Disturbed sleep index; FA, fractional anisotropy, HC, Healthy controls; *r*, correlation coefficient; SE, sleep efficiency; SFI, sleep fragmentation index; TST, total sleep time; UHR, individuals at ultra-high risk; WASO, wake after sleep onset.

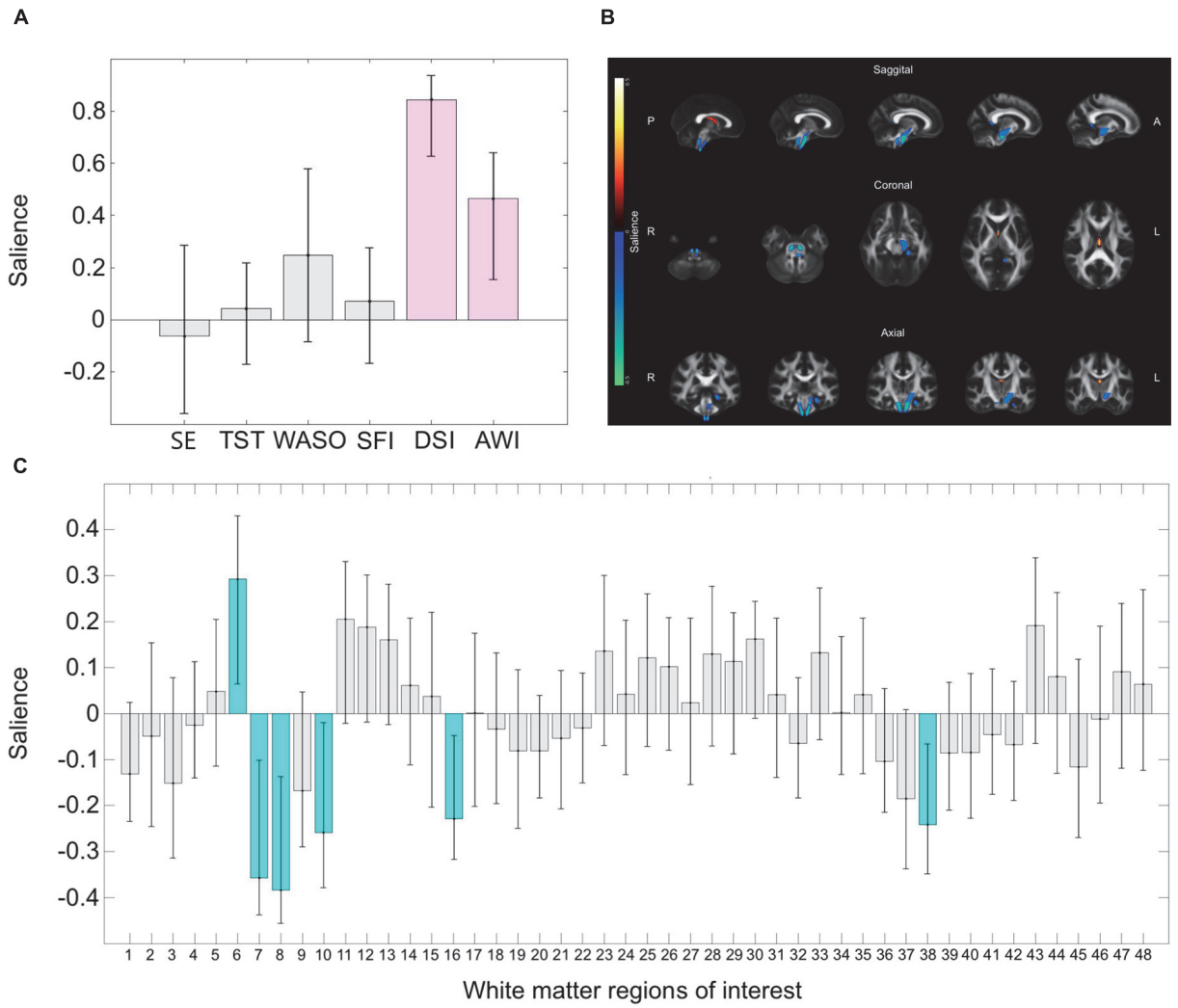

FIGURE 3
Multivariate correlations between sleep measures and regional fractional anisotropy. Figure displays the results from the multivariate PLS-C analyses on UHR individuals linking covariance in a pattern of sleep disturbances with fractional anisotropy (FA) in 48 regions of interest. **(A)** The pattern of variance six measures of sleep disturbances show that higher disturbed sleep index (DSI) and disturbed awakening index (AWI) marked with purple contributes reliably to the pattern, as the confidence interval does not cross zero. **(B)** The pattern of sleep disturbances is linked to a pattern of regional covariance in FA. The regions of interest which contributes reliably are visualized with the regions contributing reliably projected on a standard brain derived from JHU white matter atlas. Regions colored yellow indicates higher FA, and blue color indicates lower FA. Reliably contributing regions are fornix (higher FA) and left and right corticospinal tract, left cerebral peduncle, left medial lemniscus, and left cingulum (hippocampus) (lower FA). **(C)** The pattern of covariance in all 48 regions of interest, with the regions contributing reliably marked in turquoise. A list linking the numbers to the regions are displayed in the **Supplementary Text 3**. SE, sleep efficiency; JHU, John Hopkins University; L, left; R, right; SFI, sleep fragmentation index; TST, total sleep time; WASO, wake after sleep onset.

WM alterations (Wheeler and Voineskos, 2014). We identified an increased level of subjective sleep-wake disturbances (DSI and AWI) among UHR individuals compared to HC. These results indicate that both sleep continuity and awakening are disturbed in UHR individuals, congruent with a recent meta-analysis reporting significantly lower subjective sleep quality and significantly more fragmented sleep among high risk individuals (Clarke et al., 2021). We found no group difference regarding the objective measures from the actigraph. Research on objective sleep measures in UHR samples is scarce, as one trial has found significantly reduced SE and significantly higher (i.e., more negatively affected) WASO in UHR individuals compared to HC (Lunsford-Avery et al., 2015), but a recent meta-analysis could not confirm these findings (Clarke et al., 2021) and reported no group differences.

As hypothesized, lower FA in CC was associated with poorer outcomes in objective sleep-wake measures in UHR individuals, although no group difference in the actigraphy outcomes were observed. Lower FA was linked to more time spend awake after sleep had occurred and restlessness during

the sleep period, indicating more disrupted sleep in UHR individuals, but not in HC. Nonetheless, when testing all participants, the identical associations remained significant after correction for multiplicity, which may reflect a problem with power due to the smaller sample of HCs. The indication that associations between regional FA and disturbed sleep-wake measures are more pronounced in the patient group than in HC was corroborated by the multivariate PLS-C within-group analyses on all ROIs. Interestingly, this perspective has become increasingly acknowledged, as several studies have concluded that contrary to HC, behavioral measures appear more vigorously associated with and dependent on the structural characteristics of WM in UHR individuals and patients with first-episode schizophrenia (Jessen et al., 2018; Kristensen et al., 2019). A similar finding is reported by Raikes et al. (2018) examining associations between subjectively reported sleep disturbances and FA when comparing patients with mild traumatic brain injury to controls (Raikes et al., 2018). Although they did not identify any group difference on FA, they found that higher regional FA was correlated with better sleep quality in patients with mild traumatic brain injury, but not in the controls.

In the full sample, the subjective sleep-wake measure AWI was significantly correlated with FA in CC but contrary to our expectations we did not find any firm associations between DSI and FA in CC. However, the overall association between sleep-wake disturbances and lower FA in widespread WM regions was corroborated in the sensitivity PLS-C analyses including both HCs and antipsychotic free UHR individuals (**Supplementary Figure 4A**). Hence, in both HC and UHR individuals in particular SE, WASO, SFI, and AWI appear associated with FA, most pronounced bilaterally and in left hemisphere WM regions located medial and ventrally. When examining UHR individuals and HC separately, the significant association with AWI was lost, likely due to loss of power, as the effect size was similar and the direction of the correlation for the UHR individuals was identical with that of the full sample. In support for this notion, the negative correlation between FA in CC and the objective sleep-wake measure WASO and SFI in the UHR individuals may be considered as corresponding to AWI.

Although it is difficult to compare results across diverse patient populations, Altendahl et al. (2020) have reported callosal FA to be significantly associated with duration of REM-sleep in older adults but could not confirm any links between FA and subjective sleep measures or SE and TST (Altendahl et al., 2020). In another longitudinal study by Telzer et al. (2015) sleep variability in adolescents predicted callosal FA after 1.5 years (Telzer et al., 2015). Both in patients with callosal agenesis (Nielsen et al., 1992) and callosotomy (Avvenuti et al., 2019) studies have indicated that CC plays a vital role for the cross-hemispheric propagation of sleep oscillations and that aberrant callosal FA may potentially interfere with synchronization both in interhemispheric activity as well as in neuronal populations within each hemisphere. Our results confirm the involvement of callosal FA in sleep-wake disturbances as measured by actigraphy in UHR individuals, although we cannot infer any causality due to the cross-sectional design.

The multivariate correlation test revealed a link between the Karolinska sleep measures of DSI and AWI contributing reliably as indicative of sleep-wake disturbances, associated with a pattern of lower FA in 5 ROIs, as well as higher FA in fornix contributing reliably. The ROIs contributing reliably appear mainly to be located ventrally, which is in accordance with previous research locating sleep-wake regulation to sub-thalamic circuits in the brainstem (Tahmasian et al., 2021). We speculate if our findings could be extended to WM connecting deep nuclei structures involved in sleep-wake regulation, such as the brain stem with thalamus, hypothalamus, and basal forebrain. Unfortunately, the current MRI technology does not offer such resolution and our analysis therefore did not include these structures.

Interestingly, FA in CC did not contribute reliably, which indicates that the subjective sleep-wake disturbances may predominantly be linked to other WM networks, compared to the actigraphy measures. Our result may reflect the notion that different aspects of sleep-wake regulation potentially is linked to specialized and differentiated neuronal circuits and corresponding structural networks (Héricé and Sakata, 2019). Sleep-wake regulation involves a complex network including different brain regions and neurotransmitters, and studies have identified that specific damages on different parts of this network result in various types of sleep-wake disturbances (Schwartz and Roth, 2009; Brown et al., 2012; Scammell et al., 2017). Hence, our results may reflect how the discrepancy between self-reported and objective measures of sleep have been interpreted as the measurement of different constructs which present with different biological underpinnings (Rezaie et al., 2018).

The directionality of FA may depend on the patient sample or region of interest (Thomason and Thompson, 2011). FA is an averaged measure derived from the diffusion signal. Hence, being susceptible for extracellular fluids and crossing fibers (Weinberger and Radulescu, 2020), FA lacks microstructural specificity and great caution in the interpretation must be exhibited, as there is no direct correspondence between the MRI-derived measures and the biological underpinnings (Weinberger and Radulescu, 2020). In particular considering the contra intuitive directionality of FA in fornix contributing reliably in the PLS-C, the interpretation must be exhibited cautiously due to fornix' proximity to cerebrospinal fluid, which could induce volume effects (Kaufmann et al., 2017).

Our results indicate, that although use of nicotine may affect sleep measures, no substance use affected the association between WM and sleep in CC. Previous studies have reported mixed results, a metanalysis found that substance use disorder (alcohol, cocaine and opiates) was associated with FA in CC,

but for cannabis and nicotine the results were mixed (Hampton et al., 2019). However, the prevalence of substance use disorder in our sample is limited, and the study was not specifically designed to address this topic, and the result must therefore be interpreted cautiously.

Our exploratory analyses from partial correlations revealed that medication and psychopathology did not confound the association between FA and the measures of WASO and SFI. The result is not surprising, as we did not observe any group difference on these measures comparing UHR individuals to HC. However, the *post hoc* sensitivity PLS-C analyses on antipsychotic-free UHR individuals indicated a potential effect of antipsychotic medication on the association between sleep-wake measures and FA. The pattern of sleep-wake disturbances in antipsychotic free UHR individuals indicated that mainly reduced sleep-time (lower TST) and disturbed sleep (higher DSI) contributed reliably to the covariation with lower regional FA (**Supplementary Figure 4B**). When UHR individuals on antipsychotic medication were included, sleep time (TST) was no longer contributing reliably to the pattern of sleep-wake disturbances, whereas difficulties in awakening, non-refreshing sleep and exhaustion at awakening (higher AWI) were added as reliable contributors (**Figure 3**). Although the results with the reduced sample size were only at trend level, we notice that it appeared to reflect the sedative effect antipsychotic medication can have, which lends some external and clinical validity to the finding that antipsychotic medication may confound the association between sleep-wake disturbances and regional FA by inducing more sleep time yet increased sleepiness at awakening. It appears to be recommendable to examine the effect of antipsychotics when investigating sleep disturbances.

Finally, in the multivariate PLS-C, the level of depressive symptoms (MADRS) as well as the level of UHR-symptoms (CAARMS) appeared to confound the association between regional FA and AWI as well as DSI suggesting that the subjective sleep-wake measures may be more susceptible for level of psychopathology. Moreover, the group difference between UHR individuals and HCs on AWI and DSI were highly significant. As a result of this finding, we *post-hoc* explored if level of depressive and UHR-symptoms would mediate the association between regional FA contributing reliably and AWI/DSI (**Supplementary Table 9**). As one pathway between regional FA and psychopathology were only at trend level (p = 0.063), the model did not fulfill requirements for establishing a mediation effect, although all other requirements were met and a significant mediation effect appeared to be present, showing that level of depressive symptoms mediated the association between FA in fornix and DSI. We believe this trend level association may be due to reduced power, hence reflecting a Type 2 error. A recent study demonstrated how diffusion metrics within the CC partially mediated the associations between poor sleep quality/high stress and depressive symptomatology (Li et al., 2020). To confirm the finding of a potential mediating effect of level of psychopathology on the link between WM microstructure and sleep-wake disturbances (which potentially could explain the different associations in patients compared to controls), a study with a larger sample size designed for the purpose needs to be performed.

Methodological considerations

PLS-C can be difficult to interpret due to the complexity of linking multivariate data patterns. Furthermore, we did not identify any clear interaction effect. However, repeating the within-group analyses from the primary analyses appeared to confirm aspects of our univariate findings and contribute with additional and more specific information on the associations between WM ROIs and sleep-wake disturbances.

A general limitation to the study is the fact that the analyses were secondary to an RCT and this research question was formulated *post-hoc*. Furthermore, the matching between HC and UHR individuals in the main trial was not complete in this subsample. Further, we would optimally have cross-validated our results in an independent sample. As this was not possible, the results must be interpreted cautiously and should be evaluated as hypothesis generating with a need for replication in a larger sample. Nonetheless, we trust the consistent associations across multiple tests to represent a valuable contribution indicative of specific associations between regional WM and sleep in a group of vulnerable patients.

The actigraphy measures were only recorded for a 24-h period, which makes it susceptible to individual and spurious variations. Actigraphy tends to overestimate sleep length and efficiency compared to polysomnography, and overestimation is more pronounced in individuals with sleep-wake disturbances than in healthy individuals (Fekedulegn et al., 2020). To minimize this overestimation, we did supplement the actigraphy with a sleep diary, estimating time in bed more precisely, but unfortunately no data on daytime sleep were obtained. To increase the reliability of actigraphy compared to polysomnography (which determine sleep stages in contrast to actigraphy measures), studies have suggested a minimum of 5–7 consecutive nights of actigraphy, especially when measuring TST (Aili et al., 2017; Fekedulegn et al., 2020). The short duration of the actigraphic measurement reduces its power to detect between-group differences in this study. Furthermore, the one-night actigraphic measurement renders the data sensitive for bias due to lack of habituation to the equipment on the night of examination. This fact might explain why average WASO in the HC in this study was longer [55.74 min (42.64)] than what

is usually considered normative in healthy adults (Fekedulegn et al., 2020). This suggests that the primary finding in these UHR individuals are subjectively poor sleep quality. Hence, although the actigraphy data are not optimally valid we nonetheless regard the contribution valuable, as the results appear clinically meaningful as well as mutually confirming.

Strengths of this study comprise the consistent use of relevant covariates along with a meticulous examination of potential confounders. Furthermore, we believe this is the first study to investigate links between WM and sleep-wake disturbances in UHR individuals. Although our findings call for replication in larger samples, our results may contribute with preliminary hypotheses regarding neurobiological underpinnings of a modifiable risk factor for developing psychosis. Future perspectives of examining the relationship between brain structure/functioning and sleep parameters might be suggested to include AI techniques. With this approach multiple sources of information from advanced MR-scans, biological measures of sleep continuity/architecture and subjective measures of sleep quality could be modeled for purposes of prediction and eventually choice of treatment.

Conclusion

UHR individuals presented with lower global and callosal mean FA compared to HC. In UHR individuals, compromised callosal microstructure was associated with disturbed objectively measured sleep-wake functioning which was not confounded by substance use or medication. Subjectively measured sleep-wake disturbances were associated with a pattern of lower FA in ventrally located WM regions in UHR individuals. This association was not confounded by substance use or medication, but level of depressive and UHR symptoms partly explained it, pointing to a complex interaction between biological factors and psychopathology as determinants of the sleep-wake pattern. These findings suggest sleep disturbances as a potential treatment target, but future longitudinal studies are needed to address the direction of causality.

Data availability statement

The original contributions presented in this study are included in the article/**Supplementary material**, further inquiries can be directed to the corresponding author.

Ethics statement

The studies involving human participants were reviewed and approved by the Committee on Health Research Ethics of the Capital Region in Denmark (H-6-2013-015). The patients/participants provided their written informed consent to participate in this study.

Author contributions

JRs: analyzing data and writing up results. DN: designing study, preparing dataset, extracting/analyzing actigraphy data, and reviewing/writing. LG: study coordination, collecting data, and reviewing/writing. MJ: processing actigraphy data and reviewing/writing. AG: processing actigraphy data and reviewing/writing. JRg: processing MRI data and reviewing/writing. PJ: reviewing/writing. BG MN, and BE: financing and reviewing/writing. LB: designing study, financing and supervising JRs, and reviewing/writing. TK: conceptualizing and designing study, analyzing data, supervising JRs, and writing up results. All authors contributed to the article and approved the submitted version.

Funding

The original study and data collection was funded through the Danish Council for Independent Research (DFF-4004-00314); TrygFonden (ID 108119); the Mental Health Services in the Capital Region of Denmark; the Research Fund of the Capital Region of Denmark; the Lundbeck Foundation Center for Clinical Intervention and Neuropsychiatric Schizophrenia Research, CINS (R155-2013-16337); and Lundbeck Foundation grant for BYG (R316-2019-191). DN was supported by a grant from the Lundbeck Foundation (R287-2018-1485). TK was supported by a Brain and Behavior Research Foundation 2021 NARSAD Young Investigator Grant (ID 30112).

Acknowledgments

We thank all participants for their participation and the clinical staff for referrals and collaboration. Furthermore, we thank Research Partners Dana and Bill Starling for supporting TK as a Gregory and Tyler Starling Investigator.

Conflict of interest

Author BG has been the leader of a Lundbeck Foundation Centre of Excellence for Clinical Intervention and Neuropsychiatric Schizophrenia Research (CINS) (January 2009–December 2021), which was partially financed by an independent grant from the Lundbeck Foundation based on

international review and partially financed by the Mental Health Services in the Capital Region of Denmark, the University of Copenhagen, and other foundations. All grants are the property of the Mental Health Services in the Capital Region of Denmark and administrated by them. She has no other conflicts to disclose. Author BE has received lecture fees and/or is part of Advisory Boards of Bristol-Myers Squibb, Eli Lilly and Company, Janssen-Cilag, Otsuka Pharma Scandinavia AB, Boehringer Ingelheim, and Lundbeck Pharma A/S.

The remaining authors declare that the research was conducted in the absence of any commercial or financial relationships that could be construed as a potential conflict of interest.

Publisher's note

Supplementary material

The Supplementary Material for this article can be found online at: https://www.frontiersin.org/articles/10.3389/fnhum.2022.1029149/full#supplementary-material

References

Abdi, H., and Williams, L. J. (2013). Partial least squares methods: Partial least squares correlation and partial least square regression. *Comput. Toxicol.* 930, 549–579. doi: 10.1007/978-1-62703-059-5

Aili, K., Åström-Paulsson, S., Stoetzer, U., Svartengren, M., and Hillert, L. (2017). Reliability of actigraphy and subjective sleep measurements in adults: The design of sleep assessments. *J. Clin. Sleep Med.* 13, 39–47. doi: 10.5664/jcsm.6384

Åkerstedt, T., Knutsson, A., Westerholm, P., Theorell, T., Alfredsson, L., and Kecklund, G. (2002). Sleep disturbances, work stress and work hours: A cross-sectional study. *J. Psychosom. Res.* 53, 741–748. doi: 10.1016/S0022-3999(02)00333-1

Alexander, A. L., Hurley, S. A., Samsonov, A. A., Adluru, N., Hosseinbor, A. P., Mossahebi, P., et al. (2011). Characterization of cerebral white matter properties using quantitative magnetic resonance imaging stains. *Brain Connect.* 1, 423–446. doi: 10.1089/brain.2011.0071

Alexander, A. L., Lee, J. E., Lazar, M., and Field, A. S. (2007). Diffusion tensor imaging of the brain. *Neurotherapeutics* 4, 316–329. doi: 10.1016/j.nurt.2007.05.011

Ali, R., Awwad, E., Babor, T. F., Bradley, F., Butau, T., Farrell, M., et al. (2002). The Alcohol, Smoking and Substance Involvement Screening Test (ASSIST): Development, reliability and feasibility. *Addiction* 97, 1183–1194. doi: 10.1046/j.1360-0443.2002.00185.x

Altendahl, M., Cotter, D. L., Staffaroni, A. M., Wolf, A., Mumford, P., Cobigo, Y., et al. (2020). REM sleep is associated with white matter integrity in cognitively healthy, older adults. *PLoS One* 15:e0235395. doi: 10.1371/journal.pone.0235395

Andersson, J. L. R., Jenkinson, M., and Smith, S. (2007a). *Non-Linear Registration, Aka Spatial Normalisation*. FMRIB Technial Report TR07JA2. Oxford: Oxford University, . doi: 10.1016/j.neuroimage.2008.10.055

Andersson, J. L. R., Jenkinson, M., and Smith, S. M. (2007b). *Non-Linear Optimisation*. FMRIB technical report TR07JA1. Oxford: Oxford University

Andersson, J. L. R., Skare, S., and Ashburner, J. (2003). How to correct susceptibility distortions in spin-echo echo-planar images: Application to diffusion tensor imaging. *NeuroImage* 20, 870–888. doi: 10.1016/S1053-8119(03)00336-7

Andersson, J. L. R., and Sotiropoulos, S. N. (2016). An integrated approach to correction for off-resonance effects and subject movement in diffusion MR imaging. *NeuroImage* 125, 1063–1078. doi: 10.1016/j.neuroimage.2015.10.019

Avvenuti, G., Handjaras, G., Betta, M., Cataldi, J., Imperatori, L. S., Lattanzi, S., et al. (2019). Integrity of corpus callosum is essential for the cross-hemispheric propagation of sleep slow waves: A high-density EEG study in split-brain patients. *bioRxiv* 40, 5589–5603. doi: 10.1101/756676

Bernardi, G., Avvenuti, G., Cataldi, J., Lattanzi, S., Ricciardi, E., Polonara, G., et al. (2021). Role of corpus callosum in sleep spindle synchronization and coupling with slow waves. *Brain Commun.* 3:fcab108. doi: 10.1093/braincomms/fcab108

Bora, E., Yucel, M., and Pantelis, C. (2009). Theory of mind impairment in schizophrenia: Meta-analysis. *Schizophr. Res.* 109, 1–9. doi: 10.1016/j.schres.2008.12.020

Brown, R. E., Basheer, R., McKenna, J. T., Strecker, R. E., and McCarley, R. W. (2012). Control of sleep and wakefulness. *Physiol. Rev.* 92, 1087–1187. doi: 10.1152/physrev.00032.2011

Canu, E., Agosta, F., and Filippi, M. (2015). A selective review of structural connectivity abnormalities of schizophrenic patients at different stages of the disease. *Schizophr. Res.* 161, 19–28. doi: 10.1016/j.schres.2014.05.020

Carletti, F., Woolley, J. B., Bhattacharyya, S., Perez-Iglesias, R., Fusar Poli, P., Valmaggia, L., et al. (2012). Alterations in white matter evident before the onset of psychosis. *Schizophr. Bull.* 38, 1170–1179. doi: 10.1093/schbul/sbs053

Carney, R., Cotter, J., Bradshaw, T., and Yung, A. R. (2017). Examining the physical health and lifestyle of young people at ultra-high risk for psychosis: A qualitative study involving service users, parents and clinicians. *Psychiatry Res.* 255, 87–93. doi: 10.1016/j.psychres.2017.05.023

Clarke, L., Chisholm, K., Cappuccio, F. P., Tang, N. K. Y., Miller, M. A., Elahi, F., et al. (2021). Sleep disturbances and the At Risk Mental State: A systematic review and meta-analysis. *Schizophr. Res.* 227, 81–91. doi: 10.1016/j.schres.2020.06.027

Clemm Von Hohenberg, C., Pasternak, O., Kubicki, M., Ballinger, T., Vu, M. A., Swisher, T., et al. (2014). White matter microstructure in individuals at clinical high risk of psychosis: A whole-brain diffusion tensor imaging study. *Schizophr. Bull.* 40, 895–903. doi: 10.1093/schbul/sbt079

Cui, Y., Dong, J., Yang, Y., Yu, H., Li, W., Liu, Y., et al. (2020). White matter microstructural differences across major depressive disorder, bipolar disorder and schizophrenia: A tract-based spatial statistics study. *J. Affect. Disord.* 260, 281–286. doi: 10.1016/j.jad.2019.09.029

Dhollander, T., Raffelt, D., and Connelly, A. (2016). Unsupervised 3-tissue response function estimation from single-shell or multi-shell diffusion MR data without a co-registered T1 image. *ISMRM Workshop Breaking Barriers Diffusion MRI* 35:5.

Ebdrup, B. H., Raghava, J. M., Nielsen, M. Ø, Rostrup, E., and Glenthøj, B. (2015). Frontal fasciculi and psychotic with symptoms in patients schizophrenia before and after six weeks of selective dopamine D 2 / 3 receptor blockade. *J. Psychiatry Neurosci.* 41, 133–141. doi: 10.1503/jpn.150030

Fekedulegn, D., Andrew, M. E., Shi, M., Violanti, J. M., Knox, S., and Innes, K. E. (2020). Actigraphy-based assessment of sleep parameters. *Ann. Work Expo. Health.* 64, 350–367. doi: 10.1093/ANNWEH/WXAA007

First, M. B., Gibbon, M., Spitzer, R. L., Williams, J. B. W., and Benjamin, L. S. (1997). *Structured Clinical Interview for DSM-IV Axis II Personality Disorders (SCID-II)*. Washington, DC: American Psychiatric Press.

Friston, K. J. (1998). The disconnection hypothesis. *Schizophr. Res.* 30, 115–125. doi: 10.1016/S0920-9964(97)00140-0

Fusar-Poli, P., Salazar De Pablo, G., Correll, C. U., Meyer-Lindenberg, A., Millan, M. J., Borgwardt, S., et al. (2020). Prevention of psychosis: Advances in detection, prognosis, and intervention. *JAMA Psychiatry* 77, 755–765. doi: 10.1001/jamapsychiatry.2019.4779

Glenthøj, L. B., Fagerlund, B., Randers, L., Hjorthøj, C. R., Wenneberg, C., Krakauer, K., et al. (2015). The FOCUS trial: Cognitive remediation plus standard treatment versus standard treatment for patients at ultra-high risk for psychosis: Study protocol for a randomised controlled trial. *Trials* 16:25. doi: 10.1186/s13063-014-0542-8

Glenthøj, L. B., Mariegaard, L. S., Fagerlund, B., Jepsen, J. R. M., Kristensen, T. D., Wenneberg, C., et al. (2020). Effectiveness of cognitive remediation in the ultra-high risk state for psychosis. *World Psychiatry* 19, 54–55. doi: 10.1002/wps.20760

Grigg, O., and Grady, C. L. (2010). Task-related effects on the temporal and spatial dynamics of resting-state functional connectivity in the default network. *PLoS One* 5:e13311. doi: 10.1371/journal.pone.0013311

Grumbach, P., Opel, N., Martin, S., Meinert, S., Leehr, E. J., Redlich, R., et al. (2020). Sleep duration is associated with white matter microstructure and cognitive performance in healthy adults. *Hum. Brain Mapp.* 41, 4397–4405. doi: 10.1002/hbm.25132

Hampton, W. H., Hanik, I. M., and Olson, I. R. (2019). Substance abuse and white matter: Findings, limitations, and future of diffusion tensor imaging research. *Drug Alcohol Depend.* 197, 288–298. doi: 10.1016/j.drugalcdep.2019.02.005

Hayes, A. F. (2017). *Introduction to Mediation, Moderation, and Conditional Process Analysis*, Second Edi Edn. New York, NY: The Guilford Press.

Héricé, C., and Sakata, S. (2019). Pathway-dependent regulation of sleep dynamics in a network model of the sleep–wake cycle. *Front. Neurosci.* 13:1380. doi: 10.3389/fnins.2019.01380

Hjorthøj, C., Posselt, C. M., and Nordentoft, M. (2021). Development over time of the population-attributable risk fraction for cannabis use disorder in schizophrenia in denmark. *JAMA Psychiatry* 78, 1013–1019. doi: 10.1001/jamapsychiatry.2021.1471

Hua, K., Zhang, J., Wakana, S., Jiang, H., Li, X., Reich, D. S., et al. (2008). Tract probability maps in stereotaxic spaces: Analyses of white matter anatomy and tract-specific quantification. *Neuroimage* 39, 336–347. doi: 10.1055/s-0029-1237430.Imprinting

Huhn, A. S., Ellis, J. D., Dunn, Kelly, E., Scholler, D. J., Tabaschek, P., et al. (2022). Patient-reported sleep outcomes in randomized-controlled trials in persons with substance use disorders: A systematic review. *Drug Alcohol Depend.* 237:109508. doi: 10.1016/j.drugalcdep.2022.109508

Hunt, G. E., Large, M. M., Cleary, M., Lai, H. M. X., and Saunders, J. B. (2018). Prevalence of comorbid substance use in schizophrenia spectrum disorders in community and clinical settings, 1990–2017: Systematic review and meta-analysis. *Drug Alcohol Depend.* 191, 234–258. doi: 10.1016/j.drugalcdep.2018.07.011

Jenkins, L. M., Barba, A., Campbell, M., Lamar, M., Shankman, S. A., Leow, A. D., et al. (2016). Shared white matter alterations across emotional disorders: A voxel-based meta-analysis of fractional anisotropy. *NeuroImage* 12, 1022–1034. doi: 10.1016/j.nicl.2016.09.001

Jenkinson, M., Beckmann, C. F., Behrens, T. E. J., Woolrich, M. W., and Smith, S. M. (2012). Fsl. *NeuroImage* 62, 782–790. doi: 10.1016/j.neuroimage.2011.09.015

Jessen, K., Mandl, R. C. W., Fagerlund, B., Bojesen, K. B., Raghava, J. M., Obaid, H. G., et al. (2018). Patterns of cortical structures and cognition in antipsychotic-naïve patients with first-episode schizophrenia: A partial least squares correlation analysis. *Biol. Psychiatry* 4, 444–453. doi: 10.1016/J.BPSC.2018.09.006

Jones, D. K., Knösche, T. R., and Turner, R. (2013). White matter integrity, fiber count, and other fallacies: The do's and don'ts of diffusion MRI. *NeuroImage* 73, 239–254. doi: 10.1016/j.neuroimage.2012.06.081

Karlsgodt, K. H., Jacobson, S. C., Seal, M., and Fusar-Poli, P. (2012). The relationship of developmental changes in white matter to the onset of psychosis. *Curr. Pharm. Des.* 18, 422–433. doi: 10.2174/138161212799316073

Katagiri, N., Pantelis, C., Nemoto, T., Zalesky, A., Hori, M., Shimoji, K., et al. (2015). A longitudinal study investigating sub-threshold symptoms and white matter changes in individuals with an "at risk mental state" (ARMS). *Schizophr. Res.* 162, 7–13. doi: 10.1016/j.schres.2015.01.002

Kaufmann, L. K., Baur, V., Hänggi, J., Jäncke, L., Piccirelli, M., Kollias, S., et al. (2017). Fornix under water? ventricular enlargement biases forniceal diffusion magnetic resonance imaging indices in anorexia nervosa. *Biol. Psychiatry* 2, 430–437. doi: 10.1016/j.bpsc.2017.03.014

Khalsa, S., Hale, J. R., Goldstone, A., Wilson, R. S., Mayhew, S. D., Bagary, M., et al. (2017). Habitual sleep durations and subjective sleep quality predict white matter differences in the human brain. *Neurobiol. Sleep Circadian Rhythms* 3, 17–25. doi: 10.1016/j.nbscr.2017.03.001

Kocevska, D., Tiemeier, H., Lysen, T. S., De Groot, M., Muetzel, R. L., Van Someren, E. J. W., et al. (2019). The prospective association of objectively measured sleep and cerebral white matter microstructure in middle-aged and older persons. *Sleep* 42:zsz140. doi: 10.1093/sleep/zsz140

Kovacevic, N., Abdi, H., Beaton, D., and McIntosh, A. R. (2013). "Revisiting PLS Resampling: Comparing Significance vs. Reliability Across Range of Simulations," in *New Perspectives in Partial Least Squares and Related Methods*, eds H. Abdi, W. Chin, V. Esposito Vinzi, G. Russolillo, and L. Trinchera (New York, NY: Springer), 159–170. doi: 10.1007/978-1-4614-8283-3

Krakauer, K., Ebdrup, B. H., Glenthoj, B. Y., Raghava, J. M., Nordholm, D., Randers, L., et al. (2017). Patterns of white matter microstructure in individuals at ultra-high-risk for psychosis: Associations to level of functioning and clinical symptoms. *Psychol. Med.* 47, 2689–2707. doi: 10.1017/S0033291717001210

Krishnan, A., Williams, L. J., McIntosh, A. R., and Abdi, H. (2011). Partial Least Squares (PLS) methods for neuroimaging: A tutorial and review. *NeuroImage* 56, 455–475. doi: 10.1016/j.neuroimage.2010.07.034

Kristensen, T. D., Glenthøj, L. B., Ambrosen, K., Syeda, W., Ragahava, J. M., Krakauer, K., et al. (2021a). Global fractional anisotropy predicts transition to psychosis after 12 months in individuals at ultra-high risk for psychosis. *Acta Psychiatrica Scand.* 144, 448–463. doi: 10.1111/acps.13355

Kristensen, T. D., Glenthøj, L. B., Ragahava, J. M., Syeda, W., Mandl, R. C. W., Wenneberg, C., et al. (2021b). Changes in negative symptoms are linked to white matter changes in superior longitudinal fasciculus in individuals at ultra-high risk for psychosis. *Schizophr. Res.* 237, 192–201. doi: 10.1016/j.schres.2021.09.014

Kristensen, T. D., Mandl, R. C. W., Raghava, J. M., Jessen, K., Jepsen, J. R. M. J. R. M., Fagerlund, B., et al. (2019). Widespread higher fractional anisotropy associates to better cognitive functions in individuals at ultra-high risk for psychosis. *Hum. Brain Mapp.* 40:hbm.24765. doi: 10.1002/hbm.24765

Lagopoulos, J., Hermens, D. F., Hatton, S. N., Battisti, R. A., Tobias-Webb, J., White, D., et al. (2013). Microstructural white matter changes are correlated with the stage of psychiatric illness. *Trans. Psychiatry* 3:e248. doi: 10.1038/tp.2013.25

Li, C., Schreiber, J., Bittner, N., Li, S., Huang, R., Moebus, S., et al. (2020). White matter microstructure underlies the effects of sleep quality and life stress on depression symptomatology in older adults. *Front. Aging Neurosci.* 12:578037. doi: 10.3389/fnagi.2020.578037

Lunsford-Avery, J. R., LeBourgeois, M. K., Gupta, T., and Mittal, V. A. (2015). Actigraphic-measured sleep disturbance predicts increased positive symptoms in adolescents at ultra high-risk for psychosis: A longitudinal study. *Schizophr. Res.* 164, 15–20. doi: 10.1016/j.schres.2015.03.013

Mancuso, L., Uddin, L. Q., Nani, A., Costa, T., and Cauda, F. (2019). Brain functional connectivity in individuals with callosotomy and agenesis of the corpus callosum: A systematic review. *Neurosci. Biobehav. Rev.* 105, 231–248. doi: 10.1016/j.neubiorev.2019.07.004

McIntosh, A. R., and Lobaugh, N. J. (2004). Partial least squares analysis of neuroimaging data: Applications and advances. *NeuroImage* 23, 250–263. doi: 10.1016/j.neuroimage.2004.07.020

Montgomery, S. A., and Asberg, M. (1979). A new depression scale designed to be sensitive to change. *Br. J. Psychiatry* 134, 382–389.

Mori, S., and Van Zijl, P. (2007). Human white matter atlas. *Am. J. Psychiatry* 164:75390. doi: 10.1176/appi.ajp.164.7.1005

Morosini, P. L., Magliano, L., Brambilla, L., Ugolini, S., Pioli, R., MorosiniI, P.-L., et al. (2000). Development, reliability and acceptability of a new version of the DSM- IV Social Occupational Functioning Assessment Scale (SOFAS) to assess routine social functioning. *Acta Psychiatrica Scand.* 101, 323–329. doi: 10.1034/j.1600-0447.2000.101004323.x

Morrison, A. P., Stewart, S. L. K., French, P., Bentall, R. P., Birchwood, M., Byrne, R., et al. (2011). Early detection and intervention evaluation for people at high-risk of psychosis-2 (EDIE-2): Trial rationale, design and baseline characteristics. *Early Interv. Psychiatry* 5, 24–32. doi: 10.1111/j.1751-7893.2010.00254.x

Murray, R. M., Englund, A., Abi-Dargham, A., Lewis, D. A., Di Forti, M., Davies, C., et al. (2017). Cannabis-associated psychosis: Neural substrate and clinical impact. *Neuropharmacology* 124, 89–104. doi: 10.1016/j.neuropharm.2017.06.018

Murrie, B., Lappin, J., Large, M., and Sara, G. (2020). Transition of Substance-Induced, Brief, and Atypical Psychoses to Schizophrenia: A Systematic Review and Meta-analysis. *Schizophr. Bull.* 46, 505–516. doi: 10.1093/schbul/sbz102

Nägele, F. L., Pasternak, O., Bitzan, L. V., Mußmann, M., Rauh, J., Kubicki, M., et al. (2020). Cellular and extracellular white matter alterations indicate conversion

to psychosis among individuals at clinical high-risk for psychosis. *World J. Biol. Psychiatry* 22, 214–227. doi: 10.1080/15622975.2020.1775890

Nielsen, T., Montplaisir, J., and Lassonde, M. (1992). Sleep architecture in agenesis of the corpus callosum: Laboratory assessment of four cases. *J. Sleep Res.*1, 197–200. doi: 10.1111/j.1365-2869.1992.tb00038.x

Pantelis, C., Yücel, M., Wood, S. J., Velakoulis, D., Sun, D., Berger, G., et al. (2005). Structural brain imaging evidence for multiple pathological processes at different stages of brain development in schizophrenia. *Schizophr. Bull.* 31, 672–696. doi: 10.1093/schbul/sbi034

Pasternak, O., Sochen, N., Gur, Y., Intrator, N., and Assaf, Y. (2009). Free water elimination and mapping from diffusion MRI. *Magnet. Reson. Med.* 62, 717–730. doi: 10.1002/mrm.22055

Peters, B. D., Blaas, J., and de Haan, L. (2010). Diffusion tensor imaging in the early phase of schizophrenia: What have we learned? *J. Psychiatr. Res.* 44, 993–1004. doi: 10.1016/j.jpsychires.2010.05.003

Pettersson-Yeo, W., Allen, P., Benetti, S., McGuire, P., and Mechelli, A. (2011). Dysconnectivity in schizophrenia: Where are we now? *Neurosci. Biobehav. Rev.* 35, 1110–1124. doi: 10.1016/j.neubiorev.2010.11.004

Piantoni, G., Poil, S. S., Linkenkaer-Hansen, K., Verweij, I. M., Ramautar, J. R., Van Someren, E. J. W., et al. (2013). Individual differences in white matter diffusion affect sleep oscillations. *J. Neurosci.* 33, 227–233. doi: 10.1523/JNEUROSCI.2030-12.2013

Raikes, A. C., Bajaj, S., Dailey, N. S., Smith, R. S., Alkozei, A., Satterfield, B. C., et al. (2018). Diffusion Tensor Imaging (DTI) correlates of self-reported sleep quality and depression following mild traumatic brain injury. *Front. Neurol.* 9:468. doi: 10.3389/fneur.2018.00468

Reisfeld, B., and Mayeno, A. N. (2013). "On the Development and Validation of QSAR Models," in *Computational Toxicology. Methods in Molecular Biology*, Vol. 930, eds B. Reisfeld and A. Mayeno (Totowa, NJ: Humana Press), 499–526. doi: 10.1007/978-1-62703-059-5_21

Rezaie, L., Fobian, A. D., McCall, W. V., and Khazaie, H. (2018). Paradoxical insomnia and subjective–objective sleep discrepancy: A review. *Sleep Med. Rev.* 40, 196–202. doi: 10.1016/j.smrv.2018.01.002

Rigucci, S., Santi, G., Corigliano, V., Imola, A., Rossi-Espagnet, C., Mancinelli, I., et al. (2016). White matter microstructure in ultra-high risk and first episode schizophrenia: A prospective study. *Psychiatry Res. Neuroimag.* 247, 42–48. doi: 10.1016/j.pscychresns.2015.11.003

Roalf, D. R., Quarmley, M., Elliott, M. A., Satterthwaite, T. D., Vandekar, S. N., Ruparel, K., et al. (2016). The Impact of Quality Assurance Assessment on Diffusion Tensor Imaging Outcomes in a Large-Scale Population-Based Cohort. *NeuroImage* 125, 903–919. doi: 10.1016/j.neuroimage.2015.10.068

Saito, J., Hori, M., Nemoto, T., Katagiri, N., Shimoji, K., Ito, S., et al. (2017). Longitudinal study examining abnormal white matter integrity using a tract-specific analysis in individuals with a high risk for psychosis. *Psychiatry Clin. Neurosci.* 71, 530–541. doi: 10.1111/pcn.12515

Salazar De Pablo, G., Radua, J., Pereira, J., Bonoldi, I., Arienti, V., Besana, F., et al. (2021). Probability of transition to psychosis in individuals at clinical high risk: An updated meta-analysis. *JAMA Psychiatry* 78, 970–978. doi: 10.1001/jamapsychiatry.2021.0830

Samartzis, L., Dima, D., Fusar-Poli, P., and Kyriakopoulos, M. (2014). White matter alterations in early stages of schizophrenia: A systematic review of diffusion tensor imaging studies. *J. Neuroimag.* 24, 101–110. doi: 10.1111/j.1552-6569.2012.00779.x

Scammell, T. E., Arrigoni, E., and Lipton, J. O. (2017). Neural circuitry of wakefulness and sleep. *Neuron* 93, 747–765. doi: 10.1016/j.neuron.2017.01.014

Schwartz, J., and Roth, T. (2009). Neurophysiology of sleep and wakefulness: Basic science and clinical implications. *Curr. Neuropharmacol.* 6, 367–378. doi: 10.2174/157015908787386050

Sexton, C. E., Zsoldos, E., Filippini, N., Griffanti, L., Winkler, A., Mahmood, A., et al. (2017). Associations between self-reported sleep quality and white matter in community-dwelling older adults: A prospective cohort study. *Hum. Brain Mapp.* 38, 5465–5473. doi: 10.1002/hbm.23739

Smith, S. M., Jenkinson, M., Johansen-Berg, H., Rueckert, D., Nichols, T. E., Mackay, C. E., et al. (2006). Tract-based spatial statistics: Voxelwise analysis of multi-subject diffusion data. *NeuroImage* 31, 1487–1505. doi: 10.1016/j.neuroimage.2006.02.024

Smith, S. M., Jenkinson, M., Woolrich, M. W., Beckmann, C. F., Behrens, T. E. J. J., Johansen-Berg, H., et al. (2004). Advances in functional and structural MR image analysis and implementation as FSL. *NeuroImage* 23, 208–219. doi: 10.1016/j.neuroimage.2004.07.051

Song, S. K., Sun, S. W., Ramsbottom, M. J., Chang, C., Russell, J., and Cross, A. H. (2002). Dysmyelination revealed through MRI as increased radial (but unchanged axial) diffusion of water. *NeuroImage* 17, 1429–1436. doi: 10.1006/nimg.2002.1267

Tahmasian, M., Aleman, A., Andreassen, O. A., Arab, Z., Baillet, M., Benedetti, F., et al. (2021). ENIGMA-Sleep: Challenges, opportunities, and the road map. *J. Sleep Res.* 30:e13347. doi: 10.1111/jsr.13347

Telzer, E. H., Goldenberg, D., Fuligni, A. J., Lieberman, M. D., and Gálvan, A. (2015). Sleep variability in adolescence is associated with altered brain development. *Dev. Cogn. Neurosci.* 14, 16–22. doi: 10.1016/j.dcn.2015.05.007

Thomason, M. E., and Thompson, P. M. (2011). Diffusion imaging, white matter, and psychopathology. *Annu. Rev. Clin. Psychol.* 7, 63–85. doi: 10.1146/annurev-clinpsy-032210-104507

Trimmel, K., Eder, H. G., Böck, M., Stefanic-Kejik, A., Kl ösch, G., and Seidel, S. (2021). The (mis)perception of sleep: Factors influencing the discrepancy between self-reported and objective sleep parameters. *J. Clin. Sleep Med.* 17, 917–924. doi: 10.5664/jcsm.9086

Veraart, J., Fieremans, E., and Novikov, D. S. (2016a). Diffusion MRI noise mapping using random matrix theory. *Magnet. Reson. Med.* 76, 1582–1593. doi: 10.1002/mrm.26059

Veraart, J., Novikov, D. S., Christiaens, D., Ades-aron, B., Sijbers, J., and Fieremans, E. (2016b). Denoising of diffusion MRI using random matrix theory. *NeuroImage* 142, 394–406. doi: 10.1016/j.neuroimage.2016.08.016

Vijayakumar, N., Bartholomeusz, C., Whitford, T., Hermens, D. F., Nelson, B., Rice, S., et al. (2016). White matter integrity in individuals at ultra-high risk for psychosis: A systematic review and discussion of the role of polyunsaturated fatty acids. *BMC Psychiatry* 16:287. doi: 10.1186/s12888-016-0932-4

Vitolo, E., Tatu, M. K., Pignolo, C., Cauda, F., Costa, T., Ando, A., et al. (2017). White matter and schizophrenia: A meta-analysis of voxel-based morphometry and diffusion tensor imaging studies. *Psychiatry Res. Neuroimag.* 270, 8–21. doi: 10.1016/j.pscychresns.2017.09.014

Waite, F., Sheaves, B., Isham, L., Reeve, S., and Freeman, D. (2020). Sleep and schizophrenia: From epiphenomenon to treatable causal target. *Schizophr. Res.* 221, 44–56. doi: 10.1016/j.schres.2019.11.014

Weinberger, D. R., and Radulescu, E. (2020). Structural Magnetic Resonance Imaging All over Again. *JAMA Psychiatry* 78, 11–12. doi: 10.1001/jamapsychiatry.2020.1941

Wheeler, A. L., and Voineskos, A. N. (2014). A review of structural neuroimaging in schizophrenia: From connectivity to connectomics. *Front. Hum. Neurosci.* 8:653. doi: 10.3389/fnhum.2014.00653

Yung, A. R., and Nelson, B. (2011). Young people at ultra high risk for psychosis: A research update. *Early Interv. Psychiatry* 5, 52–57. doi: 10.1111/j.1751-7893.2010.00241.x

Yung, A. R., Yuen, H. P., McGorry, P. D., Phillips, L. J., Kelly, D., Dell'Olio, M., et al. (2005). Mapping the onset of psychosis: The Comprehensive Assessment of at-risk mental states. *Aust. N. Zealand J. Psychiatry* 39, 964–971. doi: 10.1111/j.1440-1614.2005.01714.x

Zaks, N., Velikonja, T., Parvaz, M. A., Zinberg, J., Done, M., Mathalon, D. H., et al. (2022). Sleep disturbance in individuals at clinical high risk for psychosis. *Schizophr. Bull.* 48, 111–121. doi: 10.1093/schbul/sbab104

Zhang, Y., Brady, M., and Smith, S. (2001). Segmentation of brain MR images through a hidden Markov random field model and the expectation-maximization algorithm. *IEEE Trans. Med. Imaging* 20, 45–57. doi: 10.1109/42.906424

Zhao, G., Lau, W. K. W., Wang, C., Yan, H., Zhang, C., Lin, K., et al. (2022). A comparative multimodal meta-analysis of anisotropy and volume abnormalities in white matter in people suffering from bipolar disorder or schizophrenia. *Schizophr. Bull.* 48, 69–79. doi: 10.1093/schbul/sbab093

Zitser, J., Anatürk, M., Zsoldos, E., Mahmood, A., Filippini, N., Suri, S., et al. (2020). Sleep duration over 28 years, cognition, gray matter volume, and white matter microstructure: A prospective cohort study. *Sleep* 43:zsz290. doi: 10.1093/sleep/zsz290

frontiers | Frontiers in Human Neuroscience

TYPE Original Research
PUBLISHED 10 November 2022
DOI 10.3389/fnhum.2022.1001692

OPEN ACCESS

EDITED BY
Felix Brandl,
Technical University of Munich,
Germany

REVIEWED BY
Feng Chen,
Hainan General Hospital, China
Eduardo Castro,
University of New Mexico,
United States
Li Kong,
Shanghai Normal University, China

*CORRESPONDENCE
Kelly Rootes-Murdy
rootesmurdy@gmail.com

†These authors have contributed equally to this work

SPECIALTY SECTION
This article was submitted to Brain Imaging and Stimulation, a section of the journal Frontiers in Human Neuroscience

RECEIVED 23 July 2022
ACCEPTED 17 October 2022
PUBLISHED 10 November 2022

CITATION
Rootes-Murdy K, Edmond JT, Jiang W, Rahaman MA, Chen J, Perrone-Bizzozero NI, Calhoun VD, van Erp TGM, Ehrlich S, Agartz I, Jönsson EG, Andreassen OA, Westlye LT, Wang L, Pearlson GD, Glahn DC, Hong E, Buchanan RW, Kochunov P, Voineskos A, Malhotra A, Tamminga CA, Liu J and Turner JA (2022) Clinical and cortical similarities identified between bipolar disorder I and schizophrenia: A multivariate approach.
Front. Hum. Neurosci. 16:1001692.
doi: 10.3389/fnhum.2022.1001692

Clinical and cortical similarities identified between bipolar disorder I and schizophrenia: A multivariate approach

Kelly Rootes-Murdy[1,2*†], Jesse T. Edmond[1,2†], Wenhao Jiang[3], Md A. Rahaman[2], Jiayu Chen[2], Nora I. Perrone-Bizzozero[4], Vince D. Calhoun[1,2], Theo G. M. van Erp[5,6], Stefan Ehrlich[7], Ingrid Agartz[8,9,10,11], Erik G. Jönsson[8,9], Ole A. Andreassen[8,10], Lars T. Westlye[8,10,12], Lei Wang[13], Godfrey D. Pearlson[14,15], David C. Glahn[15,16], Elliot Hong[17], Robert W. Buchanan[17], Peter Kochunov[17], Aristotle Voineskos[18], Anil Malhotra[19], Carol A. Tamminga[20], Jingyu Liu[2] and Jessica A. Turner[13]

[1]Department of Psychology, Georgia State University, Atlanta, GA, United States, [2]Tri-Institutional Center for Translational Research in Neuroimaging and Data Science (TReNDS), Georgia Institute of Technology, Georgia State University, Emory University, Atlanta, GA, United States, [3]Department of Psychosomatics and Psychiatry, Medical School, Zhongda Hospital, Institute of Psychosomatics, Southeast University, Nanjing, China, [4]Department of Neurosciences, University of New Mexico, Albuquerque, NM, United States, [5]Clinical Translational Neuroscience Laboratory, Department of Psychiatry and Human Behavior, University of California, Irvine, Irvine, CA, United States, [6]Center for the Neurobiology of Learning and Memory, University of California, Irvine, Irvine, CA, United States, [7]Division of Psychological and Social Medicine and Developmental Neurosciences, Faculty of Medicine, TU Dresden, Dresden, Germany, [8]Division of Mental Health and Addiction, Norwegian Centre for Mental Disorders Research (NORMENT), Institute of Clinical Medicine, Oslo University Hospital, University of Oslo, Oslo, Norway, [9]Department of Clinical Neuroscience, Centre for Psychiatry Research, Karolinska Institute and Stockholm Health Care Services, Stockholm, Sweden, [10]K. G. Jebsen Centre for Neurodevelopmental Disorders, University of Oslo, Oslo, Norway, [11]Department of Psychiatric Research, Diakonhjemmet Hospital, Oslo, Norway, [12]Department of Psychology, University of Oslo, Oslo, Norway, [13]Psychiatry and Behavioral Health, Ohio State Wexner Medical Center, Columbus, OH, United States, [14]Department of Psychiatry, Yale University, New Haven, CT, United States, [15]Olin Neuropsychiatry Research Center, Institute of Living, Hartford Hospital, Hartford, CT, United States, [16]Boston Children's Hospital and Harvard Medical School, Boston, MA, United States, [17]Department of Psychiatry, Maryland Psychiatric Research Center, University of Maryland School of Medicine, Baltimore, MD, United States, [18]Department of Psychiatry, Centre for Addiction and Mental Health, University of Toronto, Toronto, ON, Canada, [19]Division of Psychiatry Research, Zucker Hillside Hospital, Queens, NY, United States, [20]Department of Psychiatry, University of Texas Southwestern Medical School, Dallas, TX, United States

Background: Structural neuroimaging studies have identified similarities in the brains of individuals diagnosed with schizophrenia (SZ) and bipolar I disorder (BP), with overlap in regions of gray matter (GM) deficits between the two disorders. Recent studies have also shown that the symptom phenotypes associated with SZ and BP may allow for a more precise categorization than the current diagnostic criteria. In this study, we sought to identify GM alterations that were unique to each disorder and whether those alterations were also related to unique symptom profiles.

10.3389/fnhum.2022.1001692

Materials and methods: We analyzed the GM patterns and clinical symptom presentations using independent component analysis (ICA), hierarchical clustering, and n-way biclustering in a large ($N \sim 3{,}000$), merged dataset of neuroimaging data from healthy volunteers (HV), and individuals with either SZ or BP.

Results: Component A showed a SZ and BP < HV GM pattern in the bilateral insula and cingulate gyrus. Component B showed a SZ and BP < HV GM pattern in the cerebellum and vermis. There were no significant differences between diagnostic groups in these components. Component C showed a SZ < HV and BP GM pattern bilaterally in the temporal poles. Hierarchical clustering of the PANSS scores and the ICA components did not yield new subgroups. N-way biclustering identified three unique subgroups of individuals within the sample that mapped onto different combinations of ICA components and symptom profiles categorized by the PANSS but no distinct diagnostic group differences.

Conclusion: These multivariate results show that diagnostic boundaries are not clearly related to structural differences or distinct symptom profiles. Our findings add support that (1) BP tend to have less severe symptom profiles when compared to SZ on the PANSS without a clear distinction, and (2) all the gray matter alterations follow the pattern of SZ < BP < HV without a clear distinction between SZ and BP.

KEYWORDS

bipolar disorder, schizophrenia, multivariate analysis, ICA, PANSS

Introduction

Schizophrenia (SZ) and bipolar disorder (BP) are characterized by biological and clinical heterogeneity. Neuroimaging studies have found stable and replicable brain structural alterations associated with one or the other disorder [e.g., schizophrenia (Aine et al., 2017; Kochunov et al., 2019)]. There are also gray matter abnormalities related to specific symptom profiles such as psychosis (Meda et al., 2015; Clementz et al., 2016) or catatonia states (Hirjak et al., 2020), and to duration of illness instead of diagnosis, as well as confounds of medication(s) (Hartberg et al., 2015; Vita et al., 2015; Jørgensen et al., 2016; di Sero et al., 2019; Barth et al., 2020), or even structural patterns that cross diagnostic lines (Andreassen et al., 2013; Yao et al., 2017; Ruderfer et al., 2018; Kochunov et al., 2022). Untangling these unique structural features and related symptoms profiles from one another may allow us to find clinically meaningful subgroups within each disorder that may aid in the development of more precise diagnostic and treatment options.

Schizophrenia and BP are severe, heritable, and most importantly, debilitating mental illnesses both categorized by cognitive impairments, affective symptoms, and behavioral dysfunction (American Psychiatric Association, 2013). Structural neuroimaging studies have also identified similarities in the brain correlates of SZ and BP, with overlap in regions of gray matter (GM) deficits between the two disorders (Doan et al., 2017; Schwarz et al., 2019; Sorella et al., 2019; Lee D.-K. et al., 2020; Cheon et al., 2022). Accumulating evidence suggests that these two disorders may be better described along a continuum, not as two distinct disorders, of varying cognitive deficits and psychosis (Jabben et al., 2010; Hill et al., 2013). Examining SZ and BP together, as opposed to separately, may allow for the emergence of unique subgroups that may have been previously masked by diagnostic categories. Clementz et al. (2016) identified three distinct homogeneous subtypes based on a clinical profile of cognition and sensorimotor responses to functional tasks, rather than diagnostic boundaries, when SZ and BP with psychosis samples were combined (Clementz et al., 2016). This approach, and specifically these biomarkers have shown to replicate over time (Clementz et al., 2022) and have identified more precise representations of the symptom profiles associated with SZ and BP (Hudgens-Haney et al., 2020). We sought to expand upon these results through a multivariate approach

and a larger dataset ($N \sim 3{,}000$) of both individuals with schizophrenia and individuals with bipolar disorder I with psychosis.

While the heterogeneity between patients is substantial (Alnæs et al., 2019; Wolfers et al., 2021), schizophrenia has been associated with regional gray matter reductions throughout the cortex, analyzed either voxel by voxel or region by region (Honea et al., 2005; van Erp et al., 2018; Rootes-Murdy et al., 2021). Source-based morphometry (SBM), a multivariate approach, has identified covarying patterns of lower gray matter concentrations in the salience network, default mode network, insula-medial prefrontal cortex (MPFC), and the cerebellum (Turner et al., 2012; Ivleva et al., 2013; Gupta et al., 2015). One of the largest regional gray matter concentration effects was noted in the superior temporal gyrus (Gupta et al., 2015) and the cerebellum (Moberget et al., 2018). However, higher gray matter concentrations have been identified in the cerebellum (Gupta et al., 2015) and bilaterally in both the pre- and postcentral gyri (Mennigen et al., 2019). Regardless of the few discrepancies, there are clear patterns and structures with GM deficiencies in individuals with SZ. Similarly, gray matter analyses in BP have shown volumetric reductions throughout the cortex, with smaller effect sizes compared to SZ, however, these studies viewed BP in a general manner and did not specify bipolar subtype, or whether participants had psychosis (Murray et al., 2004; Bora, 2015; de Zwarte et al., 2019). Therefore, it remains unclear whether these two disorders are representations of discrete categories or if they fall along a spectrum of cognitive, affective, and behavioral disturbances.

In this study, we took a cross-disorder approach motivated by the overlapping symptoms and structural patterns observed in both schizophrenia and bipolar disorder. However, given the symptom variation within each disorder, we hypothesized that there may be subclusters within and across each disorder, that may help distinguish the underlying neural networks involved in each disorder. For example, delusions in bipolar disorder, were associated with gray matter reductions largely in the frontal cortex and amygdala and SZ showed similar patterns with additional contributions from subcortical regions (Rootes-Murdy et al., 2022). Within individuals with SZ, a symptom phenotype consisting of higher delusional symptoms, suspiciousness, hallucinations, and anxiety [measured from the Positive and Negative Syndrome Scale (PANSS); (Kay et al., 1987)] was associated with a covarying pattern of lower GM concentration in inferior temporal gyri and fusiform gyri and higher GM concentration in the sensorimotor cortex (Mennigen et al., 2019). A similar analysis in BP showed a symptom phenotype of mood symptoms (anxiety, depression, and guilt) was associated with lower GM concentration in the right middle/superior temporal gyrus (Jiang et al., 2020). The use of a large, cross-diagnostic sample may allow for examination of covarying gray matter patterns that are associated with these two disorders and with specific symptom presentations.

Structural studies in schizophrenia and bipolar disorder report inconsistencies on the patterns that are unique to each disorder, and how the shared symptoms between disorders relate to the structural deficits identified within the disorders. For this study, we sought to examine the differences and similarities in gray matter and symptom profiles between schizophrenia and bipolar disorder in a three-pronged approach. To compare the patterns of gray matter variation in a large, combined sample of schizophrenia, bipolar disorder, and healthy volunteers we used a multivariate data-driven approach, independent component analysis (ICA). Next, we used a hierarchical cluster analysis of psychosis subscales (PANSS positive, negative, and general) to identify patterns in the symptom presentation of schizophrenia and bipolar disorder and examine the groupings in symptom presentation. We also used hierarchical cluster analysis to identify pattern groupings in the gray matter concentration across participants using the ICA gray matter loading coefficients. Finally, we applied an N-way biclustering analysis (Rahaman et al., 2020) using both the PANSS subscales and the ICA loading coefficients to identify possible subgroups within and across each disorder that combine unique symptom and gray matter profiles.

Materials and methods

Participants

This study included data from 1,217 individuals diagnosed with schizophrenia, 301 individuals diagnosed with bipolar disorder I, and 1,543 unrelated healthy volunteers from the following datasets, many previously described in the literature; the Functional Imaging Biomedical Information Research Network study (FBIRN 3; multiple sites in the USA) (Potkin et al., 2009), the Center of Biomedical Research Excellence study (COBRE; Albuquerque, NM, USA) (Gupta et al., 2015), the Bipolar and Schizophrenia Network for Intermediate Phenotypes 1 study (B-SNIP 1; multiple sites in the USA) (Meda et al., 2015), the MIND Clinical Imaging Consortium study (MCIC; Albuquerque, NM, USA) (Gollub et al., 2013), the Northwestern University Schizophrenia Data study (NW; Chicago, IL, USA) (Wang et al., 2013), the Human Brain Informatics (HUBIN; Stockholm, Sweden) (Hall et al., 2002), Thematic Organized Psychosis [(TOP) research; Oslo, Norway] (Ringen et al., 2008; Rimol et al., 2012), Olin (Olin Center for Neuropsychiatric Research) (Yao et al., 2017), the Maryland Psychiatric Research Center (MPRC, Baltimore, MD, USA) (Kochunov et al., 2016, 2017), and from the Centre for Addiction and Mental Health (CAMH, Toronto, Canada) (Hawco et al., 2019). A diagnosis of SZ was confirmed by the Structured Clinical Interview for

Diagnosis (SCID) for Diagnostic and Statistical Manual of Mental Health 4th Edition (DSM-IV or DSM-IV TR) as part of each study site's protocol. For this study, participants with a diagnosis of SZ or schizophreniform were included. All data were collected under approval of local institutional review boards and all participants provided informed consent. The original study designs are described in the previous publications (cited above). Scanning information for each site can be found in **Table 1**. Participant demographic information including age, sex, diagnosis, and PANSS scores are included in **Table 2**.

MRI acquisition and preprocessing

T1-weighted structural MRI images were acquired from various scanners with information further detailed in the original studies (see **Table 1**). All T1-weighted images used the following preprocessing protocol for data harmonization. Images were co-registered and normalized to the standard Montreal Neurological Institute (MNI) template using a 12-parameter affine model, resliced to a voxel size of 2 mm × 2 mm × 2 mm and segmented into gray matter, white matter, and cerebro-spinal fluid using Statistical Parametric Mapping 12 (SPM12).[1] Individual images were correlated with the group-generated gray matter template, and images with low correlations with the template ($r < 0.87$) were removed as outliers in keeping with the standards of previous studies (Turner et al., 2012; Gupta et al., 2015). The remaining images were smoothed at 8 mm FWHM prior to analyses. These preprocessing steps resulted in a total of 3,018 gray matter concentration images (1,217 individuals diagnosed with schizophrenia, 301 individuals diagnosed with bipolar disorder I, and 1,543 unrelated healthy volunteers).

Independent component analysis

We utilized the source-based morphometry (SBM) module of the GIFT Toolbox[2] to perform independent component analysis (ICA) (Xu et al., 2009; Gupta et al., 2019). SBM identifies patterns which covary among the participants. This approach decomposes the gray matter images of the dataset into linear combinations of gray matter patterns or components. SBM is a linear model with the sum of component maps and participant loadings making up the input segmentation maps. This technique results in components (or patterns) of gray matter which covary across participants. The contribution of a component for each participant, or the individual

1 http://www.fil.ion.ucl.ac.uk/spm/software/spm12/

2 https://trendscenter.org/software/gift/

TABLE 1 Scanning and site information for each dataset.

Study	Size	Sites	Scanner (T)	Sequence	Voxel size (mm)	Orientation
BSNIP 1	773	5	GE Signa (3)	MPRAGE	1 × 1 × 1	Sagittal
			Philips Achieva (3)	IR-SPGR		
			Siemens Allegra (3)			
			Siemens Trio (3)			
			GE Signa HDxt (3)			
			Siemens Trio (3)			
CAMH	356	3	Siemens Trim Trio (3)	Grad Echo	1 × 1 × 1	
			GE Signa (3)	Grad Echo	1 × 1 × 1	
COBRE	148	1	Siemens Tim Trio (3)	MPRAGE	1 × 1 × 1	Sagittal
FBIRN3	343	8	Siemens Tim Trio (3)	MPRAGE	1.1 × 0.9 × 1.2	Sagittal
HUBIN	158	1	GE Signa (1.5)	SPGR	1 × 1 × 1	Coronal
MCIC	210	4	Siemens (1.5)	Grad Echo	0.625 × 0.625 × 1.5	Coronal
			GE Signa (1.5)	Grad Echo	0.664 × 0.664 × 1.6	
			Siemens Trio (3) Siemens (1.5)	MPRAGE	0.625 × 0.625 × 1.5	
				Grad Echo	0.625 × 0.625 × 1.5	
MPRC	389		Siemens Trio (3)	Grad Echo	1.7 × 1.7 × 3	Axial
			Allegra (3)		1.7 × 1.7 × 4	Axial
NW	136	1	Siemens (1.5)	MPRAGE	1 × 1 × 1	
Olin	159	1	Siemens Allegra (3)	Grad Echo	3.75 × 3.75 × 4	Ascending
TOP	387	1	Siemens (1.5)	MPRAGE	1.33 × 0.94 × 1	Sagittal

All scanning parameter information was obtained from the original study publications.

TABLE 2 Demographic information across sites.

	BSNIP	CAMH	COBRE	FBIRN	HUBIN	MCIC	MPRC	NW	Olin	TOP	Total
Total participants	774	356	148	343	158	210	389	136	159	387	3060
Age in years	35.62 (12.41)	32.05 (10.34)	35.51 (11.86)	38.36 (11.32)	41.65 (8.61)	33.08 (10.84)	35.69 (14.20)	32.72 (13.16)	32.74 (11.90)	33.41 (9.63)	35.41 (21.12)
Diagnosis											
BD	191	0	0	0	0	0	0	0	0	109	300
SZ	248	208	71	175	92	93	124	70	40	96	1217
HV	335	148	77	168	66	117	265	66	119	182	1543
Males (%)	376 (48.6%)	222 (62.4%)	111 (75%)	251 (73.2%)	107 (67.7%)	141 (67.1%)	205 (52.7%)	87 (64%)	87 (54.7%)	202 (52.2%)	1789 (58.5%)
Duration of illness in years	—	—	16.0 ± 12.0	18.0 ± 11.8	—	12.32 ± 10.5	—	13.09 ± 12.4	—	7.1 ± 6.3	14.27 ± 11.2
CPZ equivalent in mg/d	—	—	516.3 ± 1095.4	542.3 ± 1271.4	—	511.70 ± 721.9	—	—	—	—	653 ± 1094.9
Total PANSS scores	418	0	68	172	0	0	0	0	2	200	860
Positive subscale	15.12 (5.44)	—	15.18 (4.96)	15.37 (5.00)	—	—	—	—	11.00 (1.41)	12.11 (5.12)	14.47 (5.39)
Negative subscale	14.44 (5.64)	—	14.71 (4.62)	14.47 (5.59)	—	—	—	—	19.50 (13.44)	12.35 (5.91)	13.99 (5.70)
General subscale	30.71 (8.55)	—	29.93 (8.68)	28.63 (87.35)	—	—	—	—	30.00 (5.66)	28.28 (7.69)	29.66 (8.19)
PANSS total score	60.27 (16.70)	—	59.81 (14.40)	58.50 (14.85)	—	—	—	—	60.50 (17.68)	52.75 (16.08)	58.12 (16.28)

All values are means unless otherwise noted, SD in parenthesis. SD, standard deviation; BD, bipolar disorder; SZ, schizophrenia; HV, healthy volunteers; AP, antipsychotic medication; CPZ, chlorpromazine equivalent; PANSS, positive and negative symptom scale. Duration of illness was calculated as follows: COBRE, calculated by subtracting age at first psychiatric illness/symptoms from current age; FBIRN, calculated by subtracting age at first psychotic onset from current age; NW, DOI listed; MCIC, LENGTH_OF_ILLNESS variable which was based on diagnosis/treatment/onset through different algorithm.

10.3389/fnhum.2022.1001692

loading coefficient, indicates that that pattern of gray matter variation is specifically weighted for that individual (Xu et al., 2009).

The minimum description length (MDL) algorithm (Rissanen, 2018) estimated the number of components for the gray matter structural data to be 44. To ensure stability, the infomax ICA algorithm was applied with 10 runs and ICASSO (Himberg et al., 2004) determined the most stable run and number of components. High component stability was achieved for all but two components ($N = 42$).

Of the 44 components estimated in the ICA, the components with the highest variance percentages (>5%) were selected for the main analyses (4 total). First, we applied a linear mixed model (LMM) correction to the loading coefficients, including age and sex as fixed effects, and site (29 in total) as a random effect. The corrected loading coefficients were used in an ANOVA model as the dependent variables, with diagnostic group as a factor (healthy volunteers, bipolar disorder, and schizophrenia). Statistical results for all group comparisons (HV v BP; HV v SZ; BP v SZ) were thresholded at $\alpha < 0.0125$ with Bonferroni ($p = 0.05/4$) correction. Secondary ANOVA models for additional analyses are described below. For the secondary analyses, statistical results for all group comparisons (HV v BP; HV v SZ; BP v SZ) were thresholded at $\alpha < 0.00125$ with Bonferroni ($p = 0.05/40$) correction. All models were completed using R v3.6.2 (R Core Team, 2014).

Assessments

The Positive and Negative Syndrome Scale (PANSS) is the gold-standard symptom assessment for psychotic disorders (Kay et al., 1987) and one of the most commonly used questionnaires for symptom assessment in SZ over the last 2 weeks, and given the symptom overlap the PANSS has also been adopted to assess BP symptomatology (Kaltenboeck et al., 2016). Briefly, the PANSS allows for assessment of dimension specific abnormalities across positive, negative, and general symptoms. The positive symptom subscale includes seven items: delusions, conceptual disorganization, hallucinations, excitement, grandiosity, suspiciousness, and hostility (range: 7–49). The negative symptom subscale includes seven items: blunted affect, emotional withdrawal, poor rapport, passive/apathetic social withdrawal, difficulty in abstract thinking, lack of spontaneity and flow of conversation, and stereotyped thinking (range: 7–49). The general symptom subscale includes 16 items: somatic concerns, anxiety, guilt feelings, tension, mannerisms and posturing, motor retardation, uncooperativeness, unusual thought content, disorientation, poor attention, lack of judgment and insight, disturbance of volition, poor impulse control, preoccupation, and active social avoidance (range: 16–112). The PANSS was administered at six study sites, totaling 860 individuals with a completed PANSS (both SZ and BP diagnoses were included). For the purposes of this study, the PANSS subscales (positive, negative, and general psychopathology) were individually totaled and used for subsequent hierarchical cluster analyses and bicluster analyses (see below).

Hierarchical cluster analysis

Using individuals with PANSS scores ($N = 860$), we completed spectral clustering on the three subscales of the PANSS, which informed the number of eigenvalues. In brief, spectral clustering uses eigenvalues of the similarity matrix of the data to perform dimensionality reduction before clustering in the reduced space (von Luxburg, 2007). This analysis was completed using the normalized symmetric Laplacian matrix in MATLAB 2020b with the "*spectralcluster*" function (Ng et al., 2001). The number of eigenvalues approximating to or equaling zero was six and therefore, the three subscale scores were used to create six unique clusters. Using $k = 6$, we conducted a hierarchical cluster analysis with the PANSS subscales. A MANCOVA (FDR p corrected) was used to examine the differences in the loading coefficients from the ICA components between each of the resulting clusters of PANSS subscale scores.

The same clustering process was completed with all the loading coefficient values from the ICA ($N = 44$ components) on the same subset of individuals ($N = 860$). A hierarchical cluster analysis was utilized with $k = 4$ based on the spectral clustering estimate. Once again, a MANCOVA (FDR p corrected) was used to examine the differences in the PANSS subscale scores between each of the resulting clusters of loading coefficients.

N-way biclustering

Biclustering is a data mining technique that allows for pattern detection in large or high dimensional data. The n-way biclustering algorithm utilized in this study has been more completely described previously in the literature (Rahaman et al., 2020). We utilized the NBIC module of the GIFT Toolbox[3] to perform n-way biclustering. The algorithm uses a depth-first search (DFS) technique to explore the data matrix (subjects by measurements) with the goal of identifying submatrices with homogeneity in the pre-selected columns. It is not a requirement of the algorithm for the submatrices to involve the entire matrix and therefore, the resulting groupings may only involve a subset of the sample. In the data matrix for this study, the columns were composed of both the PANSS subscale scores and the loading

3 https://github.com/trendscenter/gift

10.3389/fnhum.2022.1001692

coefficients of 44 ICA components while participants were listed in the rows, resulting in an 860 × 47 matrix.

Results

Independent component analysis results

Gray matter clustering approach with ICA yielded 44 components. Of the 44 components, there were four components identified with high variance (>5%). From those four components, two (Components A and B) showed significant group differences; see **Figures 1**, **2** for more details. Component A identified a pattern of covarying gray matter bilaterally in the insula and cingulate gyrus and showed when comparing HV to both diagnostic groups [$F(2, 3056) = 115.42$, $p < 0.001$]. A Bonferroni's test for multiple comparisons (0.05/4) showed significant differences on the Component A loading coefficients between HV and SZ [$t(2443.73) = 14.47$, $p = 1.28E\text{-}45$] and BP [$t(1840) = 7.90$, $p < 4.78E\text{-}15$]. There were no significant differences on the loading coefficients between SZ and BP identified in this component [$t(1515) = 1.35$, $p = 0.173$]. Component B also showed more gray matter concentration in the cerebellar hemispheres and vermis when comparing HV to both diagnostic groups [$F(2, 3056) = 16.14$, $p < 0.001$]. Bonferroni's test for multiple comparisons found significant differences on the Component B loading coefficients between HV and SZ [$t(2757) = 5.53$, $p = 3.59E\text{-}8$] and BP [$t(1840) = 2.97$, $p = 0.003$]. Again, there were no significant differences between SZ and BP [$t(1515)$, $p = 0.636$].

Next, the remaining forty loading coefficients (with low variances) were compared for group differences [Bonferroni corrected for multiple comparisons (0.05/40)] using the same models as above. One component, Component C (variance = 0.62%; **Figure 3**), showed a significant group effect [$F(2, 3056) = 48.15$, $p < 0.001$] and Bonferroni's test found significant difference on the Component C loading coefficients between SZ and BP [$t(1515) = 3.95$, $p = 8.20E\text{-}5$]. This component identified a pattern of lower gray matter bilaterally in the temporal poles, with lower loading coefficients in SZ compared to BP ($p < 0.001$) and schizophrenia and healthy volunteers [$t(2757) = 9.78$, $p < 3.06E\text{-}22$]. Loading coefficients between individuals with bipolar disorder and healthy volunteers were similar for this component [$t(1840) = 1.97$, $p = 0.05$]. Component C is the only component that identified a distinction between SZ and BP.

There were 17 additional components that showed significant group effects. See **Table 3** for the component numbers, their spatial map peaks, and the statistics regarding the group effect size. See **Supplementary Table 1** for a list of all remaining components that did not show significant group differences.

Hierarchical clustering results

Schizophrenia had more severe symptoms in the PANSS positive [$t(675.649) = 11.02$, $p = 4.40E\text{-}26$], PANSS negative [$t(819.79) = 13.45$, $p = 2.10E\text{-}37$], and PANSS general [$t(658.72) = 6.16$, $p = 1.29E\text{-}9$] than BP. There was also a significant site effect ($N = 16$) for all PANSS subscales; PANSS positive [$F(15,844) = 6.266$, $p = 1.081E\text{-}12$], PANSS negative [$F(15,844) = 3.28$, $p = -2.4E\text{-}5$], and PANSS general [$F(15,844) = 7.940$, $p = 5.921E\text{-}17$]. In the hierarchical clustering analysis of the PANSS scores, while each cluster had participants with either SZ or BP diagnosis, there was a significant difference in diagnostic group membership across the six clusters [$\chi^2(5) = 86.68$, $p < 0.001$]. Cluster 6, characterized by lowest PANSS subscale scores had a significantly higher percentage of BP (53.1% of the cluster) than did any other cluster. Cluster 1, in contrast, was characterized by the highest PANSS negative, and slightly above average PANSS positive and general subscale scores, had only two individuals with BP (6.06%). See **Table 4** and **Figure 4** for more information on cluster membership, average symptoms, and diagnosis by cluster. See **Supplementary Figure 2** for the breakdown of the three PANSS subscales by each cluster. The clusters' membership was used as a grouping factor in a MANCOVA on all 44 components' loading coefficients (FDR p corrected). Cluster 2 had less gray matter in Component B [$F(5,854) = 3.44$, $p = 0.004$] than Cluster 3 and Cluster 6 but neither association passed FDR correction ($p = 0.008$ and $p = 0.007$, respectively). No other between groups association of cluster membership and loading coefficients passed FDR correction (all p values > 0.005).

In the hierarchical cluster analysis of the 44 gray matter components' loading coefficients, four clusters were identified. The four clusters appear to fall along the divisions of cortical regions, subcortical regions, and two cerebellar regions (see **Figure 5** and **Table 5** for cluster membership). There were no significant associations between membership in any of the four ICA clusters and the six PANSS clusters [$\chi^2(15) = 16.79$, $p = 0.331$]; any of the PANSS subscale scores (PANSS positive [$\chi^2(52) = 37.87$, $p = 0.929$]; PANSS negative [$\chi^2(58) = 57.20$, $p = 0.505$]; PANSS general [$\chi^2(78) = 93.33$, $p = 0.114$] or diagnostic group membership [$\chi^2(2) = 1.22$, $p = 0.543$]. **Supplementary Figure 1** details all the ICA components in the cluster groupings.

N-way biclustering

The bi-cluster analyses identified nine bi-clusters within the data matrix. Of those, three bi-clusters had high reliability ($freq > 3$). Spatial maps of the components included in these clusters, heat maps indicating the loading coefficients of each of these spatial maps, and heat maps of the related PANSS subscale scores are shown in **Figures 6–8**, respectively.

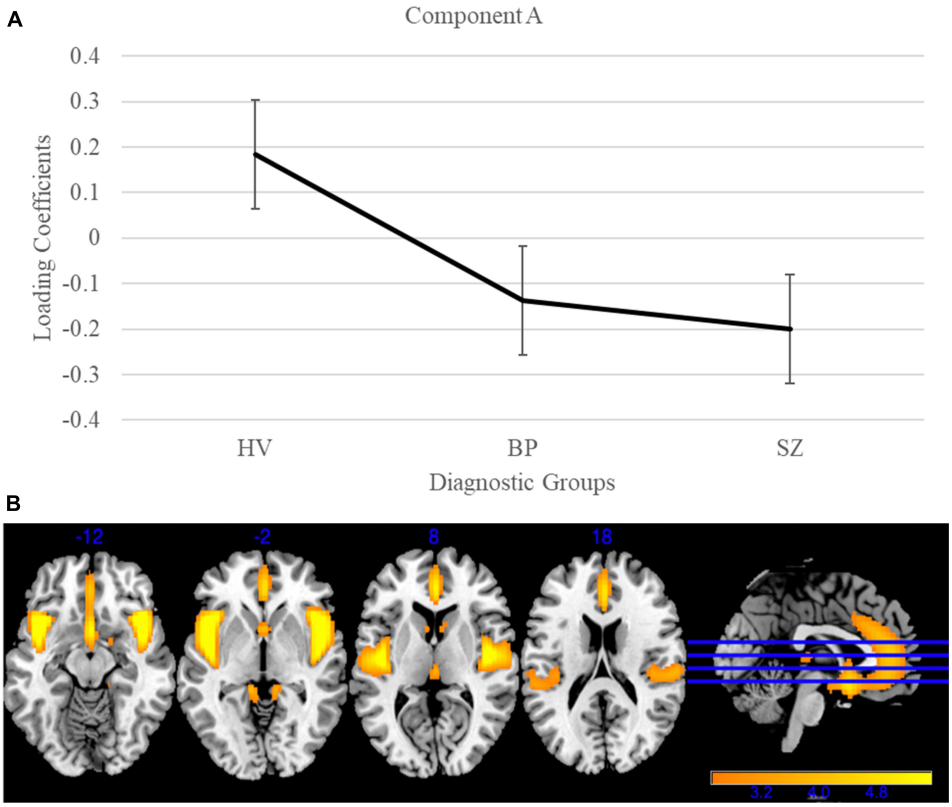

FIGURE 1
Gray matter group differences in independent component analysis (ICA) results for healthy volunteers, individuals with schizophrenia, and individuals with bipolar I disorder. **(A)** Group effects of diagnosis on loading coefficients for Component A. Schizophrenia (SZ) and bipolar disorder (BP) had significantly less gray matter when compared to healthy volunteers but did not differ significantly from each other. **(B)** Component A showed less gray matter concentration in the bilateral insula and cingulate gyrus in individuals with SZ and individuals with BP compared to healthy volunteers. Images are thresholded at 2.5.

Bicluster 1 included 80 individuals (14 BP; 66 SZ) and clustered on all three PANSS subscales (positive, negative, and general) and five ICA components. See Figure 6 for more details. The average age for bicluster 1 was 36.35 years old (SD = 11.08) and there were 50 male participants (62.50%). Bicluster 1 had more severe PANSS scores than the rest on all three subscales: positive mean = 20.14 (SD = 3.59); negative mean = 18.84 (SD = 5.44); general mean = 39.84 (SD = 6.30). The five ICA components showed varying degrees of alterations in the gray matter of the thalamus, cerebellum, occipital lobes, rectus, and the temporal poles. Of these, only two components (28 and C) showed group differences between healthy volunteers and schizophrenia.

Bicluster 2 included 76 individuals (17 BP; 59 SZ) and clustered on PANSS positive scores, PANSS general scores, and five ICA components. See Figure 7 for more details. The average for bicluster 2 was 37.09 years old (SD = 11.00) and there were 47 male participants (61.84%). Bicluster 2 had, on average, more severe PANSS positive (mean = 19.89; SD = 3.90) and lower PANSS general (mean = 16.80; SD = 6.64) scores than the rest of the sample. All five ICA components also showed lower gray matter concentration (cluster peaks identified in the insula, cerebellum, and supplemental motor and motor cortices) when compared to the rest of the sample. Of these five components, two components (A and B, described above) showed diagnostic group difference for both SZ and BP (HV > SZ; HV > BP), and one showed a significant group difference between HV and SZ.

Bicluster 3 consisted of 112 participants (32 BP; 80 SZ) and five ICA components but no PANSS subscales. See Figure 8 for more details. The average age for bicluster 3 was 36.66 years old (SD = 11.18) and there were 67 male participants (59.82%). All five ICA components within bicluster 3 showed significant group differences (A and 24: HV > SZ, HV > BP; 10: HV > SZ; C: HV > SZ, BP > SZ; 28: HV > SZ). Bicluster 3 had reduced gray matter concentration in the frontal middle gyrus, frontal inferior gyrus, insula, cerebellar Crus I, rectus, and fusiform gyrus.

To gauge consistency between the hierarchical and biclustering methods, we asked whether the participant groups identified in each overlapped. Of the four hierarchical clusters based on gray matter loading coefficients only one cluster

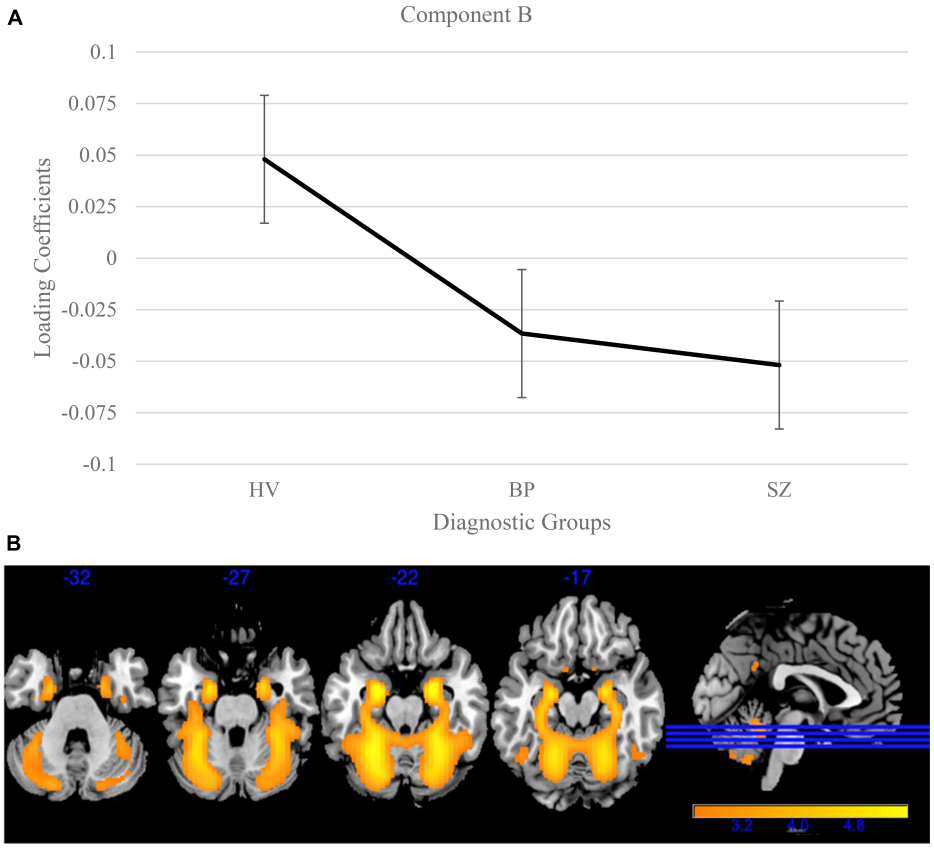

FIGURE 2
Cerebellum and vermis gray matter group differences in independent component analysis (ICA) results for healthy volunteers, individuals with schizophrenia, and individuals with bipolar I disorder. **(A)** Group effects of diagnosis on loading coefficients for Component B. Schizophrenia (SZ) and bipolar disorder (BP) had significantly less gray matter compared to healthy volunteers but did not significantly differ from each other. **(B)** Component B showed less gray matter concentration in the cerebellum and vermis in individuals with SZ and individuals with BP compared to healthy volunteers. Images thresholded at 2.5.

had the greatest amount of overlap with all the biclusters (hierarchical cluster shown in light blue, Figure 4). There were 69 (61.61%) individuals from bicluster 3, 37 (48.68%) individuals from bicluster 2, and 9 (11.25%) from bicluster 1 in this cluster. There were eight individuals who were present in all three biclusters. We would not expect to see exact overlap between the clustering as the PANSS scores are influencing the identification of reliable groups in the n-way biclustering and hierarchical clustering was used to examine either the ICA components or PANSS symptoms scores (two separate models).

We completed subsequent *post hoc* analyses with individuals for whom we had chlorpromazine equivalents (CPZ; $N = 381$) and found that component A was unaffected by CPZ scores, but that component B was significantly negatively related to CPZ scores ($r = -0.129$, $p = 0.012$). In other words, individuals with high CPZ scores had less gray matter in the cerebellum. Similarly, we completed subsequent analyses with duration of illness (DOI) and although we were limited in the amount of participant information ($N = 640$) and we found no changes to our significant association in individuals with BP but with individuals with SZ, DOI was significantly negatively related to both component A ($r = -0.165$, $p = 5.58\text{E-}5$) and B ($r = -0.101$, $p = 0.014$). In other words, individuals with longer durations of illness had less gray matter in both the insula/cingulum component and the cerebellum component.

Discussion

We examined patterns of gray matter alterations in SZ, BP, and HV. We also examined the symptom profiles of the diagnostic groups to parse out unique subgroups. We evaluated outcomes of ICA and symptom pattern analyses to link gray matter patterns with unique symptom profiles.

The ICA of gray matter variations demonstrated that individuals with SZ and BP share similar patterns of structural

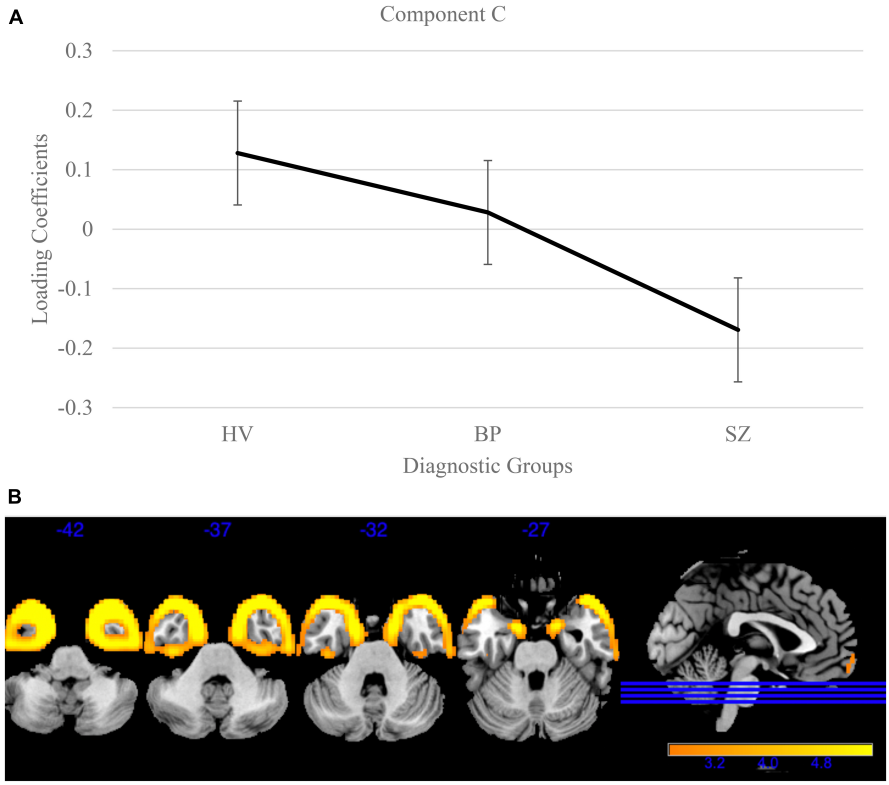

FIGURE 3
Temporal pole gray matter group differences in independent component analysis (ICA) results for healthy volunteers, individuals with schizophrenia, and individuals with bipolar I disorder. **(A)** Group effects of diagnosis on loading coefficients. Individuals with schizophrenia (SZ) had significantly less gray matter compared to individuals with bipolar disorder (BP) and healthy volunteers. Individuals with BP did not differ significantly from healthy volunteers. **(B)** Component C showed less gray matter concentration in the bilateral temporal poles in individuals with SZ compared to individuals with BP and healthy volunteers. Individuals with BP did not significantly differ from healthy volunteers. Images are thresholded at 2.5.

deficits. We identified two components that showed significant group differences between HV and BP, and HV and SZ. Component A showed less gray matter bilaterally in the insula and cingulate in both diagnostic groups compared to HV. This pattern has been previously identified robustly in the schizophrenia literature (Segall et al., 2009; Gupta et al., 2015; Meda et al., 2015; Jiang et al., 2021). Component B showed less gray matter bilaterally in the cerebellum in both diagnostic groups compared to HV. The cerebellar GM reductions supports previous literature that linked these losses to cognition (e.g., long-term and working memory) and symptoms (Moberget et al., 2018, 2019). Our results are in line with previous literature that shows a relationship between psychosis and the frontotemporal cortices in BP (Ivleva et al., 2013) and the cerebellum in adolescents, regardless of SZ or BP diagnosis (Moberget et al., 2019).

Component C showed significantly lower gray matter bilaterally in the fusiform gyrus/temporal pole of SZ vs. between BP where BP were not different from HV. The fusiform gyrus is a key region for sociality-related high-level vision (e.g., face perception) (Lee C. U. et al., 2002; Rangarajan et al., 2014). While our results may have been a function of having a smaller BP sample, this component is unique across the other components in showing no difference between BP and HV, while showing a strong reduction in SZ compared to BP. This result supports previous literature that found small effect sizes in this region in individuals with BP (Murray et al., 2004; Bora, 2015; Hibar et al., 2018; de Zwarte et al., 2019). The fusiform gyrus was also an area of discrepancy between individuals with SZ and individuals with schizotypy with the region being only reduced in SZ (Dickey et al., 2003; Onitsuka et al., 2003; Takahashi et al., 2006). We hypothesize that these results may indicate that the fusiform gyrus/temporal pole is a region strongly related to SZ but largely unaffected in other psychiatric disorders (e.g., BP, schizophrenia spectrum disorders).

Individuals with SZ and BP presented with similar symptom profiles, where individuals with SZ had more severe symptoms in the three PANSS subscale scores. ICA components identified by the N-way biclustering did not allow for diagnostic distinction between participants as it relates to structural alterations. The hierarchical clustering of the PANSS subscales produced clusters that were unique in their individual subscale

TABLE 3 Significant diagnostic group differences in the independent component analysis (ICA) components.

Direction		#	Peak location	Cohen's *F*	*P* value
HV > both	HV > SZ	8	Brainstem	0.17	7.43E-25
	HV > BP			0.06	1.58E-05
	HV > SZ	A	Insula/cingulate gyrus	0.27	4.46E-47
	HV > BP			0.14	2.44E-13
	HV > SZ	24	Medial prefrontal cortex	0.21	8.02E-06
	HV > BP			0.12	3.63E-11
	HV > SZ	26	Temporal pole	0.11	3.22E-08
	HV > BP			0.07	0.00104
	HV > SZ	27	Temporal inferior gyrus/occipital gyrus	0.06	1.52E-03
	HV > BP			0.04	4.62E-02
	HV > SZ	B	cerebellum	0.1	1.21E-07
	HV > BP			0.05	0.014
HV > SZ		5	Cerebellum/vermis	0.12	3.06E-10
		7	caudate	0.08	7.02E-05
		10	Calcarine/Crus I	0.09	5.14E-06
		18	Crus II	0.12	4.29E-09
		20	Calcarine/occipital gyrus	0.09	3.06E-05
		28	Rectus/cerebellum/fusiform gyrus	0.16	1.06E-17
		30	Insula/Rolandic operculum	0.13	1.18E-11
		C	Fusiform gyrus/temporal pole	0.18	7.76E-22
		33	Calcarine/frontal middle gyrus	0.08	1.17E-04
		34	Supplemental motor region	0.07	3.70E-04
		35	Cerebellum/parahippocampal gyrus	0.08	1.30E-04
		36	Parietal superior gyrus	0.09	1.84E-06
BP > SZ		C	Fusiform gyrus/temporal pole	0.07	7.76E-22

SZ, individuals with schizophrenia; BP, individuals with bipolar disorder; HV, healthy volunteers. Cohen's *F* and *p* values reported from Bonferroni corrected post hoc analyses. # Component number.

TABLE 4 PANSS subscale spread across clusters.

	N	PANSS positive	PANSS negative	PANSS general	PANSS total	Age	BP (%)
CLUSTER 6	309	10.62 ± 3.00	9.54 ± 2.34	22.81 ± 3.73	42.97 ± 6.75	35.66 ± 12.00	164 (53.07%)
CLUSTER 5	151	10.74 ± 2.52	17.03 ± 3.55	26.51 ± 5.59	54.28 ± 7.60	34.44 ± 11.65	43 (28.48%)
CLUSTER 1	33	14.91 ± 3.20	26.48 ± 2.74	35.85 ± 4.67	77.24 ± 5.85	27.27 ± 7.99	2 (6.06%)
CLUSTER 3	159	17.48 ± 3.42	13.11 ± 3.08	30.70 ± 2.38	61.28 ± 5.02	36.30 ± 12.05	37 (23.27%)
CLUSTER 4	146	19.21 ± 3.15	14.19 ± 3.78	38.09 ± 3.32	71.49 ± 6.76	36.36 ± 11.69	40 (27.39%)
CLUSTER 2	62	23.56 ± 4.25	23.90 ± 5.47	45.71 ± 5.22	93.18 ± 8.19	34.05 ± 11.83	8 (12.90%)
TOTAL	860	14.47 ± 5.39	13.76 ± 5.59	29.66 ± 8.19	58.12 ± 16.28	35.25 ± 11.86	300 (38.37%)

PANSS subscale scores for each of the hierarchical cluster membership. All scores and ages are presented as mean ± standard deviation unless otherwise noted. BP, bipolar disorder. There was no significant associations between the PANSS clusters and the ICA components.

totals, but there were no significant relationships between any of the clusters and the ICA components, indicating that the clusters were not identifying symptom profiles that related to a unique structural correlate. Of the six clusters, one had significantly more BP participants than the others and one had significantly fewer BP participants than the others. Similar to our results, Clementz et al. (2016) found a homogeneous subgroup with more severe clinical symptoms (e.g., negative symptoms and social functioning) that was majority SZ (56%) (Clementz et al., 2016, 2020). Both these previous findings and those discussed here support the main difference between SZ and BP being the severity of symptoms with no discerning differences in brain structure.

A limitation of the hierarchical cluster analysis is that the entirety of the data matrix is utilized for cluster profiling. We hypothesized that additional symptom profiles may appear if the analysis was not required to include all the PANSS subscales. Therefore, we explored the potential relationship

10.3389/fnhum.2022.1001692

TABLE 5 Description of the peak locations of each independent component analysis (ICA) component.

Component	Positive loadings	Negative loadings
15	Putamen L/R	
20	Calcarine R/L	
8	Vermis; cerebellum 9	Caudate R/L; putamen L/R; thalamus L/R
42	Cerebellum L/R	
35		Superior temporal gyrus
B	Cerebellar hemisphere; vermis L/R	
44	Thalamus L/R	
43	Parietal sup L	Thalamus L/R
29	Cingulum	Frontal mid L/R
40	Insula L/R	Fusiform L/R
19	Angular L/R; temporal sup R	Parietal inf L/R; angular L
3	Calcarine L/R	Cuneus L/R; occipital Sup R; precuneus R
9	Occipital sup R; occipital mid L	Calcarine L/R; precuneus L/R; posterior Cingulum
14		Cerebellum L; Crus I L/R; cerebellum 7b
32		Precentral L/R
34		Supp motor area R; precuneus
41	Frontal mid L	Vermis 4 5; cingulum post L/R; lingual L/R
18		Crus II L/R
26	Temporal inferior gyrus L/R; fusiform L/R	Temporal inferior gyrus L/R; fusiform L/R
1	Crus II L/R	
12	Cerebellum/vermis	
5	Cerebellum 9 L/R	
7	Ventricles	
39	Fusiform L/R; lingual L; Crus I L/R	Cerebellum 6 L/R; Crus I L/R; vermis 7
10	Cerebellum Crus I L/R; calcarine L	
C	Temporal poles L/R	
25	Cerebellum 8 L/R	Lingual R; calcarine R
28	Rectus L/R	Cerebellum 8 L; fusiform L
A	Insula L/R; cingulate gyrus L/R; temporal pole sup L/R; temporal sup R	
24	Frontal mid L/R; frontal inf Tri L/R	
16	Occipital mid L; parietal inf L/R; angular L/R; temporal mid L/R	Temporal mid L/R; angular L/R; occipital sup L/R
2	Frontal inf tri L/R; frontal sup L/R	Frontal mid L/R; insula L/R
4	Temporal sup L; insula L	Temporal mid L; temporal sup R
22	Precentral L/R	Frontal inf oper L/R; frontal mid L/R; precentral L/R
13	Cuneus L; insula R; angular R; temporal mid R; temporal sup R; temporal inf R	Temporal mid R; temporal sup R
30	Temporal mid L/R; parietal inf L; cuneus L/R; frontal inf oper R; supramarginal R	Rolandic oper L/R; temporal pole sup L/R; Calcarine L/R; Rectus L/R; insula L/R
38	Parietal inf lobule L/R; angular L/R	Cuneus L/R; precuneus L/R
6	Calcarine L; Crus II L; temporal inf R; Crus I R; lingual L	Crus II R; lingual R; calcarine R
11	Frontal inf tri L/R; frontal sup L; frontal mid L/R	Frontal mid L/R; frontal inf tri L/R; frontal inf oper L/R
33	Calcarine L/R	Parietal inf L; frontal Mid L/R; supra marginal R; angular R; frontal sup L/R
36	Parietal sup L/R; parietal inf R	
17	Occipital mid L; temporal mid R; angular R	Occipital mid L/R; occipital sup L/R
27	Temporal inf L/R; temporal mid L/R; angular L/R	Temporal mid L/R; occipital mid L

Table is in matching order to the hierarchical clustering of the ICA depicted in Figure 5. The color separation shows the four (4) clusters of the hierarchical cluster (tan, purple, green, and yellow). Description of the locations of the peak(s) identified within each component. L, left; R, right; peak regions identified using the aal.nii template.

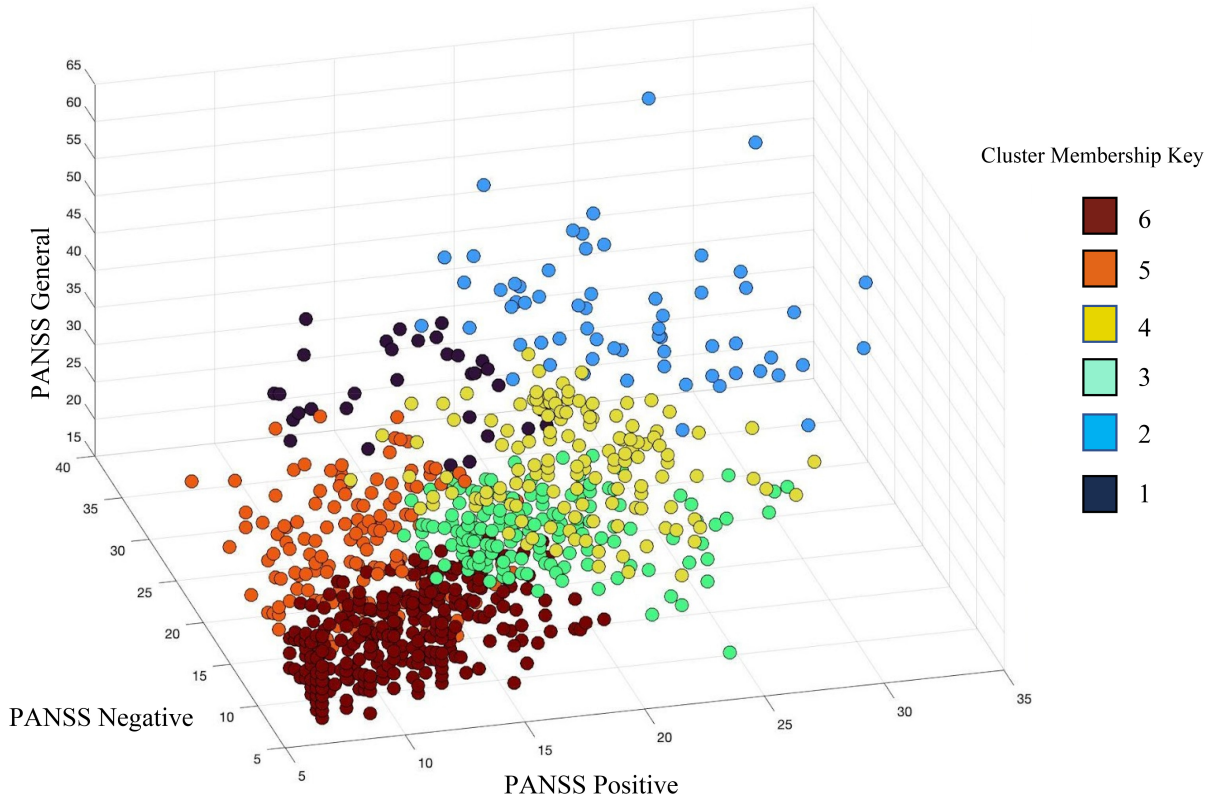

FIGURE 4
Hierarchical clustering of PANSS subscale scores identified six (6) clusters across individuals with schizophrenia (SZ) and individuals with bipolar disorder (BP). PANSS positive scores are plotted on the X-axis, PANSS negative scores on the Y-axis, and PANSS general psychopathology scores are on the Z-axis. See legend for cluster membership key.

between the PANSS symptom profiles and the ICA components by adding both to a n-way biclustering analysis. A strength of the biclustering approach is that the data matrix is examined using every possible combination within the data, and therefore, submatrices or clusters may arise that do not include all participants, subscales, or components.

Our results found three biclusters; Bicluster 1 included all three subscales of the PANSS, Bicluster 2 included PANSS positive and PANSS general, and Bicluster 3 did not include any PANSS subscales. Bicluster 1 ($N = 80$) included both individuals with SZ and individuals with BP who had more severe symptom scores on all three PANSS subscales. The five ICA components that were identified in bicluster 1 included peaks in the occipital lobe, cerebellum, bilateral temporal poles, thalamus, and bilateral rectus. However, the directionality of these peaks was not uniform (see **Figure 5**) across participants. Therefore, we conclude that, this cluster identifies a subgroup in which more severe positive, negative, and general psychopathology symptoms are related to less gray matter in the cerebellum, thalamus, and bilateral rectus; but we also note that there is inconsistency in the directionality of the gray matter alteration in the bilateral temporal poles and occipital lobes. These inconsistencies may be explained by the range of symptom presentations included in the bicluster. More severe PANSS positive scores have been associated with *regional* cortical thinning whereas more severe PANSS negative scores were associated with *global* cortical thinning (van Erp et al., 2018). Regardless, this bicluster represents a group of people that, regardless of diagnosis, share both a pattern of low gray matter concentration and severe total symptom profiles.

Recently, the rectus has been shown to be associated with individuals with high genetic risk for either SZ, BP, or psychosis (Luna et al., 2022). As mentioned in the previous section, component C (part of this bicluster) has also been studied extensively in the schizophrenia spectrum literature (Takahashi et al., 2006). Previous literature has also found that poor facial recognition is associated with the genetic risk for SZ (Martin et al., 2020). Therefore, this bicluster may give insight into the genetic risk of developing psychosis, but further research is needed.

Bicluster 2 ($N = 76$) included both individuals with SZ and individuals with BP who had more severe PANSS positive and lower PANSS general scores than the rest of the sample. All five ICA components identified in this bicluster indicated

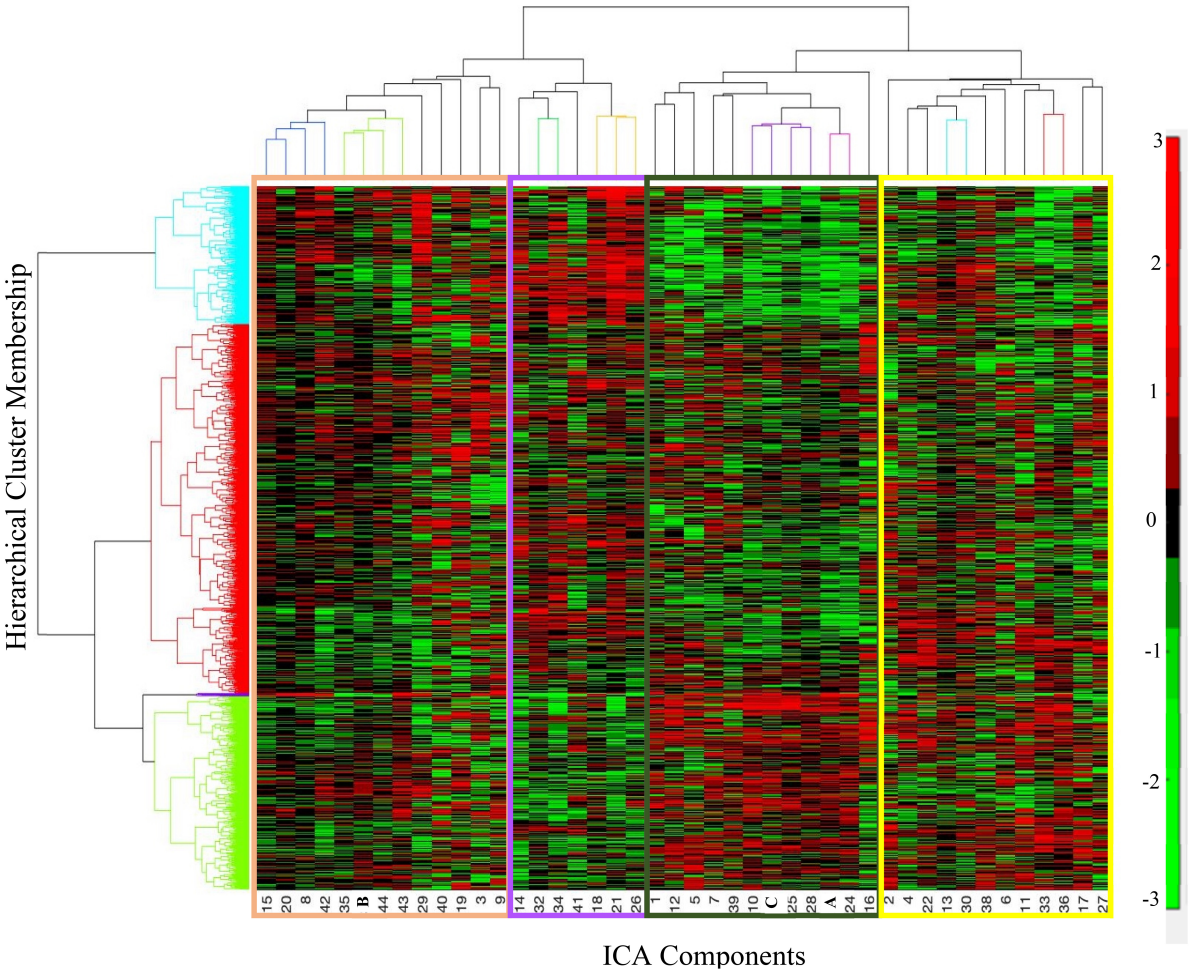

FIGURE 5
Hierarchical cluster analysis of independent component analysis (ICA) loading coefficients resulted in four clusters of participants (Y-axis, rows). The y-axis shows the cluster membership, the X-axis shows the ordering of the ICA components. The organization of the components along the X-axis is color-coordinated with **Table 5**. The tan cluster is largely comprised of posterior cortical regions. The purple cluster is largely negatively weighted on the cerebellar regions. The dark green cluster includes Components A and C as well as cerebellar and subcortical components. The yellow cluster includes most of the frontal as well as cortical components from every other lobe. See **Table 5** for more details on the peak locations of each component. In the color bar, red represents positive loading coefficients and green represents negative loading coefficients.

less gray matter concentration than the rest of the sample. In other words, this bicluster showed a negative relationship with more severe PANSS positive scores, low PANSS general scores, and less gray matter in all five ICA components. Component A and Component B which each showed significant reductions in both diagnostic groups, SZ and BP, were both included in bicluster 2. In addition, there were three other components (involving the precentral gyrus, thalamus, left parietal supplemental gyrus, and right supplemental motor region) where bicluster 2 had less gray matter concentration than the rest of the sample. And as mentioned above, three of these components identified significant diagnostic group differences. Therefore, bicluster 2 indicates that more severe positive symptoms and less prominent general psychopathology symptoms are related to less gray matter in the cerebellum, insula, and other subcortical regions.

Bicluster 3 (N = 112) identified a subset of the sample that presents with a unique structural set of patterns but there are no clinical features (symptom scores, age, gender, and site) that distinguish this cluster from the rest of the sample. Given the directionality of gray matter alteration, we hypothesize that this bicluster may be identifying individuals with similar cortical measures (e.g., smaller brain volumes overall) and not necessarily unique clinical presentations. In addition, one component showed lower gray matter concentration in the rectus gyrus, which has been associated with genetic risk for SZ, BP, and psychosis (Luna et al., 2022). It is possible that this bicluster is mapping onto a genetic profile instead of a clinical profile. However, we caution that further research is

10.3389/fnhum.2022.1001692

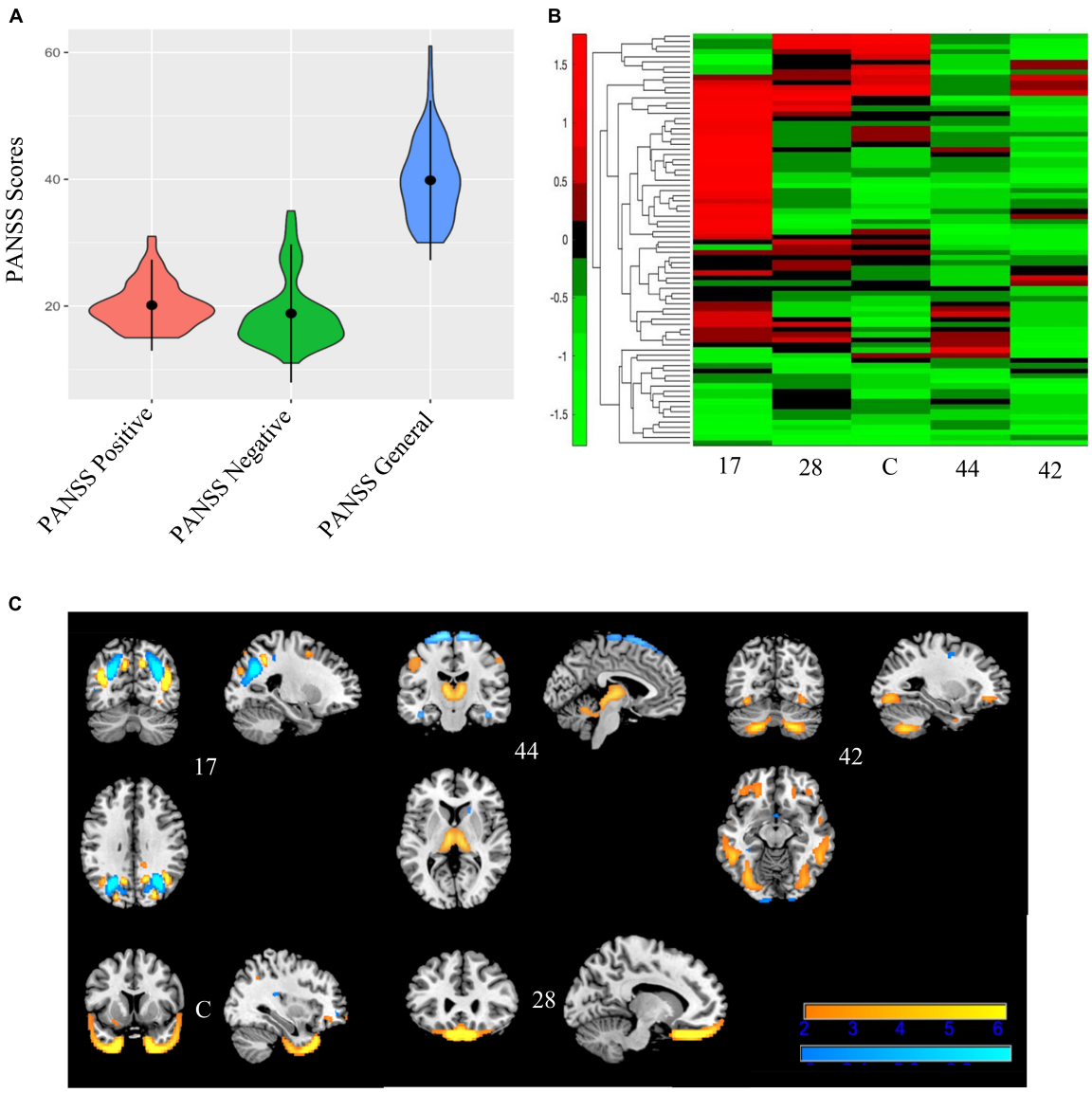

FIGURE 6
Bicluster 1: PANSS scores, heat map of loadings of independent component analysis (ICA) components, and ICA components. Bicluster 1 (N = 80) had more severe scores on all three PANSS subscales **(A)** than the rest of the sample. This bicluster included 5 ICA components (17, 44, 42, C, and 28) representing the occipital lobes, rectus, cerebellum, and the temporal poles that were generally low in the loading coefficients **(B)**. Images in **(C)** 6C are thresholded at |2.5|. Warm colors represent positive values and cool colors represent negative values.

needed to confirm the role of this bicluster in genetic risk for psychiatric disorders.

The addition of n-way biclustering to the analyses allowed for identification of reliable grouping of the sample based on both the symptom profiles and the gray matter patterns. These results included unique, homogeneous subclusters that were not identified in the ICA results or the hierarchical cluster analyses. The bicluster approach identified anatomic substrates that related to different symptoms profiles in both SZ and BP, supporting a dimensional view of these disorders.

Limitations

There are a few limitations of this study. The number of BP individuals (N = 301) across all the sites was significantly less than the number of SZ individuals (N = 1217). We acknowledge that this imbalance in diagnostic groups may have masked some of the BP specific results, especially in the ICA components. However, *post hoc* analyses of group differences in HV v. BP and BP v. SZ showed significant differences and strong effect sizes. Although there is an imbalance in our diagnostic group sizes, we were still able to identify some

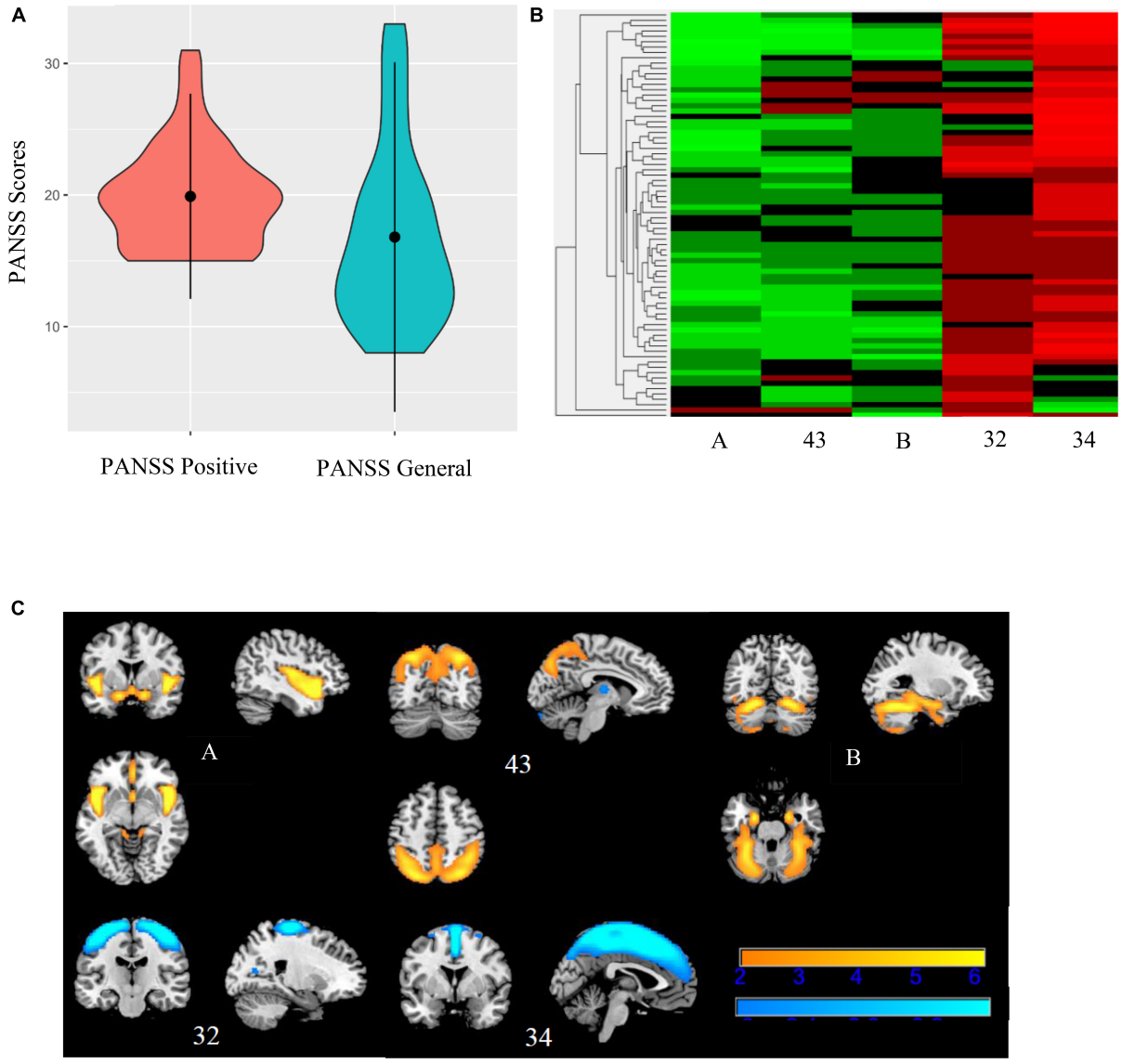

FIGURE 7
Bicluster 2: PANSS scores, heat map of loadings of independent component analysis (ICA) components, and ICA components. Bicluster 2 (N = 76) consisted of more severe PANSS positive and PANSS general scores **(A)** and 5 ICA components (A, 43, B, 32, and 34) representing the insula, cerebellum, and supplemental motor and motor cortices **(B)**. Images in **(C)** 7C are thresholded at |2.5|. Warm colors represent positive values and cool colors represent negative values.

valid representations of gray matter alterations in BP. The imbalance in the number of BP and SZ participants may also have contributed to the significant site effects that were observed in the PANSS subscales as not every site had the same distribution. We also acknowledge that our findings can be confounded by medication effects. We do not have medication information for every individual in the sample and we cannot conclude that our results are not at least somewhat driven by medication differences. There were also a large number of sites (N = 29) included in the study. Site effects were addressed in the preprocessing pipelines and the subsequent analyses, but site-specific effects may still occur as detailed in Supplementary Table 2.

Another limitation of this study is the utilization of the PANSS subscales for symptom profiling. Although the PANSS is a gold-standard assessment for SZ and widely utilized in BP, this assessment is not all-encompassing of the multitude of symptoms presenting in both schizophrenia and bipolar disorder over time. Especially for individuals with BP, there may be some symptom presentations that fluctuate with mood or psychosis and therefore, cross-sectional assessments may not capture all symptoms. Further research

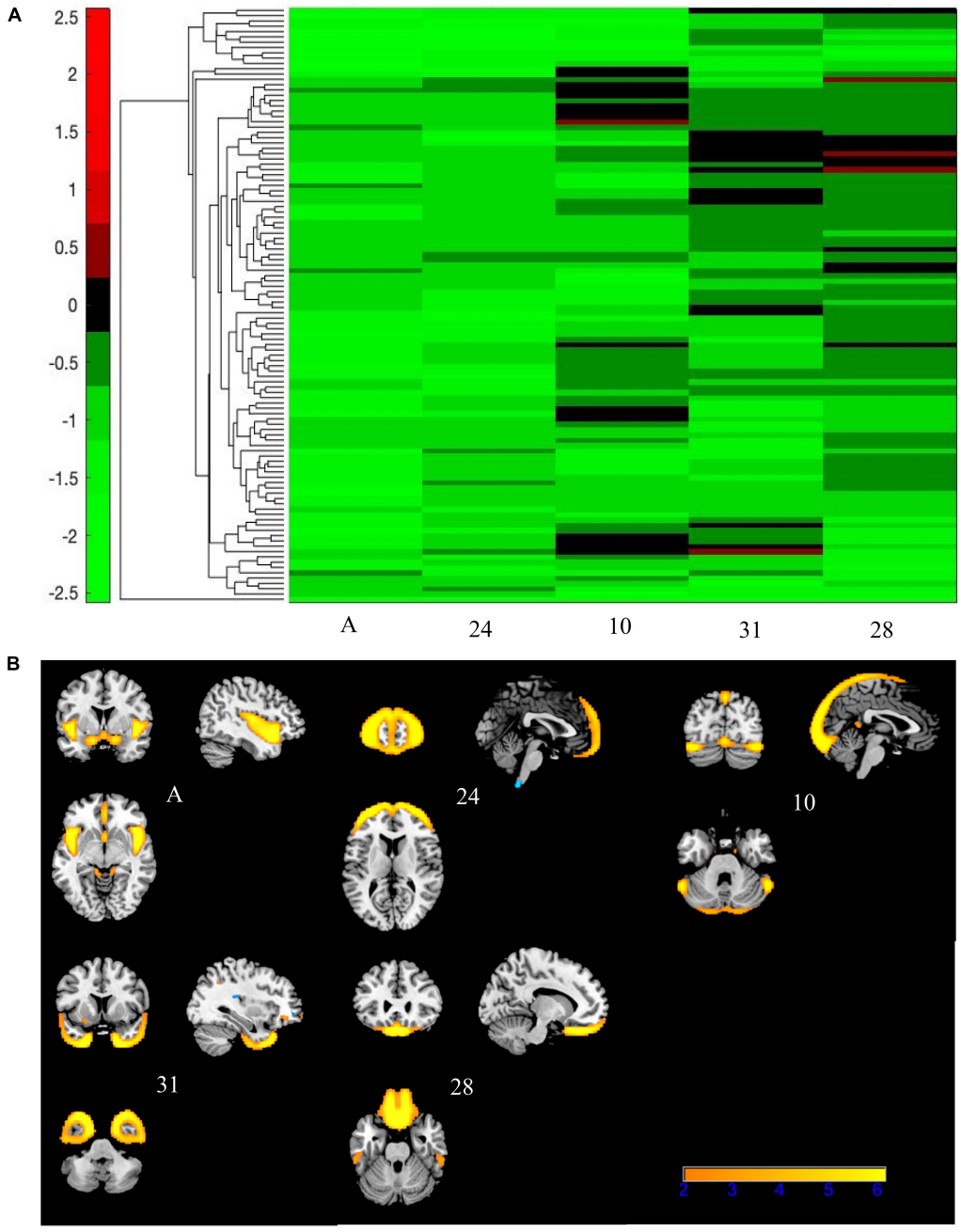

FIGURE 8
Bicluster 3: heat map of loadings of independent component analysis (ICA) components and related ICA components. Bicluster C (N = 112) was comprised of five ICA components (A, 24, 10, 31, and 28) shown above that had mostly negative loading coefficients **(A)**. There were no PANSS subscales associated with bicluster C. Images in **(B)** 8B are thresholded at |2.5|. Warm colors represent positive values.

may want to examine additional scales (e.g., Montgomery-Aberg Depression Rating Scale) that capture other symptoms that may round out the symptom profile as previous studies have done with their subtyping of psychosis-related disorders (Clementz et al., 2020) and scales that examine these symptoms over the lifetime (as opposed to recent or the previous 2 weeks).

Conclusion

Our study examined multivariate relationships between the symptom profiles and gray matter patterns of individuals with SZ and individuals with BP. Our results identified one gray matter pattern that differed between SZ and BP. However, this pattern (less gray matter concentration in the temporal

poles) was not significantly different between individuals with BP and healthy volunteers. Therefore, we conclude that this region is much less affected, if at all, in BP. The remainder of our results indicate that SZ and BP lie along an extensive spectrum of symptoms and brain correlates but there are no clear distinctions between the disorders in these areas.

However, we note that there are still meaningful distinctions between the disorders. The category of symptoms differ, the prognosis and diagnostic timeline often differ, and most importantly, the prescribed treatments often differ between individuals with SZ and individuals with BP. Overall, we conclude that the cortical alterations seen in individuals with SZ and individuals with BP trend together and are not significantly different from one another; similar patterns of gray matter loss particularly in the cerebellum and thalamus or insula appear to cluster with more severe symptoms. All components identified in this study showed the same direction of gray matter concentration (SZ < BP < HV). Based on these findings, it appears that BP and SZ may track along the same spectrum, with individuals with BP having less severe cortical alterations and less severe symptom profiles when compared to individuals with SZ, but without a clear distinction in cortical alterations between these disorders.

Data availability statement

The data analyzed in this study is subject to the following licenses/restrictions: Some of the datasets are already publicly available (see citations in manuscript). Some are still privately owned. Requests to access these datasets should be directed to http://fcon_1000.projects.nitrc.org/indi/retro/cobre.html.

Author contributions

WJ, KR-M, and JT: conceptualization. WJ, KR-M, JE, and MR: methodology. KR-M and JE: writing—original draft preparation. NP-B, VC, TE, SE, IA, EJ, OA, LWe, LWa, GP, DG, EH, RB, PK, AV, AM, CT, and JL: data collection and curation. JT: supervision. All authors writing—review and editing, read, and agreed to the published version of the manuscript.

Funding

This work was funded by the National Institutes of Mental Health grants (3R01MH121246-02S2 to VC and 5R01MH094524-1 to JT).

Conflict of interest

The authors declare that the research was conducted in the absence of any commercial or financial relationships that could be construed as a potential conflict of interest.

Publisher's note

All claims expressed in this article are solely those of the authors and do not necessarily represent those of their affiliated organizations, or those of the publisher, the editors and the reviewers. Any product that may be evaluated in this article, or claim that may be made by its manufacturer, is not guaranteed or endorsed by the publisher.

Supplementary material

The Supplementary Material for this article can be found online at: https://www.frontiersin.org/articles/10.3389/fnhum.2022.1001692/full#supplementary-material

References

Aine, C. J., Bockholt, H. J., Bustillo, J. R., Cañive, J. M., Caprihan, A., Gasparovic, C., et al. (2017). Multimodal neuroimaging in schizophrenia: Description and dissemination. *Neuroinformatics* 15, 343–364. doi: 10.1007/s12021-017-9338-9

Alnæs, D., Kaufmann, T., van der Meer, D., Córdova-Palomera, A., Rokicki, J., Moberget, T., et al. (2019). Brain heterogeneity in schizophrenia and its association with polygenic risk. *JAMA Psychiatry* 76:739. doi: 10.1001/jamapsychiatry.2019.0257

American Psychiatric Association (2013). *Diagnostic and statistical manual of mental disorders*, 5th Edn. Washington, DC: American Psychiatric Association, doi: 0.1176/appi.books.97808904255596

Andreassen, O. A., Thompson, W. K., Schork, A. J., Ripke, S., Mattingsdal, M., Kelsoe, J. R., et al. (2013). Improved detection of common variants associated with schizophrenia and bipolar disorder using pleiotropy-informed conditional false discovery rate. *PLoS Genet.* 9:e1003455. doi: 10.1371/journal.pgen.1003455

Barth, C., Jørgensen, K. N., Wortinger, L. A., Nerland, S., Jönsson, E. G., and Agartz, I. (2020). Trajectories of brain volume change over 13 years in chronic schizophrenia. *Schizophr. Res.* 222, 525–527. doi: 10.1016/j.schres.2020.05.014

Bora, E. (2015). Developmental trajectory of cognitive impairment in bipolar disorder: Comparison with schizophrenia. *Eur. Neuropsychopharmacol.* 25, 158–168. doi: 10.1016/j.euroneuro.2014.09.007

Cheon, E., Bearden, C. E., Sun, D., Ching, C. R. K., Andreassen, O. A., Schmaal, L., et al. (2022). Cross disorder comparisons of brain structure in schizophrenia, bipolar disorder, major depressive disorder, and 22q11.2 deletion syndrome: A review of <scp>ENIGMA</scp> findings. *Psychiatry Clin. Neurosci.* 76, 140–161. doi: 10.1111/pcn.13337

Clementz, B. A., Parker, D. A., Trotti, R. L., McDowell, J. E., Keedy, S. K., Keshavan, M. S., et al. (2022). Psychosis biotypes: Replication and validation

from the B-SNIP consortium. *Schizophr. Bull.* 48, 56–68. doi: 10.1093/schbul/sbab090

Clementz, B. A., Sweeney, J. A., Hamm, J. P., Ivleva, E. I., Ethridge, L. E., Pearlson, G. D., et al. (2016). Identification of distinct psychosis biotypes using brain-based biomarkers. *Am. J. Psychiatry* 173, 373–384. doi: 10.1176/appi.ajp.2015.14091200

Clementz, B. A., Trotti, R. L., Pearlson, G. D., Keshavan, M. S., Gershon, E. S., Keedy, S. K., et al. (2020). Testing psychosis phenotypes from bipolar–schizophrenia network for intermediate phenotypes for clinical application: Biotype characteristics and targets. *Biol. Psychiatry* 5, 808–818. doi: 10.1016/j.bpsc.2020.03.011

de Zwarte, S. M. C., Brouwer, R. M., Agartz, I., Alda, M., Aleman, A., Alpert, K. I., et al. (2019). The Association between familial risk and brain abnormalities is disease specific: An enigma-relatives study of schizophrenia and bipolar disorder. *Biol. Psychiatry* 86, 545–556. doi: 10.1016/j.biopsych.2019.03.985

di Sero, A., Jørgensen, K. N., Nerland, S., Melle, I., Andreassen, O. A., Jovicich, J., et al. (2019). Antipsychotic treatment and basal ganglia volumes: Exploring the role of receptor occupancy, dosage and remission status. *Schizophr. Res.* 208, 114–123. doi: 10.1016/j.schres.2019.04.002

Dickey, C. C., McCarley, R. W., Voglmaier, M. M., Niznikiewicz, M. A., Seidman, L. J., Frumin, M., et al. (2003). A MRI study of fusiform gyrus in schizotypal personality disorder. *Schizophr. Res.* 64, 35–39. doi: 10.1016/S0920-9964(02)00529-7

Doan, N. T., Kaufmann, T., Bettella, F., Jørgensen, K. N., Brandt, C. L., Moberget, T., et al. (2017). Distinct multivariate brain morphological patterns and their added predictive value with cognitive and polygenic risk scores in mental disorders. *Neuroimage* 15, 719–731. doi: 10.1016/j.nicl.2017.06.014

Gollub, R. L., Shoemaker, J. M., King, M. D., White, T., Ehrlich, S., Sponheim, S. R., et al. (2013). The MCIC collection: A shared repository of multi-modal, multi-site brain image data from a clinical investigation of schizophrenia. *Neuroinformatics* 11, 367–88. doi: 10.1007/s12021-013-9184-3

Gupta, C. N., Calhoun, V. D., Rachakonda, S., Chen, J., Patel, V., Liu, J., et al. (2015). Patterns of gray matter abnormalities in schizophrenia based on an international mega-analysis. *Schizophr. Bull.* 41, 1133–42. doi: 10.1093/schbul/sbu177

Gupta, C. N., Turner, J. A., and Calhoun, V. D. (2019). Source-based morphometry: A decade of covarying structural brain patterns. *Brain Struct. Funct.* 224, 3031–3044. doi: 10.1007/s00429-019-01969-8

Hall, H., McNeil, T., Arnborg, S., Terenius, L., and Sedvall, G. (2002). HUBIN — human brain informatics: A database project on schizophrenia. *Eur. Psychiatry* 17:71. doi: 10.1016/S0924-9338(02)80324-8

Hartberg, C. B., Jørgensen, K. N., Haukvik, U. K., Westlye, L. T., Melle, I., Andreassen, O. A., et al. (2015). Lithium treatment and hippocampal subfields and amygdala volumes in bipolar disorder. *Bipolar Disord.* 17, 496–506. doi: 10.1111/bdi.12295

Hawco, C., Buchanan, R. W., Calarco, N., Mulsant, B. H., Viviano, J. D., Dickie, E. W., et al. (2019). Separable and replicable neural strategies during social brain function in people with and without severe mental illness. *Am. J. Psychiatry* 176, 521–530. doi: 10.1176/appi.ajp.2018.17091020

Hibar, D. P., Westlye, L. T., Doan, N. T., Jahanshad, N., Cheung, J. W., Ching, C. R. K., et al. (2018). Cortical abnormalities in bipolar disorder: An MRI analysis of 6503 individuals from the ENIGMA bipolar disorder working group. *Mol. Psychiatry* 23, 932–942. doi: 10.1038/mp.2017.73

Hill, S. K., Reilly, J. L., Keefe, R. S. E., Gold, J. M., Bishop, J. R., Gershon, E. S., et al. (2013). Neuropsychological impairments in schizophrenia and psychotic bipolar disorder: Findings from the bipolar-schizophrenia network on intermediate phenotypes (B-SNIP) Study. *Am. J. Psychiatry* 170, 1275–1284. doi: 10.1176/appi.ajp.2013.12101298

Himberg, J., Hyvärinen, A., and Esposito, F. (2004). Validating the independent components of neuroimaging time series via clustering and visualization. *NeuroImage* 22, 1214–1222. doi: 10.1016/j.neuroimage.2004.03.027

Hirjak, D., Rashidi, M., Kubera, K. M., Northoff, G., Fritze, S., Schmitgen, M. M., et al. (2020). Multimodal magnetic resonance imaging data fusion reveals distinct patterns of abnormal brain structure and function in catatonia. *Schizophr. Bull.* 46, 202–210. doi: 10.1093/schbul/sbz042

Honea, R., Crow, T. J., Passingham, D., and Mackay, C. E. (2005). Regional deficits in brain volume in schizophrenia: A meta-analysis of voxel-based morphometry studies. *Am. J. Psychiatry* 162, 2233–2245. doi: 10.1176/appi.ajp.162.12.2233

Hudgens-Haney, M. E., Clementz, B. A., Ivleva, E. I., Keshavan, M. S., Pearlson, G. D., Gershon, E. S., et al. (2020). Cognitive impairment and diminished neural responses constitute a biomarker signature of negative symptoms in psychosis. *Schizophr. Bull.* 46, 1269–1281. doi: 10.1093/schbul/sbaa001

Ivleva, E. I., Bidesi, A. S., Keshavan, M. S., Pearlson, G. D., Meda, S. A., Dodig, D., et al. (2013). Gray matter volume as an intermediate phenotype for psychosis: Bipolar-schizophrenia network on intermediate phenotypes (B-SNIP). *Am. J. Psychiatry* 170, 1285–1296. doi: 10.1176/appi.ajp.2013.13010126

Jabben, N., Arts, B., van Os, J., and Krabbendam, L. (2010). Neurocognitive functioning as intermediary phenotype and predictor of psychosocial functioning across the psychosis continuum. *J. Clin. Psychiatry* 71, 764–774. doi: 10.4088/JCP.08m04837yel

Jiang, W., Andreassen, O. A., Agartz, I., Lagerberg, T. V., Westlye, L. T., Calhoun, V. D., et al. (2020). Distinct structural brain circuits indicate mood and apathy profiles in bipolar disorder. *Neuroimage* 26:101989. doi: 10.1016/j.nicl.2019.101989

Jiang, W., Rootes-Murdy, K., Chen, J., Bizzozero, N. I. P., Calhoun, V. D., van Erp, T. G. M., et al. (2021). Multivariate alterations in insula - medial prefrontal cortex linked to genetics in 12q24 in schizophrenia. *Psychiatry Res.* 306:114237. doi: 10.1016/j.psychres.2021.114237

Jørgensen, K. N., Nesvåg, R., Gunleiksrud, S., Raballo, A., Jönsson, E. G., and Agartz, I. (2016). First- and second-generation antipsychotic drug treatment and subcortical brain morphology in schizophrenia. *Eur. Arch. Psychiatry Clin. Neurosci.* 266, 451–460. doi: 10.1007/s00406-015-0650-9

Kaltenboeck, A., Winkler, D., and Kasper, S. (2016). Bipolar and related disorders in DSM-5 and ICD-10. *CNS Spectr.* 21, 318–323. doi: 10.1017/S1092852916000079

Kay, S. R., Fiszbein, A., and Opler, L. A. (1987). The positive and negative syndrome scale (PANSS) for schizophrenia. *Schizophr. Bull.* 13, 261–276. doi: 10.1093/schbul/13.2.261

Kochunov, P., Coyle, T. R., Rowland, L. M., Jahanshad, N., Thompson, P. M., Kelly, S., et al. (2017). Association of white matter with core cognitive deficits in patients with schizophrenia. *JAMA Psychiatry* 74:958. doi: 10.1001/jamapsychiatry.2017.2228

Kochunov, P., Ganjgahi, H., Winkler, A., Kelly, S., Shukla, D. K., Du, X., et al. (2016). Heterochronicity of white matter development and aging explains regional patient control differences in schizophrenia. *Hum. Brain Mapp.* 37, 4673–4688. doi: 10.1002/hbm.23336

Kochunov, P., Hong, L. E., Dennis, E. L., Morey, R. A., Tate, D. F., Wilde, E. A., et al. (2022). ENIGMA-DTI: Translating reproducible white matter deficits into personalized vulnerability metrics in cross-diagnostic psychiatric research. *Hum. Brain Mapp.* 43, 194–206. doi: 10.1002/hbm.24998

Kochunov, P., Thompson, P. M., and Hong, L. E. (2019). Toward high reproducibility and accountable heterogeneity in schizophrenia research. *JAMA Psychiatry* 76:680. doi: 10.1001/jamapsychiatry.2019.0208

Lee, C. U., Shenton, M. E., Salisbury, D. F., Kasai, K., Onitsuka, T., Dickey, C. C., et al. (2002). Fusiform gyrus volume reduction in first-episode schizophrenia. *Arch. Gen. Psychiatry* 59:775. doi: 10.1001/archpsyc.59.9.775

Lee, D.-K., Lee, H., Park, K., Joh, E., Kim, C.-E., and Ryu, S. (2020). Common gray and white matter abnormalities in schizophrenia and bipolar disorder. *PLoS One* 15:e0232826. doi: 10.1371/journal.pone.0232826

Luna, L. P., Radua, J., Fortea, L., Sugranyes, G., Fortea, A., Fusar-Poli, P., et al. (2022). A systematic review and meta-analysis of structural and functional brain alterations in individuals with genetic and clinical high-risk for psychosis and bipolar disorder. *Prog. Neuropsychopharmacol. Biol. Psychiatry* 117:110540. doi: 10.1016/j.pnpbp.2022.110540

Martin, D., Croft, J., Pitt, A., Strelchuk, D., Sullivan, S., and Zammit, S. (2020). Systematic review and meta-analysis of the relationship between genetic risk for schizophrenia and facial emotion recognition. *Schizophr. Res.* 218, 7–13. doi: 10.1016/j.schres.2019.12.031

Meda, S. A., Wang, Z., Ivleva, E. I., Poudyal, G., Keshavan, M. S., Tamminga, C. A., et al. (2015). Frequency-Specific neural signatures of spontaneous low-frequency resting state fluctuations in psychosis: Evidence from bipolar-schizophrenia network on intermediate phenotypes (B-SNIP) Consortium. *Schizophr. Bull.* 41, 1336–1348. doi: 10.1093/schbul/sbv064

Mennigen, E., Jiang, W., Calhoun, V. D., van Erp, T. G. M., Agartz, I., Ford, J. M., et al. (2019). Positive and general psychopathology associated with specific gray matter reductions in inferior temporal regions in patients with schizophrenia. *Schizophr. Res.* 208, 242–249. doi: 10.1016/j.schres.2019.02.010

Moberget, T., Alnæs, D., Kaufmann, T., Doan, N. T., Córdova-Palomera, A., Norbom, L. B., et al. (2019). Cerebellar gray matter volume is associated with cognitive function and psychopathology in adolescence. *Biol. Psychiatry* 86, 65–75. doi: 10.1016/j.biopsych.2019.01.019

Moberget, T., Doan, N. T., Alnæs, D., Kaufmann, T., Córdova-Palomera, A., Lagerberg, T. V., et al. (2018). Cerebellar volume and cerebellocerebral structural

covariance in schizophrenia: A multisite mega-analysis of 983 patients and 1349 healthy controls. *Mol. Psychiatry* 23, 1512–1520. doi: 10.1038/mp.2017.106

Murray, R. M., Sham, P., van Os, J., Zanelli, J., Cannon, M., and McDonald, C. (2004). A developmental model for similarities and dissimilarities between schizophrenia and bipolar disorder. *Schizophr. Res.* 71, 405–416. doi: 10.1016/j.schres.2004.03.002

Ng, A., Jordan, M. I., and Weiss, Y. (2001). "On spectral clustering: Analysis and an algorithm," in *Proceedings of NIPS*.

Onitsuka, T., Shenton, M. E., Kasai, K., Nestor, P. G., Toner, S. K., Kikinis, R., et al. (2003). Fusiform gyrus volume reduction and facial recognition in chronic schizophrenia. *Arch. Gen. Psychiatry* 60:349. doi: 10.1001/archpsyc.60.4.349

Potkin, S. G., Turner, J. A., Brown, G. G., McCarthy, G., Greve, D. N., Glover, G. H., et al. (2009). Working memory and DLPFC inefficiency in schizophrenia: The FBIRN study. *Schizophr. Bull.* 35, 19–31. doi: 10.1093/schbul/sbn162

R Core Team (2014). *R: A Language and Environment for Statistical Computing*. Vienna: R Foundation for Statistical Computing.

Rahaman, M. A., Mathalon, D., Lee, H. J., Jiang, W., Mueller, B. A., Andreassen, O., et al. (2020). N-BiC: A method for multi-component and symptom biclustering of structural mri Data: Application to schizophrenia. *IEEE Trans. Biomed. Eng.* 67, 110–121. doi: 10.1109/TBME.2019.2908815

Rangarajan, V., Hermes, D., Foster, B. L., Weiner, K. S., Jacques, C., Grill-Spector, K., et al. (2014). Electrical stimulation of the left and right human fusiform gyrus causes different effects in conscious face perception. *J. Neurosci.* 34, 12828–12836. doi: 10.1523/JNEUROSCI.0527-14.2014

Rimol, L. M., Nesvåg, R., Hagler, D. J., Bergmann, Ø, Fennema-Notestine, C., Hartberg, C. B., et al. (2012). Cortical volume, surface area, and thickness in schizophrenia and bipolar disorder. *Biol. Psychiatry* 71, 552–560. doi: 10.1016/j.biopsych.2011.11.026

Ringen, P. A., Lagerberg, T. V., Birkenæs, A. B., Engn, J., Færden, A., Jónsdottir, H., et al. (2008). Differences in prevalence and patterns of substance use in schizophrenia and bipolar disorder. *Psychol. Med.* 38, 1241–1249. doi: 10.1017/S003329170700236X

Rootes-Murdy, K., Goldsmith, D. R., and Turner, J. A. (2022). Clinical and structural differences in delusions across diagnoses: A systematic review. *Front. Integr. Neurosci.* 15:726321. doi: 10.3389/fnint.2021.726321

Rootes-Murdy, K., Zendehrouh, E., Calhoun, V. D., and Turner, J. A. (2021). Spatially covarying patterns of gray matter volume and concentration highlight distinct regions in schizophrenia. *Front. Neurosci.* 15:708387. doi: 10.3389/fnins.2021.708387

Ruderfer, D. M., Ripke, S., McQuillin, A., Boocock, J., Stahl, E. A., Pavlides, J. M. W., et al. (2018). Genomic dissection of bipolar disorder and schizophrenia, including 28 subphenotypes. *Cell* 173, 1705–1715.e16. doi: 10.1016/j.cell.2018.05.046

Rissanen, J. (2018). Modeling by shortest data description. *Automatica* 14, 465–471. doi: 10.1016/0005-1098(78)90005-5

Schwarz, E., Doan, N. T., Pergola, G., Westlye, L. T., Kaufmann, T., Wolfers, T., et al. (2019). Reproducible grey matter patterns index a multivariate, global alteration of brain structure in schizophrenia and bipolar disorder. *Transl. Psychiatry* 9:12. doi: 10.1038/s41398-018-0225-4

Segall, J. M., Turner, J. A., van Erp, T. G. M., White, T., Bockholt, H. J., Gollub, R. L., et al. (2009). Voxel-based morphometric multisite collaborative study on schizophrenia. *Schizophr. Bull.* 35, 82–95. doi: 10.1093/schbul/sbn150

Sorella, S., Lapomarda, G., Messina, I., Frederickson, J. J., Siugzdaite, R., Job, R., et al. (2019). Testing the expanded continuum hypothesis of schizophrenia and bipolar disorder. neural and psychological evidence for shared and distinct mechanisms. *Neuroimage* 23:101854. doi: 10.1016/j.nicl.2019.101854

Takahashi, T., Suzuki, M., Zhou, S.-Y., Tanino, R., Hagino, H., Niu, L., et al. (2006). Temporal lobe gray matter in schizophrenia spectrum: A volumetric MRI study of the fusiform gyrus, parahippocampal gyrus, and middle and inferior temporal gyri. *Schizophr. Res.* 87, 116–126. doi: 10.1016/j.schres.2006.04.023

Turner, J. A., Calhoun, V. D., Michael, A., van Erp, T. G. M., Ehrlich, S., Segall, J. M., et al. (2012). Heritability of multivariate gray matter measures in schizophrenia. *Twin Res. Hum. Genet.* 15, 324–335. doi: 10.1017/thg.2012.1

van Erp, T. G. M., Walton, E., Hibar, D. P., Schmaal, L., Jiang, W., Glahn, D. C., et al. (2018). Cortical brain abnormalities in 4474 individuals with schizophrenia and 5098 control subjects via the enhancing neuro imaging genetics through meta analysis (ENIGMA) consortium. *Biol. Psychiatry* 84, 644–654. doi: 10.1016/j.biopsych.2018.04.023

Vita, A., de Peri, L., Deste, G., Barlati, S., and Sacchetti, E. (2015). The effect of antipsychotic treatment on cortical gray matter changes in schizophrenia: Does the class matter? a meta-analysis and meta-regression of longitudinal magnetic resonance imaging studies. *Biol. Psychiatry* 78, 403–412. doi: 10.1016/j.biopsych.2015.02.008

von Luxburg, U. (2007). A tutorial on spectral clustering. *Stat. Comput.* 17, 395–416. doi: 10.1007/s11222-007-9033-z

Wang, L., Kogan, A., Cobia, D., Alpert, K., Kolasny, A., Miller, M. I., et al. (2013). Northwestern university schizophrenia data and software tool (NUSDAST). *Front. Neuroinform.* 7:25. doi: 10.3389/fninf.2013.00025

Wolfers, T., Rokicki, J., Alnæs, D., Berthet, P., Agartz, I., Kia, S. M., et al. (2021). Replicating extensive brain structural heterogeneity in individuals with schizophrenia and bipolar disorder. *Hum. Brain Mapp.* 42, 2546–2555. doi: 10.1002/hbm.25386

Xu, L., Groth, K. M., Pearlson, G., Schretlen, D. J., and Calhoun, V. D. (2009). Source-based morphometry: The use of independent component analysis to identify gray matter differences with application to schizophrenia. *Hum. Brain Mapp.* 30:711–24. doi: 10.1002/hbm.20540

Yao, N., Winkler, A. M., Barrett, J., Book, G. A., Beetham, T., Horseman, R., et al. (2017). Inferring pathobiology from structural MRI in schizophrenia and bipolar disorder: Modeling head motion and neuroanatomical specificity. *Hum. Brain Mapp.* 38, 3757–3770. doi: 10.1002/hbm.23612

Frontiers in
Human Neuroscience

Bridges neuroscience and psychology to understand the human brain

The second most-cited journal in the field of psychology, that bridges research in psychology and neuroscience to advance our understanding of the human brain in both healthy and diseased states.

Discover the latest Research Topics

See more →

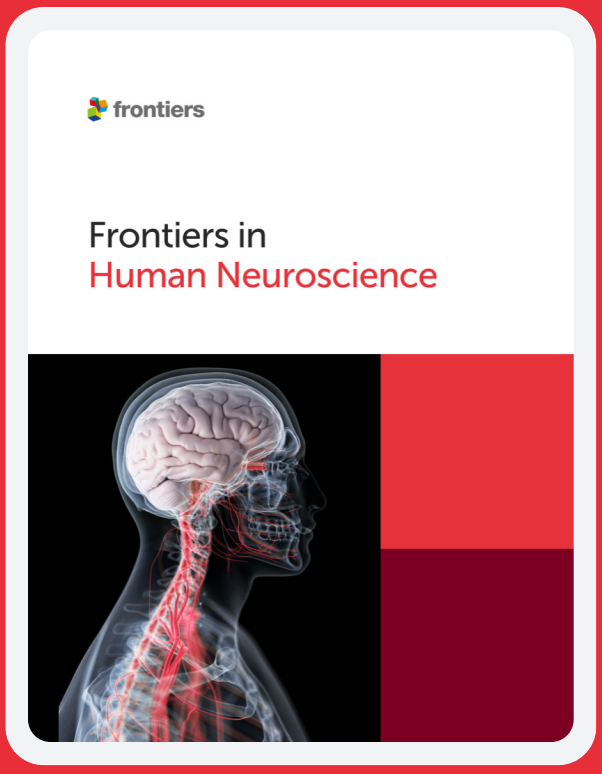

Frontiers

Avenue du Tribunal-Fédéral 34
1005 Lausanne, Switzerland
frontiersin.org

Contact us

+41 (0)21 510 17 00
frontiersin.org/about/contact